The role of Sulf1 during Sonic hedgehog mediated neural patterning

Simon Alexander Ramsbottom

PhD

The University of York
Department of Biology

2011

Abstract

Heparan sulphate proteoglycans (HSPGs) are large molecules distributed ubiquitously, both at the cell surface and within the extracellular matrix. These molecules are known to play essential roles in developmental cell signalling, and the differential sulfation of HSPG chains gives rise to a high degree of variability in their binding specificity.

Sulf1, an N-acetlyglucosamine O-6 endosulfatase, specifically removes sulphate groups from HSPG chains in regions of high sulfation, and removal of these groups by Sulf1 leads to the attenuation of both BMP and FGF signalling.

The expression profile of *Sulf1* within the neural tube of *X. tropicalis* is similar to that of *Sonic Hedgehog* (*Shh*) and work in both chick and *Drosophila* has shown that Sulf1 is able to modify the distribution of hedgehog proteins during development. Taken together, this suggests that Sulf1 may act within the ventral neural tube to modify the distribution and activity of Shh and so regulate vertebrate neural patterning.

Using the paradigm of dorsoventral patterning within the vertebrate neural tube, this thesis establishes a role for Sulf1 in modulating the distribution and activity of Shh, and demonstrates that this regulation is an important factor during neural development.

List of figures

List of Tables

Acknowledgements

I would like to thank Betsy Pownall and Harv Isaacs for their help and guidance, as well as James Chong and Paul Genever for their assistance throughout the project. Additionally a number of people within the technology facility have been an enormous help over the course of my PhD. These include Naveed Aziz, Celina Whalley, Peter O'Toole, Karen Hodgkinson, Karen Hogg, Graeme Park, Meg Stark, Jo Marrison and Andrew Leech. A massive thank you to all of you, particularly those from imaging and cytometry, who have put up with a huge amount of nagging and given up a lot of their time to help me.

I would also like to thank all the members of the frog lab past and present for their years of suffering guiding me through, in no particular order; Steve Freeman, Emily Guiral, Emily Winterbottom for her extensive help teaching me a number of biological techniques, Wendy Moore, Laura Faas for showing me that gas injectors are the way forward, Di Quinn for her amazing ability to get anything to work no matter how difficult it seems, Julie Affleck, Richard Maguire for teaching me almost everything I know about lab work and proving you don't need to work with mercury to be completely mental, Fiona Warrander for her help with a number of techniques and ensuring that everything is fairly allotted, Simon Fellgett for helping to develop the method to visualise animal caps and reminding me that a 15 hour day builds character and should not be considered strange in any way, and Nick Bland for so many things but above all for showing me that data should always be viewed with suspicion, especially if it shows you what you want it to.

I would like to thank all the people that weren't but would love to be part of the frog lab including, Andy Taylor for his friendship, critical eye, encyclopaedic knowledge and above all his amazing perseverance which is an example for us all, Louise Ridley for constantly reminding me that teaching children is not for me, Sarah Aynsley for a surprising amount of reagents and help with protocols despite the disparity of our respective fields, as well as her friendship and the fact that her door is always open, Tom Brabbs for his ability to always provide comic relief and someone to talk to in the lab at 3am, Tom Smith, Naomi Voke, Eleanor Walton, and Jo Hepworth for reminding me that no matter how annoying animal work may be sometimes, it's better than working with plants. I

would like to thank the following people for providing reagents or protocols: Ana Ribeiro, James Briscoe, Nancy Papalopulu, Raphael Thuret, Jim Smith, Andrew McMahon, Roger Tsien, Makoto Mochii, Asako Shindo.

Mostly I would like to thank my loving wife Jen for her support, without which the completion of this work would not have been possible.

Author's declaration

None of the work presented in this thesis has been previously published or submitted for a qualification either at the University of York or at any other institution. Some parts of this work have however been presented in posters at the British Society for Developmental Biology Spring meeting (2008) the 12th/13th International *Xenopus* Meeting (2008/2010); and the 16th International Society for Developmental Biology Meeting (2009). All of the work presented here is that of the author.

.....

Simon Ramsbottom

1.0 Introduction

1.1 Morphogens in development

During development it is imperative that cells communicate with one other. For an organism to function properly it requires cells of a specific type to be in the correct place and in the correct number to be able to establish functional tissues and organs. Signalling between cells can take many forms from direct contact between cells, to the production of long range signals which spread throughout a cell population and signal to many cells simultaneously. With some long range signals, the concentration of the signal provides positional information to the cell and allows the formation of polarised tissues; these signalling molecules have been termed morphogens. Cells may respond to these signals based on a number of factors including properties of the signal itself, such as the concentration and longevity of the signal, or on their competence to respond based on their lineage. Due to the complexity of cells and their surrounding environment, long range signals may not always simply diffuse away from their source but may instead interact with the local environment. By adapting the environment through which signals pass, the nature, concentration and longevity of a signal can be modified, allowing one signal to be interpreted in a number of different ways.

In this thesis I will be investigating the impact that the extracellular environment has on hedgehog signalling and how modification of the extracellular matrix by specific enzymes can affect the way the hedgehog protein moves and signals. The sonic hedgehog (*Shh*) gene codes for a secreted signalling molecule that is expressed in regions important in patterning the vertebrate embryo. Shh signalling has been shown to be critical during vertebrate neuronal development, acting as a long range signal within the neural tube to induce polarity and provide positional information. As Shh interacts with the local environment, modification of the extracellular matrix may affect the way in which it is able to move and signal, thus impacting on early neuronal patterning.

1.2 The role of hedgehog during *Drosophila* development

Hedgehog was first discovered in a screen for mutations that perturb the larval body plan in *Drosophila* (Nusslein-Volhard and Wieschaus, 1980), taking its name from the lawn of denticles which arise in the mutant and resemble the spines on a hedgehog. A number of other genes were identified both in this screen and in other works, and classified into a group called the segment polarity genes (Counce, 1956; Nusslein-Volhard and Wieschaus, 1980; Sharma and Chopra, 1976).These genes were proposed to regulate the development of each segment, acting to control the polarity of every repeating unit, with each gene having a role in specifying a certain aspect of the segment (Nusslein-Volhard and Wieschaus, 1980). Further work shed light on the mechanisms that control segment-polarity gene expression and function, identifying crucial roles for two genes *wingless* (*wg*) and *engrailed* (*en*) in the establishment and maintenance of segment identity (DiNardo et al., 1988). A role for hedgehog in the regulation of these genes was proposed following the discovery that in the absence of the putative hedgehog receptor *patched* (*ptc*), the domain of wg expression is broadened and leads to the induction of *en* in anterior regions (DiNardo et al., 1988; Martinez Arias et al., 1988). *Ptc* is initially expressed in broad domains and normally acts to inhibit wg expression; this repressive action is inhibited by Hh which is secreted from *en* expressing cells (Ingham et al., 1991). In addition to its role in segment polarity, hedgehog also plays a role in the development of the fly wing, leg and eye (Basler and Struhl, 1994; Dominguez, 1999).

1.3 The role of hedgehog during vertebrate development

Unlike in *Drosophila* which has only one *hedgehog* gene, vertebrates have a number of related *hedgehog* genes. The three genes *Desert hedgehog* (*Dhh*), *Indian hedgehog*, (*Ihh*) and *Sonic hedgehog* (*Shh*) are widely conserved, while gene duplication events have lead to additional genes in certain species (reviewed in Ingham and McMahon, 2001). Of the three main hedgehog genes, *Shh* has garnered the greatest interest due to its expression in a number of regions within the vertebrate embryo which comprise major signalling centres, namely the notochord and floor plate within the midline, as well as the zone of polarising activity (ZPA) within the developing limb bud.

1.3.1 Development of axial structures

Shh is a major determinant in the formation of axial structures and the dorsal ventral patterning of the vertebrate neural tube. During early vertebrate development, axial mesoderm expresses the winged helix transcription factor *HNF3β* (also known as FoxA2) and is specified to form notochord (Ang and Rossant, 1994; Weinstein et al., 1994). HNF3β has been shown to be required for the expression of *Shh*; mice lacking *HNF3β*, do not form a notochord and fail to initiate *Shh* expression (Ang and Rossant, 1994; Weinstein et al., 1994), while ectopic expression of *HNF3β* leads to ectopic sites of Shh expression within the neural tube (Ruiz i Altaba et al., 1995).

Another important structure which arises from this region is the floor plate of the neural tube. During the differentiation of the floor plate, cells along the midline undergo a morphological change, such that they take on a wedge-like appearance (Schoenwolf and Franks, 1984). In the absence of notochord, floor plate cells do not develop (Placzek et al., 1990). HNF3β$^{-/-}$ mice, which fail to form notochord, are able to develop a neural tube, but lack floor plate cells (Ang and Rossant, 1994), again suggesting that the notochord is essential for the differentiation of the floor plate. Grafting of notochord to the lateral part of the neural tube gives rise to cells, which are morphologically similar to the floor plate (Smith and Schoenwolf, 1989) supporting the idea that the notochord induces floor plate identity. Using a floor plate specific chemoattractant as a floor plate marker (Tessier-Lavigne et al., 1988), explant studies showed that notochord was sufficient to induce floor plate identity (Placzek et al., 1990).

Interestingly, notochord is not the only tissue able to induce floor plate identity. Grafting segments of floor plate on to neural tube gives rise to ectopic floor plate induction in a similar manner to notochord grafts (Yamada et al., 1991). Similarly, growth of neural plate explants grown in contact with either notochord or floor plate induces floor plate identity (Placzek et al., 1993). This inductive property of floor plate and notochord propagates through cells, up to a distance of ten cell diameters from the grafted tissue (Placzek et al., 1993). This ability is not diminished in the presence of either mitomycin C which blocks proliferation, or cytochalasin D which inhibits cell migration, which suggested that a

homeogenetic signal spread through the tissue to expand the size of the floor plate (Placzek et al., 1993).

Mice which have a targeted mutation in the *Shh* gene fail to form floor plate (Chiang et al., 1996), while blocking Shh function with antibodies similarly results in floor plate loss (Ericson et al., 1996). In Shh mutant mice however, notochord does develop early on but is not maintained, as indicated by changes to Brachyury expression, which is lost rostrally and is not expressed uniformly along the midline (Chiang et al., 1996). The fact that Shh mutant mice form a notochord but fail to form a floor plate, and that inhibition of Shh function blocks floor plate development, suggests that Shh is the active factor in the notochord required for floor plate induction. In agreement with this idea, when neural plate explants are grown in contact with COS cells expressing hedgehog, they differentiate in a similar manner to when they are grown in contact with notochord (Roelink et al., 1994).

In vivo, ectopic expression of either *Shh*, or downstream effectors of Shh signalling, results in the emergence of ectopic floor plate cells (Hynes et al., 2000; Roelink et al., 1994). If Shh is presented as an external source however, it is not sufficient to induce floor plate identity *in vivo* (Patten and Placzek, 2002). This suggests that additional factors present in notochord and floor plate are required for indiction. When beads were implanted containing both Shh and the BMP inhibitor chordin, dramatic effects can be seen, with a massive expansion of the region in which cells take on floor plate identity (Patten and Placzek, 2002).

Taken together this evidence points to a mechanism whereby notochord differentiates as a result of *FoxA2* expression, which induces the expression of Shh within the notochord. The notochord then induces the overlaying neural tissue to form floor plate in a contact dependent and Shh mediated manner. This inductive signal is the propagated through the adjacent neural cells, thus expanding the floor plate (Placzek et al., 1993). Despite the mass of evidence for this model, it may not represent a universal mechanism of floor plate induction. Mutations in Zebrafish indicate a reduced importance for the notochord and Shh in floor plate specification. The mutations no tail (*ntl*) and

floating head (*flh*), which code for Not and Brachyury respectively, both affect the formation of the notochord (Halpern et al., 1993; Talbot et al., 1995). In mice and chick, loss of notochord leads to a lack of floor plate (Ang and Rossant, 1994; Placzek et al., 1990). In the *ntl* and flh mutants however, medial floor plate cells persist (Halpern et al., 1993; Talbot et al., 1995). Furthermore, while surgical removal of the early embryonic shield leads to a loss of notochord, morphologically distinct floor plate cells can be seen, although these are only found anteriorly and cannot be seen within the trunk (Shih and Fraser, 1996). Mutation of the Shh gene, or blocking Shh function in mice leads to lack of floor plate (Chiang et al., 1996; Ericson et al., 1996). Studies analysing mutation of the zebrafish sonic hedgehog gene sonic-you (syu), or mutation of downstream effectors of Shh signalling however, indicate that only lateral floor plate cells require the presence of Shh for their differentiation (Chen et al., 2001; Schauerte et al., 1998).

The zebrafish mutants *cyclops* (cyc), which codes for nodal-related2 (ndr2) and *one-eyed pinhead* (*oep*), which encodes a cofactor required for nodal signalling (Gritsman et al., 1999) do lack floor plate cells (Hatta et al., 1991; Schier et al., 1997; Strahle et al., 1997) suggesting that nodal signalling, and not Shh is the predominant factor in floor plate specification. Additionally while Shh is a key factor in chick, it appears that floor plate induction is achieved by different mechanisms along the anteroposterior axis (Patten et al., 2003). Cells from a region of the prenodal epiblast termed “area a” undergo rapid induction through the co-ordinated activity of Shh and nodal, and do not require prolonged contact with underlying notochord, as seen further posteriorly (Patten et al., 2003). Floor plate induction in this region therefore resembles induction of the medial floor plate in zebrafish, suggesting that while floor plate induction overall may be achieved by divergent mechanisms, parallels do exist between amniotic and anamniotic species.

While originally identified from its morpholocial appearance and later by its ability to homeogenetically induce cells of a similar characteristic, it must be noted that the floor plate is not made up from a homogenous group of cells. Instead it is comprised of a number of different subpopulations which differ along the dorsoventral and anteroposterior axes (Placzek and Briscoe, 2005).

These different groups are derived from distinct origins, are able to differentially induce specific cell types and each express a distinct subset of transcription factors. Within the spinal cord, the floor plate can be spatially separated along the dorsoventral axis into the medial floor plate (MFP) which occupies the midline, and lateral floor plate (LFP). These two subpopulations express different transcription factors, and exhibit a differential requirement for Shh in their induction (Halpern et al., 1993; Talbot et al., 1995) It is however unclear as to whether the lateral population of cells constitutes a *bona fide* floor plate population. These cells were originally described as being floor plate due to a number of defining characteristics (Odenthal et al., 2000). However while MFP does not give rise to cells of a neuronal subtype, cells deriving from the LFP differentiate into interneurons (Charrier et al., 2002). Whether or not these lateral cells can be described *per se* as floor plate therefore remains under discussion. Work in chick has shown that along the midline, cells initially express transcription factors associated with a later floor plate identity (Ribes et al., 2010). Over time the expression profile within these cells changes, and cells take on a medial identity, indicating not only a spatial, but also a temporal element to the specification of these cell types.

1.3.2 Determination of cell lineage

Other experiments reveal the ability of Shh to promote cell lineage determination. Shh has a role in controlling the specification of muscle precursors, being important in regulating the myogenic genes MyoD and Myf5 in avian somites (Borycki et al., 1998)**.** Shh null mice lose *Myf5* expression within the epaxial dermomyotome giving rise to abnormal somites showing that Shh plays a key role in the determination of myogenic precursors in mice (Borycki et al., 1999). Injection of retrovirus engineered to express Sonic hedgehog, or growth of presomitc mesoderm in contact with Shh expressing 10T1/2 cells leads to an increase in Paxl expression in the sclerotome but a decrease in Pax3 in the dermatome (Fan and Tessier-Lavigne, 1994; Johnson et al., 1994). Ectopic *MyoD* expression can also be seen in chick and zebrafish over expressing *Shh* (Johnson et al., 1994). Additionally a Gli1 binding site was shown to be located within an epaxial somite enhancer region within the Myf4/Myf5 locus, and it has been shown that Shh can transcriptionally regulate Mfy5 expression (Gustafsson et al., 2002).

Expression of Shh within the notochord and floor plate leads to polarisation of the neural tube, specifying cells of a ventral characteristic. The mechanism by which Shh patterns the neural tube will be discussed in further detail in chapter 3.

1.3.3 Development of the limb bud

Within the developing vertebrate limb bud Shh specifies positional identity along the anterior–posterior axis. Shh is expressed in a region known as the zone of polarising activity (ZPA), which is found within the posterior of the limb bud. A gradient of Shh can be detected across the limb bud (Zeng et al., 2001), such that high levels of Shh specify digits as posterior while progressively lower concentrations of Shh give rise to digits of a more anterior character. If Shh expression within the ZPA is reduced, digits with the most posterior identity are lost (Lewis et al., 2001). Ectopic Shh within the anterior of the limb induces the formation of additional digits in a concentration-dependent manner, and these supernumerary digits take on a more posterior identity as the level of Shh increases (Yang et al., 1997). Although Shh is not the only signalling molecule that acts to specify the polarity of the limb bud (Duprez et al., 1996), the formation of a hedgehog gradient (Lewis et al., 2001; Zeng et al., 2001) as well as the wide-ranging expression of Shh target genes (Lewis et al., 2001), demonstrates that Shh is able to act over a long distance to specify positional identity within the developing limb. As well as its role in AP patterning, Shh is also required for continued outgrowth of the limb bud as it is required for continued expression of FGF within the apical ectodermal ridge (AER) (Laufer et al., 1994; Niswander et al., 1994). FGF4 expression within the AER is then required for the maintenance of Shh expression; removal of the AER leads to a down regulation of Shh expression, but expression can be maintained by replacement of the AER with a bead soaked with FGF4 protein (Laufer et al., 1994). Shh is therefore an integral part of a positive feedback loop which controls patterning and outgrowth of the limb bud.

1.3.4 Axon guidance

As well as being able to provide graded positional information to pattern tissues and specify cell fates, Shh is able to act as a guidance cue for axons. *Xenopus*

spinal axons grown in dispersed cell culture grow towards a source of Shh, while culturing cells expressing *Shh* adjacent to rat spinal cord explants can induce the reorientation of commissural axons (Charron et al., 2003). In both cases, directional growth can be perturbed by the inhibition of hedgehog signalling with the chemical inhibitor cyclopamine (Charron et al., 2003). When the reception of the hedgehog signal is specifically inhibited in commissural axons in mice, although they ultimately reach the midline and form a normal ventral commisure, the path they take is very convoluted (Charron et al., 2003). Conversely Shh acts as a negative regulator of retinal ganglion cell (RGC) growth. When chick RGCs are grown in culture in the presence of SHH soaked beads, the length and number of projecting axons is reduced (Trousse et al., 2001). Furthermore when *Shh* is expressed ectopically throughout the ventral forebrain, axons do not advance along the optic nerve, whilst confined *Shh* over expression leads to axonal routing defects (Trousse et al., 2001).

1.3.5 Cell proliferation

As well as a role in providing positional information and promoting differentiation, Shh is able to control the number of cells within a population of progenitors. In neocortical neurospheres (nsps) treatment with SHH alone is not sufficient to induce proliferation, however treatment with epidermal growth factor (EGF) does promote proliferation in a SHH concentration dependent manner (Palma and Altaba, 2004). Additionally, the ability of nsps to form secondary colonies is increased in the presence of SHH, and this ability can be abrogated by inhibition of the hedgehog pathway (Palma and Altaba, 2004). Furthermore, when hedgehog signalling is inhibited in mice by peritoneal injection of the chemical inhibitor cyclopamine, a large reduction in the number of proliferative cells within the subventricular zone (SVZ) can be observed, concomitant with a reduction in downstream targets of hedgehog signalling in the same region (Palma et al., 2005). An increase in neuronal precursor proliferation can also be seen in *Xenopus* explants from the neocortex and tectum following the addition of SHH (Dahmane et al., 2001) whilst inhibition of hedgehog signalling leads to loss of precursors within the chick cerebellum (Dahmane and Ruiz i Altaba, 1999).

1.4 Hedgehog synthesis

Shh is initially synthesised as a 46 kDa precursor and is subsequently cleaved and modified to produce the mature protein (Lee et al., 1994; Porter et al., 1996b). Signal cleavage is followed by autoproteolysis which gives rise to a 19 kDa N-terminal fragment (Shh-N) and a 25 kDa C-terminal fragment (Lee et al., 1994). A cholesterol group is added to the C-terminal end of the N-fragment during autoproteolysis, with the C-terminal fragment acting as a cholesterol transferase (Porter et al., 1996b). A palmitoyl group is subsequently added the Shh-N molecule at Cys-24 (Pepinsky et al., 1998), giving rise to an extremely hydrophobic molecule (now termed Shh-Np for N-processed) (Figure 1.1). The addition of palmitate is made within the secretory pathway and is mediated by a palmitoylacyltransferase which is coded for by the Skinny hedgehog gene (*Ski/Skn*) (Chamoun et al., 2001). This gene is also known as sightless (Sit) (Lee and Treisman, 2001), rasp (Micchelli et al., 2002) and hedgehog aceyl transferase (Hhat) (Buglino and Resh, 2008). Mice deficient in *Skn* exhibit similar defects to *Shh* mutants, and lack a differentiated floor plate as well as having patterning defects within the neural tube indicating that this modification is essential for Shh function (Chen et al., 2004). The addition of cholesterol and palmitate increases the efficacy of Shh-Np (Chen et al., 2004; Zeng et al., 2001), whereas it has been shown that addition of hydrophilic adducts to the N terminus reduces the activity of Shh (Taylor et al., 2001).

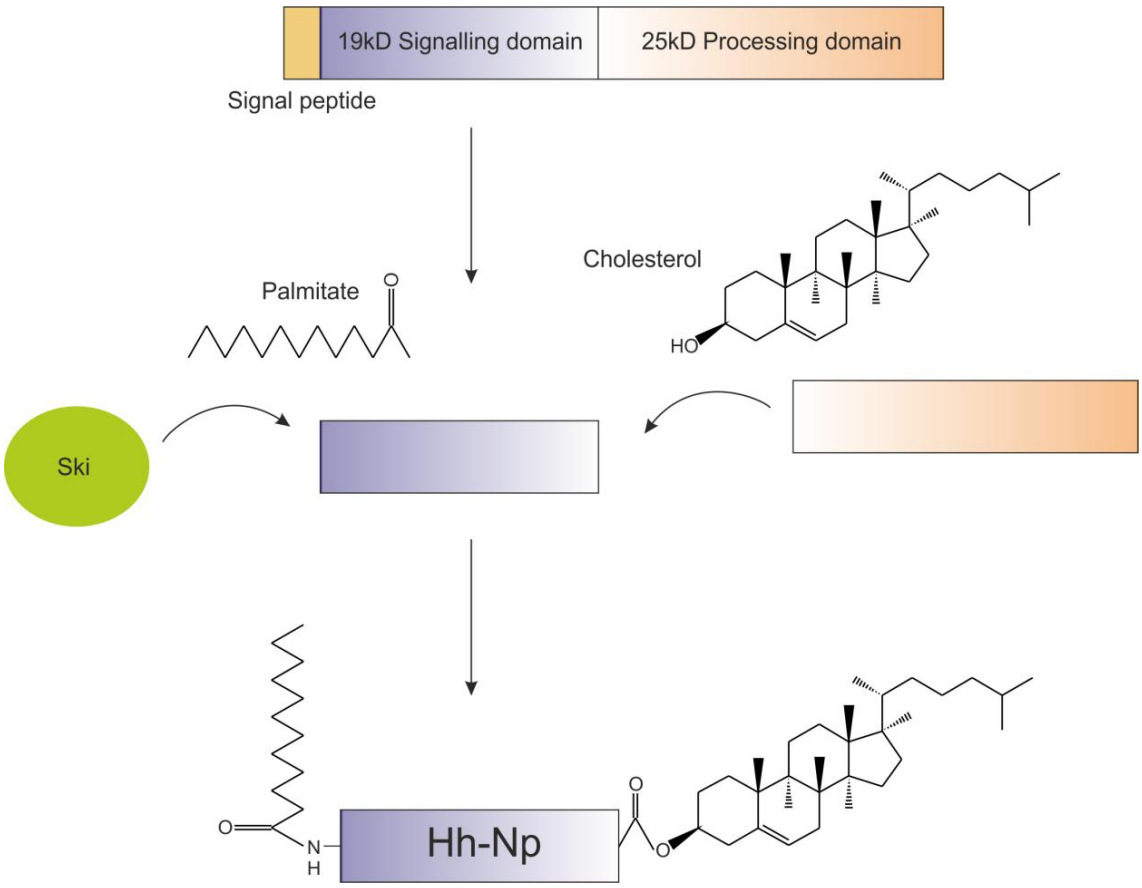

Figure 1.1 Synthesis of functional lipid modified hedgehog protein
Following cleavage of the signal peptide, the hedgehog protein undergoes autoproteolysis to give N and C terminal fragments. The C-terminal fragment acts as a cholesterol transferase to attach cholesterol to the N-terminal fragment. The skinny hedgehog gene attaches palmitate to the N-terminus of hedgehog to give rise to the fully processed form (Hh-Np/Shh-Np).

The presence of a cholesterol adduct on hedgehog would suggest that it is membrane bound and thus restricted in its diffusive ability. In agreement with this, when expressed in cells most of the lipid-modifed form of Shh (Shh-Np) is found to be associated with cells, and is not released into the surrounding medium (Bumcrot et al., 1995; Lee et al., 1994; Porter et al., 1995). Additionally hedgehog which does not undergo autoproteolysis and thus has no cholesterol adduct (termed Hh-Nu), is released by cells (Porter et al., 1995). Hh-Nu has also been shown to have an increased range compared with Hh-Np (Porter et al., 1996a) further supporting the idea the cholesterol has a role in hedgehog tethering. As discussed previously however, Shh displays the characteristics of a freely diffusible molecule, and is able to act from a distance in a morphogenic manner (Briscoe et al., 2001). These seemingly contradictory factors of the existence of an adduct associated with membrane tethering and the ability of

Shh to diffuse and act at long range, suggests that Shh release and subsequent diffusion is facilitated in some way.

1.4.1 Controlled release of the hedgehog ligand

A gene closely related to *Ptc*, *Dispatched* (*Disp*), has been shown to be required for the release of Hh-Np (Burke et al., 1999). Disp contains a sterol sensing domain (SSD), which can be found in other proteins that directly bind cholesterol (Radhakrishnan et al., 2004), suggesting that Disp recognises the cholesterol adduct on the modified form of Shh**.** Loss of Disp leads to retention of Hh-Np in producing cells (Burke et al., 1999). Hh-Nu however, which is not cholesterol modified, is not retained following loss of Disp, demonstrating that addition of cholesterol during Shh processing is responsible for Hh tethering at the membrane and that this is overcome by the action of Disp (Burke et al., 1999). Mice homozygous for disp exhibit cyclopia and holoprosencephaly and display reduced levels of Shh target genes (Kawakami et al., 2002). As seen in *Drosophila*, hedgehog in mouse *disp* mutants fails to be released from its site of synthesis indicating a conserved role for hedgehog release (Kawakami et al., 2002).

As well as dispatched, a number of other factors are required for correct hedgehog release and diffusion away from its site of synthesis. Many of these are extracellular matrix (ECM) proteins, or are involved in the synthesis or modification of components of the ECM, and will be discussed further in chapter 4.

1.5 Hedeghog signal transduction

1.5.1 Patched

Patched (*Ptc*) codes for a transmembrane protein and acts as the receptor for the hedgehog ligand (Ingham et al., 1991; Marigo et al., 1996). Ptc was known for its role in segment polarity in *Drosophila*, but its role as the receptor for hedgehog was first suggested following a study which analysed the role of Ptc and Hh on *wingless* (*wg*) expression (Ingham et al., 1991). *Drosophila* has only one *ptc* gene while in vertebrates there are two related genes *Ptc*1 and *Ptc*2 (Carpenter et al., 1998; Lewis et al., 1999; Motoyama et al., 1998; Smyth et al.,

1999; Takabatake et al., 2000; Zaphiropoulos et al., 1999) Mutations of *Ptc* have shown that unlike many receptors, Ptc acts to suppress hedgehog target genes, (Goodrich et al., 1997; Ingham et al., 1991) and this repression is released upon binding of hedgehog. The extracellular domain of Ptc consists of two large hydrophilic loops which are required for hedgehog binding (Marigo et al., 1996). Mutation of these domains prevents ligand receptor binding and inhibits the ability of cells to receive the hedgehog signal (Briscoe et al., 2001). The addition of palmitoyl and cholesterol groups during the synthesis of the hedgehog protein (as previously discussed) does not appear to be a pre-requisite for binding to Ptc. Mutation of the SSD of Ptc does not compromise Hh binding (Martin et al., 2001; Strutt et al., 2001), and neither cholesterol or palmitoyl modifications appear to increase the Hh-Ptc interaction (Pepinsky et al., 1998), although these modifications do increase the level of activity of Hh as previously discussed. Upon Hh binding, Ptc and Hh are internalised as a complex in Hh responding cells (Martin et al., 2001; Torroja et al., 2004). By binding hedgehog and promoting its internalisation, Ptc not only acts to transduce the Hh signal but also to control its dispersal through sequestration of the Hh ligand (Chen and Struhl, 1996). These two roles can be separated out by mutation of different domains. Deletion of the extracellular loop of ptc inhibits Hh binding and thus its ability to regulate the hedgehog morphogen gradient, but has no effect on the inhibition signal transduction (Briscoe et al., 2001) Conversely, truncation of the C-terminus of ptc abolishes its ability to inhibit downstream signalling, but not to bind Hh (Johnson et al., 2000).

1.5.2 Smoothened

While Ptc acts to bind the hedgehog ligand, another protein named Smoothened (Smo), has a conserved integral role in the hedgehog pathway, and is essential for hedgehog signal transduction in *Drosophila* and vertebrates (Alcedo et al., 1996; Chen and Struhl, 1998; van den Heuvel and Ingham, 1996; Zhang et al., 2001). Smo is a seven-pass G-protein coupled integral membrane protein (Alcedo et al., 1996; Chen and Struhl, 1998), and is closely related to Frizzled, a receptor in the Wnt signalling pathway (Dann et al., 2001). The level of Smo protein is hedgehog dependent and in the absence of Hh ligand, Smo levels are low (Alcedo et al., 2000). Over expression of *Ptc* reduces levels of the Smo protein, whereas levels are high in *Ptc* mutants (Alcedo et al., 2000).

Genetic evidence from *Drosophila* showed that Ptc acts to inhibit Smo activity in the absence of ligand and that Hh binding releases this inhibition resulting in signal transduction (Chen and Struhl, 1996; Fuse et al., 1999). The exact mechanism by which Ptc inhibits Smo however is still unclear. Originally it was hypothesised that Ptc inhibited Smo via a direct physical interaction, however this interpretation is unlikely due to a number of factors. Firstly, Ptc and Smo are not co-localised in Shh responding cells (Denef et al., 2000). Secondly, the repression of Smo by Ptc does not require a 1:1 stochiometry, in fact, even when Smo is present in a 50-fold molar excess, Ptc is still able to repress Smo activity by 50% (Taipale et al., 2002). It has been suggested therefore that Smo activity is instead regulated by the action of small molecules. *Ptc*1-transfected cells display elevated levels of 3b-hydroxysteroid ((pro-)vitamin D3), which is released into the surrounding medium and is able to effectively block Gli activity (Bijlsma et al., 2006). Treatment of zebrafish with vitamin D3 leads to a loss of engrailed expression within muscle pioneer cells and a down regulation of *ptc* expression, both of which are indicative of reduced hedgehog signalling (Bijlsma et al., 2006). Additionally, these embryos display a change in the patterning and number of slow muscle fibres, which closely resembles the phenotype of $Smo^{-/-}$ embryos (Bijlsma et al., 2006). Conversely, oxysterols which are also an intermediate product in the cholesterol biosynthetic pathway are able to activate *Smo* (Corcoran and Scott, 2006). Smo activity may therefore depend on the relative concentrations of different small molecules, modulated by the action of Ptc, however the specifics of how this is controlled have yet to be resolved.

As well as the main two signal transduction proteins Ptc and Smo, a number of other proteins act at the cell surface to regulate hedgehog signalling. These proteins may promote or inhibit signalling and provide an additional level of control within the hedgehog signalling pathway.

1.5.3 Gas1

Gas1 (Growth arrest specific 1) was originally identified as a gene transcriptionally up regulated in NIH/3T3 cells arrested in G_0 (Schneider et al., 1988). Gas1 encodes a 45-kDa GPI-anchored cell surface protein (Stebel et al., 2000) which binds Shh with high affinity (Kd ~ 6 nM) (Lee et al., 2001). Over

expression of *Gas1* can suppress cell cycle progression (Del Sal et al., 1992) and requires p53 for this activity (Del Sal et al., 1995). The link of Gas1 with hedgehog signalling was recognised following a screen to identify Shh binding proteins (Lee et al., 2001). Gas1 is negatively regulated by Shh; *Smo*$^{-/-}$ embryos display an increase in Gas1 levels whereas in *Ptc*1$^{-/-}$ embryos Gas1 is almost completely lost (Allen et al., 2007). *Gas1* is expressed throughout the neural tube of mice early on but becomes dorsally restricted in later development (Allen et al., 2007). *Gas*$^{-/-}$ embryos display incorrect neuronal patterning within the ventral neural tube, with *Nkx2.2* and *FoxA2* showing overlapping expression domains within the ventral midline (Allen et al., 2007). Additionally within these embryos, ventral neural tube expression of *Shh* is almost completely lost. *Gas1* over expression conversely gives rise to cell autonomous up regulation of *Nkx2.2*, *Olig2* and *Nkx6.1* (Allen et al., 2007). Co-expression of *Gas1* with *Ptc1*$^{\Delta loop2}$ which does not bind Shh, blocks the ability of Gas1 to promote ectopic expression of ventral neural marker genes suggesting that Gas1 acts at the level of the Shh ligand (Allen et al., 2007).

1.5.4 The ihog family

Another cell surface protein which acts to promote hedgehog signalling is the *Drosophila* type-1 transmembrane protein *interference hedgehog* (*ihog*) (Yao et al., 2006). Ihog interacts with hedgehog, is required for Hh signal response in *Drosophila* cultured cells and when mutated leads to fusion of denticle belts in developing *Drosophila* embryos (Yao et al., 2006). Ihog represents one gene of a family of genes which also act to promote hedgehog signalling, comprised of brother of ihog (boi) and the mammalian proteins Cdo and Boc (Kang et al., 1997; Kang et al., 2002; Yao et al., 2006). Boi and Ihog display redundancy, as while single mutations of each give rise to only minor effects, *boi/ihog* double mutant flies die 24 to 48 hours after hatching (Camp et al., 2010). In mosaic mutants, cells which lack *boi* and *ihog* show low levels of the downstream effector Ci155 (which will be discussed later) and Ptc indicating that Ihog and Boi are required cell-autonomously in Hh responding cells (Camp et al., 2010).

While acting to promote Hh signalling, the expression of ihog family members is down regulated in response to active signalling. The mammalian homologues of *ihog* and *boi*, *cdo* and *boc*, are expressed in regions of low hedgehog activity,

and loss of hedgehog signalling in *shh*$^{-/-}$ or *smo*$^{-/-}$ embryos leads to a spread of both Cdo and Boc, consistent with them being negatively regulated by Shh (Tenzen et al., 2006). Similar to Gas1 mutants, Cdo$^{-/-}$ embryos show a reduction in midline expression of *Shh* and *FoxA2* along with a ventral shift in *Nkx2.2* expression (Tenzen et al., 2006). Loss of *Boc* in rat commissural axons prevents correct axonal guidance and the ability to turn toward an ectopic source of Shh (Okada et al., 2006), while ectopic expression of *Boc* and *Cdo* promotes ectopic Shh-dependent ventral marker expression (Tenzen et al., 2006).

1.5.5 Hip

One cell surface protein which acts to negatively regulate hedgehog signalling is the type1 transmembrane glycoprotein Hip (Hedeghog interacting protein), which binds all three mammalian hedgehog genes. The expression of *Hip* maps to regions in which hedgehog genes control development including *Shh* in the ventral neural tube and adjacent sclerotome, *Ihh*, within the prehypertrophic chondrocytes, and *Dhh* in Sertoli cells. Over expression of *Shh*, or activation of the hedgehog pathway via expression of a transgene encoding a dominant-negative form of cyclic AMP-dependent protein kinase A, leads to up regulation of *Ptc* as well as *Hip*. Hip acts to inhibit the hedgehog pathway; the phenotype of mice expressing a *Hip* transgene (*Hiptg*) closely resembles the Indian hedgehog mutant, with a reduction in the zone of undifferentiated chondrocytes and ectopic calcification. Proliferative chondrocytes in these animials show a reduction in *Ptc* expression but not *Ihh*, consistent with the idea that Hip inhibits hedgehog signalling. Hedgehog inhibition is achieved by ligand sequestration whereby Hip interacts with hedgehog directly and retains it at the membrane. (Chuang and McMahon, 1999).

1.5.6 Downstream of ptc and smo

Activation of Smo leads to the up regulation of hedgehog target genes, a process mediated in *Drosophila*, by *cubitus interruptus* (*Ci*). In the absence of Hh, Ci undergoes proteolytic cleavage (Forbes et al., 1993) to form a truncated protein (Ci75), which acts as a transcriptional repressor (AzaBlanc et al., 1997).

In the presence of Hh however, the full length Ci (Ci155) remains un-cleaved and is able to activate Hh responsive genes.

Ci processing is regulated by a number of different proteins which act to sequester and phosphorylate Ci, controlling its activity and translocation to the nucleus (see Hooper and Scott, 2005 for review). A key regulator of Ci processing is the kinesin-related protein Costal-2 (Cos-2). Over expression of Cos-2 promotes Ci cleavage and is sufficient to inhibit hedgehog signal transduction (Wang et al., 2000), whereas loss of Cos-2 leads to Ci155 accumulation although this in itself in not sufficient to activate hedgehog signalling (Wang et al., 2000; Wang and Holmgren, 1999). Cos-2 associates with both Ci (Wang and Jiang, 2004), and Smoothened (Ogden et al., 2003), as well as microtubules (Sisson et al., 1997), and the affinity of Cos-2 for microtubules appears to be controlled by hedgehog, whereby addition of hedgehog results in release of Cos-2 (Robbins et al., 1997). By binding microtubules, Cos-2 provides the scaffold for a complex of proteins which contribute to the processing of Ci, known as Complex I, comprised of four kinases, Protein Kinase A (PKA), casein kinase I (CKI), glycogen synthase kinase-3β (GSK3β), the serine/threonine kinase Fused (Fu) as well as Ci (Zhang et al., 2005). Ci contains several PKA sites suggesting that its cleavage may be facilitated by PKA phosphorylation, and mutation of these sites has been shown to be sufficient to inhibit Ci cleavage (Chen et al., 1998). Similarly loss of PKA function leads to accumulation of full length Ci and subsequent activation of hedgehog target genes in the absence of Hh ligand (Johnson et al., 1995). PKA activity however does not seem to be moderated by hedgehog activity (Jiang and Struhl, 1995), suggesting that PKA activity is only a permissive factor in Ci regulation. Once phosphorylated Ci binds to a component of the scf ubiquitin e3 ligase complex named Supernumerary limbs (Slmb). Slmb acts to facilitate processing of Ci into its repressor form (Jiang and Struhl, 1998), which then translocates to the nucleus to inhibit the transcription of hedgehog target genes. Ci is also regulated by Suppressor of fused (Su(fu)). Su(fu) acts to sequester Ci within the cytoplasm in both its cleaved and full length form, preventing its translocation to the nucleus (Methot and Basler, 2000). In the absence of ligand therefore, hedgehog signalling is repressed,

both actively by the production of a repressor form of Ci, and passively by the retention of unprocessed Ci within the cytoplasm.

Binding of the hedgehog ligand to *ptc* leads to the release of Smo inhibition (as discussed above). Smo is phosphorylated by CKI, PKA and GSK3β, and translocates to the membrane (Apionishev et al., 2005; Jia et al., 2004). CKI, PKA and GSK3β dissociate, and the remaining parts of complex I separate from microtubules (Robbins et al., 1997). Cos-2, Smo and Fu form a complex which allows Fu to undergo autophosphorylation (Zhou and Kalderon, 2011). Subsequent CKI dependent phosphorylation leads to full activation of Fu, which is then able promote Ci-155 stabilisation via the phosphorylation of Cos-2 and, along with CKI, inhibit the action of Su(fu) (Zhou and Kalderon, 2011). Activated Ci(155) translocates to the nucleus and interacts with CREB binding protein (CBP) to activate target gene transcription (Akimaru et al., 1997). A summary of the events during hedgehog signal transduction is shown in Figure 1.2.

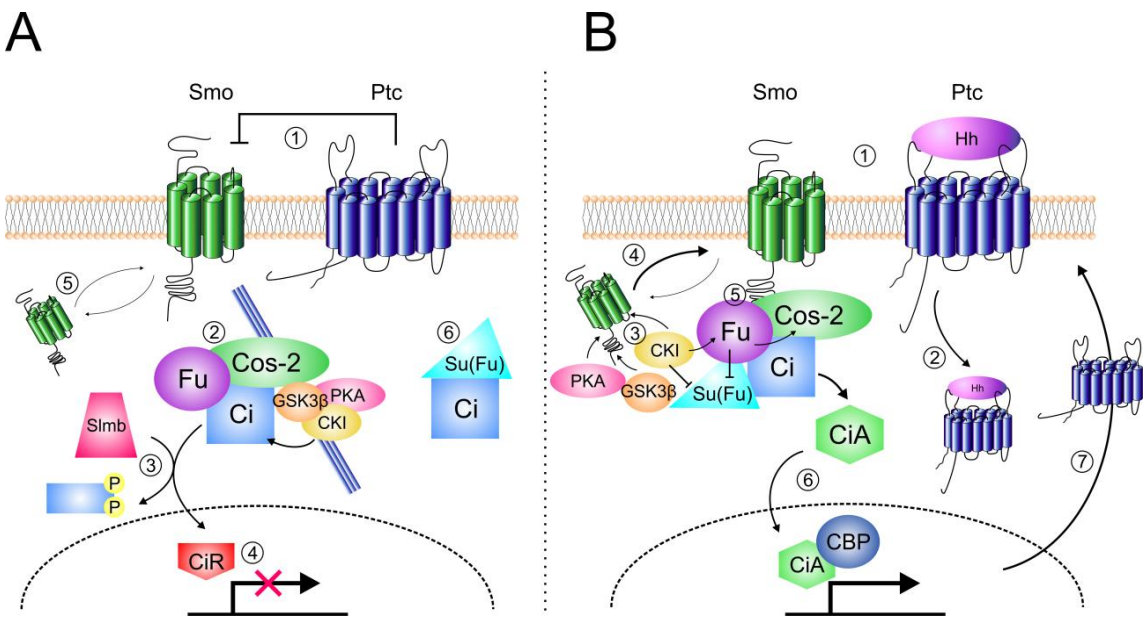

Figure 1.2 Transduction of the hedgehog signalling pathway
(A) (1) In the absence of hedgehog ligand Ptc acts to repress Smo inhibiting downstream signalling. (2) Cos-2 is bound to microtubules and forms a scaffold for complex I, which phosphorlyates Ci. (3) Phosphrylated Ci is released and then bound by Slmb which facilitates Ci cleavage to form a repressor, which then (4) translocates to the nucleus and represses hedgehog target genes. (5) Smo levels at the membrane are low being mostly located within intracellular stores. (6) Full length inactive Ci is sequestered within the cytoplasm by Su(Fu). **(B)** (1) Upon binding of hedgehog, Smo inhibition by Ptc is released. (2) The hedgehog ptc complex is internalised. (3) Smo is phosphorylated by PKA, GSK3β and CK1 leading to its activation. (4) Membrane levels of Smo increase. (5) Cos-2 dissociates from microtubules and binds to activated Smo, along with Fu, which undergoes autophosphorylation, is activated by CKI and promotes stabalisation of Ci by phosphrylation of Cos-2 and inhibiton of Su(Fu). (6) Ci(155) is activated and translocates to the nucles to activate hedgehog target genes. (7) *Ptc* is a target of hedgehog signalling, so upon hedgehog activation, Ptc levels increase leading to pathway inactivation in the absence of additional ligand.
Adapted from (Hooper and Scott, 2005; Ingham and McMahon, 2001)

In vertebrates Ci is replaced by multiple transducing factors, Gli1, 2 and 3 (Altaba, 1998), which are differentially regulated by Shh signalling. Gli1 is transcriptionaly regulated by Shh (Lee et al., 1997), whereas Gli2 and Gli3 are not (Pan et al., 2006), their activity instead being controlled in a similar manner to Ci in *Drosophila* (Dai et al., 1999). In the absence of Shh protein, Gli2 undergoes proteolytic cleavage to form a repressor, and is subsequently targeted for degradation, whereas in the presence of Shh, Gli2 is stabilised to form an activator (Pan et al., 2006). Gli3 likewise contains activation and repression domains and is similarly cleaved to form a repressor of Shh signalling (Dai et al., 1999) Although Gli1 acts exclusively as an activator and is

transcriptionaly up regulated in response to Shh signalling, it is Gli2 that is required for transduction of the Shh pathway (Ding et al., 1998). Mice mutant for Gli2 lack differentiated floor plate cells and show a reduction in HNF3β, a floor plate marker, Shh and Gli1 (Ding et al., 1998).

Following signal transduction, a number of genes are up regulated in response to Hh signalling, one of which is the Hh receptor *ptc* (Goodrich et al., 1996). Up regulation of *ptc* leads to a reduction in Smo levels (Alcedo et al., 2000), providing a mechanism to rapidly inhibit the Hh pathway in the absence of additional ligand. This mechanism has been suggested to allow not only a way of preventing aberrant Hh signalling, but also a readout of positional identity, and an additional way to control the overall level of Hh signalling which a cell receives. Perceived Hh levels can in this way be controlled not only spatially but also temporally, allowing for a greater level of control (Briscoe, 2004; Dessaud et al., 2007).

1.5.7 Role of cilium in vertebrate hedgehog signal transduction

A forward genetic screen by (Huangfu et al., 2003) identified two mutations *wimple* (*wim*) (also known as IFT172) and *flexo* (*fxo*) (a hypomorphic allele of *polaris*) that prevented the specification of a subset of neurons within the ventral neural tube, a role attributed to hedgehog signalling. The mutations however did not map to hedgehog or any of the downstream components of the hedgehog pathway, but instead to two proteins required for intraflagellar transport (IFT). IFT is required for the assembly and maintenance of cilia, microtubule-based cell surface protrusions present on most vertebrate cells (Rosenbaum and Witman, 2002). Similar studies identified other IFT mutants which were deficient in ventral neuronal subtypes (Huangfu and Anderson, 2005). Within the murine limb bud, embryos mutant for the IFT protein polaris show reduced levels of hedgehog target genes despite normal levels of hedgehog expression (Haycraft et al., 2005). Exogenous hedgehog yielded no increase in hedgehog target genes within these mutants suggesting that the role of cilium in vertebrate hedgehog signalling is reception of the hedgehog signal. Loss of function experiments showed that IFT lay downstream of hedgehog signal transduction; while patched mutations give rise to ectopic ventral subtypes, patched IFT double mutants have a phenotype which mimics the IFT single mutation

(Huangfu et al., 2003). Thus while the presence of hedgehog normally leads to the de-repression of smoothened to activate signal transduction, loss of IFT renders this de-repression ineffectual. Interestingly, mutations in IFT proteins do not give the same phenotype as a mutation of just *Shh*. This is because IFT mutants have been implicated in the processing of the downstream effectors of hedgehog signalling, the Glis. As mentioned above, Gli1 and Gli2 act mainly as activators of hedgehog signalling while Gli3 normally acts as a repressor. Gli3 is able to act as an activator but is proteolytically processed to form a transcriptional repressor (Dai et al., 1999). As hedgehog signal transduction switches the balance between the activator and repressor forms of the Glis, loss of Shh alone promotes the repressor form of Gli3 which inhibits hedgehog target genes. Loss of IFT function however affects Gli processing and so does no recapitulate loss of Shh alone. Mouse IFT172 mutants display a reduction in the amount of Gli3 repressor compared with wild type litter mates (Huangfu and Anderson, 2005). Similarly murine cells which lack *polaris* are unable to efficiently convert Gli3 from its full-length activator form, to its cleaved repressor form (Haycraft et al., 2005). These cells were also unable to induce *patched* expression in response to Gli2, suggesting that full Gli2 activity requires IFT (Haycraft et al., 2005). Consequently in the absence of IFT there is no repression or significant activation downstream of hedgehog (May et al., 2005). Therefore while hedgehog levels are not high enough to specify ventral neuronal subtypes following the loss of IFT proteins, some neuronal precursors which rely on low levels of signalling can still be specified (Huangfu et al., 2003).

Cilia act as a site where hedgehog components are enriched. When cultured in Shh-conditioned medium MDCK (Madin–Darby canine kidney) cells display high ciliary levels of Smo (Corbit et al., 2005), while in zebrafish Smo translocates to the cilia in the presence of the hedgehog agonist purmorphamine (Aanstad et al., 2009). Cells cultured with the Smo agonist SAG similarly show Smo translocation into cilia (Rohatgi et al., 2007). When MDCK cells are exposed to the hedgehog antagonist cyclopamine, levels of Smoothened are undetectable within cilia, a response which is also seen in mouse embryos *in vivo* (Corbit et al., 2005). Another report however showed that cyclopamine promoted Smo translocation to the cilia in NIH/3T3 cells (Wang et al., 2009). This result was

confirmed by (Rohatgi et al., 2009), who see a translocation of Smo to cilia in response to cyclopamine treatment in NIH/3T3 cells and mouse embryonic fibroblasts (MEFs).

Smo contains a hydrophobic and basic residue motif within its carboxy terminus, and mutation of this motif renders Smo unable to promote hedgehog signal transduction either *in vitro* or *in vivo* (Corbit et al., 2005). Wild type Smo is able to restore hedgehog signalling in *Smo*$^{-/-}$ cells whereas Smo which contains a point mutation (C151Y) within its extracellular domain (ECD) is unable to do so (Aanstad et al., 2009). Both of these mutations prevent Smo from translocating to cilia in response to either exogenous hedgehog or purmorphamine (Aanstad et al., 2009; Corbit et al., 2005). Chemical inhibition of Shh signal activation with the antagonists SANT-1 and SANT-2 similarly prevents hedgehog induced translocation of Smo to the cilia (Wang et al., 2009). Taken together these data suggest that translocation of Smo is a necessary step for Shh signal transduction in vertebrates.

Smo is not the only hedgehog signal component to be present within cilia; all three Gli family members have been shown to be localised to the distal tip of cilia (Haycraft et al., 2005). Addition of Shh to NIH/3T3 cells leads to the accumulation of Gli2 within cilia and the nucleus which displays a concomitant switch from its cleaved repressor form to its full length activator form (Kim et al., 2009). Addition of hedgehog agonists SAG and purmorphamine, which bind Smo and result in its ciliary translocation as discussed previously, also lead to ciliary and nuclear accumulation of Gli2. Transfection of cells with the constitutively active form of Smo (SmoA1), gives rise to similar effects (Kim et al., 2009). When Smo translocation is blocked by addition of the pharmalogical hedgehog inhibitor SANT-1, Gli2 translocation is similarly blocked. It would appear then that movement of Gli2 into cilia is simply dependent on the movement of Smo. It seems however that Smo needs to be active for Gli2 accumulation. As discussed previously, treatment with cyclopamine, leads to the translocation of Smo into cilia but prevents hedgehog signal transduction. Cyclopamine treatment does not however lead to an increase in ciliary or nuclear Gli2 levels, and the level of the repressor form of Gli2 within the nucleas remains constant, even in the presence of exogenous Shh (Kim et al., 2009).

If retrograde trafficking within the cilium is blocked via mutation of the cytoplasmic dynein 2 heavy chain (Dync2h1), both Smo and Gli2 show accumulation within cilia, even in the absence of Shh suggesting that they constantly cycle in and out of the cilium regardless of whether ligand is present or not (Kim et al., 2009). It has been suggested therefore that Smo activation leads to Gli2 accumulation where some change occurs, either to Gli2 itself, or to the proteins which associate with Gli2, conferring an activated state and subsequent translocation to the nucleus (Kim et al., 2009).

While the presence of cilia is not required for hedgehog signalling in *Drosophila*, it appears that translocation of signalling components to the membrane is a conserved feature. Ectopic expression of *Hh* in *Drosophila* salivary gland cells increases the ratio of membrane localised Smo to internal Smo by 10 fold. Additionally, following expression of *Hh*, Ptc moves away from the plasma membrane and becomes concentrated perinuclearly (Zhu et al., 2003). These data indicate that while hedgehog signalling in *Drosophila* may not require cilia, the shuttling of proteins is a conserved mechanism for signal transduction.

1.5.8 Hedgehog interacts with the extracellular environment

So far I have discussed the specifics of hedgehog signalling and the role which it plays in the development of *Drosophila* and vertebrates. Many of the regions in which hedgehog functions dictate the requirement of hedgehog to act at long range, and it has previously been eluded to that the ability to act at long range is not immediately obvious due to the nature of the hydrophobic properties of the fully processed protein. Hedgehog release, as previously discussed is aided by the protein Dispatched, and following its release, hedgehog interacts with the extracellular matrix in order to facilitate is diffusion. A major component of the extracellular matrix is made up of Heparan sulfate proteoglycans (HSPGs). Hh is able to bind to the side chain of HSPGs (Rubin et al., 2002) and work in *Drosophila* has shown a requirement for HSPG synthesis for correct Hh diffusion (The et al., 1999). Below I will discuss the synthesis of HSPGs and the role they play in developmentally important signalling events. The interaction of Hh with HSPGs will however not be discussed here. Chapter 4 of this work describes the role that HSPG modification has on Shh diffusion in *Xenopus*, and

as such the specifics of the way in which HSPGs affect hedgehog signalling will be discussed in that section.

1.6 Heparan sulphate proteoglycans

1.6.1 Structure

Heparan sulfate proteoglycans (HSPGs) are large molecules distributed ubiquitously, and are found both at the cell surface and within the extracellular matrix (Bernfield et al., 1999; Lamanna et al., 2007). Discovered forty years ago on the surface of Chinese hamster ovary cells (Kraemer et al 1971), these proteoglycans are now known to be a common feature and have been identified as a component of the surface of all animal cells (Bernfield et al., 1999; Bishop et al., 2007). HSPGs are comprised of a core protein covelantly linked to long glycosaminoglycan (GAG) chains via specific serine residues (Turnbull et al., 2001). The GAG chains are made up of a tetrasaccharide linker followed by repeating disaccharide units consisting of glucuronic acid and N-acetyl glucosamine (Lamanna et al., 2006). The GAG chains are modified during their synthesis giving rise to a large extent of heterogeneity along their length, particularly in the degree to which certain regions are sulphated. The specifics of chain synthesis will be discussed in further detail in section 1.6.2.

HSPGS can be present either on the surface of cells, or within the extracellular matrix. Their location is specified by the protein core, which takes three major forms; the syndecans, glypicans and the perlecans. Syndecans are type I transmembrane proteins, and although they mostly have heparan sulphate (HS) chains attached, they may also carry chondroitin sulphate (CS) and dermatan sulphate (DS) chains (Lee et al., 2004; Rapraeger et al., 1985). HS chains are normally located toward the N-terminus, while CS chains are attached closer to the cell surface (Kokenyesi and Bernfield, 1994). The extracellular domain of the syndecans is particularly long, meaning that HS chains attached close to the N-terminus can reside far from the surface of the cell (Bernfield et al., 1992). In vertebrates there are four members of the syndecan family. The accepted nomenclature for these is Syndecan 1-4 although they have been previously known by different names: fibroglycan (syndecan-2), N-syndecan (syndecan-3) and amphiglycan (syndecan-4) (Bernfield et al., 1992). Syndecan homologues

have also been identified in both *Drosophila and C. elegans (Carey, 1997; Spring et al., 1994).*

Glypicans do not contain a transmembrane domain but are instead tethered to the plasma membrane by a glycosylphosphatidylinositol (GPI) link (Lin, 2004). As with the syndecans, vertebrates have multiple members of the glypican family, also prescribing to the accepted nomenclature glypican 1-6 (previously cerebroglycan (glypican-2), OCI-5 (glypican-3) and K-glypican (glypican-4)). Glypicans exclusively carry HS chains which, in contrast to their distal location when linked to syndecans, are in close proximity with the plasma membrane, due to the relatively short glypican extracellular domain (David, 1993). *Drosophila* has two known glypicans; *division abnormally delayed* (*Dally*) (Nakato et al., 1995), which is most similar in sequence to glypicans 3 and 5, and *dally-like protein* (*dlp*), which is most similar to glypicans 4 and 6 (Khare and Baumgartner, 2000). *Dally* mutants display cell cycle progression defects, from which the name derives, as well as morphological defects in the eye, antenna, wing and genitalia (Nakato et al., 1995). The zebrafish gene knypek encodes a zebrafish homolog of glypican-4 (LeClair et al., 2009; Topczewski et al., 2001). Knypek mutants exhibit aberrant convergent extension movements, cyclopia and craniofacial skeletal defects (LeClair et al., 2009; Marlow et al., 1998; Solnica-Krezel et al., 1996; Topczewski et al., 2001).

One characteristic that sets glypicans and syndecans apart is the fact the glypicans can be released into the extracellular matrix. The GPI link which tethers glypicans to the cell surface can be cleaved by the enzyme *notum*, an α/β-hydrolase which is secreted from cells and is able to act non cell-autonomously (Giraldez et al., 2002; Traister et al., 2007). *Drosophila notum* mutants display a variation of phenotypes ranging from duplication of the wing pouch to an almost complete loss of the thorax (Giraldez et al., 2002).

The third class of HSPGs is made up by the agrins the perlecans, and collagen XVIII, which are not bound to the membrane but secreted into the extracellular matrix. The core protein of perlecan is very large (~400KDa) (Noonan et al., 1991) and shows widespread expression, although it is found predominantly in connective tissues where it is generally localised to the basement membrane

(Murdoch et al., 1994). Perlecan (Hspg2) null mice exhibit defective endochondral ossification and disorganized collagen fibrils within the cartilage matrix (Arikawa-Hirasawa et al., 1999). Mutation of the *C. elegans* homolog of perlecan (unc-52) leads to irregular skeletal muscle formation (Rogalski et al., 1993), while the *Drosophila* perlecan *terribly reduced optic lobes* (*trol*) affects neuroblast proliferation, and a complete null of this locus leads to lethality (Voigt et al., 2002). Perlecan is also implicated as having a role in accelerating Alzheimer's disease. Perlecan binds directly to the β-amyloid peptide accelerating the rate of Aβ fibril formation *in vitro* (Castillo et al., 1997).

Agrin was first identified in the electric organ of the Pacific electric ray *Torpedo californica* named for its ability to induce the aggregation of acetylcholine receptors (Nitkin et al., 1987). Agrin is also a large protein (~200KDa) and displays a similar C-terminal domain structure to perlecan (Rupp et al., 1991). A missense mutation in agrin leads to congenital myasthenic syndrome, characterised by disorganisation of the neuromuscular junction (Huze et al., 2009). The spatial and temporal expression of agrin within the central and peripheral nervous system suggests that it has a role in the development of axonal pathways (Halfter et al., 1997; Tsen et al., 1995).

Whereas most collagens which are associated with glycosaminoglycan chains display attachement of chondroitin sulphate, Collagen XVIII is a heparan sulphate proteoglycan (Halfter et al., 1998). Collagen XVIII shows a molecular mass of 300KDa which is reduced to 180KDa following heparitinase treatment (Halfter et al., 1998). Abundant expression of collagen XVIII can be seen in the basal lamina of numerous tissues. Mutations in the COL18A1 gene lead to Knobloch syndrome (Sertie et al., 2000), characterised by vitreoretinal degeneration with retinal detachment and neural tube closure defects (for review on human phenotype see Passos-Bueno et al., 2006). An overview of the overall structure of the three main HSPGs is shown in Figure 1.3.

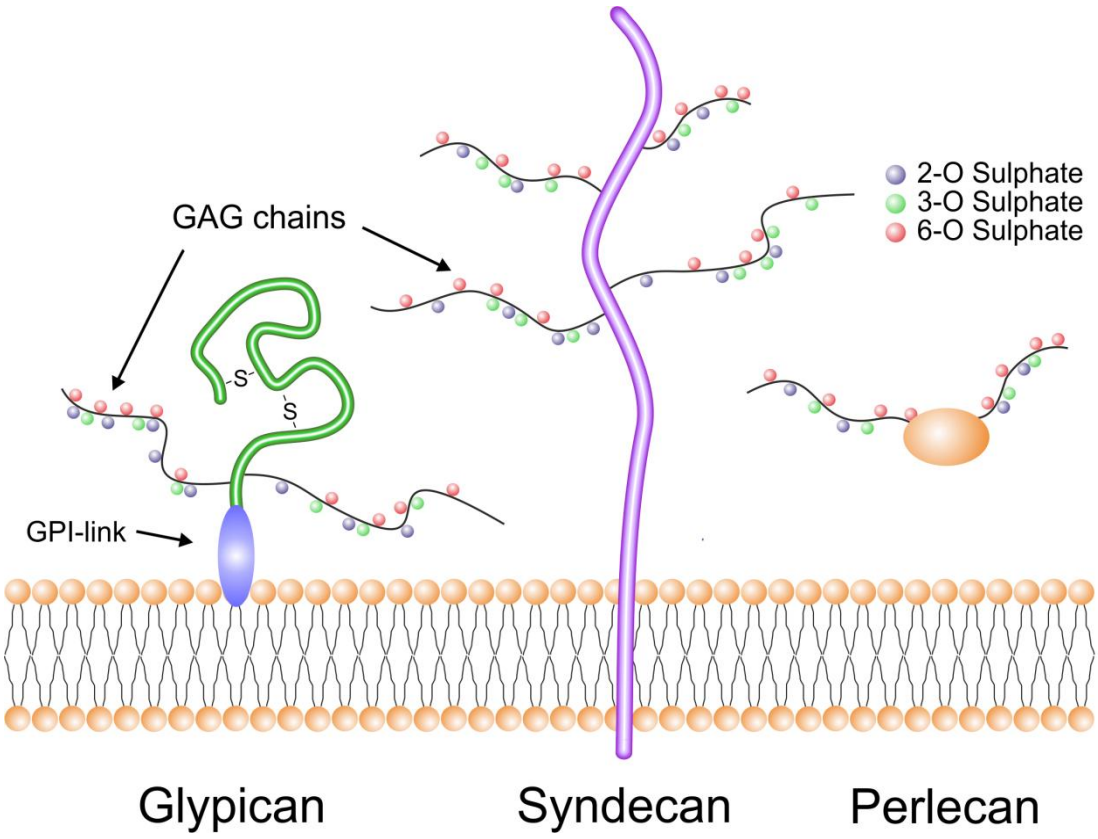

Figure 1.3 Structure of HSPGs
HSPGs take three major forms, and are attached to the cells surface via a GPI link (Glypicans), are transmembrane proteins (syndecans) or are secreted into the ECM (perlecans). The GAG chains which are attached to the core proteins by a tetrasaccharide linker are modified during synthesis and contain regions of both high and low sulphation.
Diagram adapted from (Hacker et al., 2005)

1.6.2 Synthesis

During their synthesis, HSPGs undergo a number of different modifications which give rise to a massive amount of structural heterogeneity. Synthesis of the GAG chain is initiated on a GAG-protein linkage region, (GlcAb1–3Galb1–3Galb1–4Xylb1-*O*-Ser), by the action of the 1,4-N-acetylhexosaminyltransferase *Extosin-like2* (*EXTL2*), which transfers N-acetylglucosamine (GlcNAc) to the tetrasaccharide linker (Kitagawa et al., 1999). A closely related gene EXTL3 is also able to initiate this reaction (Kim et al., 2001). Chondroitin sulphate chains are attached via the same linker region, and their elongation is initiated by the attachment of N-acetylgalactosamine (GalNAc) (Kitagawa et al., 1999). As EXTL2 also functions to add N-acetylgalactosamine to the extending chain, it is an important factor in the determination of the type of GAG chain which is attached to the core protein (Kitagawa et al., 1999).

The GAG chain is elongated via the attachment of monosaccharide units of GlcNAc and GlcA from UDP-sugars. *Sugarless* (*sgl*) sgl encodes a homolog of bovine UDP glucose dehydrogenase (Häcker et al., 1997), which catalyzes the conversion of UDP-D-glucose to UDP-D-glucuronic acid. This gene was first characterised by Binari et al 1997 and Haerry et al 1997, who gave the gene the name *kiwi* and *suppenkasper* (*ska*) respectively. As UDP- glucuronic acid provides an essential substrate for the biosynthesis of glucosaminoglycan chains (Lin et al., 1999), loss of *sgl* leads to defective glycosaminoglycan synthesis.

Chain elongation is regulated by the Exostosin genes (EXT1 and EXT2). Mutation of these genes leads to hereditary multiple exostoses (HME) (Lind et al., 1998), characterised by the development of nodules at the end of the bones. Patients with HME also have a higher propensity to form tumors of the bone (chondrosarcomas and osteosarcomas), suggesting a tumor-supressor role of EXT1 and EXT2 (Ahn et al., 1995; Stickens et al., 1996). These genes represent co-polymerases and successively add alternate N-acetylglucosamine (GlcNAc) and glucuronic acid (GlcA) residues to the developing HS chain (Lind et al., 1998). Mice which lack EXT1 are unable to synthesise heparan sulphate and display aberrant contralateral projection of retinal ganglion cells, as well as more general defects to overall brain morphology (Inatani et al., 2003).The *Drosophila* homologues of EXT1 and EXT2 are encoded by the *tout-velu* (*ttv*) and *sister of tout-velu* (*sotv*) genes respectively (Bellaiche et al., 1998; Bornemann et al., 2004). Loss of ttv or sotv gives rise to segment polarity defects (Bornemann et al., 2004; Han et al., 2004; The et al., 1999) revealing a developmentally important role for these genes.

Extosin-like-3 (EXTL3), which as previously mentioned is able to initiate chain elongation, also harbours N-acetylglucosaminyltransferase II activity and can attach GlcNac to the extending HS chain (Kim et al., 2001). EXTL3 is however not able to attach GlcA to oligosaccharides with non-reducing terminal GlcNAc residues showing that unlike EXT1 and EXT2, EXTL3 is not a co-polymerase (Kim et al., 2002). The *Drosophila* homologue of EXTL3 is *brother of tout-velu* (*botv*) (Han et al., 2004). *Botv* mutants display a loss of engrailed expression

within the ectoderm of stage 11 *Drosophila* embryos, indicating that, similar to *ttv* and *sotv*, *botv* is a segment polarity gene (Han et al., 2004).

Following elongation, glucosamine residues are N-deacetylated and N-sulfated *by* N-deacetylase/N-sulfotransferase (Figure 1.4 1-1A), which is coded for in *Drosophila* by *Sulfateless* (*sfl*) (Lin and Perrimon, 1999). Within a chain, only 40-50% of the residues are N-sulfated in this way, and are usually grouped, creating highly sulfated regions of GlcA and GlcNS repeats, which have been termed S-domains (Maccarana et al., 1996). Within these domains GlcA is converted to iduronic acid (IdoA) via epimerisation by C5 epimerase (Figure 1.4 2-2A), which requires the adjacent glucosamine residue toward the non-reducing end to be *N*-sulfated (Hagner-McWhirter et al., 2004; Hook et al., 1974). Subsequentlly, sulfotransferases (2-O, 3-O and 6-O) add sulphate groups to GlcNS and IdoA at the C2,C3 and C6 positions respectively (Figure 1.4 3-5). As with N-sulfation and subsequent epimerisation, sulfation at these sites is not uniform along the whole length of the chain. This variability in the sulfation and structural state of residues along the length of the chain allows for binding of a massive range of proteins. A summary of the biosynthetic pathway described above is shown in Figure 1.5.

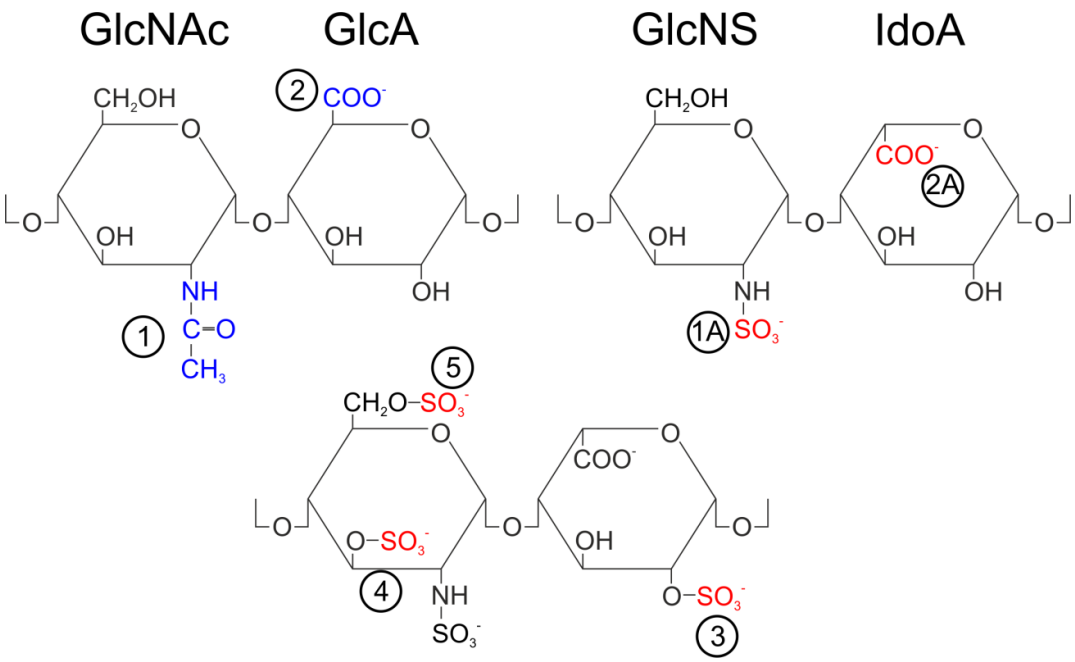

Figure 1.4 N-deacetylation/N-sulfation and epimerisation of GcNAc/GlcA disaccharide
N-acetylglucosamine (GlcNAc) is N-deacetylated and N-Sulfated by N-deacetylase/N-sulfotransferase to give N-sulfoglucosamine(GlcNS) (1-1A). Subsequently glucuronic acid (GlcA) is epimerised by C5 epimerase to form Iduronic acid (IdoA). (2-2A). Sulfotransferases then add sulphate groups to C2 (3), C3 (4) and C6 (5) positions.

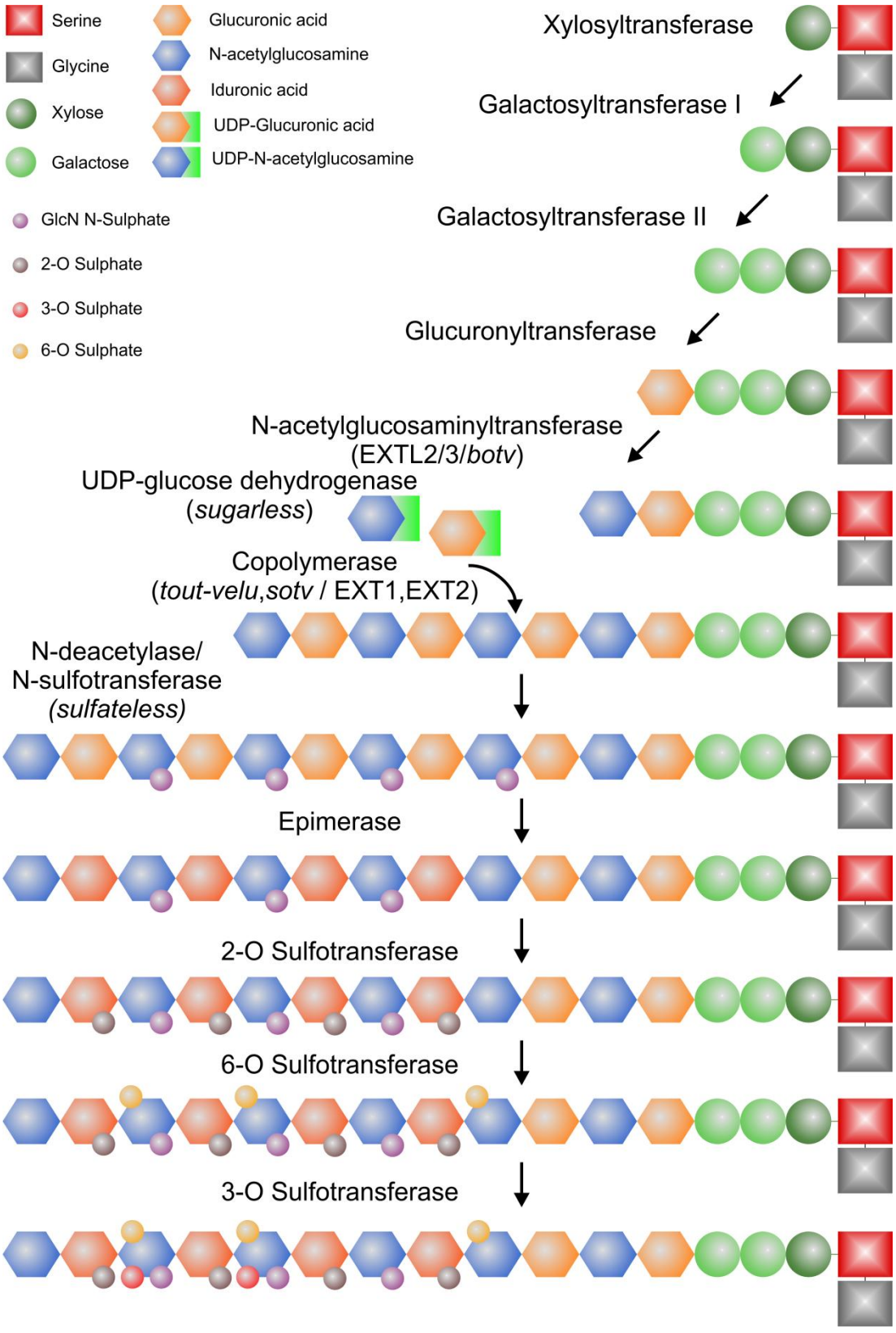

Figure 1.5 HSPG biosynthesis

Attachment of a tetrasaccharide linker by the sequential addition of sugar residues is followed by the addition of a disaccharide by two specific enzymes. Further attachment of the disaccharide by a co-polymerase leads to extension of the sugar chain which undergoes sulfation and epimerisation to give rise to the fully modified HSPG. Modifications are specific but not uniformly added resulting in a large degree of heterogeneity.

Adapted from (Esko and Selleck, 2002; Hacker et al., 2005)

1.6.3 Loss of HSPGs impacts on developmental signalling processes.

Mutation to either HSPGs themselves or genes required for their synthesis leads to developmental defects as described above. Many of the defects described are reminiscent of aberrant developmental signalling suggesting that HSPGs are a key regulator for a variety of different signalling pathways during development.

Treatment of Swiss 3T3 fibroblasts with heparitinase to degrade heparan sulphate reduced binding of bFGF to HS by 80% (Rapraeger et al., 1991). This reduction of binding to HS is mirrored by a reduction in the ability of bFGF to bind to its receptor by a similar degree (Rapraeger et al., 1991). Similarly mutant Chinese hamster ovary cells (CHO-803), which lack about 95% of the HSPGs found in wild-type CHO cells, are unable to bind bFGF. Binding can however be restored following the addition of exogenous heparin or heparan sulphate (Yayon et al., 1991).

Ectodermal explants from *Xenopus* (referred to commonly as animal caps) provide a useful tool to display changes to signalling pathways. If cultured in isolation, cells from this region differentiate to form ectoderm, however they can be easily promoted to differentiate and form tissues from other germ layers in response to certain signals. When treated with activin, FGF or Wnt, cells undergo convergent extension and mesodermal differentiation. If treated with heparinise however, animal caps are no longer able to undergo changes in response to these signals (Itoh and Sokol, 1994), suggesting that HSPGs are required for signal transduction.

Perhaps the most revealing studies about the role of HSPGs during developmental signalling however have come from *Drosophila* mutants. Mutation of all of the HSPG synthesis genes described above (*sfl*,*sgl*,*ttv*,*sotv*,*botv*), as well as mutants for HSPGs themselves (*dally* and *dlp*) result in defects within a number of signalling pathways including wg, hh, dpp, and FGF (Bornemann et al., 2004; Häcker et al., 1997; Han et al., 2004; Lin et al., 1999; Lin and Perrimon, 1999; Wu et al., 2010). These studies reveal that HSPGs are not only required for the transduction of the signal but in some cases such as Wnt/Wg signalling, are responsible for controlling the movement

of the ligand from its source to target cells. This apparent wide range of activities in regulating the distribution and transduction of developmentally important signalling molecules is vastly different from the originally suggested passive role of HSPGs during development.

1.6.4 Additions to HSPGs are critical for their function

As discussed above, the loss of HSPGs impacts on developmentally important signalling events. However it is not only HSPGs as a whole that are required for correct signalling, but the modifications that are made to the HS chain during its synthesis. The addition of sulphate groups to the disaccharide backbone is not only critical for the formation of the basic structure, as in the case of *sfl*, but for the correct functioning of the molecule. Mutants that lack the ability to add sulphate groups display defects in a number of signalling processes that are critical for proper development.

Mice with a null mutation in the *N-deacetylase/N-sulfotransferase1* (NDST1) gene, which is the homologue of *Drosophila* sfl (Lin and Perrimon, 1999), show incorrect lung morphogenesis and suffer from severe respiratory distress (Fan et al., 2000). Mice lacking heparin sulphate *2-O-sulfotransferase-1* (HS2ST) display aberrant kindney, eye and skeletal development (Bullock et al., 1998), while in chick, inhibition of HS2ST with siRNA leads to truncation of the developing limb bud and inhibition of FGF8 expression within the apical ectodermal ridge (AER) (Kobayashi et al., 2007).

Mice homozygous for a null mutation in Hs2st display a 40% reduction in the proliferation of cortical precursors as revealed by BrdU incorporation, although the migration of these cells as they differentiated was unaffected (McLaughlin et al., 2003). Retinal ganglion cells in *Hs2st*$^{-/-}$ mice do however show erratic path formation as they grow towards the optic chiasm, resulting in growth outside of the normal chiasm territory (Pratt et al., 2006), demonstrating that Hs2st participates differentially within distinct cell populations.

Another enzyme within the HSPG biosynthetic pathway, heparan sulfate 6-O-sulfotransferase (HS6ST), which specifically transfers sulfate residues to position 6 of N-sulfoglucosamine, has also been shown to affect neuronal

development. Retinal ganglion cells in *Hs6st*$^{-/-}$ mice exhibit increased growth into the contralateral optic nerve compared with controls, rather than aberrant growth outside of the normal chiasm terriotory as seen in *Hs2st*$^{-/-}$ mice (Pratt et al., 2006). As seen for HS2ST, inhibition of HS6ST with siRNA leads to truncation of the developing limb bud in chick (Kobayashi et al., 2010). HS6ST also has a role in the regulation of guidance cues in *Drosophila*, where inhibition of HS6ST function with RNAi, leads to the disruption of tracheal branching (Kamimura et al., 2001). Loss of *Hs6st* expression can also impact on the determination of cell fate within the developing embryo. In zebrafish, Hs6st morphants display high levels of MyoD expression within the somites which is maintained for longer than in control embryos (Bink et al 2003). Analysis of muscle architecture via DIC microscopy and Bodipy-ceramide staining revealed abnormal muscle fibre structure and the presence of undifferentiated cells, demonstrating a requirement of Hs6st for correct muscle differentiation (Bink et al 2003). Additionally, targeted inhibition of Hs6st in zebrafish gives rise to a reduction in white matter (nerve tracts), and to a lesser extent grey matter (somata) (Bink et al 2003), indicating that, similar to 2-O sulfotransferase, 6-O sulfotransferase is involved in the regulation of cell proliferation as well as migration, outgrowth and differentiation.

1.6.5 HSPG sulfation is required for developmental signalling pathways

Defects following the loss of HSPGs are mainly due to the inability to regulate specific signalling pathways. Developmental problems in sulphation mutants are similarly due to a loss in the regulation of developmental signalling. As discussed above, treatment of Swiss 3T3 fibroblasts with heparitinase reduces binding of bFGF to HS (Rapraeger et al., 1991). Removal of the whole HS chain however is not necessary to obtain this result; treatment with sodium chlorate to block sulfation reduces binding of bFGF to HS by the same degree, and similarly leads to a reduction in the capacity of bFGF to bind to its receptor (Rapraeger et al., 1991). The inability of mutant Chinese hamster ovary cells to bind bFGF can be restored by addition of highly sulphated heparan sulphate, but not under-sulphated heparan sulphate (Yayon et al., 1991). Inhibition of sulfation by sodium chlorate treatment gives rise to downstream effects in MM14 skeletal muscle cells, whereby they exit from the cell cycle and

differentiate to form myotubes (Rapraeger et al., 1991), a result consistent with the removal of FGF (Clegg et al., 1987).

Additional studies showed that binding of FGF requires distinct sulphate groups on specific sugar residues and that binding of FGF can be inhibited to different extents when sulphate groups are removed individually (Loo and Salmivirta, 2002). N- as well as 2-O and 6-O desulphated heparin shows a large reduction in the ability to bind FGF8b, suggesting that the tri-sulphated iduronic acid-N-sulpho-glucosamine disaccharides are important for interaction with FGF8b (Loo and Salmivirta, 2002). Tri-sulphated disaccharides are however not required to bind all FGFs. While N and 2-O sulphation are required for FGF2 binding to heparin, 6-O sulphation is not (Lundin et al., 2000). 6-O sulphation is however required for stimulation of FGFR-1 and Erk2 kinases by FGF2 (Lundin et al., 2000), demonstrating that specific sulphate groups are differentially required for binding of different ligands.

FGF signalling is not the only pathway to require HSPG sulphation. The *Drosophila* cell line S2 expresses the secreted glycoprotein *wingless* (*wg*), which can be detected bound to the cell surface. Bound *wg* can be removed from these cells by addition of heparan sulphate, while treatment of cells with chlorate, which removes sulphate groups, inhibits the response to wingless signalling (Reichsman et al., 1996). Treatment of embryonic stem cells with chlorate similarly leads to a reduction in the level of *wg* signalling as well as other signalling pathways. Following chlorate treatment a reduction can be seen in the level of nuclear β-catenin, phosphrylated Smad1 and di-phosphorylated ERK1/2 (Sasaki et al., 2010), indicating a reduction in the level of Wnt, BMP and FGF signalling respectively.

1.7 Post-synthetic modification of HSPG structure; the Sulfs

All of the enzymes discussed above act within the HS synthetic pathway, modifying the protein and GAG chains before they are exported to the cell surface. Although these enzymes create massive diversity within the HS structure, the complexity of HS can be increased subsequent to export, by enzymes which act at the cell surface. These enzymes can be controlled in a

cell specific and temporal manner to modulate an already heterogeneous population of HS chains.

1.7.1 Sulf1

Sulf1 is a heparan sulphate-specific 6-O-endosulfatase which acts at the cell surface to modify HS chains. Sulf1 contains four distinct domains, an N-terminal signal peptide, a catalytic domain, a hydrophilic domain and a C-terminal domain (Dhoot et al., 2001). The catalytic domain of Sulf1 is homologous to that of the lysosomal *N*-acetyl glucosamine exo-sulfatase Glucosamine-6-Sulphatase (G6S), which hydrolyses the terminal 6-O-sulfate groups of HS chains during their degradation (Robertson et al., 1992). Sulf1 is however not an exosulfatase but an endosulfatase with substrate specificity for a subset of trisulfated disaccharide residues within the HS chains (Ai et al., 2006; Morimoto-Tomita et al., 2002) (Figure 1.6). The catalytic domain of Sulf1 shows a high degree of conservation between species (Figure 1.7). Within its catalytic domain XtSulf1 has a conserved cystein residue at position 86 (Figure 1.7), which is post-translationally modified to *N*-formylglycine. This change is unique to sulfatases, happens within the active site and is essential for activity (Knaust et al., 1998). Although the catalytic site is homologous to Glucosamine-6-Sulphatase, through the action of the signal peptide and the hydrophilic domain, Sulf1 does not act within the degradation pathway but instead at the cell surface (Ai et al., 2006; Dhoot et al., 2001; Morimoto-Tomita et al., 2002).

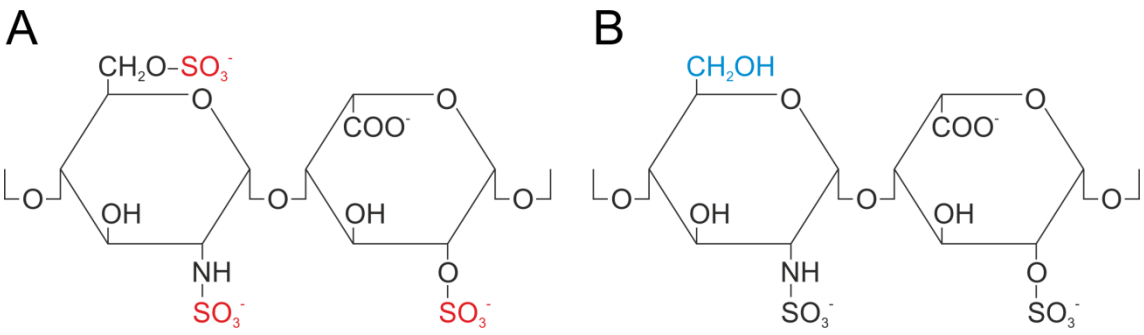

Figure 1.6 A trisulphated disaccharide provides the substrate for Sulf1
(A) The trisulphated form of the gucosamine/Iduronic acid disaccharide (IdoA2S-GlcNS6S) provides the substrate for Sulf1(sulphate groups at the 2-O, N and 6-O positions shown in red). (B) Sulf1 acts to specifically remove the sulphate group at the 6-O position (desulphated form shown in blue) and does not remove sulphate from any other position.

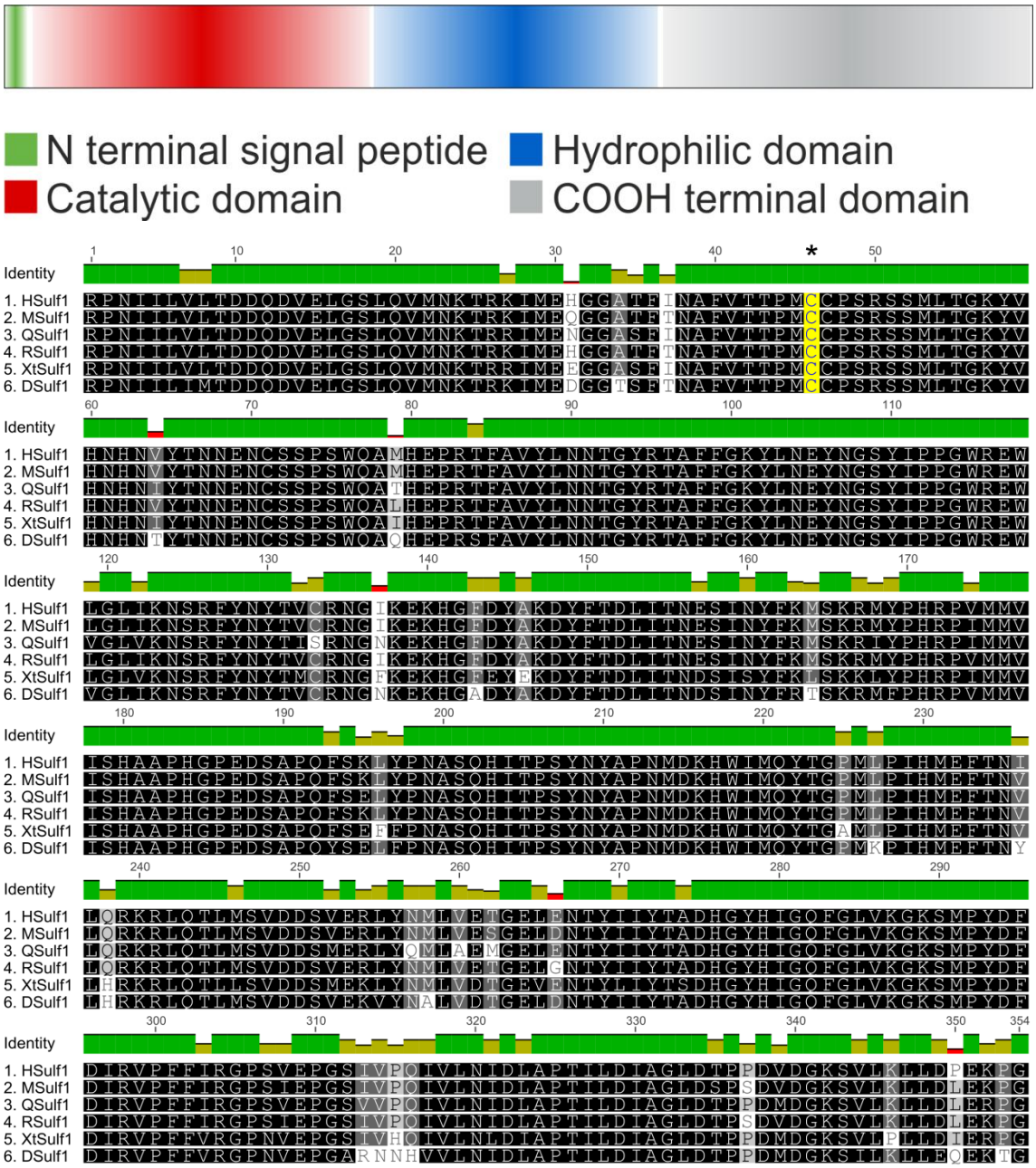

Figure 1.7 Sulf1 displays four distinct domains including a highly conserved catalytic domain **Top:** Sulf1 contains four distinct domains which are laid out as shown. **Bottom:** Sulf1 shows a high degree of conservation within its catalytic domain; Zebrafish displays the greatest amount of deviation from the consensus sequence.

The conserved cysteine residue which undergoes post-translational modification is shown in yellow. Universally conserved residues are shown in black and overlayed with green while highly variable residues are shown in white and overlayed in red. Partially conserved residues are shown in varying shades of grey and overlayed with yellow. Alignment performed using Geneious Basic.

1.7.2 Sulf2

A second member of this family named Sulf2 has also been identified. Like Sulf1, Sulf2 is an HS-specific 6-O-endosulfatase and has the same substrate specificity as Sulf1 (Ai et al., 2006; Morimoto-Tomita et al., 2002). While only having approximately 60% identity with Sulf1 overall, Sulf2 shows a greater than 80% identity with Sulf1 within its catalytic domain (Figure 1.8). Most of the differences observed between Sulf1 and Sulf2 are however variable within Sulf1 of different species, and when this variation is taken into account, Sulf1 and Sulf2 only show a 7% disparity within the sequences of their catalytic domains (Figure 1.8).

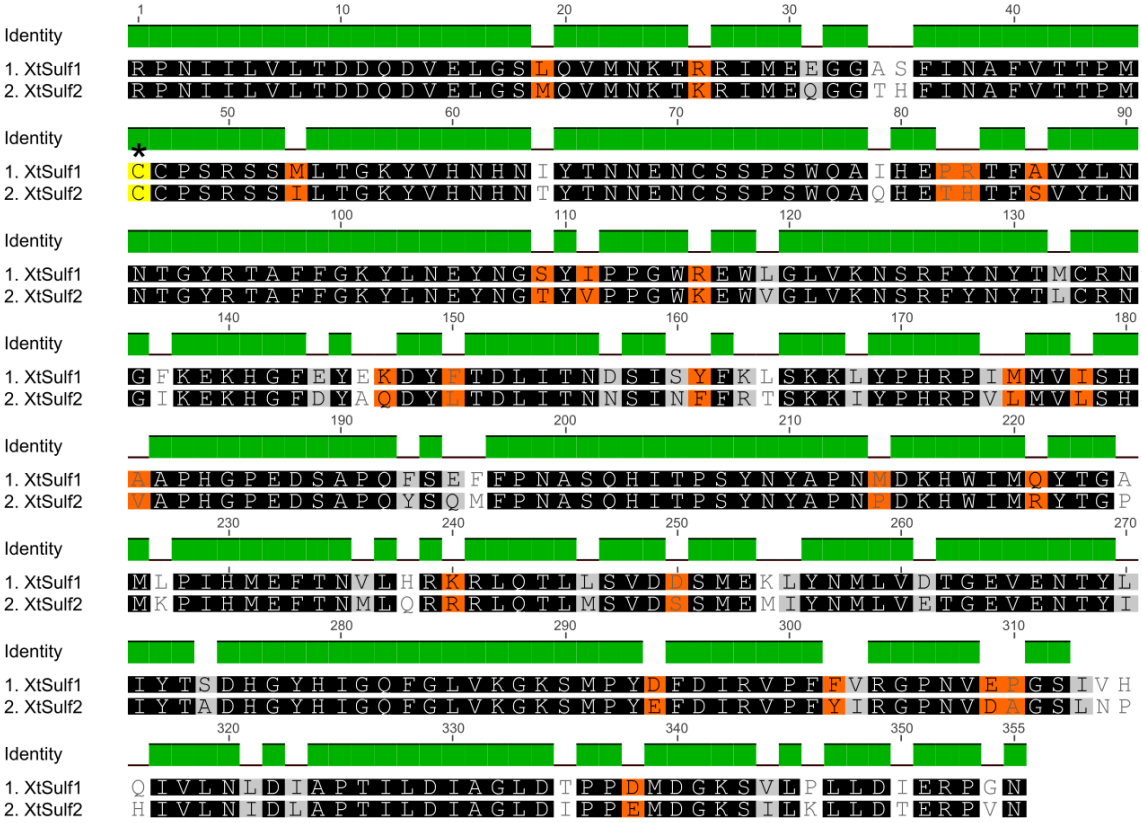

Figure 1.8 The catalytic domains of Sufl1 and Sulf2 are highly conserved
The catalytic domain of Sulf2, displays a high degree of conservation with that of Sulf1. A significant proportion of the differences seen between Sulf1 and Sulf2 are represented by residues which show variability within Sulf1 from different species.
The conserved cysteine residue which undergoes post-translational modification is shown in yellow. Residues which differ between Sulf1 and Sulf2 but are conserved in Sulf1 between species are shown in orange. Residues which differ between Sulf1 and Sulf2, but show a high amount of variability in Sulf1 are shown in grey. Alignment performed using Geneious Basic.

1.7.3 Sulf effects on signalling pathways

HSPG-ligand interactions play an important role in many different signalling pathways, including FGF signalling (Pye et al., 2000), Wnt signalling (Ai et al., 2003b) and BMP signalling (Paine-Saunders et al., 2002). Many of these interactions have been shown to require sulphate groups, suggesting that Sulf1 may have a role in modulating cell signalling.

A role for Sulf1 within a signalling context was first eluded to in quail, where knockdown of QSulf1 was shown to inhibit activation of the muscle specific transcription factor MyoD (Dhoot et al., 2001). As *MyoD* is induced by Wnt signalling (Cossu and Borello, 1999), the authors suggested that inhibition of *MyoD* induction following Sulf knockdown is a result of an effect on Wnt signalling. In agreement with this idea, chlorate treatment of C2C12 cells reduced the activation of a Wnt inducible luciferase reporter compared with controls (Dhoot et al., 2001). Further work showed that HSPGs interact with the wnt ligand with high affinity when sulfated, preventing interaction with the frizzled receptor (Ai et al., 2006). Removal of 6-O sulfate groups by Sulf1 lead to dissociation of the wnt ligand from HSPGs allowing the formation of a ligand-receptor complex (Ai et al., 2003b). In addition, Wg signalling has been shown to up regulate Sulf1 expression at the DV border of the *Drosophila* wing disc, where it acts to reduce extracellular levels and facilitate the lateral diffusion of the Wg protein (Kleinschmit et al., 2010; You et al., 2011).

During FGF signalling, sulfated HSPGs are required for the formation of ligand receptor complexes (Pye et al., 2000). Over expression of Qsulf-1 in *Xenopus* ectodermal explants inhibits the phosphorylation of ERK, the downstream effector of FGF signalling, as well as expression of the FGF-inducible mesodermal marker *xbra* (Wang et al., 2004). Over expression of a constitutively active FGF receptor however is able to abrogate these effects suggesting that Sulf1 acts at the level of the ligand receptor interaction (Wang et al., 2004).

Sulf1 has also been shown to have a role in regulating BMP signalling. Sulf1 is able to extend the range of the BMP antagonist noggin, by reducing its binding affinity for HSPGs via specific sulfate removal (Viviano et al., 2004). In *Xenopus*

ectodermal explants, Sulf1 is able to inhibit phosphorylation of SMAD1, which is phosphorylated in response to activated BMP (Freeman et al., 2008). Using GST and HA fusions of the BMP receptor and BMP4 it was shown that Sulf1 directly inhibits the interaction between the BMP ligand and its receptor (Freeman et al., 2008).

1.7.4 The role of Sulf during development

As Sulf activity is able to impact on so many different signalling pathways it would be expected that it plays a crucial role during development and that in its absence, aberrant developmental signalling would lead to major morphological defects. When Sulf1 or Sulf2 are knocked out independently however, mice appear normal, are viable and display no long term defects (Holst et al., 2007). $Sulf1^{-/-}$,$Sulf2^{-/-}$ mice display no major morphological defects; these mice are however generally perinatally lethal (Holst et al., 2007). Mice which do survive to adulthood are generally smaller than their wildtype littermates and display subtle defects in bone and kidney development. Another study in the same year reported a similar growth defect and showed that the Sulfs are essential for the transmission and reception of GDNF signals from muscle to innervating neurons (Ai et al., 2007).

Disruption of Sulf1 has been shown to effect the development of certain tissues in other organisms. (Dhoot et al.) (2001) showed that knockdown of Sulf1 results in the inhibition of *MyoD* induction, a crucial regulator of muscle development. Knockdown of Sulf1 in *Xenopus*, has similarly been shown to affect *MyoD* expression and morphant exbryos exhibit a lack of segmented paraxial mesoderm (Freeman et al., 2008). More recently, work in *Xenopus* has shown a crucial role for Sulf1 and Sulf2 during the migration of cranial neural crest (Guiral et al., 2010). Sulf2 over expression results in abnormal expression of cranial neural markers (Guiral et al., 2010). Additionally, knockdown of both Sulf1 and Sulf2 results in aberrant marker expression as well as a reduction in the ability of crest cells to migrate in a directional manner. Grafting experiments showed that Sulf1 expression was not only important the migrating cells but also in the cells through which the crest cells migrate (Guiral et al., 2010).

1.7.5 Sulf and cancer

Sulf1 is down regulated a number of cancer cell lines including breast, pancreatic, and hepatocellular carcinoma (Lai et al., 2003). Loss of HSulf-1 in head and neck squamous cell carcinoma cell lines potentiates both FGF mediated MAP kinase signalling, and hepatocyte growth factor mediated MAP kinase and Akt signalling (Lai et al., 2004a). Furthermore HSulf-1 expressing clones show a reduced ability to invade basement membrane and an increased propensity to undergo apoptosis in response to the broad-spectrum kinase inhibitor straurosporine (Lai et al., 2004a). HSulf1 was also shown to inhibit growth and promote apoptosis in HCC lines (Lai et al., 2004b). *In vivo* xenograft models also identify a role for Sulf1 and Sulf2 in tumorigenesis. Human breast cancer cell lines MDA-MB-231 stabally transfected with either Sulf1, Sulf2 or both together, were injected subcutaneously in to mice (Peterson et al., 2010). While tumor xenografts expressing either Sulf1 or Sulf2 alone showed partial regression, those expressing both together exhibited complete regression (Peterson et al., 2010). Similar results assessing the effects of cells from a human myeloma cell line tranfected with Sulf1 or Sulf2 were reported by (Dai et al., 2005). Using another breast cancer cell line, MDA-MB-468, which lacks endogenous HSulf1, (Narita et al., 2006) showed that expression of Hsulf1 results in decreased proliferation. Furthermore tumours in mice injected with cells from HSulf1expressing MDA-MB-468 clonal lines, display a significant reduction in volume compared with the vector transfected clones. After 27 weeks the tumours derived from Sulf expressing clones showed a 5-fold reduction in size, compared with vector-derived xenografts. Together with a reduction in size, the authors report more than 60% reduction in blood vessel growth in xenografts expressing HSulf1 derived from both the MDA-MB-468 myeloma clonal lines and also from SKOV3 ovarian cancer cells, when compared with xenografts derived from cells transfected with empty vector (Narita et al., 2006). Combined these results suggest that down regulation of both Sulf1 and Sulf2 aids proliferation, angiogenesis, avoidance of stress induced apoptosis and the metastatic ability cancerous cells. Over expression of Sulf1 therefore seems like it may provide a good candidate as a cancer therapeutic. However an increase in Sulf expression has recently been reported to be associated with a poor prognosis in lung adenocarcinoma (Bret et al.,

2011). Furthermore, in renal carcinoma and myeloid leukaemia Sulf levels were raised compared with normal tissues (Bret et al., 2011). Sulf1 was additionally identified as a biomarker for gastric cancer (Junnila et al., 2010), while Sulf2 has been shown to promote human lung carcinogenesis (Lemjabbar-Alaoui et al., 2010). It seems therefore that aberrant Sulf expression, be it high or low, can promote tumorigenesis.

1.8 Aims of this study

During the development of the vertebrate nervous system, the establishment of a gradient of Sonic hedgehog is crucial for the correct dorsoventral patterning of the neural tube. However, being hydrophobic in nature, the Shh ligand does not have the properties associated with a freely diffusible molecule. Studies in *Drosophila* have established a role for heparan sulphate proteoglycans during hedgehog signalling, indicating that the hedgehog ligand interacts with the extracellular environment. Additionally, work in chick and *Drosophila* has shown that modification of HSPGs by the endosulfatase Sulf1, can change the way in which the hedgehog protein both moves and signals. Sulf1 is co-expressed with Shh in the ventral neural tube, suggesting that it acts to regulate Shh signalling during the establishment of the Shh gradient.

The aims of this thesis are to determine whether or not:

- Sulf1 and Shh regulate each others expresson levels during early *Xenopus* development
- The expression and activity of Shh is reduced in the absence of Sulf1
- Knockdown of Sulf1 affects the establishment of neural progenitor populations along the dorsoventral axis of the neural tube
- Sulf1 regulates neural patterning by changing the spatial distribution and activity of Shh

2.0 Relationship between Shh and Sulf1

2.1 Introduction

A number of studies have identified a role for the extracellular environment in the establishment of a hedgehog morphogen gradient (Bellaiche et al., 1998; Bornemann et al., 2004; The et al., 1999). Shh contains the consensus sequence associated with the binding of heparan sulphate proteoglycans (HSPGs), and has been shown to interact with the sulfate groups located on glycosaminoglycan (GAG) chains (Rubin et al., 2002). Enzymes which modify the sulfation state of HSPGs may affect the way Shh interacts with the extracellular matrix and could therefore contribute to the modulation of signalling.

The 6-O endosulfatase Sulf1, which removes the 6-O sulphate group from tri-sulfated disaccharides present on HSPGs, was first identified in a screen for Shh response genes activated during somite formation (Dhoot et al., 2001). Implantation of beads impregnated with Shh are able to induce *Sulf1* expression within quail somites. Conversely inhibition of *Shh* expression with antisense oligonucleotides blocked *Sulf1* expression in a tissue specific manner, inhibiting expression of *Sulf1* in epaxial somite and neural tube progenitors, but not in the floor plate or notochord (Dhoot et al., 2001).

Sulf1 expression is also regulated by a number of other factors. Within the developing chick limb, implantation of beads containing FGF4 promotes an increase in *Sulf1* expression (Zhao et al., 2007). A similar result is obtained in micromass cultures of limb bud mesenchyme treated with FGF4, which display a dose dependent response in *Sulf1* expression following the addition of FGF4 (Zhao et al., 2007). Induction of *Sulf1* by FGF4 however shows a bimodal response whereby levels increase at intermediate concentrations (5ng/ml) but are reduced when the does is increased (10ng/ml). Additionally implantation of beads containing the FGF inhibitor SU5042 leads to ectopic *Sulf1* expression in the distal tip of digit III (Zhao et al., 2007), which is most likely due to a similar bimodal response. Sulf1 also exhibits a bimodal dose dependent response to TGF-β1 in normal human lung fibroblast (NHLF) cells, and is up regulated within the lungs of mice treated with adenovirus encoding active TGF-β1 (Yue et al., 2008). These studies indicate that Sulf1 is switched on in precise locations in response to the specific level of signalling from a number of different signalling

pathways. The ability of Sulf1 to inhibit some of these pathways (Freeman et al., 2008; Wang et al., 2004) suggests that up regulation of Sulf1 provides a mechanism by which signalling pathways are regulated.

The co-expression of *Sulf1* and *Shh* within the ventral neural tube, suggested that Sulf1 may have a role in the regulation of Shh signalling. However although Sulf1 was originally identified as a target of Shh, it was proposed not to act within the Shh signal transduction pathway as inhibition of Sulf1 expression failed to inhibit the expression of the Shh targets Pax1, Pax3 and Myf5 (Dhoot et al., 2001). Further studies however revealed a role for Sulf1within the neural tube, whereby it acts to increase the local concentration of Shh to direct the switch from neuronal to oligodendroglial precursors (Danesin et al., 2006). More recently studies in *Drosophila* have similarly revealed a role for Sulf1 in the regulation of Hh signalling (Wojcinski et al., 2011).

2.2 Aims

This chapter will outline the expression of *Shh* and *Sulf1* during the development of *X. tropicalis* and provide evidence for an interaction between them. *Shh* and *Sulf1* will be over expressed and inhibited to investigate the relationship between Shh signalling and Sulf1 activity. In this chapter I report the developmental expression patterns of *Shh* and *Sulf1* in *X. tropicalis* and test the following hypotheses:

- Inhibition of Shh signalling affects the expression of Sulf1
- Knockdown of Sulf1 affects the expression of Shh
- Modifying the sulfation state of HSPGs by over expression or knockdown of Sulf1 changes the activity of Shh

2.3 Methods

2.3.1 Perturbation of Shh signalling

In this chapter the expression of *Sulf1* and *Shh* will be considered in relation to one another. The action of each protein will be perturbed in different ways. Shh signalling will be inhibited by culturing embryos in a solution containing cyclopamine. Cyclopamine is a teratogenic compound which inhibits hedgehog signalling at the level of Smoothened, preventing its activation in the presence of Shh and thus blocking downstream signalling (Chen et al., 2002). Cyclopamine treatment is relatively easy in *Xenopus* as it can simply be introduced into the medium in which embryos are cultured. One problem with this methodology is that the drug is unable to pass through the vitelline membrane surrounding the embryos, and this has to be mechanically removed before treatment. To ensure that this process is not the causative factor for any effects seen, control embryos were subjected to the same treatment and cultured in solution containing 2% ethanol as a vehicle control (Cyclopamine stock in 100% ethanol diluted 1/50). Figure 2.1 outlines how cyclopamine blocks Shh signalling. During signalling, the presence of the Shh ligand inhibits the repressive action of Ptc on Smo, thus permitting active signalling. Cyclopamine binds to Smo and prevents it being activated following the de-repression by Ptc, thus preventing downstream signalling.

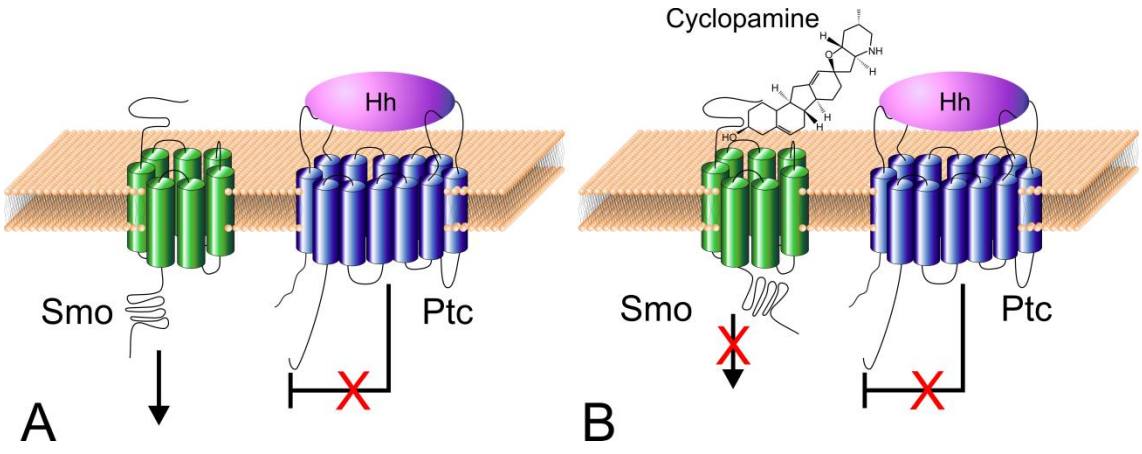

Figure 2.1 Action of cyclopamine at the cell surface
(A) In the presence of Shh, inhibition of Smoothened (green) by Patched (blue) is released leading to downstream signalling. (B) Cyclopamine binds to Smoothened which results in it taking on its inhibited state. The release of inhibition by patched due to the presence of Shh therefore has no effect and downstream signalling is inhibited.

2.3.2 Ptc2 as an indicator of Shh activity

As *Ptc* is up regulated in response to Shh signalling, the relative expression of *Ptc* can be used to show Shh signalling levels. There are two vertebrate Ptc genes, Ptc1 and Ptc2, and *Xenopus* Ptc1 and Ptc2 proteins closely resemble their amniote counterparts at the level of the amino acid sequence. However, while chick and mouse *Ptc1* expression is used as an indicator of Shh activity, in *Xenopus*, it is *Ptc2* that responds to Shh signalling (Takabatake et al., 2000).

Figure 2.2 shows *Ptc2* expression in NF stage 23 *X. tropicalis* embryos following the over expression or knockdown of Shh signalling by injection of mRNA coding for *Shh* or treatment with cyclopamine respectively.

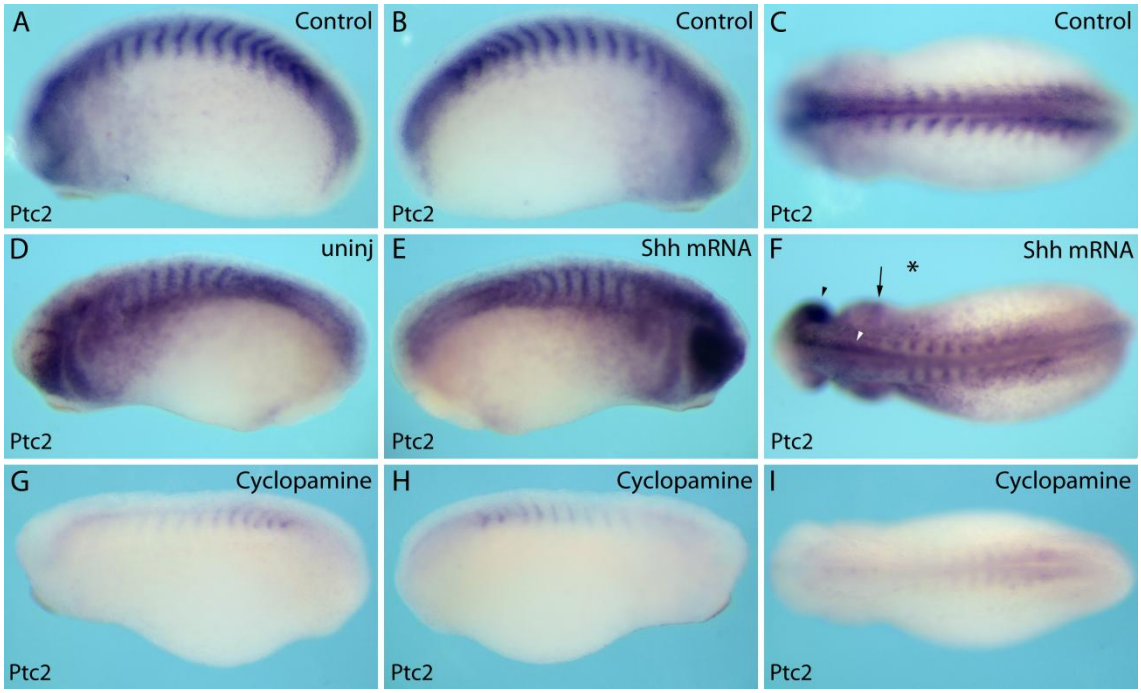

Figure 2.2 Whole mount *in situ h*ybridization analysis of *X. tropicalis* embryos unilaterally injected with 1ng Shh or treated with 100µM cyclopamine

(A-C) In control embryos *Ptc2* expression can be seen within the ventral neural tube, neural crest and somites. (D,F) Unilateral injection of *Shh* leads to the induction of *Ptc2* expression within the eye (black arrow head) and neural tube (white arrow head). (G-I) Treatment of embryos with 100µM cyclopamine leads to a large down regulation in *Ptc2* expression.

* Indicates injected side

2.3.3 Knockdown of Sulf1

Knockdown of Sulf1 was achieved by injection of an antisense morpholino oligonucleotide (AMO) which will be referred to as S1MO3 (Sulf1 morpholino 3). This morpholino blocks splicing upstream of the catalytic site of Sulf1 and leads to the introduction of a stop codon, preventing production of the active protein (Figure 2.3). The effects of Sulf1 were also abrogated via the over expression of the sulfotransferase 6-OST which adds a sulphate group to the C6 position which Sulf1 acts to de-sulphate. AMOs and mRNA were injected at the 2 cell stage.

To confirm that the Sulf1 antisense morpholino S1MO3 effectively blocks splicing, cDNA was generated from Sulf1 morphant embryos and analysed by PCR using the primers shown in Figure 2.3 which either amplify exon 2 or the region between exons 2 and 3. Figure 2.3 shows the two products generated from control or morphant embryos using these primer pairs, which have been resolved on an agarose gel (left) or acrylamide gel (right). While the product generated from exon 2 is the same in control and morphant embryos (Figure 2.3 below lanes 1 and 2), the region amplified between exons2 and 3 shows a marked increase in size following Sulf1 knockdown (Figure 2.3 below lanes 3 and 4). Resolution via acrylamide shows that the larger product generated following Sulf1 knockdown is present in two sizes indicating the activation of a cryptic splice site, which has previously been reported following the use of splice-blocking morpholinos (Madsen et al., 2008). Premature stop codons were located throughout intron 2 in all three reading frames, and so even splicing at a cryptic site does not give rise to a functional protein.

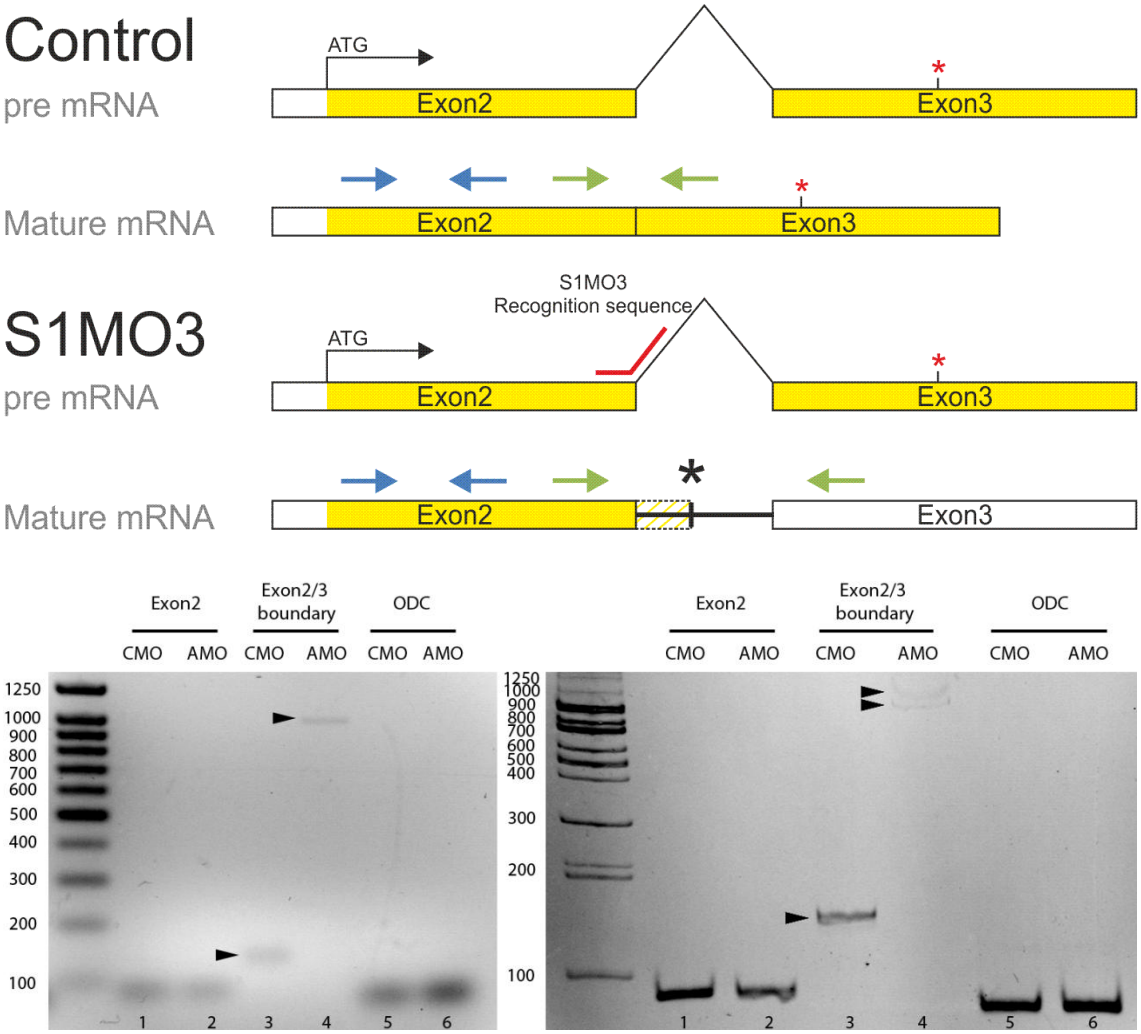

Figure 2.3 S1MO3 blocks the correct splicing of exons 2/3 of Sulf1

Above: Schematic showing splicing of Sulf1 between exons2 and 3.The Sulf1 antisense morpholino oligonucleotide (S1MO3) is complimentary to a sequence which spans the splice junction betweeen exon2 and exon3 and acts to inhibit splicing of the pre-mRNA at this site. Inhibiton of splicing results in retention of intron2 within the mature RNA, which introduces a premature a stop codon (*) and results in the formation of a truncated protein. Inclusion or exclusion of intron2 can be detedcted by PCR using the primer pairs shown. Sulf1 CDS shown in yellow. Conserved cysteine required for catalytic activity in exon 3 shown by red asterisk.

Below: The inhibiton of Splicing by S1MO3 can be detected by using PCR primers which span intron 2. The retention of intron2 following blockage of splicing can be detected by a change in the size of the amplicon from primers which span the exon2/3 boundary (green primer pair shown above) (arrow heads, gel lane 3,4 increase in size from 146 to 992 bp). Gel lanes 1,3 and 5 show PCR products from control samples while lanes 2,4 and 6 show the PCR procucts from Sulf1 morphants. Lanes 1 and 2 show amplification of exon2 (blue primer pairshown above), lanes 3 and 4 show the products from the primer pair which span exons 2 and 3 (green primer pair shown above) while lanes 5 and 6 show amplification of ODC. Left image shows product resovled by agarose electrophoresis while the right image shows products resoved on an acrylamide gel. Acrylamide gel reveals the presence of two higher bands in the Sulf1 knockdown (double arrow head). 200bp band runs as a doublet on the acrylamide gel.

2.3.4 Unilateral injections

One useful feature of *Xenopus* development is that the first cell cleavage separates the left and right halves of the embryo. Another useful trait is that if mRNA is injected into Xenopus at any stage, it is taken up by all of the cells that derive from the cell into which the RNA was injected. Consequently if mRNA is injected at the two-cell stage, it will be translated in all of the cells in one half of the embryo while the un-injected cell will give rise to wild-type cells. This permits the effects of the over expression of a particular gene product to be compared with a contra-lateral control, allowing the analysis of subtle effects within the same embryo.

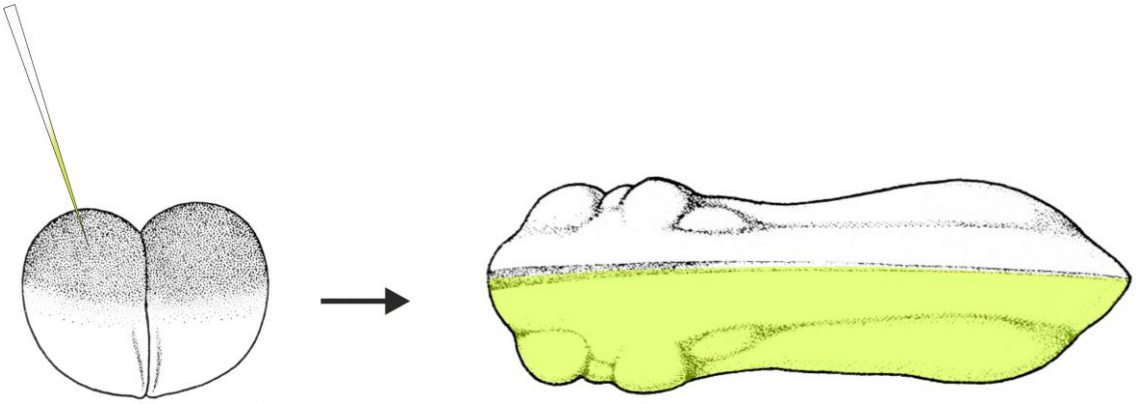

Figure 2.4 Unilateral injection of *Xenopus* oocytes
The first cleavage in Xenopus separates the left and right hemispheres. If mRNA is injected into one of the two cells (left), all of the cells on that side of the embryo express the exogenous mRNA (right). The contra-lateral side provides an internal control.
Left image shows a 2-cell stage embryo while the right image shows a stage 24 embryo from a dorsal perspective with the anterior oriented to the left of the image and the left and right side of the embryo oriented to the bottom and top respectively.

2.4 Results

2.4.1 Shh and Sulf1 expression in *Xenopus*

To understand the relationship between Shh and Sulf1, the expression of each gene was analysed first by *in situ* hybridisation to examine the spatial distribution of each of the genes. In *Xenopus* the mid blastula transition (MBT) marks the onset of zygotic transcription; this begins at the 13th cell division, which occurs during NF stage 8 (Newport and Kirschner, 1982). Transcripts detected prior to MBT therefore represent maternally deposited mRNA.

When analysed by *in situ* hybridisation, no *Shh* transcript can be detected at early blastula stages before MBT (Figure 2.5A). *Shh* is initially expressed during gastrulation within the involuting mesoderm (Figure 2.5B). Following gastrulation *Shh* shows expression within the axial mesoderm and neurectoderm (Figure 2.5E,E'), and as development progresses continues to be expressed along the midline within the notochord and ventral neural tube (Figure 2.5F,F',I,I',K,K'). At tadpole stages, *Shh* is not only expressed within the midline but also within the gall bladder, pancreas and pharynx (Figure 2.5K,K').

At early blastula stages shown in Figure 2.5C, maternal *Sulf1* transcripts are present peri-nuclearly, typical of the mRNAs that comprise germ plasm. The zygotic expression of *Sulf1* begins during gastrula stages, and can be seen in the newly formed mesoderm surrounding the blastopore (Figure 2.5D). Maternally deposited *Sulf1* persists within the germ cells (arrow head). *Sulf1* continues to be expressed within the paraxial mesoderm through open neural plate stages (Figure 2.5G,G',H,H'). Although from whole mount images *Sulf1* appears to be excluded from the midline at stage 15, sections reveal that *Sulf1* is expressed within the midline at this stage where it is localised to the neurectoderm (Figure 2.5H'). From stage 15 Sulf1 continues to be co-expressed with *Shh* within the midline which forms the floor plate as development progresses (Figure 2.5J,J',L,L''). As the paraxial mesoderm segments to form somites, *Sulf1* expression is similarly divided and outlines the blocks of muscle precursors (Figure 2.5J,L). Later on *Sulf1* can also be seen within the migrating muscles (Figure 2.5L). During tadpole stages, Sulf1 also shows additional regions of expression anteriorly in the branchial arches and the eye.

Figure 2.5 Whole mount *in situ h*ybridization analysis of *X. tropicalis* embryos showing the expression of Shh and Sulf1

(A) Shh is not maternally deposited and cannot be detected before MBT. (B) During gastrulation *Shh* is expressed within the involuting mesoderm. (C) Maternally deposied *Sulf1* can be detected in stage 7 embryos and is localised to the germ cells. (D) During gastrulation zygotic *Sulf1* is expressed in the region surrounding the blastopore while maternal *Sulf1* remains localised to the germ cells. (E,F) At open neural plate stages, *Shh* is expressed within the midline. (E',F') Sectioning reveals that midline *Shh* expression is located in the axial mesoderm which differentiates to form the notochord and within the overlying neurectoderm. (G) *Sulf1* is not expressed whtin the midline at stage 13 but within the paraxial mesoderm. (G') Transverse sections reveal that *Sulf1* expression is excluded from the midline. (H) At stage 15 *Sulf1* expression appears to be similar to that seen at 13. (H') Transverse sections of stage 15 embryos reveal midline expression within the neurectoderm. (I) Axial expression continues into tailbud stages. (I') Sections reveal strong staining within the notochord and the ventral neural tube. (J) At tailbud stages *Sulf1* expression is maintained within the midline and paraxial mesoderm, where the somites begin to form. (J') Strong *Sulf1* expression can be detected within the ventral neural tube at stage 23. (K) As development progresses *Shh* shows additional regions of expression within the gall bladder, pancreas and pharynx. (K') Sagittal sections reveal that expression within the brain is localised to the ventral hindbrain. Further anteriorly expression can be seen within the posterior tubercle, zona incerta, zona limitans intrathalamica, mammillary band, suprachiasmatic nucleus and preoptic area. (L) Expression of *Sulf1* can be detected within the neural tube and somites along the trunk of the embryo at stage 37. Further anteriorly expression can also be seen within the branchial arches and the lens within the eye. (L') Sagittal sections of the brain reveal that expression overlaps with *Shh* in the zona incerta, zona limitans intrathalamica, suprachiasmatic nucleus and preoptic area. *Sulf1* expression also extends further anteriorly into the subpallium where *Shh* is not expressed. No *Sulf1* expression can be seen within the mammillary band or posteriorly within the tuberal area. (M) A dorsal view reveals that along the trunk of the embryo, expression of *Shh* is restricted to the midline.
(N) *Sulf1* expression within the lens and somites can clearly be seen from a dorsal view
(K'') Transverse sections shows that *Shh* is still localised to the ventral neural tube. (L'') *Sulf1* expression also remains strong within the ventral neural tube at this stage.

Images indicated by ' show sections corresponding to the letter shown. Double black arrow heads on wholemount images indicate the position of the sections.

Regions of the brain described are shown in Figure 2.6, and are not marked on this figure for simplicity.

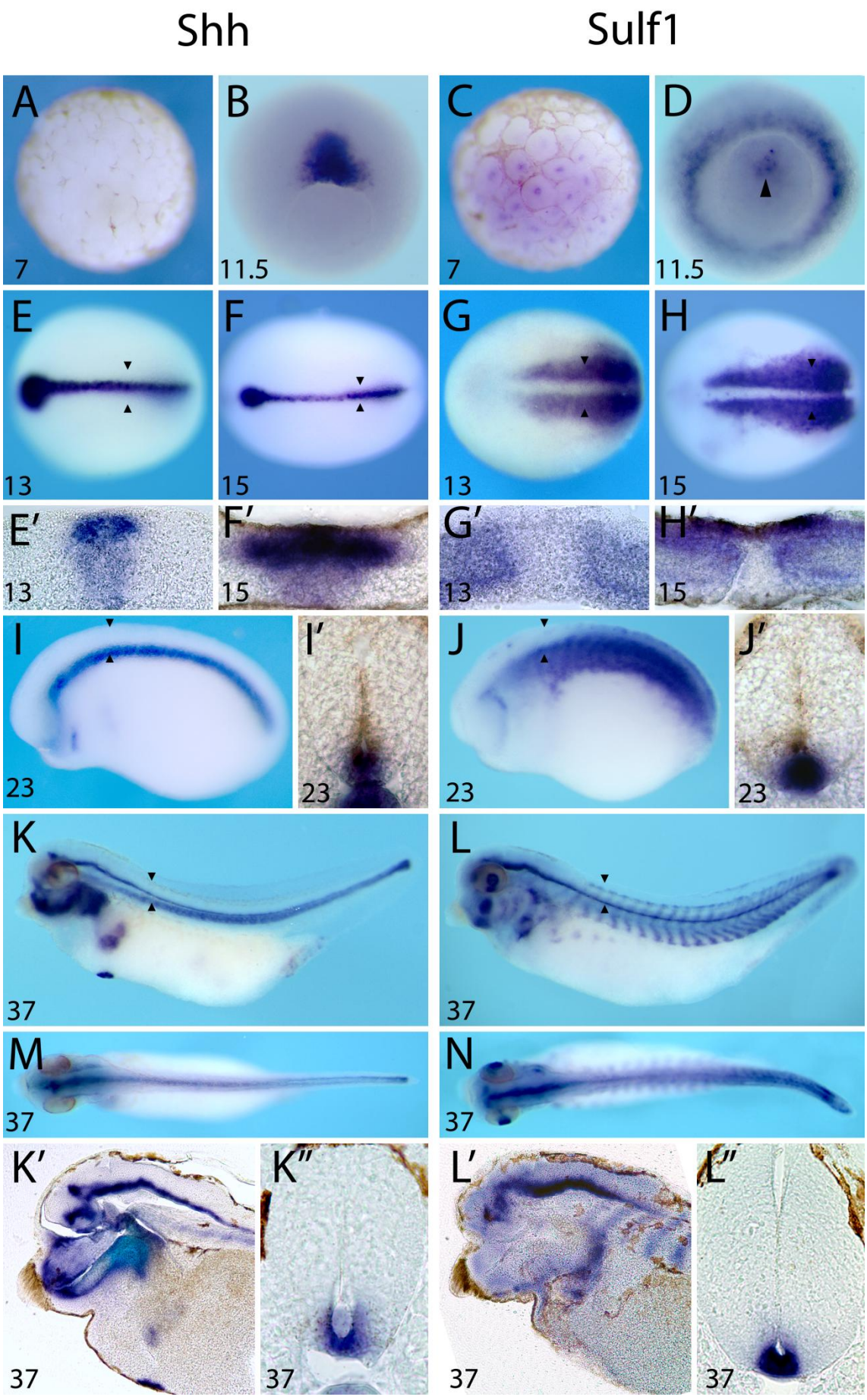
Shh
Sulf1
A
7
B
11.5
C
7
D
11.5
E
13
F
15
G
13
H
15
E′
13
F′
15
G′
13
H′
15
I
23
I′
23
J
23
J′
23
K
37
L
37
M
37
N
37
K′
37
K″
37
L′
37
L″
37

Closer inspection of *Shh* and *Sulf1* expression within the brain reveals that they are expressed in some overlapping regions. Figure 2.6 shows a schematic of the brain at stage 37 overlaid with the expression of *Shh* and *Sulf1* as shown in Figure 2.5K' and L'. Expression of *Shh* is confined to the ventral hindbrain. Further anteriorly, expression can be seen within the posterior tubercle (TP) and zona incerta (Zi). A region of expression can also be seen with the zona limitans intrathalamica (Zli). Expression continues to be confined posteriroly and ventrally within the forebrain, exhibiting regions of expression within the mammillary band (BM), suprachiasmatic nucleus (SC) and preoptic area (PO). Sulf1 expression is generally wider and extends further dorsally than *Shh*. Expression overlaps with *Shh* in the zona incerta and zona limitans intrathalamica. No expression can be seen within the mammillary band or posteriorly within the tuberal area. Overlapping expression can be seen within the suprachiasmatic nucleus and preoptic area. Unlike *Shh* however, *Sulf1* expression extends further anteriorly into the Subpallium.

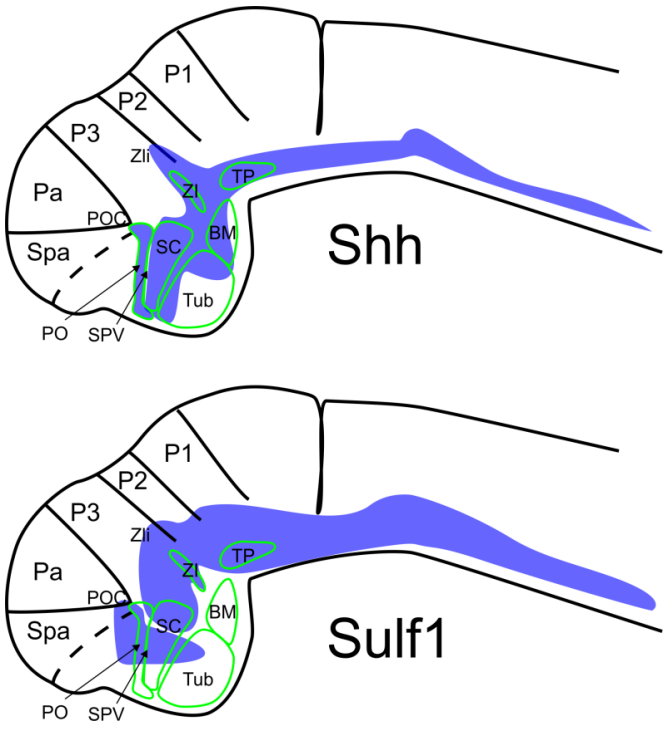

Figure 2.6 Schematic of the brain in *Xenopus* at stage 37
Shh and *Sulf1* display broadly overlapping regions of expression within the ventral neural tube, the hindbrain, midbrain and caudal forebrain
BM mammillary band; **P1/2/3**, Diencephalic prosomere1/2/3; **Pa**, Pallium; **Spa**, Subpallium; **PO**, Preoptic area; **POC**, preoptic commissural area; **SPV**, supraoptoparaventricular area; **SC** suprachiasmatic nucleus; **TP**, posterior tubercle; **Tub** tuberal area; **Zi**, zona incerta; **Zli** zona limitans intrathalamica

Schematic and annotation adapted from (Dominguez et al., 2010)

To further analyse the relationship between *Shh* and *Sulf1* qPCR was undertaken to determine the relative gene expression level through the early period of development analysed by *in situ* hybridisation. The expression of Ptc2 was also analysed as an indicator of Shh activity. Figure 2.7 shows the expression level of *Shh*, *Sulf1* and *Ptc2* from NF stage 7 to NF stage 23 relative to the expression level seen at stage 23. Maternally deposited Sulf1 mRNA seen at stage7 displays a gradual decrease until stage 11. As observed by *in situ* hybridisation, *Shh* is not expressed until after MBT where it shows low levels of expression until stage11.5. The level of *Shh* expression steadily increases from mid-gastrula stages (11.5) and throughout neurulation (14-23). Shh activity increases in line with *Shh* expression throughout neurulation as shown by *Ptc2* expression. Between stages 11.5 and 14 *Sulf1* increases in line with *Shh* but does not continue to follow this trend after stage 14.

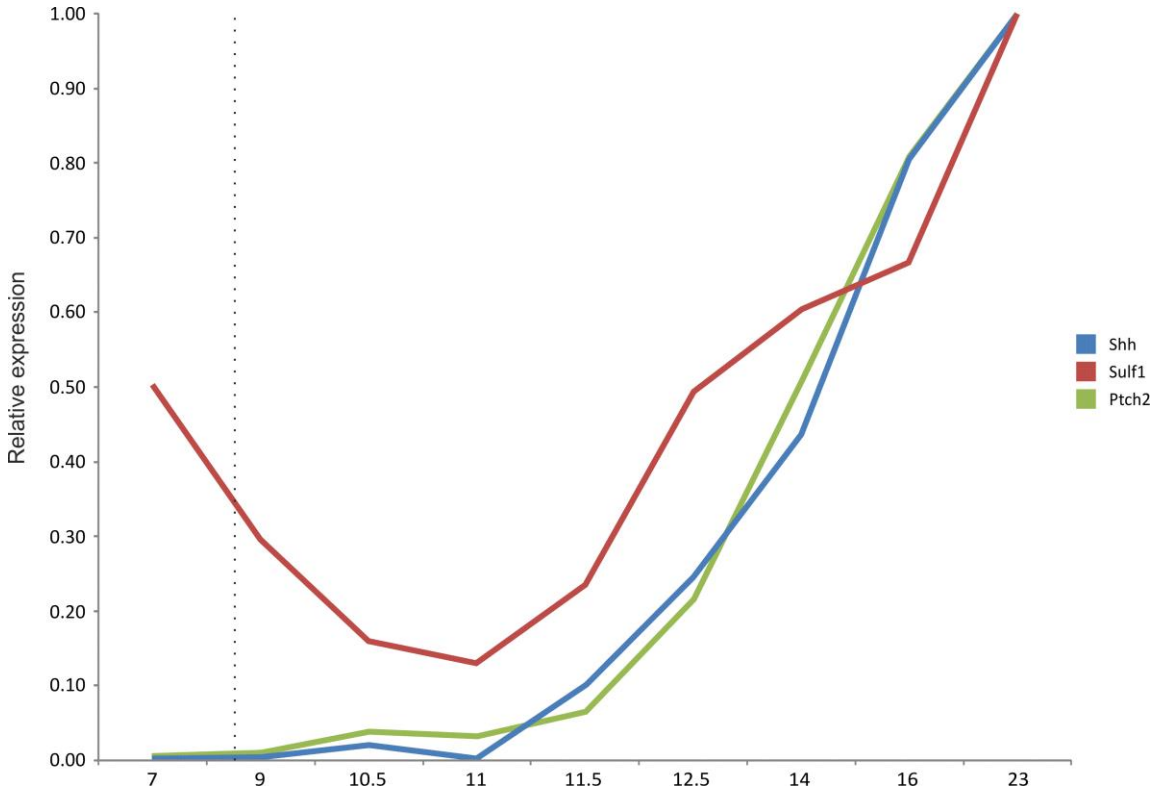

Figure 2.7 Expression level of Shh, Ptc2 and Sulf1 as determined by qPCR
Sulf1 (red) is maternally deposited in high levels before MBT (dashed line). Shh (blue) begins to be expressed at low levels as gastrulation begins (10.5), and shows a steady increase in its level from mid-gastrula (11.5). Ptc2 (green) is a downstream target of Shh and mirrors its expression. Sulf1 expression also mirrors that of Shh until around stage 14. Expression levels were normalised to ODC and are shown relative to the expression level at stage 23.

2.4.2 Shh activity affects *Sulf1* expression within the open neural plate

To assess whether Shh is able to regulate *Sulf1* expression, embryos were unilaterally injected with Shh mRNA at the two cell stage or treated with cyclopamine at stage 9. *Sulf1* expression was assessed at stage 12.5 and 15 by *in situ* hybridisation. At stage 12.5 the ability of Shh to up regulate *Sulf1* expression appears limited. A slight increase in anterior *Sulf1* levels can be seen on the injected side, however over expression of Shh does not seem to lead to ectopic expression of *Sulf1* (Figure 2.8E). Cyclopamine treatment does however give rise to a reduction in *Sulf1* expression indicating a role for Shh in the establishment of *Sulf1* expression. By stage 15, expression of *Sulf1* is shifted medially as the neural plate rolls up (Figure 2.8C). Injection of *Shh* mRNA does not expand the expression domain of *Sulf1* at this stage. An additional domain of expression which flanks the neural plate and extends up to the most anterior point of the expression seen at the midline, can however be observed (Figure 2.8F arrow head). This expression may represent an ectopic region of *Sulf1* expression or may represent a region which has failed to down regulate Sulf1 between stage 12.5 and stage 15. Treatment with cyclopamine leads to the same dysregulation of expression seen at stage 12.5, with a general expansion of expression throughout the embryo (Figure 2.8I). This suggests that Shh not only governs the activation of *Sulf1* but also defines its specific region of expression.

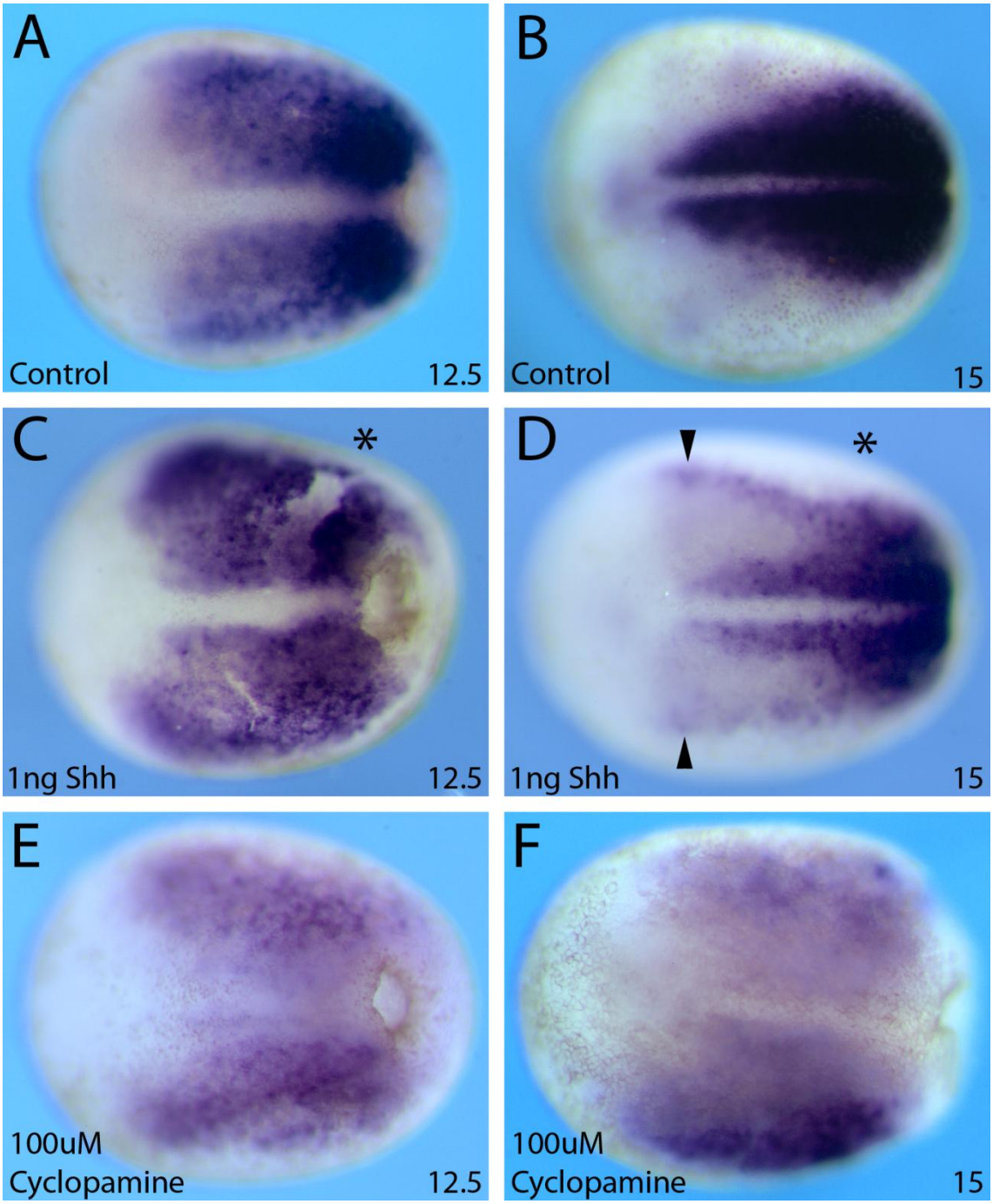

Figure 2.8 Whole mount *in situ h*ybridization analysis of Sulf1 expression in *X. tropicalis* embryos unilaterally injected with 1ng Shh or treated with 100µM cyclopamine
(A) At stage 12.5 *Sulf1* is expressed posteriorly within the paraxial mesoderm.
(C) *Shh* over expression leads to a slight increase in anterior expression of *Sulf1* but does not induce ectopic expression. (E) Cyclopamine treatment leads to a down regulation of *Sulf1* expression within the paraxial mesoderm. (B) The level of *Sulf1* expression continues to increase as development progresses. Anterior expression shifts medially as the neural plate folds. (D) Unilateral injection of *Shh* mRNA gives rise to an additional region of expression which flanks the neural plate (arrow head). Medial regions do not show any increase in expression levels however. (I) At stage 15 cyclopamine treatment leads to an overall reduction in *Sulf1* expression. *Sulf1* is also not medially restricted but can be seen throughout the paraxial mesoderm.
Embryos are viewed from a dorsal perspective with the anterior facing left.
* indicates the injected side.

While over expression of *Shh* does appear to increase the overall level of *Sulf1* expression this change is difficult to quantify by *in situ* hybridisation. Furthernore, while cyclopamine treatment appears to reduce the level of zygotic *Sulf1* during gastrulation, it is difficult however to assess whether there is any reduction in the level of *Sulf1* later during development as the area over which *Sulf1* is expressed is much greater following cyclopamine treatment.

To assess more quantitatively whether cyclopamine treatment results in a reduction of *Sulf1* expression, the level of *Sulf1* was analysed by qPCR. Figure 2.9 shows the expression of *Sulf1* at stage 12.5, 16 and 23 following treatment with cyclopamine. *Ptc2* expression was also analysed to provide a readout of Shh activity. While a reduction in *Sulf1* expression can be observed at stage 12.5 (~ 3 fold), almost no change is observed at stage 16 and 23. Inhibition of Shh signalling is shown by a reduction in *Ptc2* expression at all stages. This

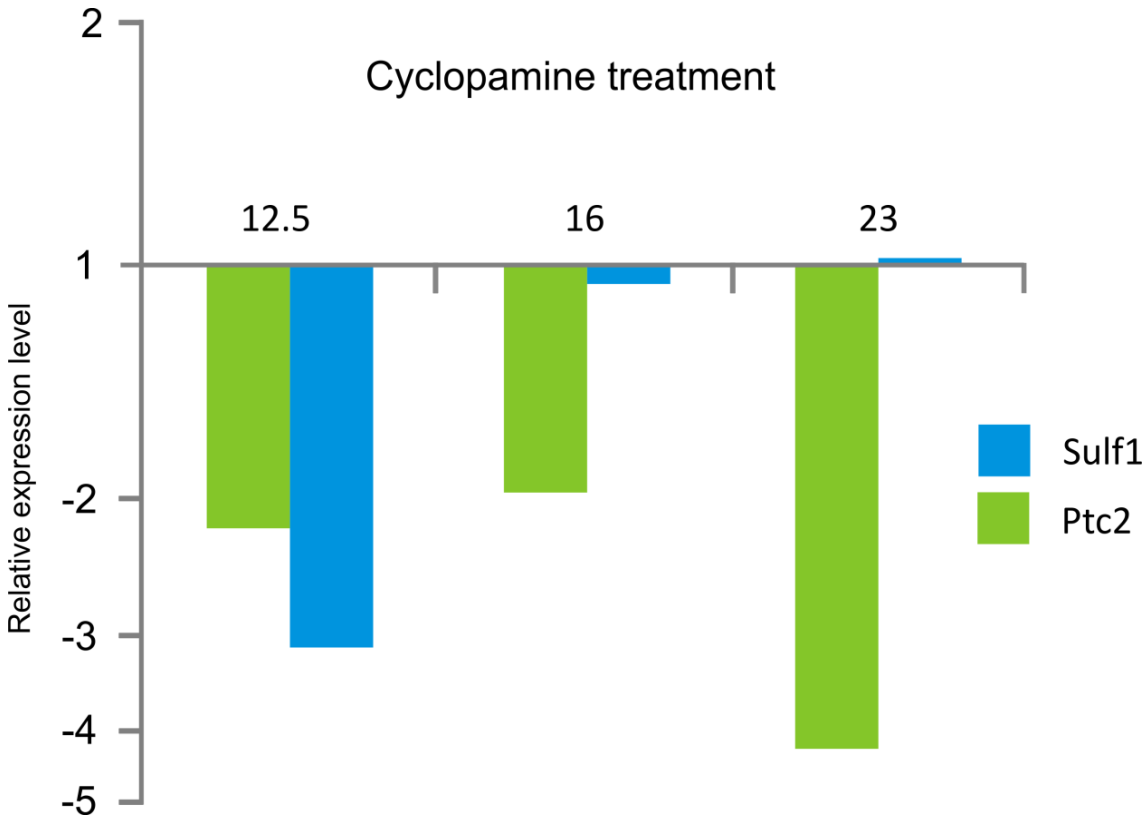

Figure 2.9 Expression levels of *Sulf1* and *Ptc2* following inhibition of Shh signalling
qPCR showing the expression of *Sulf1* and *Ptc2* following treatment with cyclopamine. While expression of *Sulf1* is reduced at 12.5, no change is observed at stage 16 or 23. The downstream target of Shh *Ptc2* is reduced at all stages indicating that Shh signalling has been reduced by the treatment. Embryos were treated with 100µM cyclopamine. Expression levels were normalised with ODC and are shown relative to embryos cultured in a 1/50 diltuion of ethanol. Data is log transformed such that relative values less than one are shown as negative.

suggests that while Shh signalling may promote early expression of *Sulf1* during gastrula and early neurula stages, the continued expression of *Sulf1* does not require Shh activity.

At stage 15, *Sulf1* is expressed much more widely following cyclopamine treatment. This ectopic expression of *Sulf1* in cyclopamine treated embryos may explain why expression levels appear to be restored to normal by stage 23. To investigate whether *Sulf1* is expressed ectopically at stage 23, *Sulf1* expression was analysed by *in situ* hybridisation. While in control embryos, *Sulf1* is confined to the paraxial mesoderm in the posterior of the embryo, cyclopamine treated embryos exhibit ectopic *Sulf1* expression throughout this region (Figure 2.10B black arrow head). Anterior neural expression is reduced however (Figure 2.10 arrow).

Although *Sulf1* is reduced at gastrula stages following cyclopamine treatment, overall expression levels are restored later on during development due to ectopic expression of *Sulf1*.

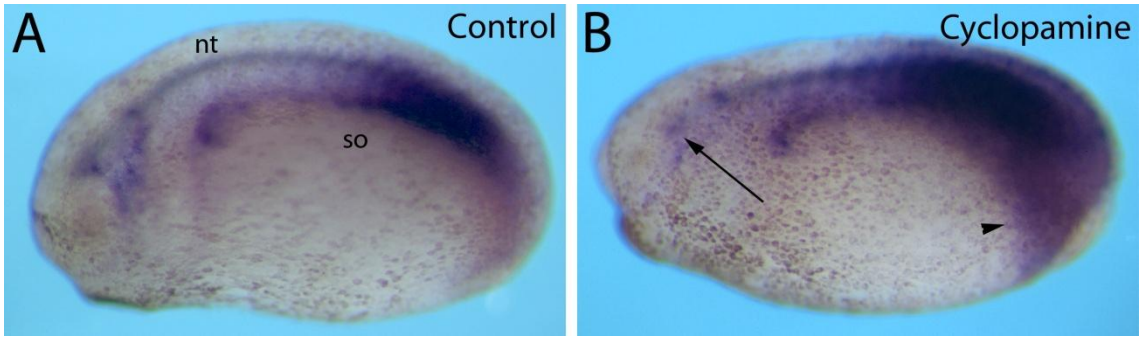

Figure 2.10 Whole mount *in situ h*ybridization analysis of *Sulf1* expression in stage 23 *X. tropicalis* embryos treated with 100μM cyclopamine
(A) *Sulf1* expression can be seen posteriorly within the paraxial mesoderm which is undergoing segmentation to form somites. Expression can also be seen within the ventral neural tube.
(B) In cyclopamine treated embryos ectopic expression can be seen throughout the posterior of the embryo (arrow head). Anterior neural expression however appears reduced.

2.4.3 Regulation of *Shh* expression by Sulf1

The above results provide evidence that Shh in *Xenopus*, as in other organisms, is able to regulate the expression of *Sulf1*. To investigate whether Sulf1 has any role in the regulation of *Shh* expression, embryos were injected with *Sulf1* mRNA or with an antisense morpholino oligonucleotide (referred to as S1MO3 – Sulf1 morpholino number 3) designed to prevent splicing of Sulf1, thus rendering it inactive. Embryos were also treated with 100µM cyclopamine to investigate whether blocking Shh signalling gives rise to similar effects to blocking the function of Sulf1. At stage 11.5, over expression or knockdown of Sulf1 seems to have no effect on the expression of Shh (Figure 2.11D,G). Treatment with 100µM cyclopamine however, narrows the expression domain of *Shh*. At stage 12.5, over expression of Sulf1 still appears not to have any effect on *Shh* expression (Figure 2.11E). Following Sulf1 knockdown at this stage however, Shh expression can be seen further anteriorly than in controls (Figure 2.11H). Treatment of embryos with 100µM cyclopamine leads to a widening of the expression domain of Shh. Expression does however not extend any further anteriorly (Figure 2.11K). At stage 15, Shh is expressed in a narrow line alone the midline of the embryo, which widens out at the anterior to form a circle (Figure 2.11C). Following over expression of Sulf1, the anterior region of Shh expression is much narrower than observed in controls, such that expression is almost the same as that seen along the midline (Figure 2.11F). As seen earlier during development, knockdown of Sulf1 has no affect on Shh expression at stage 15 (Figure 2.11I). Expression in cyclopamine treated embryos is generally much wider than in controls and does not widen significantly in the anterior of the embryo, such that expression is almost uniform along the whole axis of the embryo (Figure 2.11L).

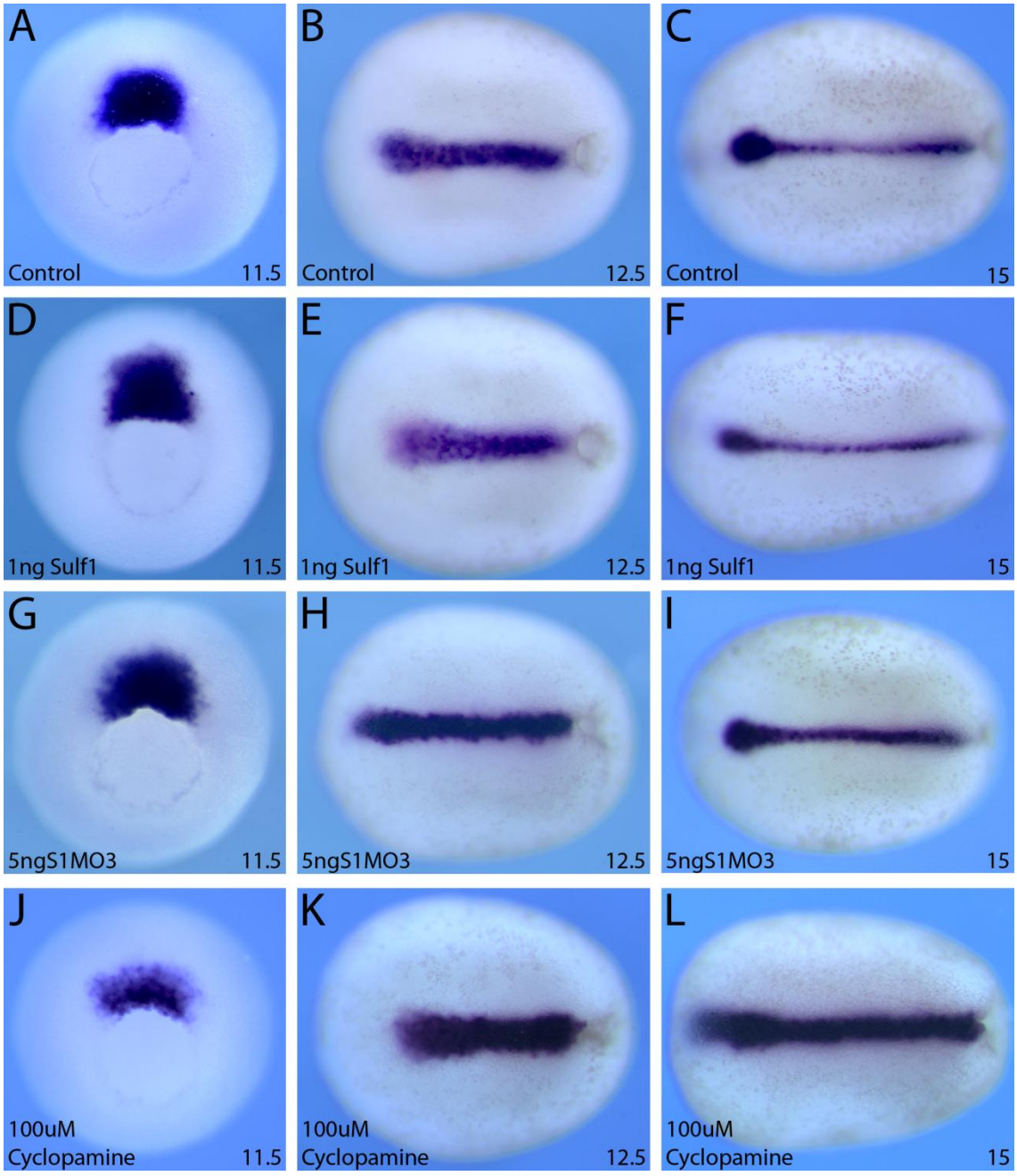

Figure 2.11 Whole mount *in situ h*ybridization analysis of *Shh* expression in *X. tropicalis* embryos bilaterally injected with 1ng Sulf1 mRNA, 5ng S1MO3 or treated with 100µM cyclopamine

(A) At stage 11.5 *Shh* is expressed in the dorsal lip of the blastopore. (D,G) Over expression or knockdown of *Sulf1* has no effect on *Shh* expression at stage 11. (J) Cyclopamine treatment slightly reduces the *Shh* expression region. (B) By stage 12.5 *Shh* is expressed along the midline. (E) As at stage 11.5 *Sulf1* over expression has does not alter *Shh* expression. (H) Sulf1 knockdown extends the region of *Shh* expression in the anterior of the embryo. (K) Cyclopamine treatment expands the region of *Shh* expression laterally, although expression is reduced anteriorly. (C) Expression of *Shh* is still restricted to the midline at stage 15 although an expansion of expression can be seen anteriorly within the open neural plate. (F) *Sulf1* over expression restricts anterior *Shh* expression. (I) As at earler stages Sulf1 knockdown has no significant impact on *Shh* expression. (L) Cyclopamine treatment leads to a lateral expansion of *Shh* expression along the length of the embryo.
Stage 11.5 embryos are oriented dorsal up. Stage 12.5 and 15 embryos are viewed from a dorsal perspective with the anterior facing left.

2.4.4 .The activity of Sulf1 and 6-OST can modulate Shh signalling

The above results indicate that while over expression or inhibition of Shh alters *Sulf1* expression, Sulf1 does not seem to regulate *Shh* expression. In quail embryos inhibition of *Sulf1* was shown not to affect Shh target expression suggesting that it does not act to regulate Shh signalling (Dhoot et al., 2001). To investigate whether Sulf1 is able to promote or inhibit hedgehog activity in *Xenopus*, embryos were unilaterally injected with mRNA coding for either Sulf1, or 6-OST giving rise to hypo- or hyper-sulfated HSPGs respectively. Additionally to assess the endogenous role of Sulf1 on hedgehog activity embryos were unilaterally injected with the Sulf1 morpholino S1MO3. Shh signalling was assayed via *in situ* hybridisation using *Ptc2* expression as a readout of Shh activity. Figure 2.12 shows the expression of *Ptc2* following unilateral injection of Sulf1, 6-OST or S1MO3. Unilateral over expression of *Sulf1* appears to

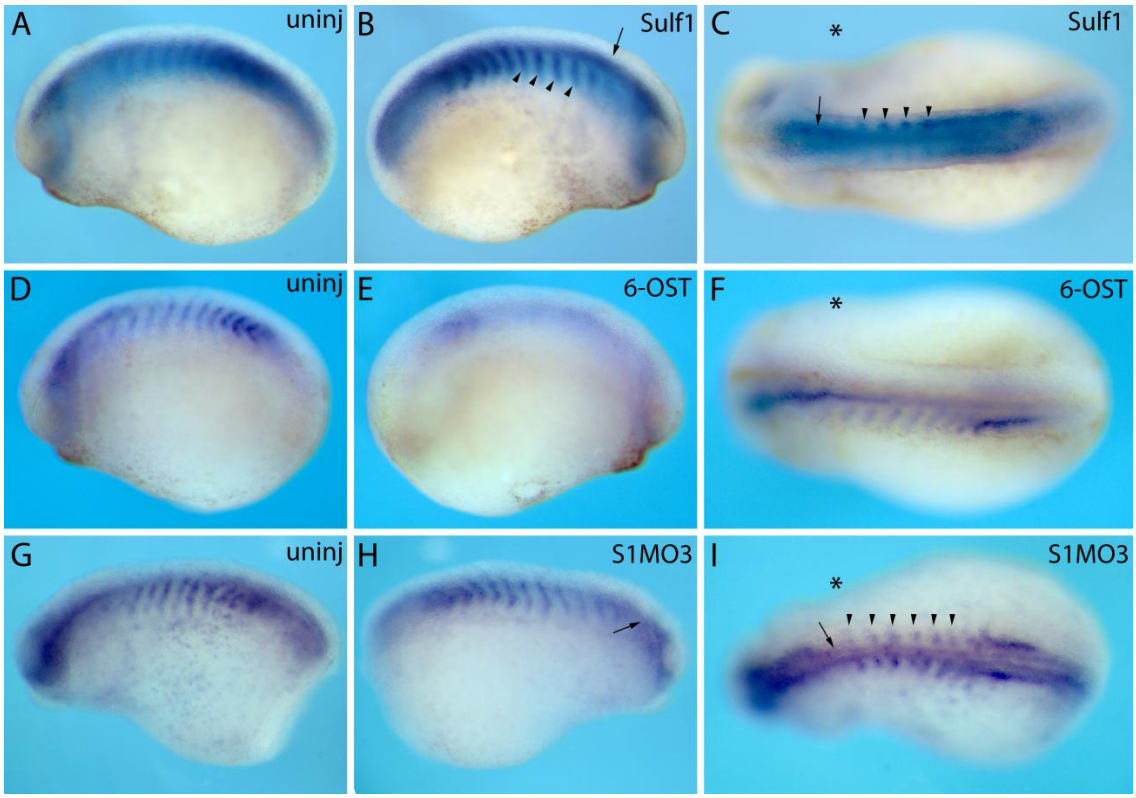

Figure 2.12 Whole mount *in situ h*ybridization analysis of *Ptc2* expression in *X. tropicalis* embryos unilaterally injected with 1ng Sulf1 mRNA, 1ng 6-OST mRNA or 5ng S1MO3
(A,D,G) By neural tube closure, Ptc2 expression can be seen within the ventral neural tube and somites. (B,C) Over expression of Sulf1 promotes stronger *Ptc2* expression within the somites (arrow heads) and neural tube (arrow). (E,F) Unilateral injection of 6-OST almost completely inhibits *Ptc2* expression on the injected side. (H,I) Knockdown of *Sulf1* reduces *Ptc2* expression within the somites (arrow heads) and neural tube (arrow).
* indicates injected side.

promote *Ptc2* expression both within the neural tube and the somites (Figure 2.12B,C), suggesting that Sulf1 acts to enhance Shh activity. Expression of *Ptc2* is not observed in any ectopic regions however. Injection of 6-OST conversely leads to an almost complete inhibition of *Ptc2* expression on the injected side (Figure 2.12E,F), again suggesting that HSPG de-sulfation is important for Shh activity. When *Sulf1* is knocked down by injection of the antisense morpholino S1MO3, *Ptc2* expression is reduced on the injected side (Figure 2.12H,I), although not to the extent seen following the over expression of 6-OST.

2.4.5 Sulf1 is required for correct levels of Shh signalling

The results thus far indicate that Shh acts to promote *Sulf1* expression within the midline and suggest that Sulf1 activity may be required for correct Shh signalling. Knockdown of *Sulf1* leads to a reduction in the expression of *Ptc2* within the somites on the injected side and also appears to reduce expression within the neural tube (Figure 2.12I). To more fully understand the role which Sulf1 has in modulating Shh activity within the ventral neural tube, Sulf1 was knocked down bilaterally, and the expression and activity of Shh was assayed via *in situ* hybridisation using probes targeted against Shh and Ptc2. Figure 2.13 shows *Shh* and *Ptc2* expression in transverse sections through stage 23 *X. tropicalis* embryos. Expression of *Shh* is strong within the notochord and floor

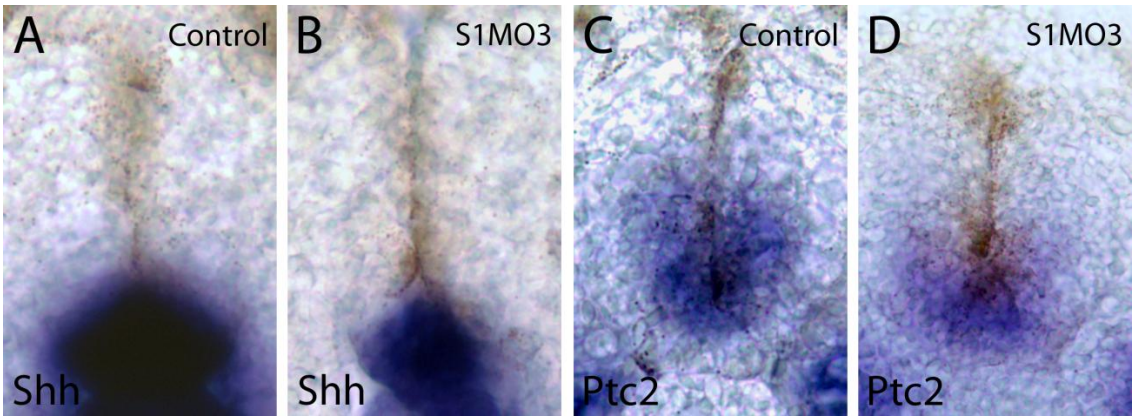

Figure 2.13 Transverse sections from whole mount *in situ h*ybridization analysis of stage 23 *X. tropicalis* embryos bilaterally injected with 5ng of S1MO3

(A) At stage 23 Shh is strongly expressed within the floor plate and notochord. (B) Knockdown of Sulf1 leads to a reduction in the level of *Shh* expression within the floor plate. (C) *Ptc2* is expressed in cells responding to Shh signalling, in the ventral neural tube and paraxial mesoderm. (D) Sulf1 knockdown results in a reduced and more diffuse expression pattern of *Ptc2*.

plate at stage 23 (Figure 2.13A). Cells responding to high levels of Shh signalling express *Ptc2*, which shows a tight region of expression within the ventral neural tube as well as the adjacent paraxial mesoderm (Figure 2.13C). Knockdown of Sulf1 leads to a reduction in the expression of *Shh* within the floor plate (Figure 2.13B). Sulf1 knockdown also leads to reduced *Ptc2* expression, which does not show the same level of tight regulation of its expression domain, but is instead more diffuse (Figure 2.13D).

To quantify the changes in Shh expression and activity following the knockdown of *Sulf1* observed by *in situ* hybridisation, expression levels of *Shh* and *Ptc2* were analysed by qPCR (Figure 2.14). At stage 12.5, Shh shows very little reduction in either its expression level of activity following Sulf1 knockdown. By stage 16 when *Sulf1* and *Shh* are co-expressed within the midline, *Shh* expression and activity show a small change, being down regulated by 1.5 fold. By stage 22 however, Shh activity, as shown by *Ptc2* expression is reduced by almost 3.5 fold, a change similar to that seen when cyclopamine is used to inhibit hedgehog signalling (Figure 2.10). Expression of *Shh* itself is down regulated by over 2 fold.

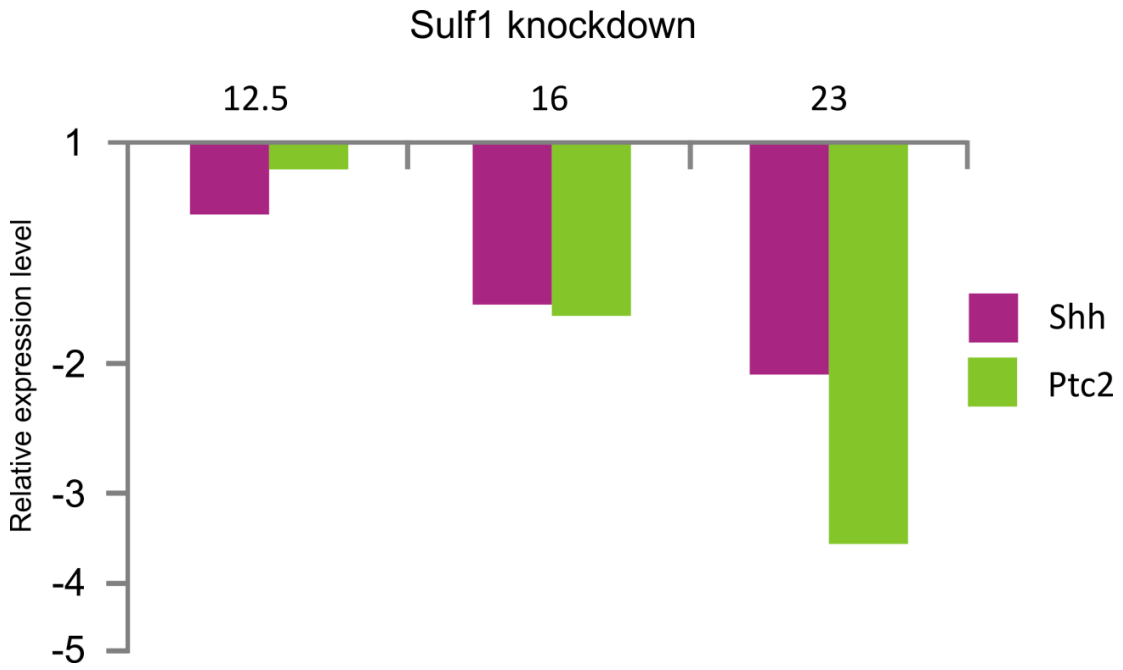

Figure 2.14 Expression levels of *Shh* and *Ptc2* following knockdown of Sulf1
qPCR showing the expression of *Shh* and *Ptc2* following Sulf1 knockdown. At stage 12.5 expression of *Shh* and *Ptc2* is almost unchanged. At stage 16 the expression of both *Shh* and *Ptc2* is reduced by almost 2 fold. By stage 23, *Shh* expression is reduced slightly more, while *Ptc2* expression is greatly decreased showing almost a 4 fold reduction. Expression levels were normalised with ODC and are shown relative to embryos injected with 15ng CMO. Data is log transformed such that relative values less than one are shown as negative.

2.5 Discussion

2.5.1 Shh and Sulf1 show regions of co-expression

To investigate the relationship between Shh and Sulf1, the expression of each gene was analysed via *in situ* hybridisation. Early expression of *Sulf1* does not overlap with that of *Shh*, but is instead expressed in adjacent cells within the paraxial mesoderm. *Sulf1* is first co-expressed with *Shh* in the midline at stage 15, and continues to be co-expressed within the ventral neural tube throughout development. The strong co-expression within the ventral neural tube from early neurula stages and throughout development suggests that Sulf1 may act within the ventral neural tube to regulate Shh signalling.

2.5.2 Sulf1 is a Shh response gene in *Xenopus*

Previous research has shown that Sulf1 is a Shh response gene, and is positively up regulated in response to exogenous Shh protein (Dhoot et al., 2001). In agreement with this, the results shown here indicate that *XtSulf1* is also up regulated by Shh, which when over expressed can give rise an increase in the level of *Sulf1* expression (Figure 2.8). Knockdown of Shh activity with cyclopamine conversely leads to a reduction in the overall level of *Sulf1* expression during gastrula stages (Figure 2.8,Figure 2.9). Interestingly while it appears that the level of *Sulf1* is reduced at stage 16 following cyclopamine treatment when assayed by *in situ* hybridisation, it appears that this is not the case when analysed by qPCR, and this is also true at stage 23 (Figure 2.9). Until stage 15, *Sulf1* is not co-expressed with *Shh* but in cells surrounding the Shh source (Figure 2.5). In Quail, blocking Shh does not inhibit the expression of *QSulf1* within the floor plate and notochord (Dhoot et al., 2001). Taken together, this suggests that while Shh may control *Sulf1* expression in cells adjacent to the Shh source, midline expression of *Sulf1* is not under the control of Shh.

It is interesting that early expression of *Sulf1*, which is not expressed in the same cells as *Shh* appears to be regulated by Shh, while later on when *Shh* and *Sulf1* are co-expressed within the midline, Shh does not regulate *Sulf1*. The ability of Shh to regulate *Sulf1* expression in distant cells is not surprising, as Shh is able to diffuse and induce gene expression far from its source. The fact

that *Sulf1* expression within the floor plate is not responsive to changes in Shh does appear at first to be surprising. However, one aspect of Shh signalling, is that cells become increasingly refractory to Shh signalling over time due to the up-regulation of *Ptc*. Recently it has been shown in chick, that Shh is only required transiently for the induction of the floor plate markers FoxA2 and Arx (Ribes et al., 2010). Blocking Shh signalling with $Ptc1^{\Delta loop2}$ after this period does not affect their expression level, while over activation of Shh signalling with $Gli3^{HIGH}$ leads to the down regulation of FoxA2 and a complete loss of Arx. This indicates that down regulation of Shh signalling within the floor plate region after its induction is essential for the specification of floor plate identity (Ribes et al., 2010). A reliance on continued Shh signalling for *Sulf1* expression in the floor plate would consequently lead to its down regulation. Shh may therefore only be required transiently for *Sulf1* expression in the midline. The fact that cyclopamine treatment does not abolish midline Sulf1 expression however suggests that Sulf1 does not require Shh at all, but is instead induced by another factor. Similarly, the inability of cyclopamine to totally inhibit Sulf1 at gastrula stages suggests that although Shh may contribute to Sulf1 induction, it is not required for expression.

Shh may not be required for *Sulf1* expression, however it does appear that it is required to ensure that *Sulf1* expression is correctly regulated in regard to its spatial restriction. Although *Sulf1* levels appear not to be reduced by mid-neurula stages following cyclopamine treatment, *Sulf1* is not up regulated within its normal expression domain but is instead expressed in a much wider domain. *Sulf1* expression is induced by a number of different growth factors including FGF and TGFβ (Yue et al., 2008; Zhao et al., 2007), so this ectopic expression may be due to induction by factors other than Shh. A number of FGFs show high levels of expression during gastrulation (Fletcher and Harland, 2008; Pownall et al., 1996; Tannahill et al., 1992). As Sulf1 has been shown to inhibit FGF signalling (Freeman et al., 2008; Wang et al., 2004), a reduction in the level of Sulf1 as a result of cyclopamine treatment, would lead to an increase in the level of FGF signalling at this time, which would in turn give rise to an increase in Sulf1 expression later on during development. At stage 23, ectopic Sulf1 expression can be seen posteriorly. FGFs continue to be expressed at

high levels in this region (Hayashi et al., 2004; Lea et al., 2009), again suggesting that ectopic Sulf1 expression may be due to increased FGF activity.

2.5.3 Sulf1 regulates Shh activity but not *Shh* expression

As discussed above, over expression of Shh is able to induce ectopic *Sulf1* expression. Over expression of Sulf1 however is not sufficient to induce ectopic regions of *Shh* at any stage of development, while knockdown similarly does not lead to any changes in Shh expression (Figure 2.11). This indicates that Sulf1 does not regulate *Shh* during open neural plate stages. The inability of Sulf1 to regulate *Shh* expression within the neural plate is not surprising as Sulf1 acts cell-autonomously (Ai et al., 2003a) and *Shh* and *Sulf1* are not co-expressed until stage15. As well as its inability to regulate *Shh* expression, previous research has suggested that Sulf1 does not have a role in the regulation of Shh target genes (Dhoot et al., 2001). More recently however it has been shown that Sulf1 is able to induce the ectopic expression of the Shh target Nkx2.2 within the neural tube of chick (Danesin et al., 2006). Similarly in *Drosophila* is has been shown that Sulf1 is able to regulate Hh activity (Wojcinski et al., 2011). In *Drosophila* it has been suggested that in cells receiving the Hh signal, Sulf1 acts in an inhibitory manner (Wojcinski et al., 2011). In chick however, the ability of Sulf1 to cell-autonomously induce the expression of *Nkx2.2*, suggests that it acts to positively regulate Shh signalling. In *Xenopus*, *Shh* is expressed in the midline; cells within the paraxial mesoderm receive the signal and consequently express *Ptc2*. If Sulf1 acts in an inhibitory manner, *Ptc2* levels within the somites should decrease following over expression of *Sulf1*, while an increase in *Ptc2* levels would indicate a positive role. When Sulf1 mRNA is unilaterally injected, *Ptc2* levels show an increase within the somites (Figure 2.12). Conversely when HSPGs are hyper-sulfated following the over expression of 6-OST, *Ptc2* expression is completely lost within the somites on the injected side (Figure 2.12). These results agree with the findings in chick that Sulf1 acts to promote Shh signalling. Sulf1 may however not simply act to inhibit or promote signalling cell autonomously. The work in *Drosophila* also shows that when *Sulf1* is co-expressed with *Hh*, release of Hh from expressing cells is increased. As over expression of *Sulf1* by injection of mRNA leads to an increase in *Sulf1* levels in both *Shh* expressing and Shh receiving cells, it may be that Sulf1 does not act to promote signalling at the level of cells perceiving

the signal, but acts to increase in the level of Shh released from *Shh* expressing cells. Therefore although these results show that the HSPG sulfation state is important for correct Shh signalling, they do not dissect out the specific role of Sulf1.

2.5.4 Loss of Sulf1 leads to a reduction in Shh expression and activity within the floor plate

To further assess the role of Sulf1 within the neural tube, Sulf1 morphant embryos were sectioned. As observed in whole embryos, Shh activity as indicated by *Ptc2* expression is reduced following the loss of Sulf1 (Figure 2.13). Interestingly however, when *Shh* expression was also analysed in Sulf1 morphants at stage 23, it was found to also be significantly reduced, which seems to disagree with the previous findings at open neural plate stages. During the differentiation of the floor plate, Shh activity is essential for cells to take on a floor plate identity, and consequently inhibition of Shh leads to inhibition of floor plate development (Ericson et al., 1996). As cells with a floor plate identity express *Shh*, a reduction in Shh activity during floor plate induction leading to a decrease in the size of the floor plate, would result in a reduction of *Shh* expression. The decrease in *Shh* expression following Sulf1 knockdown is therefore likely to be an indirect consequence of perturbed Shh signalling.

Shh expression within the floor plate is essential for the correct regulation of neuronal patterning in vertebrates (Briscoe and Ericson, 2001; Ericson et al., 1997a). The reduction in *Shh* expression and activity following Sulf1 knockdown therefore suggests that Sulf1 may be an important factor in the regulation of vertebrate neuronal patterning. The effect that Sulf1 loss has on the patterning of the neural tube in *Xenopus* will be discussed in the following chapter.

3.0 Patterning the vertebrate neural tube

3.1 Introduction

3.1.1 Shh and neural patterning

An extensive body of work describes the role of Shh in establishing populations of precursor cells along the axis of the neural tube. *Shh* expression is activated within the floor plate in response to notochord signals, where it maintains its own expression through homeostatic induction. Shh protein is secreted and diffuses dorsally, setting up a concentration gradient. This gradient of Shh exhibits the properties of a morphogen, whereby cells respond to Shh differently at different threshold concentrations (Gurdon et al., 1999). At a given concentration of Shh protein therefore, cells will express specific genes (Briscoe et al., 2000). Within the chick neural tube two classes of homeodomain transcription factors have been shown to be negatively (class I) and positively (class II) regulated by Shh, and are important for establishing different pools of neural progenitor cells (Briscoe et al., 2000). The class II transcription factors are up regulated in response to Shh signalling in a concentration dependent manner (Briscoe and Ericson, 1999; Briscoe et al., 2000). Cells in ventral regions, receive the highest concentration of Shh and express class II genes such as Nkx2.2 and Nkx6.1. Nkx2.2 is only expressed in the most ventral cells, requiring a high concentration of Shh (approximately 3-4nM) for its activation (Ericson et al., 1997b) while Nkx6.1 which requires a lower concentration of Shh for its transcriptional activation (~0.25nM), is expressed in cells dorsal to those expressing Nkx2.2 (Briscoe et al., 2000).

Class I transcription factors in contrast are repressed by increasing concentrations of Shh (Ericson et al., 1997b). In a similar way to class II transcription factors, different genes respond in different ways to levels of Shh. While the expression of Pax7 can be almost completely repressed by 1nM of Shh, Pax6 requires a much higher dose to reduce its expression to comparable levels (Ericson et al., 1997b). The genes coding for class I proteins are promoted by Bone Morphogenetic Proteins (BMPs), which are expressed within most dorsal cells of the neural tube (Liem et al., 1997). As with class I transcription factors, class II genes respond to levels of BMPs in a dose dependant manner. Addition of BMP7 to cells in a defined concentration of Shh can direct cells toward a more dorsal fate changing their subtype identity (Liem et al., 2000). The genes Dbx1 and Dbx2 are expressed midway along the

dorsoventral axis of the neural tube, in a region where both Shh and BMP levels are low (Pierani et al., 1999). These genes are inhibited by high levels of Shh and BMP signalling, while reduction to the levels of either Shh or BMP moves their expression domains ventrally or dorsally respectively (Pierani et al., 1999; Timmer et al., 2002). These results describe an antagonistic relationship between BMPs and Shh which allows precise positioning of neural progenitor cells along the dorsoventral axis of the neural tube.

While levels of Shh and BMPs account for the initial expression of transcription factors along the dorsal ventral axis of the neural tube, the precise dorsal and ventral boundaries of expression domains are defined by cross repressive interactions between specific class I and class II genes giving rise to mutually exclusive areas of expression. The ventral boundary of the Class I gene Pax6, lies dorsal to cells expressing Nkx2.2 (Briscoe et al., 2000; Ericson et al., 1997b). If Pax6 expression is abolished then the dorsal boundary of Nkx2.2 extends dorsally with no requirement for increased Shh levels (Ericson et al., 1997b). The precise dorsal boundary of Nkx2.2 expression is therefore not defined by the level of Shh directly but is instead due to its repression by Pax6. These cross repressive interactions allow the initial gradient of Shh and BMP activity to be interpreted and refined as precise sharp boundaries of cells expressing distinct combinations of transcription factors. These boundaries demark neural progenitor domains which give rise to specific cell lineages. The formation of these boundaries therefore is a crucial step in the patterning of the neural tube (Briscoe et al., 2000; Lee and Pfaff, 2001), Figure 3.1).

Although Shh controls the induction of homeodomain transcription factor expression during the establishment of progenitor domains, their continued expression does not require sustained Shh signalling (Briscoe et al., 2000). Shh however retains the ability to modulate their expression patterns later on (Danesin et al., 2006). In chick embryos, the region of *Nkx2.2* expression expands dorsally due to a local rise in *Shh* expression subsequent to the establishment of the progenitor domains (Danesin et al., 2006). Cells which now co-express *Olig2* and *Nkx2.2* will differentiate to form oligodendrocytes (Agius et al., 2004). These oligodendrocytes are generated in this ventral region and then migrate dorsally to colonise the entire neural tube (Miller et al., 2004).

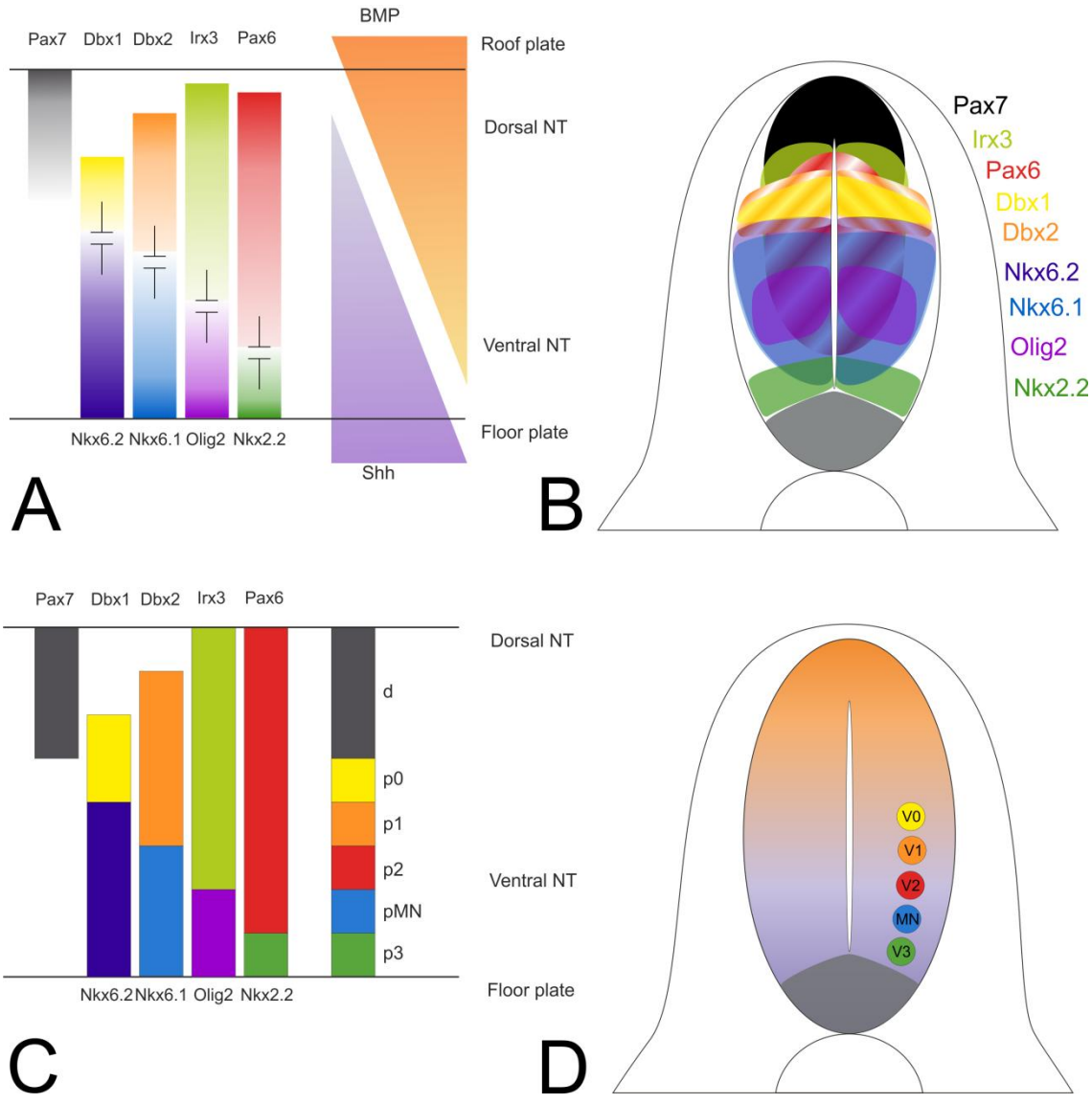

Figure 3.1 Expression boundaries of class I and class II homeodomain transcription factors within the chick neural tube.
(A) Gradients of Shh and BMP expression give rise to class II and class I transcription factor expression respectively, in a gradient dependent manner. (B) Spatial distribution of class I and II transcription factors within the neural tube. (C) Class I and II transcription factors cross repress each other (as shown in A), leading to the formation of sharp expression boundaries that define neural progenitor domains. (D) Each progenitor domain is characterised by a specific expression profile which defines the regions in which distinct neuronal subtypes form.
(Diagram adapted from Ayers et al., 2010; Briscoe et al., 2000; Lee and Pfaff, 2001)

If Shh levels are artificially increased, the onset of oligodendrogenesis is early, and markers of neural progenitors such as ngn2 are down regulated prematurely (Danesin et al., 2006), suggesting that although Shh is able to potentiate proliferation it also has the ability to drive the differentiation of cells in certain circumstances later during development. BMP4 is able to inhibit the differentiation of oligodendrocytes (Miller et al., 2004), pointing to a continued antagonistic relationship with Shh. Addition of Shh soaked beads into dorsal

regions gives rise to ectopic oligodendrocytes, while increasing the levels of BMP4 can inhibit the usual switch from neurogenesis to oligodendrogenesis (Miller et al., 2004)

3.1.2 Sulf1 and neuronal patterning

Sulf1 expression can be up regulated by Shh in quail embryos (Dhoot et al., 2001). Implantation of beads containing Shh induces ectopic Sulf1 expression while antagonising Shh signalling using anti-sense oligonucleotides inhibits Sulf1 within its usual expression domain (Dhoot et al., 2001). In the previous chapter I showed that Shh over expression can induce ectopic Sulf1 expression, while induction of Sulf1 requires Shh activity Figure 2.8.

Sulf1 is co-expressed with Shh within the floor plate and has been shown to affect the localisation of Shh (Danesin et al., 2006). Sulf1 may therefore be an important factor controlling patterning events or precursor specification during primary and secondary neurogenesis. Sulf2 has the same substrate specificity as Sulf1 (Ai et al., 2006) and is also expressed ventrally within the anterior neural tube (Winterbottom and Pownall, 2008). It may therefore similarly be a contributing factor in neuronal patterning.

6-OST is an important factor during HSPG biogenesis, catalysing the addition of sulfate groups to the 6-O position of the disaccharides of HS chains, and is expressed dorsally within the developing neural tube (Winterbottom and Pownall, 2008). BMPs are expressed in this region and are important for the specification of dorsal neuronal subtypes (Liem et al., 1997). Sulf1 has been shown to inhibit BMP signalling in animal caps (Freeman et al., 2008). The complimentary expression domains of Sulf1/2 and 6-OST within the neural tube, along with their opposing roles in the modification of HSPG chains, suggests that the polarisation of the sulfation state of HSPGs may be a factor in the determination of neuronal subtypes.

During the previous chapter the expression and interaction of Shh and Sulf1 was considered. The expression of *Ptc2* was also discussed as it indicates cells which respond to Shh signalling. The main focus of this chapter is the role which Sulf1 has during neural patterning. As discussed in chapter 1, there are two members of the Sulf family, Sulf1 and Sulf2. These two genes display differential patterns of expression, with *Sulf2* being expressed exclusively within anterior neural tissue. Within this region, *Sulf2* is expressed further dorsally than *Sulf1*. Figure 3.2 shows the expression of *Shh*, *Ptc2*, *Sulf1* and *Sulf2* at stage 23. While this work is mainly focussed on the role of Sulf1 during neuronal patterning, as Sulf1 and Sulf2 have the same substrate specificity, the role of Sulf2 will also be explored.

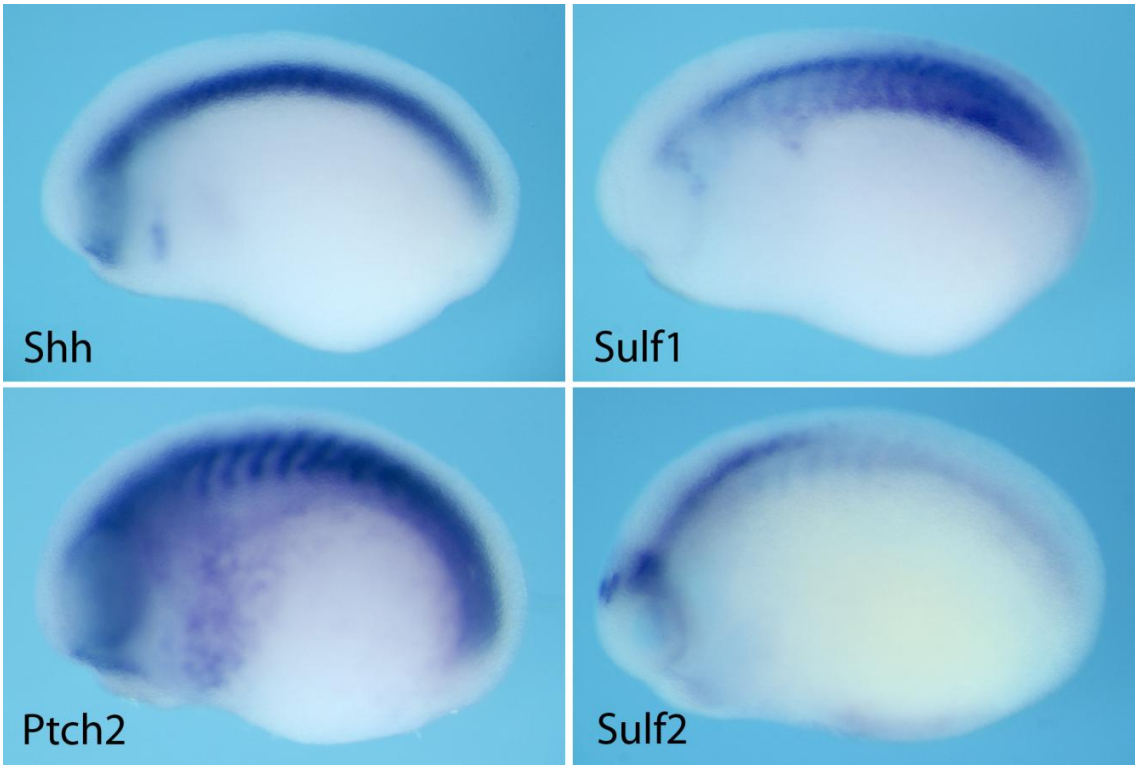

Figure 3.2 Whole mount *in situ h*ybridization analysis of stage 23 *X. tropicalis* embryos
At stage 23, *Shh* is expressed throughout the notochord and ventral neural tube, and extends through into the telencephalon. *Ptc2* is expressed within the ventral neural tube as well as the paraxial mesoderm which lies adjacent to the *Shh* expressing cells. *Sulf1* is similarly expressed within the ventral neural tube, as wll as the paraxial mesoderm; within the mesoderm however expression is strong posterirly and weak anteriorly. *Sulf1* is also expressed within the brain at this stage but not strongly. *Sulf2* is expressed anteriorly within the neural tube in a region dorsal to *Sulf1*, which extends through the the forebrain.

3.2 Aims

The aims for this chapter are to analyse the effects of Sulf knockdown on the development of the neural tube. This will be done using antisense morpholino oligonucleotides to inhibit the splicing or translation of Sulf1 and Sulf2 transcripts. Neural tube development will be analysed using histology, *in situ* hybridisation and immunohistochemistry. This analysis will specifically test the following hypotheses:

- Sulf1 is required for the establishment of neural progenitor populations along the dorsal ventral axis of the neural tube
- Sulf1 is required for the establishment of neural progenitor populations within the anterior neural tube
- Loss of Sulf1 affects the proliferation of neural progenitors
- Loss of Sulf1 affects the differentiation of cell types along the dorsal ventral axis of the neural tube

3.3 Methods

To investigate the role of Sulf1 during patterning of the neural tube, Sulf1 will be knocked down using the antisense morpholino oligonucleotide (AMO) S1MO3 as described in chapter 2. This chapter will also consider the role of Sulf2, which will also be knocked down using an AMO (S2MO4). Unlike the AMO used to knock down Sulf1 however, S2MO4 does not inhibit splicing of the mRNA but inhibits translation, preventing synthesis of the Sulf2 protein.

Throughout, when Sulf1 is knocked down the abbreviation S1MO3 will be used, while knockdown of Sulf2 will be indicated with S2MO4.

3.4 Results

3.4.1 Neuronal transcription factors are conserved between vertebrates

Chick has been used extensively to study the patterning of the neural tube, which has given rise to a standard model of dorsal-ventral neural patterning where cells express a specific set of transcription factors in response to differing levels of growth factors (Briscoe and Ericson, 2001). Using this established system therefore provides a good platform to analyse changes to growth factor signalling. A subset of the transcription factors that have been used to demark neuronal subtypes in chick were initially assessed to see whether they exhibit the same spatial distribution in *Xenopus* at stage 23 (Figure 3.3).

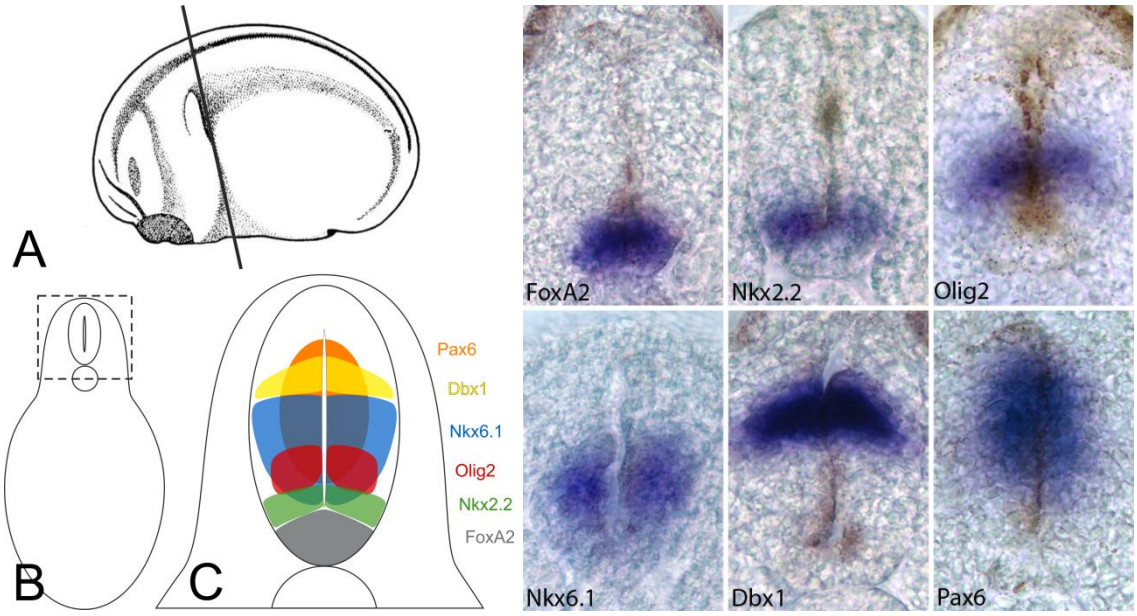

Figure 3.3 Whole mount *in situ h*ybridization analysis of stage 23 *X. tropicalis* embryos
(A) Embryos were transversely sectioned, and analysed at the same point along the anterior-posterior axis (black line). (B) Transverse sections as shown in (A) reveal a cross-section allowing visualisation of the neural tube (boxed) along the dorsal ventral axis. (C) Schematic showing the expression patterns of each of the genes analysed by *in situ* hybridization (shown right).

All of the genes analysed show the same spatial distribution in *Xenopus* as they do in chick, indicating a conserved mechanism for dorsal-ventral patterning. These transcription factors have been shown to be expressed in specific regions in response to growth factors, principally the concentration of Shh and BMP (Briscoe et al., 2000; Liem et al., 1997; Pierani et al., 1999). As the combination of these transcription factors present within cells gives rise to

discrete neuronal progenitor subtypes, any changes to the expression domains of these genes will alter the location and abundance of the cells that originate from those regions, resulting in an incorrectly patterned nervous system.

3.4.2 Shh signalling is required for floor plate and neuronal marker expression in *Xenopus*

Shh signalling has been shown to play a crucial role during floor plate induction and ventral neuronal patterning (Briscoe and Ericson, 1999; Chiang et al., 1996; Ericson et al., 1996). Recent work however has suggested that as in fish (Hatta et al., 1991; Schier et al., 1997; Strahle et al., 1997), the requirement of Shh for floor plate induction in *Xenopus* is not as crucial as it is in chick and mouse (Peyrot et al., 2011). The authors of this paper suggest that Shh only plays a minor role in floor plate induction. They show that the expression of *Nkx2.2* in the lateral floor plate requires Shh signalling while *FoxA2* expression is not dependent on the presence of Shh. Previous research however has identified a role for Shh in floor plate induction in *Xenopus* (Lopez et al., 2003; Ruiz i Altaba et al., 1995). To reconcile these conclusions in a quantitative manner, the expression of the floor plate marker *FoxA2*, the ventral marker *Nkx2.2* and a more dorsal marker *Dbx1* were analysed by qPCR. Figure 3.4 shows the

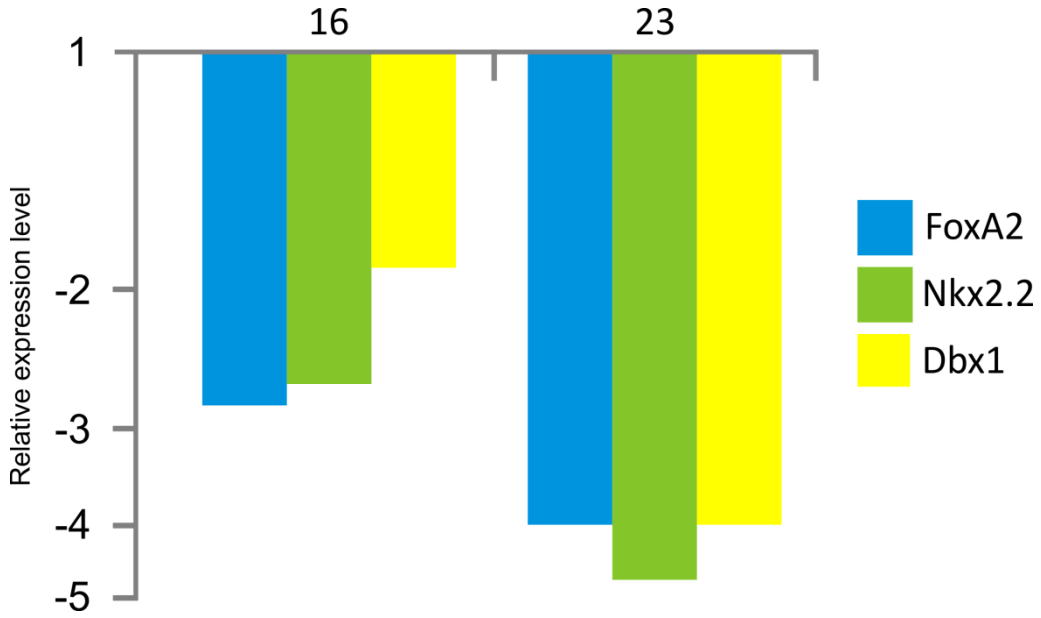

Figure 3.4 Expression levels of target genes following inhibition of Shh signalling
qRT PCR analysis of target genes following knockdown of Sulf1. At stage 16 cyclopamine treamtnet leads to the down regulation of *FoxA2*, *Nkx2.2* and *Dbx1*. Down regulation of all three genes is increased at stage 23 indicating a role for Shh signalling in the regulation of these genes throughout neurulation. Data is log transformed such that relative values less than one are shown as negative.

expression levels of *FoxA2*, *Nkx2.2* and *Dbx1* following treatment with 100µM cyclopamine, compared with ethanol treated controls. At the open neural plate stage (16), when neurectoderm overlaying the notochord is induced to form floor plate, cyclopamine treatment leads to a reduction in the expression of all three genes, with *FoxA2* showing almost a 3 fold reduction in its expression level (Figure 3.4 left). By stage 23 when the neural tube has closed and *Shh* expression is strong in both the notochord and floor plate, *FoxA2* and *Dbx1* exhibit approximately a 4 fold reduction in their expression levels following cyclopamine treatment, while *Nkx2.2* is reduced almost 5 fold (Figure 3.4 right). A reduction in FoxA2 expression following cyclopamine treatment can also be observed when analysed by *in situ* hybridisation (ISH) (Figure 3.5). While ISH does not provide an accurate measure of the relative level of expression between different samples, it is clear that expression is reduced following cyclopamine treatment. The reduction in the expression of *Nkx2.2* and *Dbx1* suggests that, as in other vertebrates, Shh is a crucial regulator of neuronal patterning. Additionally the reduction in *FoxA2* expression indicates that Shh is also required for the specification of floor plate identity. The persistence of *FoxA2* medially within the floor plate suggests that Shh is not absolutely required for the initiation of medial floor plate identity, but that Shh is required during the expansion of the floor plate region. Therefore despite the recent report that *FoxA2* expression is unchanged following cyclopamine treatment in *Xenopus* (Peyrot et al., 2011), the evidence reported here suggests that Shh signalling does have a role in the regulation of *FoxA2* expression within the floor plate, at least under the experimental conditions used within this study, and it will be assumed that this is the case for the remainder of this work.

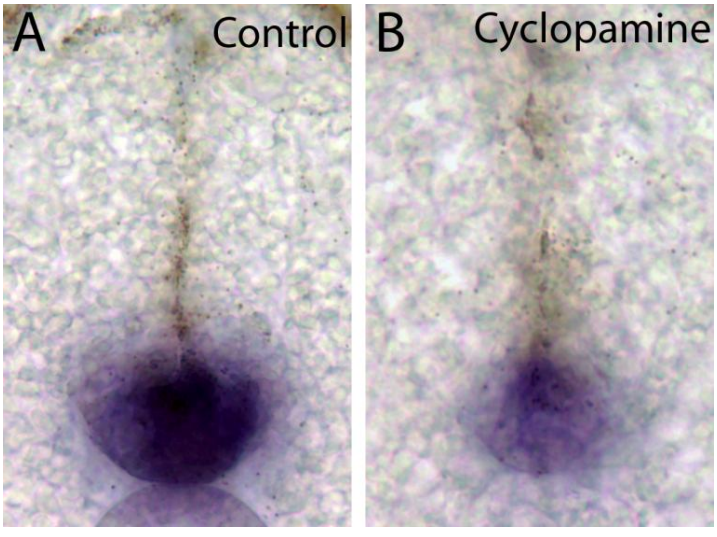

Figure 3.5 Transverse sections from whole mount *in situ* hybridization analysis of *FoxA2* expression in stage 23 *X. tropicalis* treated with cyclopamine
While *FoxA2* is strongly expressed within the floor plate of control embryos (A), treatment with 100µM cyclopamine results in a significant reduction in expression levels (B).

3.4.3 *Sulf1* over expression promotes ventral neuronal markers

It has been shown in chick that over expression of *Sulf1* can promote ectopic expression of the ventral neuronal marker *Nkx2.2* (Danesin et al., 2006). To investigate whether this ability is conserved in *Xenopus*, *Sulf1* was over expressed by injection of mRNA. Figure 3.6 shows the expression of *Nkx2.2* within the ventral neural tube of stage 23 *X tropicalis* embryos. Following bilateral injection of *Sulf1*, expression of is *Nkx2.2* up regulated and extends dorsally compared with the expression seen in controls. This indicated that, as in chick, Sulf1 is able to promote ectopic expression of Shh target genes within the neural tube of *Xenopus*.

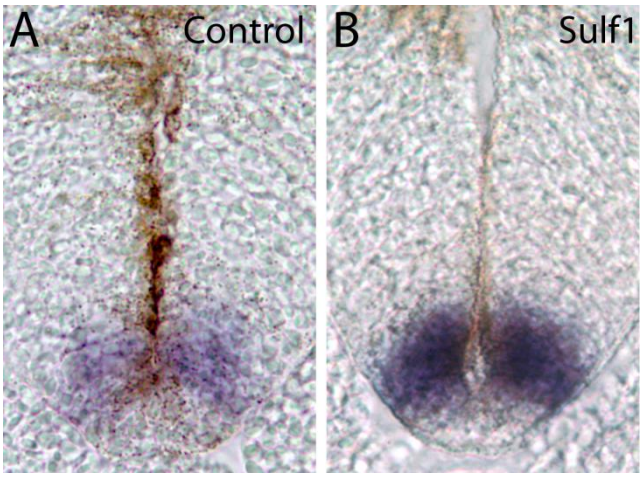

Figure 3.6 Transverse sections from whole mount *in situ hybridization* analysis of *Nkx2.2* expression in stage 23 *X. tropicalis* embryos bilaterally injected with 2ng Sulf1
Nkx2.2 is expressed within the ventral neural tube, in a domain adjacent to the floor plate (A). Following over expression of *Sulf1*, *Nkx2.2* expression is increased, and extended slightly dorsally (B).

3.4.4 Sulf1 is required for correct neural patterning

As described in the previous chapter, *Shh* and *Sulf1* show overlapping expression in the midline from open neural plate stages, and continue to be co-expressed within the floor plate throughout development. This co-expression, together with the well documented requirement for HSPGs during Hh signalling in flies (Bellaiche et al., 1998; Bornemann et al., 2004; The et al., 1999), raises the possibility that Sulf1 may act to regulate hedgehog signalling within the ventral neural tube. Ectopic expression of *Sulf1* has been shown to effect *Nkx2.2* expression in chick (Danesin et al., 2006) and *Xenopus* (above). These experiments however do not establish whether endogenous Sulf1 is required for correct neural progenitor specification. To analyse whether Sulf1 and Sulf2 are required for correct neuronal patterning, embryos were bilaterally injected with antisense morpholino oligonucleotides (AMOs) to knock

down either the function of Sulf1 (single knockdown), or Sulf1 and Sulf2 simultaneously (double knockdown). Embryos were subsequently analysed via *in situ* hybridisation using the genes outlined in Figure 3.3. Following the knockdown of Sulf1, the floor plate marker FoxA2 is expressed in a more restricted region such that expression within the lateral floor plate is lost and expression is confined to the ventral midline (Figure 3.7B). In the double knockdown, a similar restriction in the expression domain of *FoxA2* can be seen (Figure 3.7C). In both cases, the reduction in *FoxA2* is very similar to that seen following inhibition of Shh signalling following treatment with cyclopamine (Figure 3.5). *Nkx2.2* expression is normally restricted to a group of cells just dorsal to the floor plate (Figure 3.7D). In single and double knockdowns the entire expression domains is shifted ventrally such that expression is now seen within the ventral midline occupying the same region that *FoxA2* does in control embryos (Figure 3.7E-F). Sulf1 knockdown extends the region of Nkx6.1 dorsally, although this expansion is very subtle compared with the changes observed for other genes (Figure 3.7K). The interneuron marker Dbx1 shows a similar change in its expression pattern following the knockdown of either Sulf1 or Sulf1 and Sulf2 simultaneously. In control embryos the ventral boundary of Dbx1 is flat (Figure 3.7M). Following Sulf knockdown however, its medial region of expression moves dorsally while laterally, expression moves ventrally such that when viewed transversely the expression region resembles a chevron (Figure 3.7N-O). Pax6 shows rather a marked change in response to the knockdown of Sulf1, with a large lateral expansion of its expression domain. Its ventral boundary however does move slightly dorsally (Figure 3.7Q). When Sulf1 and Sulf2 are knocked down simultaneously, the lateral expansion of Pax6 expression remains, however the ventral boundary returns to its original position (Figure 3.7R).

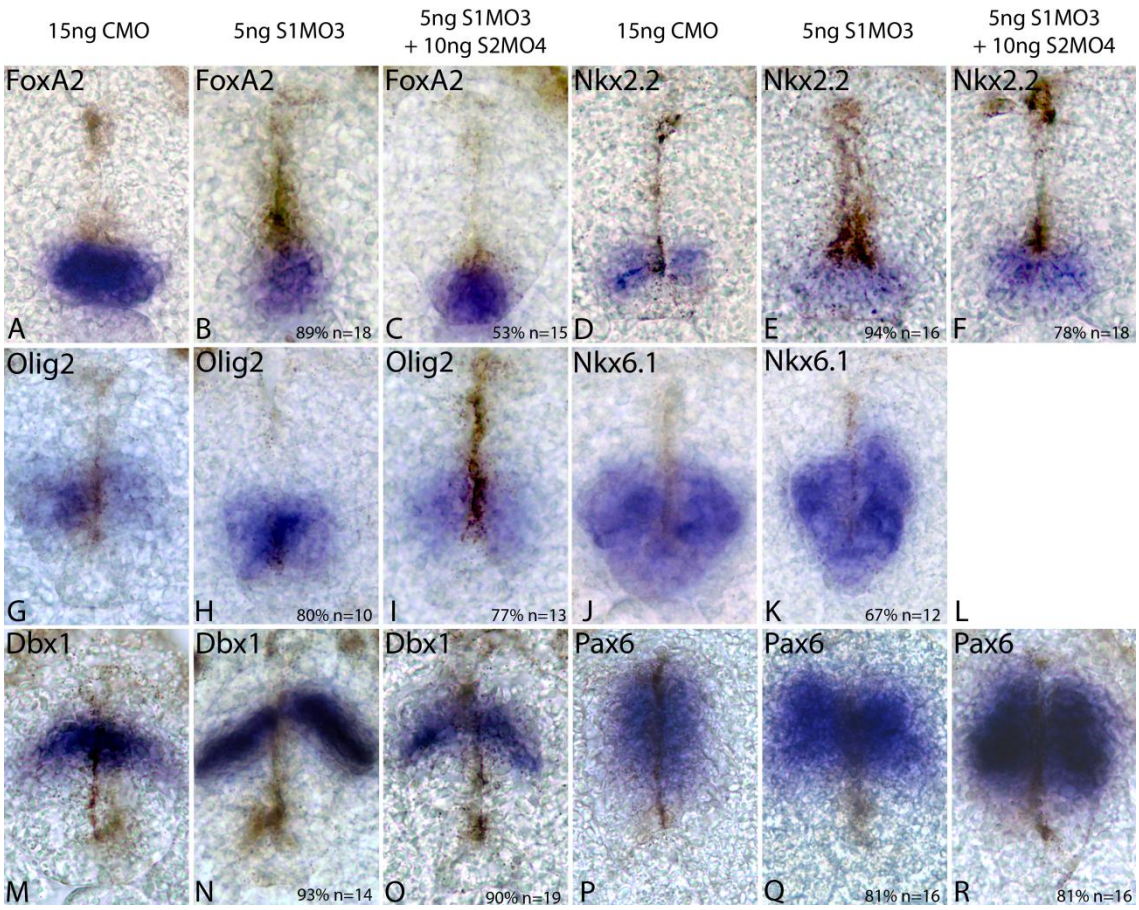

Figure 3.7 Transverse sections from whole mount *in situ h*ybridization analysis of stage 23 *X. tropicalis* embryos bilaterally injected with either 5ng of S1MO3 or 5ng S1MO3 + 10ng S2MO4
(A) FoxA2 is expressed throughout the floor plate. (B) Following Sulf1 knockdown, FoxA2 expression is reduced and confined to the medial cells of the ventral neural tube.
(C) Knockdown of Sulf2 with Sulf1 has a similar effect to single knockdown, with a loss of lateral regions of FoxA2 expression (D) Nkx2.2 expression is restricted to a band of cells just dorsal to the medial floor plate. (E) Sulf1 knockdown results inNkx2.2 being expressed further ventrally such that it occupies the ventral midline. (F) Knockdown of Sulf2 with Sulf1 also gives rise to midline expression of Nkx2.2. (G) Olig2 is expressed in a ventral region of the neural tube just dorsal to the Nkx2.2 expression domain. (H) Sulf1 knockdown leads to a ventral shift in the entire expression domain of Olig2. (I) Simultaneous knockdown of Sulf1 and Sulf2 leads to a partial recovery of the Olig2 expression domain, although the level of expression appears reduced. (J) Nkx6.1 is expressed in a region from just dorsal to Olig2, down to floor plate. (K) Sulf1 knockdown extends the region of Nkx6.1 expression dorsally particularly within the medial region. (M) Dbx1 is expressed in a region of the neural tube which lies dorsal to that of the Nkx6.1 region, with expression levels higher medially than laterally. (N) Sulf1 knockdown results in Dbx1 being expressed further dorsally in medial regions, but further ventrally in lateral regions. (O) Concomitant Sulf2 knockdown gives rise to a similar change in Dbx1 expression as the single knockdown. (P) Pax6 shows extensive expression within the neural tube extending from a region dorsal to that of Dbx1 to just dorsal of Nkx2.2. (Q) Sulf1 knockdown gives rise to a lateral expansion of the Pax6 domain. Expression does however not extend as far ventrally as in controls. (R) Knockdown of Sulf2 with Sulf1 restores the ventral boundary to the position observed inn control embryos. The lateral expansion of Pax6 seen in single knockdowns is also found in double knockdowns.
(L) No in situ hybridisation was carried out for this probe and set of injections

Although transverse sections give an accurate view of the dorsal ventral axis, they only provide information about a very small section of the overall expression within the embryo. When viewed transversely *Dbx1* does not change dramatically following Sulf knockdown. Similarly, *Olig2* only seems to change following Sulf1 knockdown, and its expression pattern is almost restored when Sulf2 is knocked down along with Sulf1, although its expression does appear to be weaker. When each of these genes is looked at wholemount however, a much different picture of the expression dynamics emerges. Figure 3.8 Shows expression of *Dbx1* and *Olig2* from both lateral and dorsal views. *Dbx1* is expressed throughout the neural tube, and extends anteriorly into the forebrain. From a lateral view, *Dbx1* expression does not seem to show any dramatic changes following Sulf1 knockdown (Figure 3.8B). When observed from a dorsal view however, differences can be seen. In control embryos *Dbx1* is expressed in two thin stripes down the midline (Figure 3.8D). Following Sulf1 knockdown, these thin expression regions are expanded laterally (Figure 3.8E). Additionally if looked at closely, the expression of *Dbx1* is not in a continuous line but more in distinct regions which abut each other to form a line of expression. Following Sulf1 knockdown these expression regions appear to be fewer in number but larger. Furthermore, there are some regions where there is no expression such that the continuous line is broken up (Figure 3.8E black arrow heads). While in control embryos, expression within the brain appears stronger that that further posteriorly, this difference is reduced following Sulf1 knockdown. When Sulf2 is knocked down along with Sulf1, the observed gaps in expression are larger and more numerous, and expression appears to be weaker generally (Figure 3.8F). Reduced expression is particularly apparent within the brain.

Olig2 expression is more varied, than *Dbx1*, being expressed ventrally within the neural tube, dorsally within the hindbrain, within the neural crest, the eye and the forebrain (Figure 3.8G,J). Following Sulf1 knockdown, all anterior regions of expression are reduced, especially within the neural crest (Figure 3.8H black arrow head) and hindbrain (Figure 3.8K black arrow head). More posteriorly, *Olig2* is no longer even expressed throughout the neural tube displaying a reduction within the anterior neural tube, but an increase posteriorly (Figure 3.8H). When Sulf2 is also knocked down, some anterior regions of

expression are almost completely lost, such as the neural crest and forebrain (Figure 3.8I). Expression within the neural tube is reduced further compared with the single knockdown, although posterior expression is still higher (Figure 3.8I,L).

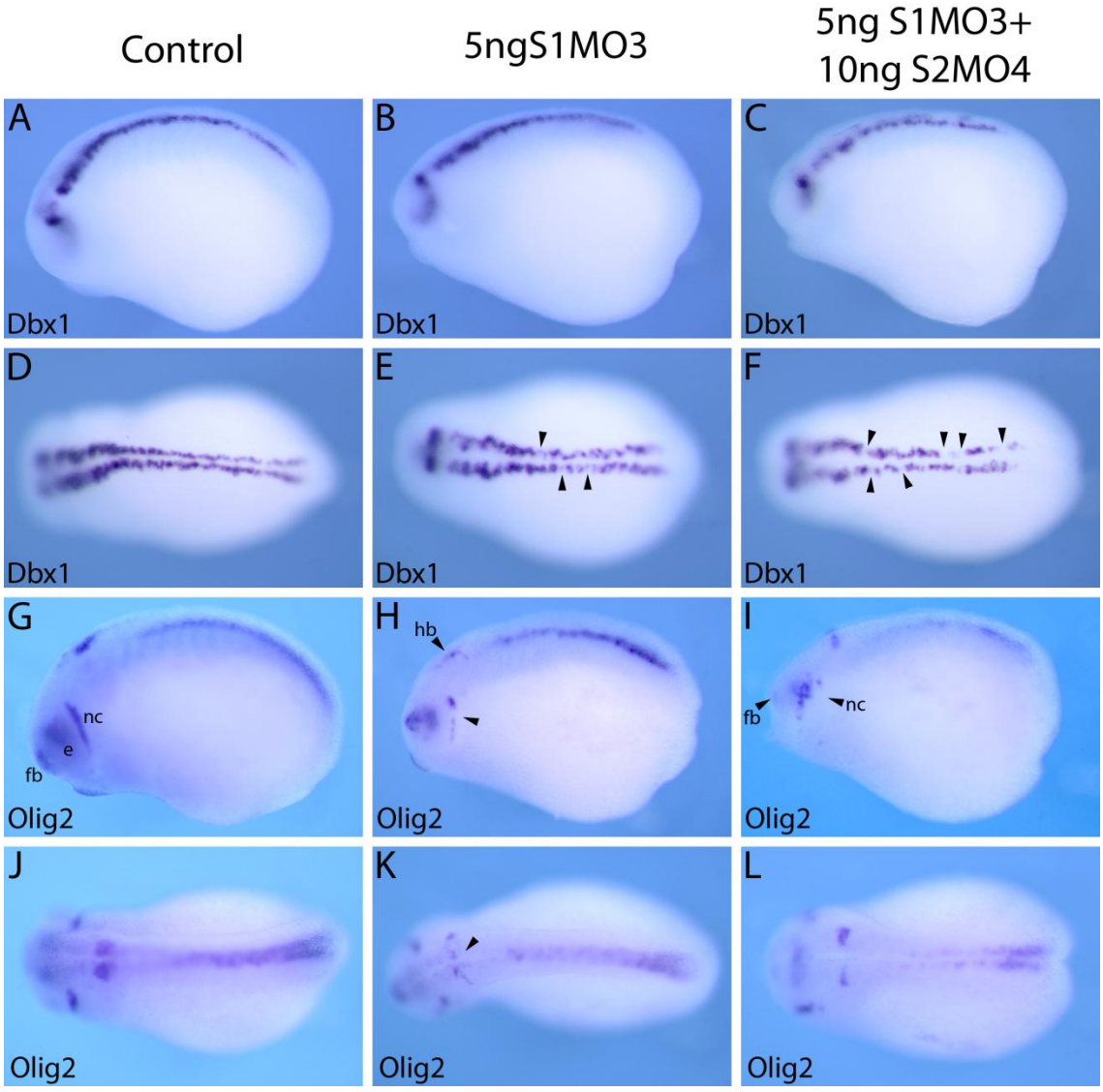

Figure 3.8 Whole mount *in situ h*ybridization analysis of stage 23 *X. tropicalis* embryos bilaterally injected with either 5ng of S1MO3 or 5ng S1MO3 + 10ng S2MO4

(A,D) *Dbx1* is expressed dorsally within the neural tube throughout the anterior posterior axis, and extends into the brain. (B,E) Following Sulf1 knockdown, *Dbx1* expression is expanded laterally, while gaps appear between increasingly discrete domains of expression (black arrow heads). (C,F) *Dbx1* expression is increasingly scattered and discontinuous when Sulf2 is additionally knocked down. (G,J) *Olig2* is expressed ventrally within the neural tube, dorsally within the hindbrain, within the neural crest, the eye and the forebrain. (H,K) *Olig2* expression is reduced in anterior regions following knockdown of Sulf1. Within the neural tube, expression is reduced anteriorly, whereas posterior expression remains high. (I,L) Knockdown of Sulf1 and Sulf2 results in an almost complete loss of expression within the neural crest and forebrain. Expression within the neural tube is also reduced further.

fb - forebrain,e - eye, nc - neural crest, hb - hindbrain

3.4.5 Expression levels of neuronal markers are reduced in response to Sulf knockdown

While *in situ* hybridisation data can give information about changes to the spatial distribution of genes, the degree to which their expression level changes cannot be satisfactorily determined. To more accurately determine the degree to which each gene changes following Sulf knockdown, expression levels were analysed via qPCR (Figure 3.9). Each of the genes was normalised to ODC and expression levels were compared to those seen in control embryos injected with 15ng CMO. Every gene analysed was down regulated following the knockdown of both Sulf1 singly and Sulf1 and Sulf2 together. No significant difference was seen between the single and double knockdown, with the exception of *Gsh2*, where knockdown of Sulf2 lead to a partial recovery of expression. Double knockdown also appears to further reduce *Dbx1* levels compared with the single knockdown, although due to the variation observed between the different biological samples it is not possible to say with certainty whether this is the case. These results show that neuronal transcription factors exhibit a significant reduction in their expression level as well as a change to their spatial distribution following Sulf knockdown.

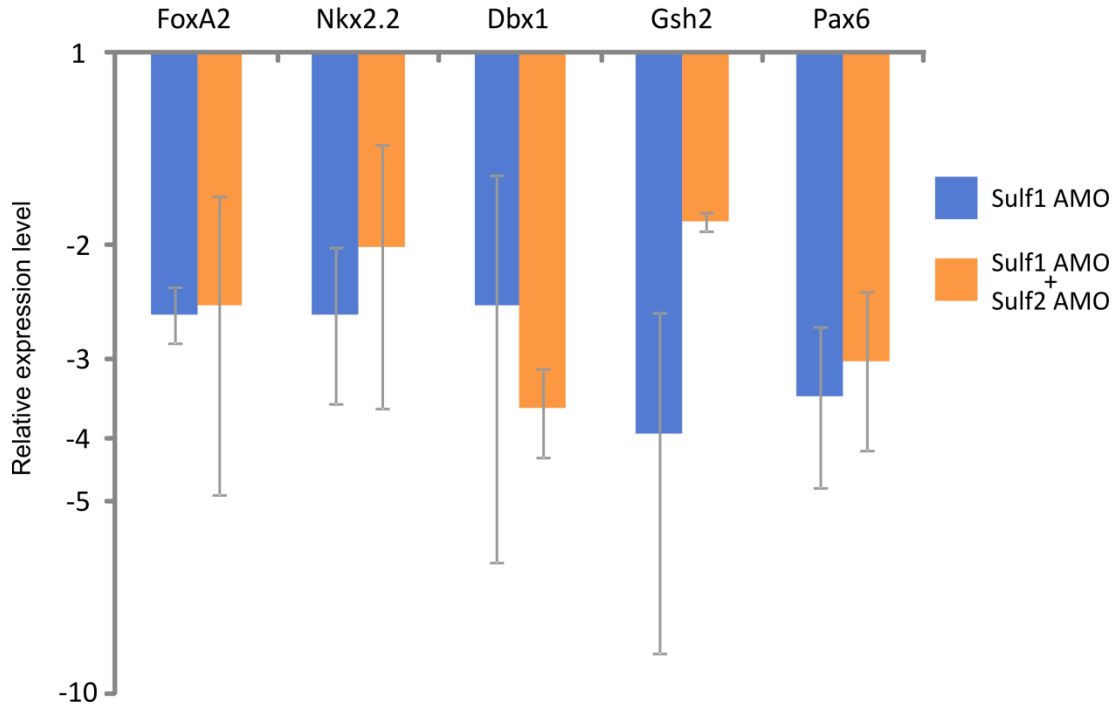

Figure 3.9 Expression levels of target genes following knockdown of Sulf1 and Sulf2
qRT-PCR analysis of target genes following knockdown of Sulf1 alone (blue bars) or Sulf1 and Sulf2 together (orange bars). Expression level is relative to embryos injected with 15ng of a control non-specific morpholino (CMO), and normalised to ODC. Data is log transformed such that relative values less than one are shown as negative. Means calculated from 2 biological replicates. Error bars show the standard error of the mean.

3.4.6 Pax6 expression is increased within the neural tube following Sulf knockdown

One unexpected result from the qPCR data is that the level of *Pax6* expression is reduced following Sulf knockdown. From the *in situ* hybridisation data shown in Figure 3.7 an enlargement of the expression domain of *Pax6* can be observed following Sulf knockdown. Additionally the level of staining was greatly increased, especially in the double knockdown (Figure 3.7R), suggesting an increase in the expression level of *Pax6*. Although these results seem at odds, they can be resolved if the embryo is looked at as a whole. Sulf knockdown leads to a large change to the morphology of the embryo, with a marked decrease in the size of the head structures. *Pax6* expression is a crucial factor for the development of the eye and is expressed throughout the eye field during stage 23; the stage at which embryos were analysed (Figure 3.10). The change to the size of the developing head, results in a significant reduction in *Pax6* expression, so any small increase in *Pax6* observed within the neural tube is masked.

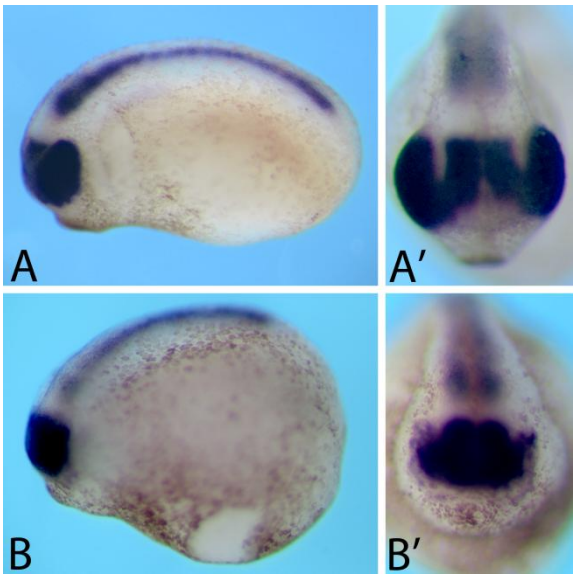

Figure 3.10 Whole mount *in situ hybridization* analysis of stage 23 *X. tropicalis* embryos bilaterally injected with 5ng S1MO3 + 10ng S2MO4
(A) *Pax6* is expressed dorsally within the neural tube but shows particularly strong expression within the forebrain and eyes. (B) Following knockdown of Sulf1 and Sulf2, anterior structures are reduced in size leading to a large reduction in the size of the eyes and loss of *Pax6* expression. A' and B' show anterior views of the embryos pictured in A and B respectively.

To attempt to separate out the confounding factor of the loss of the head on Pax6 expression levels, embryos were dissected before RNA extraction so separating the head from the main body (as shown in Figure 3.11), allowing analysis of changes to expression levels specifically within the neural tube. When the expression of the same genes is analysed using cDNA generated from only the posterior of the embryo a similar reduction in expression level can be seen for most of the genes (Figure 3.12). *Pax6* however is no longer seen to

be reduced but shows a slight increase in its expression level following Sulf1 knockdown.

Figure 3.11 Separation of anterior and posterior
Diagram showing the separation of the head from the body before RNA extraction to allow analysis of expression changes within the neural tube. Embryos were cut along their dorsal-ventral axis as shown by the black line (picture left) to give an anterior and posterior section (picture right).

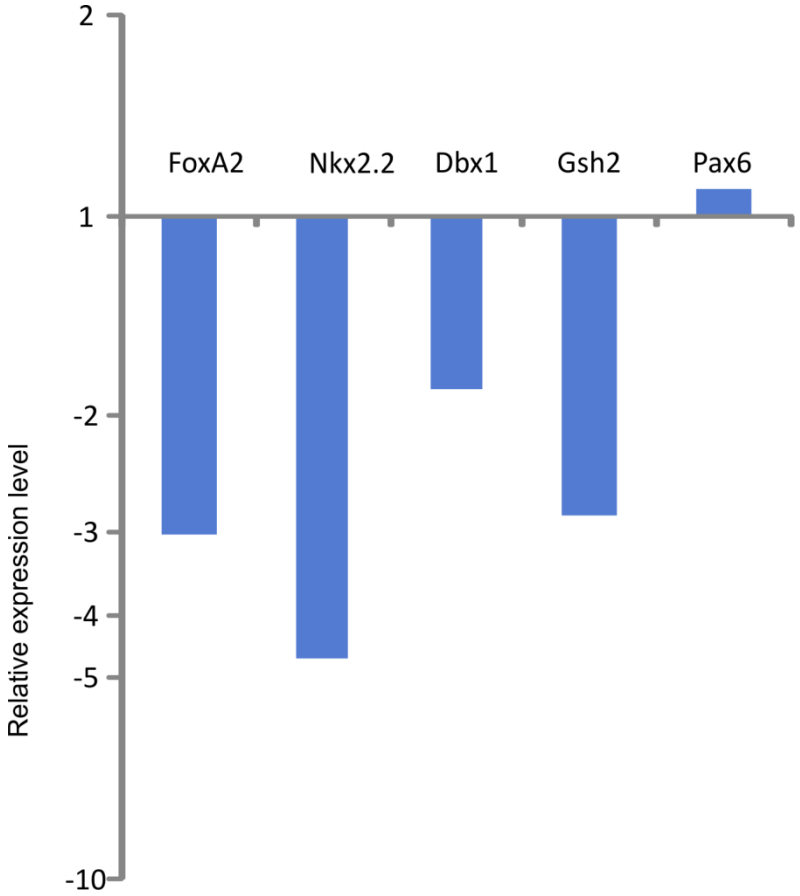

Figure 3.12 Expression levels of target genes within the neural tube following knockdown of Sulf1
qRT PCR analysis of target genes reveals that all are down regulated within the neural tube following Sulf1 knockdown, with the exception of Pax6 which shows a small increase in its level of expression. Expression level is relative to embryos injected with 15ng of a control
non-specific morpholino (CMO), and normalised to ODC. Data is log transformed such that relative values less than one are shown as negative.

3.4.7 A microarray screen to find genes affected by Sulf1

To identify additional genes that may be affected by Sulf1 a microarray screen was undertaken. Embryos were injected with either 2ng Shh or 2ng Sulf1, cultured until stage 23 and then snap frozen. RNA was extracted and used to synthesise cDNA. Targets were selected on the basis that they show the same directional response to *Shh* and *Sulf1* over expression. Table 3.1 shows the most interesting targets based on their expression changes and on their function. Many of the targets identified were expressed within anterior domains. Although *Foxg1* does not show a large change in response to either Sulf1 or *Shh* over expression it was added to the target list due to its role in forebrain development.

Gene		Fold difference	
		Shh	Sulf1
Evi-1	Antagonist of BMP/TGFbeta/activin	2.53	3.20
Frizzled 8	Transmembrane receptor in the Wnt signalling pathway	1.81	1.58
Fezf2	Zinc-finger DNA binding protein	1.69	1.61
Dlx2a	homeodomain and LIM zinc binding domain transcription factor	1.50	1.68
Foxg1b	Forkhead domain transcription factor	1.43	1.29
Vent2	Homeobox transcription factor BMP target	-1.83	-1.75

Table 3.1 Genes showing the greatest change following over expression of either Sulf1 or Shh from microarray analysis
Genes selected on the basis that they exhibit a change greater than 1.5 fold following over expression of either *Shh* or *Sulf1*. Although Foxg1 does not fit this category, it was selected as a potential candidate due to its role during forebrain development.

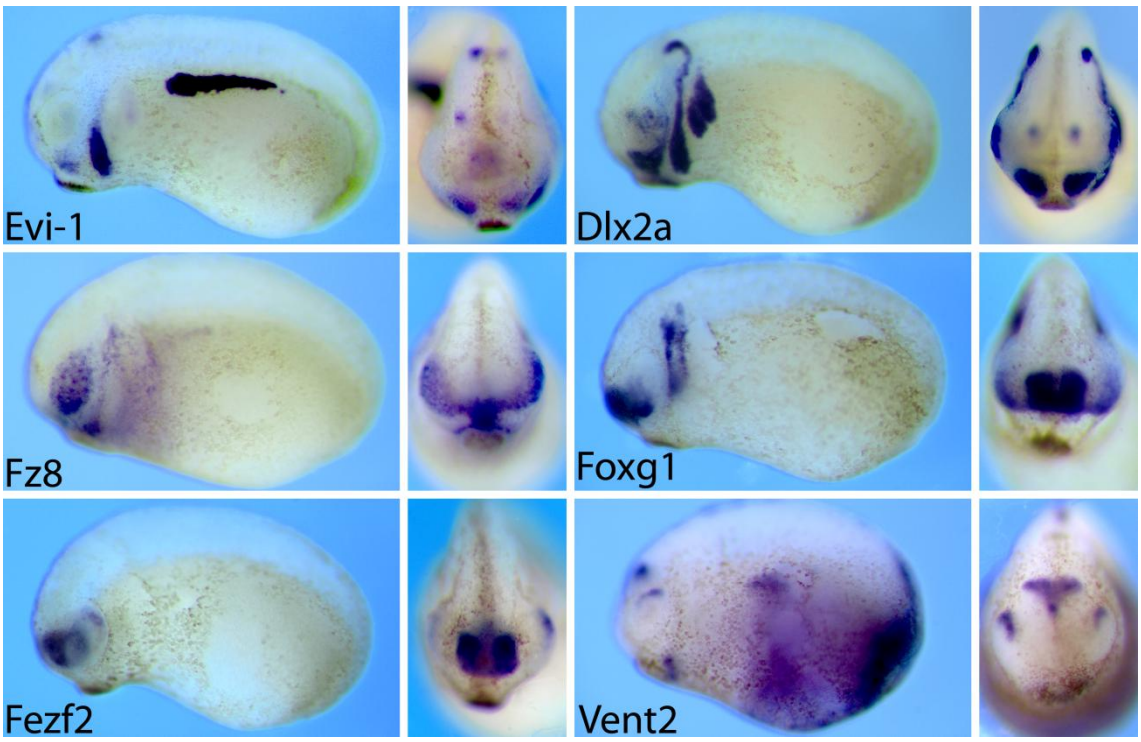

Figure 3.13 Whole mount *in situ* hybridization analysis of microarray targets in NF stage 23 *X. tropicalis* embryos
Expression domains of 6 genes identified from the microarray analysis. All of the genes show anterior regions of expression, specifically within the forebrain (Fezf2,Foxg1), eyes (Fz8,Dlx2a,Vent2) and neural crest (Evi-1,Fz8,Dlx2a,Foxg1).

In situ hybridization probes were synthesised to analyse the expression patterns of each of the top targets. Figure 3.13 shows side and anterior views of each of the six genes at NF stage 23. All of the targets that are positively regulated by Shh and Sulf1 show predominantly anterior regions of expression while Vent2, which is negatively regulated by Shh and Sulf1, is predominantly expressed posteriorly.

Targets were validated using *in situ* hybridization. Sulf1 was over expressed as for the microarray study, and Sulf1 and Sulf2 waere knocked down as previously discussed. *Evi-1* is expressed within a number of discrete regions within the anterior of the embryo including the forebrain, midbrain, rhombomere 4 and neural crest. Further posteriorly *Evi-1* is expressed within the pronephros (Figure 3.14A,A'). Following Sulf knockdown, Evi-1 expression is completely lost in all anterior regions. The only remaining expression is located within the pronephric duct, and this expression region is shortened in the anterior-posterior axis but expanded in the dorsal-ventral axis (Figure 3.14C,C'). When

Sulf1 is over expressed however, expression within neural crest is expanded, while the expression within the brain increased, although no ectopic regions of expression are observed (Figure 3.14E,E'). *Dlx2a* is strongly expressed within the migrating neural crest, and more weakly within the eye. Two expression regions within the forebrain can also be seen (Figure 3.14B,B'). Following Sulf knockdown, neural crest expression is severely reduced, while expression within the eye and brain is completely lost (Figure 3.14D,D'). Over expression of Sulf1 gives rise to a change in the neural crest expression of *Dlx2a* similar to that observed in other neural crest markers following over expression of Sulf2 (Guiral et al., 2010). Expression within the eyes is significantly increased, while ectopic expression can be seen within the forebrain (Figure 3.14F,F' arrow head). *Foxg1* is expressed in the forebrain and neural crest (Figure 3.14G,G'). Following Sulf knockdown, neural crest expression is significantly reduced. Although the expression domain within the forebrain is reduced in size, this appears only to be due to an overall reduction in the size of anterior structures as *Foxg1* expression remains strong (Figure 3.14I,I'). Sulf1 over expression slightly expands the *Foxg1* positive region, but not to any significant degree. Neural crest expression also appears unaffected (Figure 3.14K,K'). *Vent2* is expressed in a number of discrete regions in a similar manner to *Evi-1*. Expression can be seen within the forebrain, midbrain, dorsally within the eye, the otic vesicle and the roof plate (Figure 3.14H,H'). *Vent2* is also expressed widely within the endoderm (Figure 3.14H end). Following Sulf knockdown, ventral posterior expression of *Vent2* remains mainly unchanged (Figure 3.14J). Expression within the otic vesicle is lost, while dorsal eye expression is reduced, although this is expected due to the large reduction in the size of the eye field following Sulf knockdown (Figure 3.14J). The two regions of expression within the brain, which are normally separated, are now juxtaposed (arrow) and expanded laterally (arrow head) (Figure 3.14J'). As seen in the microarray, over expression of Sulf1 leads to a large reduction in the expression of *Vent2* (Figure 3.14L). Expression within the eyes is reduced and shifted dorsally while expression within the brain is completely lost (Figure 3.14L,L'). Posterior expression is greatly reduced, although strong *Vent2* expression remains within the tail and pronephros (Figure 3.14L).

.

Figure 3.14 Whole mount *in situ h*ybridization analysis of stage 23 *X. tropicalis* embryos bilaterally injected with either 5ng S1MO3 + 10ng S2MO4 (Sulf1/2 KD), or 2ng Sulf1
(A,A') *Evi1* is expressed within the forebrain and midbrain as well as rhombomere 4. *Evi1* also shows domains of expression within the neural crest and the pronephros.(C,C') Following knockdown of Sulf1 and 2 all anterior expression is lost. Expression within the pronephros is shortened in the anterior posterior axis, while expanded dorsally. (E,E') Over expression of Sulf1 leads to up regulation of *Evi1* in all anterior domains. Expression is particularly high within the diencephalon (black arrow head) and the second arch (arrow). Pronephric expression remains largely unaffected, although there is a small gap within its expression domain.
(B,B') *Dlx2a* is strongly expressed within the neural crest. Weaker expression can also be seen within the eye and two discrete regions in the forebrain. (D,D') Knockdown of Sulf1 and 2 leads to a large reduction in neural crest expression, as well as a complete loss of expression within the eye and forebrain. (F,F') Sulf1 over expression results in defective neural crest migration. Expression within the eye is significantly increased and ectopic expression can be seen within the forebrain (arrow head). (G,G') *Foxg1* is expressed within the neural crest and strongly within the forebrain. (I,I') Knockdown of Sulf1 and 2 does not significantly affect expression within the forebrain, whereas neural crest expression is reduced. (K,K') Over expression of Sulf1 gives rise to only minor changes in *Foxg1* expression in both the forebrain and neural crest.
(H,H') *Vent2* is expressed in distinct regions anteriorly, within the eye dorsally, as well as the forebrain, diencephalon and otic vesicle. Weak expression can also be seen within the roof plate. (J,J') Knockdown of Sulf1 and 2 leads to a lateral expansion of midbrain expression (arrow head), while the forebrain expression is shifted rostrally (arrow). Expression within the dorsal eye is reduced in line with the reduction in the size of the eye field. (L,L') Sulf1 over expression leads to a reduction in all expression domains, except the most posterior expression within the tail.

Images shown with ' are the anterior view of the adjacent lateral view

Abbreviations: **e**, eye; **end**, endoderm; **fb**, forebrain; **nc**, neural crest
mb, midbrain; **ov**, otic vesicle; **pn**, pronephros; **r4**, rhombomere 4; **rp** roof plate

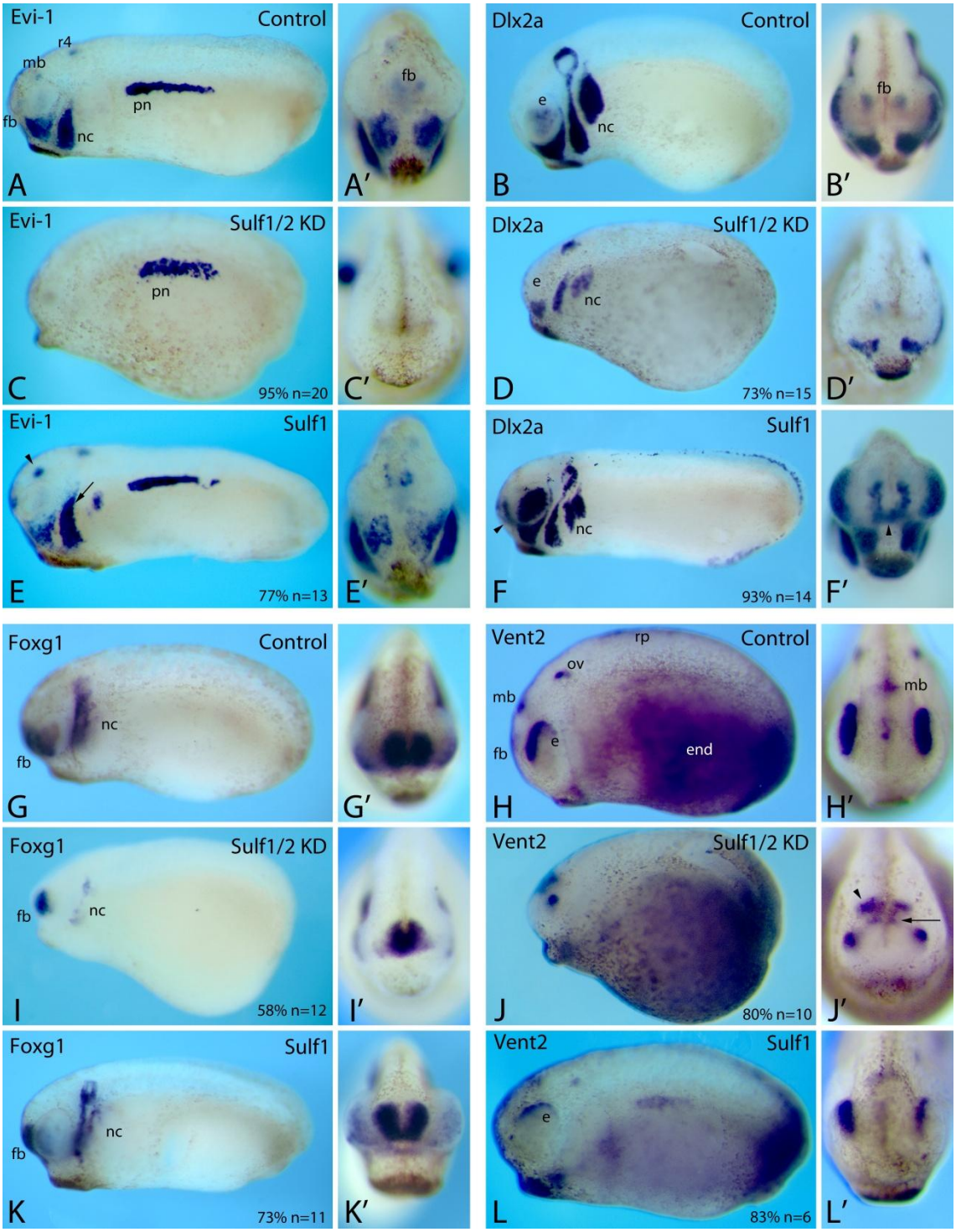
Evi-1
Control
r4
mb
pn
fb
nc
A
A′
Dlx2a
Control
e
nc
fb
B
B′
Evi-1
Sulf1/2 KD
pn
95% n=20
C
C′
Dlx2a
Sulf1/2 KD
e
nc
73% n=15
D
D′
Evi-1
Sulf1
77% n=13
E
E′
Dlx2a
Sulf1
nc
93% n=14
F
F′
Foxg1
Control
nc
fb
G
G′
Vent2
rp
Control
ov
mb
e
fb
end
H
H′
Foxg1
Sulf1/2 KD
fb
nc
58% n=12
I
I′
Vent2
Sulf1/2 KD
80% n=10
J
J′
Foxg1
Sulf1
nc
fb
73% n=11
K
K′
Vent2
Sulf1
e
83% n=6
L
L′

3.4.8 Shh and Sulf1 work synergistically

For the microarray screen discussed above, targets were chosen based on the fact that they were regulated in a similar fashion by both Shh and Sulf1. Thus far, all of the analysis has focussed on the role which either Shh or Sulf have independently. The data suggests however that Shh and Sulf1 act together, and that loss or gain of function of one impacts on the other. To further analyse the ability of Sulf1 to modulate Shh signalling, Sulf1 was over expressed at a level which in itself has very little impact on either morphology or gene expression. Shh was then expressed at low level either alone or with Sulf1 to see whether Sulf1 was able to alter the effects of Shh.

Figure 3.15 shows the anterior expression of *Nkx2.2* and *Vent2* following over expression of either Shh or Sulf1 alone, or both together. Following injection of 500pg of Sulf1 alone, *Nkx2.2* shows no change in its expression pattern or level (Figure 3.15B). Injection of 500pg of Shh however leads to an increase in the level of Nkx2.2 expression, and ectopic expression can be seen within the eyes (Figure 3.15C). Co-injection of Sulf1 with Shh leads to an expanse in the region expressing *Nkx2.2* and ectopic expression within the eyes is significantly stronger (arrow) (Figure 3.15D). *Vent2* similarly shows little change following injection of Sulf1, with only a minor increase in the level of telencephalic expression (arrow) (Figure 3.15F). Over expression of Shh leads to ectopic *Vent2* expression within the telencephalon which connects up the usually discrete telencephalic and diencephalic regions of expression within the brain (Figure 3.15G). Co-injection of Sulf1 with Shh leads to a significant expansion of this region (arrow) (Figure 3.15H).

The ability of Sulf1 to extend the range over which Shh can exert an effect can also be seen within the neural tube. Transverse sections of the embryos shown in Figure 3.15 reveal that as well as increasing the ability of Shh to promote *Nkx2.2* expression ectopically within the brain and eyes, Sulf1 also extends the expression region of *Nkx2.2* induced by Shh within the neural tube. Figure 3.16 shows the expression of *Nkx2.2* in stage 23 *X tropicalis* embryos following over expression of Shh and Sulf1. As observed in whole embryos, over expression of 500pg of Sulf1 alone does not significantly change the expression of Nkx2.2

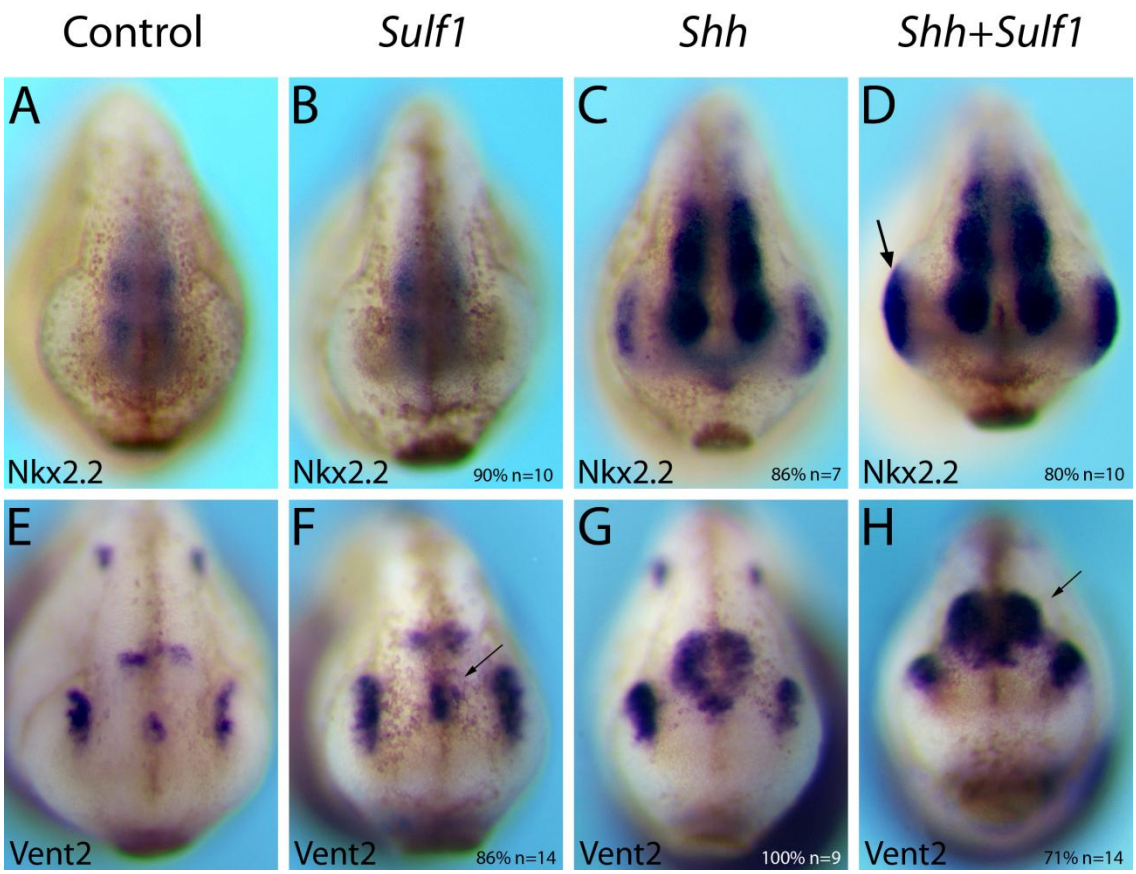

Figure 3.15 Whole mount *in situ h*ybridization analysis of stage 23 *X. tropicalis* embryos bilaterally injected with either 500pg*Sulf1*, 500pg *Shh* or *Sulf1* and *Shh* together
(A) *Nkx2.2* is normally expressed in the midbrain and forebrain. (B) Following over expression of Sulf at a low level (500pg) *Nkx2.2* shows no change in its expression domain.(C) Over expression of *Shh* leads to an up regulation of *Nkx2.2* expression within the brain. Additional regions of expression can also be seen within the eyes. (D) When *Sulf1* and *Shh* are co-expressed *Nkx2.2* shows an increase in its region of expression within the brain compared with over expression of Shh singly. The increase in *Nkx2.2* expression however is most notable in the eyes (arrow).(E) *Vent2* is expressed within the telencephalon, the diencephalon and dorsally within the eyes. (F) *Sulf1* over expression (500pg) has verry little effect on *Vent2* expression; telencephalic (arrow) and eye expression are slightly increased. (G) Over expression of *Shh* leads to an upregulation of *Vent2* wthin the brain, such that the two distinct regions of expression are now joined together. (H) Co-expression of *Shh* and *Sulf1* further increases the level of *Vent2* expression within the brain (arrow).

(Figure 3.16B,C). When *Shh* is over expressed at a low level, *Nkx2.2* is slightly up regulated but not significantly (Figure 3.16C). Co-injection of *Shh* and *Sulf1* together however dramatically changes the expression of *Nkx2.2* such that it occupies nearly half of the neural tube (Figure 3.16D). These results again suggest that Sulf1 acts within the neural tube to promote hedgehog signalling.

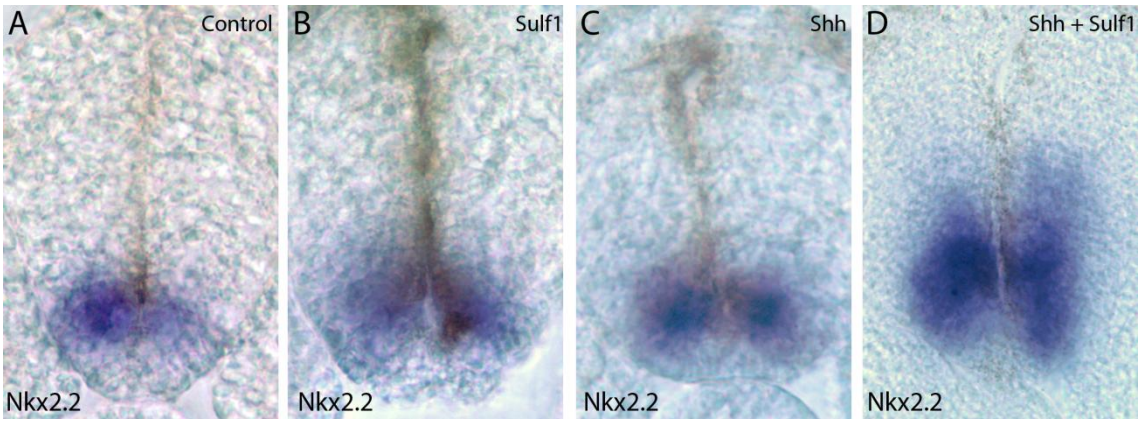

Figure 3.16 Transverse sections showing *Nkx2.2* expression in stage 23 *X. tropicalis* embryos bilaterally injected with either 500pg *Sulf1*, 500pg *Shh* or *Shh* and *Sulf1* together
(A) Expression of *Nkx2.2* in the ventral neural tube. (B) Following injection of 500pg *Sulf1*, the region of *Nkx2.2* expression does not significantly change. (C) Injection of 500pg *Shh* increases *Nkx2.2* expression slightly, extending its dorsal boundary. (D) Co-expression of *Shh* and *Sulf1* dramatically increases the expression of *Nkx2.2*, leading to a shift in its dorsal boundary.

3.4.9 *Isl1* expresion within the MN domain requires Sulf1

The expression data shown above indicates that transcription factors which specify cell fate are altered following changes to endogenous sulfation (Figure 3.7), and that within the ventral neural tube, Sulf1 is able to promote the expression of Shh target genes. Within the ventral neural tube, motor neurons are specified in cells in response to Shh signalling (Ericson et al., 1996). For the differentiation of motor neurons, Shh is not only required initially but in a sustained way such that if levels are lowered following the initial expression of progenitor markers, differentiation of motor neurons will still not occur (Ericson et al., 1996). Loss of Sulf1 leads to a change in the expression regions of transcription factors which define the motor neuron domain (Nkx6.1, Olig2 Figure 3.7) as well as a reduction in the level of *Ptc2*, indicating reduced levels of Shh signalling (Chapter 2 Figure 2.14). Taken together this suggests that the sulfation state of HSPGs, as defined by *Sulf1* expression, is a crucial factor in the ability to specify motor neuron fate. The *Islet1* (*Isl1*) gene is expressed in cells which differentiate into motor neurons, and *Isl1* expression is a prerequisite for motor neuron differentiation (Pfaff et al., 1996; Shi et al., 2009). *Isl1* expression can therefore be used as a marker of motor neuron differentiation within the ventral neural tube.

To further investigate the role of HSPG sulfation in the establishment of motor neurons within the neural tube, HSPGs were hypo- or hyper-sulfated by the

unilateral injection of Sulf1 or 6-OST respectively. To investigate the endogenous role of Sulf1 in motor neuron specification, Sulf1 was knocked down by the injection of S1MO3. Additionally, embryos were unilaterally injected with Shh or treated with cyclopamine to examine the effects of the potentiation or inhibition of Shh hedgehog signalling on *Isl1* expression within the neural tube of *Xenopus*. Figure 3.17 shows the expression of *Isl1* within the neural tube of stage 23 *X. tropicalis* embryos. Expression can be seen within three distinct domains corresponding to regions of motor neuron (MN), ventral interneuron (VIN) and dorsal interneuron (DIN) populations (Figure 3.17A). Following the unilateral injection of *Sulf1*, the ventral and dorsal interneuron populations appear to move laterally and are reduced in size (Figure 3.17B VIN,DIN). The ventral motor neuron domain however is significantly expanded on the injected side (Figure 3.17B MN). Unilateral injection of 6-OST leads to expansion of the ventral interneuron *Isl1* domain (Figure 3.17C VIN). The motor neuron domain however appears to no longer be present following 6-OST expression (Figure 3.17C MN). Cyclopamine treatment leads to a significant reduction in the expression of ventral *Isl1*, and a dorso-lateral shift of dorsal expression (Figure 3.17D). The differential repression of *Isl1* expression on each side of the embryo is most likely due to the insolubility of cyclopamine which leads to incomplete penetrance of the drug. Over expression of *Shh* gives rise to an expansion of ventral and dorsal *Isl1* expression on the injected side, but also on the un-injected side to a lesser degree (Figure 3.17E). Knockdown of Sulf1 appears to shift the *Isl1* positive motor neuron population ventrally as well as narrowing the region which these cells occupy (Figure 3.17F MN).

When the changes in hedgehog signalling following over expression of Shh are compared with changes in HSPG sufation following the over expression of Sulf1, it can be seen that *Isl1* expression within the motor neuron domain is very similar (Figure 3.17B,E). Furthermore *Isl1* expression within the motor neuron domain following 6-OST over expression is reminiscent of *Isl1* expression in

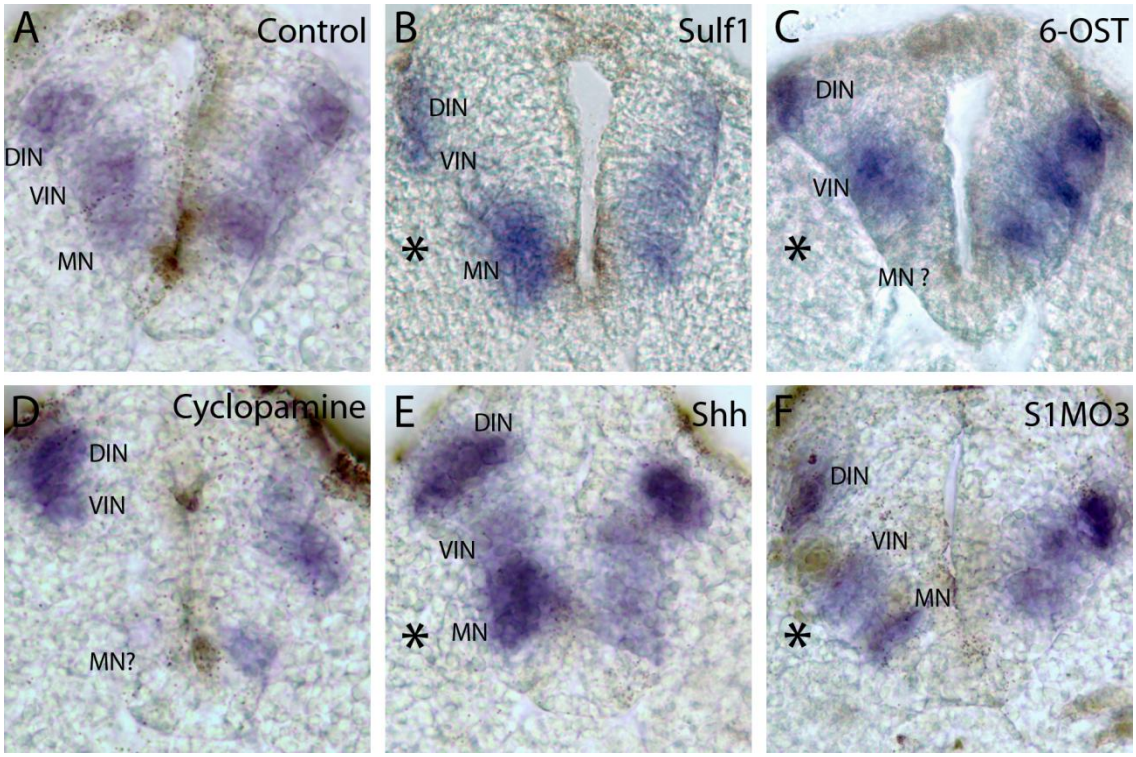

Figure 3.17 Transverse sections from whole mount *in situ h*ybridization analysis of Isl1 expression in stage 23 *X. tropicalis* embryos

(A) *Isl1* is expressed in three discrete regions within the neural tube corresponding to precursor populations of motor neurons (MN), ventral interneurons (VIN) and dorsal interneurons (DIN). (B) Following unilateral injection of *Sulf1* the two most dorsal domains appear reduced and are shifted laterally. The expression region corresponding to motor neurons is expanded dorsally on the injected side. (C) Unilateral over expression of 6-OST leads to a dorsal shift in *Isl1* expression with an apparent loss of the motor neuron domain. The intermediate region of expression does however appear to be expanded. (D) Cyclopamine treatment of embryos leads to a loss of ventral *Isl1* expression within the motor neuron domain. Dorsal expression remains but is shifted further dorsally. (E) Over expression of *Shh* expands the motor neuron doman. Dorsal expression is similarly expanded while ventral interneuron *Isl1* expression appears to be unaffected. (F) Sulf1 knockdown gives rise to a ventral shift in the motor neuron and ventral interneuron regions of *Isl1* expression. Dorsal interneuron expression appears to be largely unaltered.

* indicates injected side

cyclopamine treated embryos. The reason for this may be that 6-OST over expression leads to a reduced level of Shh signalling (Chapter2 Figure 2.12). In contrast to the result seen following hyper-sulfation of HSPGs by 6-OST, loss of Sulf1 does not completely inhibit ventral *Isl1* expression but shifts it further ventrally, suggesting that Sulf1 normally acts to regulate the precise location in which motor neurons will differentiate.

3.4.10 Sulf1 knockdown leads to an expansion of the dorsal neural tube

While changes to transcription factor levels following Sulf knockdown can be seen at stage 23, more general changes to morphology can be observed at this stage. Following analysis of sections of the neural tube, it was observed that there were changes to the shape of the neural tube in single and double knockdown embryos. To quantify the shape change in neural tube, the ratio of the width of the floor plate to the width of the neural tube at its widest point was measured. In control embryos, the neural tube is 2.4 times the width of the floor plate (Figure 3.18 CMO). This relative width is increased to 3.7 times and 3.6 times when Sulf1 is knocked down singly (Figure 3.18 S1MO3) or together with Sulf2 (Figure 3.18 S1MO3 + S2MO4) respectively, representing a significant change in width ($p<0.001$).

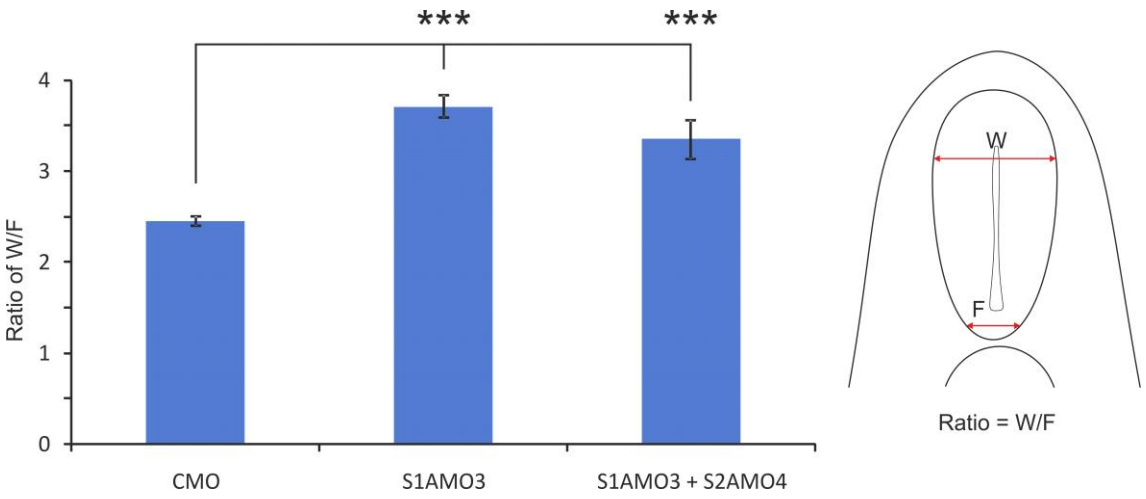

Figure 3.18 Ratio of the width of the neural tube at its widest point to the width of the floor plate

The width of the neural tube at its widest point (W) was measured and this was compared with the width of the floor plate (F) (shown diagram right). The mean ratio value is shown. Mean ratio values were compared using a 1-way ANOVA. The difference in the W/F ratio is significant between CMO and S1 and CMO and S1+S2 ($p<0.001$***).There is however no significant difference between S1 and S1+S2. Error bars display standard error of the mean, n=11.

3.4.11 Expansion of dorsal neural tube is not a result of increased proliferation

The observed change in the shape of the neural tube may be due to an increase in proliferation of cells within the dorsal neural tube compared with the ventral neural tube giving rise to an increase in the ratio of the widths observed. To analyse whether an increased number of proliferative cells arises following Sulf knockdown, antibody staining using the proliferation marker Phospho-histone 3 (PH3) was undertaken. Figure 3.19 shows sections through the neural tube of *X. tropicalis* embryos at stage 23 stained for PH3 (green) and

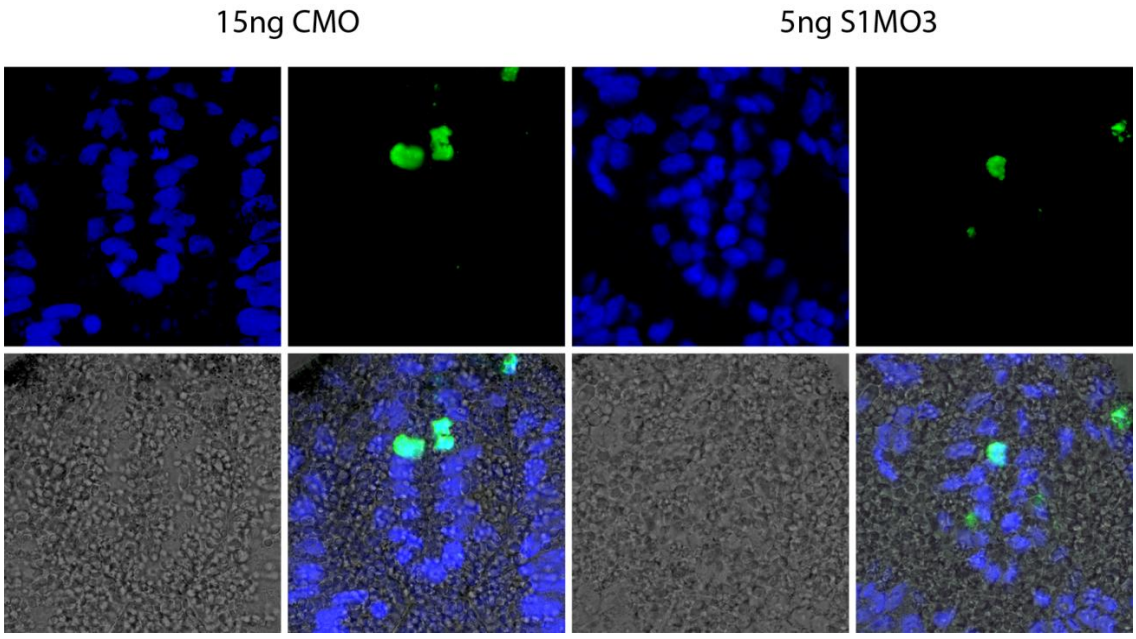

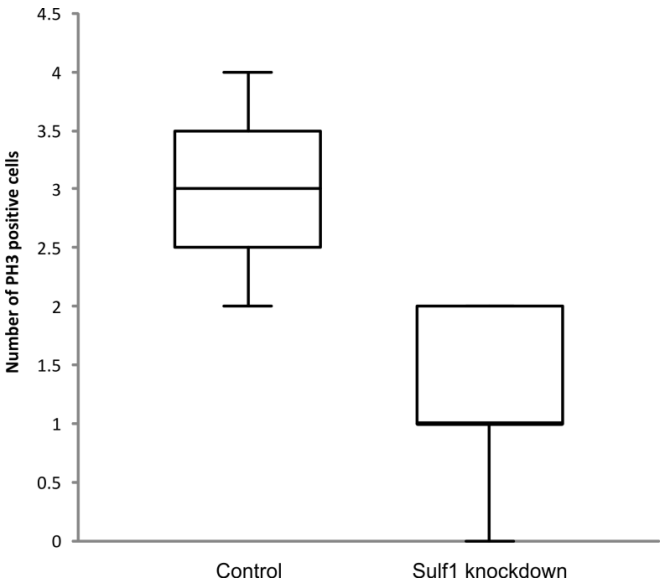

Figure 3.19 PH3 staining in transverse sections through *X. tropicalis* embryos at NF stage 22
Top: Antibody staining with the mitotic cell marker Phospho-histone3 (PH3) reveals a small number mitotic cells within the neural tube. Following knockdown of Sulf1 the number of cells positive for PH3 is reduced.
Bottom: Box plot showing the number of PH3 positive cells in control and Sulf1 knockdown embryos. Sulf1 knockdown leads to a significant reduction in the number of actively mitotic cells (Student's T-test $P<0.001$, $n=9$).

counterstained with DAPI (blue). In control embryos injected with 15ng of CMO, 3 mitotic cells can be seen within the neural tube. Following knockdown of Sulf1 however, only 1 cell within the neural tube is actively proliferative. Due to the very small number of positively stained cells, samples were taken over a number of experiments and the number of PH3 positive cells counted. In control samples the number of positive cells ranged from 2 to 4, with an average of 3. In samples where Sulf1 had been knocked down, the number of PH3 positive cells ranged from 0 to 2 with an average of 1.22. This reduction in the number of cells represents a significant difference (Student's T-test $p<0.001$). This shows that the change to the shape of the neural tube is not due to an increase in proliferation and that proliferation is actually significantly reduced following the loss of Sulf1.

3.4.12 Loss of proliferative cells coincides with a change in differentiation

The mitosis marker PH3 only stains cells actively undergoing mitosis and therefore does not give any indication as to the number of cells that remain in the proliferative pool of cells within the neural tube. The reduction in PH3 positive cells does however suggest that the number of actively proliferating cells within the neural tube is diminished following Sulf1 knockdown. Therefore cells which would normally be present in the population of proliferative precursors may have been induced to differentiate prematurely. To assess this possibility, expression of X-Myt1 was analysed. X-Myt1 acts during the determination of neurons, allowing cells to escape lateral inhibition and undergo differentiation (Bellefroid et al., 1996). X-Myt1 marks cells that have withdrawn from the cell cycle and have begun to differentiate and can therefore be used to assess whether there is an increase in the number of cells differentiating within the neural tube in the absence of Sulf1. At a glance it would appear that the number of X-Myt1 positive cells is increased following Sulf1 knockdown (Figure 3.20). This observation is consistent with the idea that Sulf1 knockdown reduces the number of cells within the proliferative population. X-Myt-1 positive cells were quantified, and the average number observed within a 10µM section was increased from 14 in control embryos, to 17 in Sulf1 knockdown embryos. Despite the apparent increase however, due to the variability in the data, this increase is not significant (Student's t-test $p=0.1$). It is therefore not possible to

determine whether Sulf1 knockdown does increase the number of cells induced to undergo differentiation prematurely from these data.

Although no difference in the number of X-Myt1 positive cells was observed following Sulf1 knockdown, differences can be seen in the position of those cells. In control embryos, X-Myt1 positive neurons are located within the lower two thirds of the neural tube. The most ventral are situated more medially than those dorsal to them, thus forming a V shape (Figure 3.20 CMO). Following Sulf1 knockdown however, Myt1 positive cells can be found throughout the dorsal ventral axis of the neural tube and those seen within the dorsal half of the neural tube are located medially compared with those seen in control embryos (Figure 3.20).

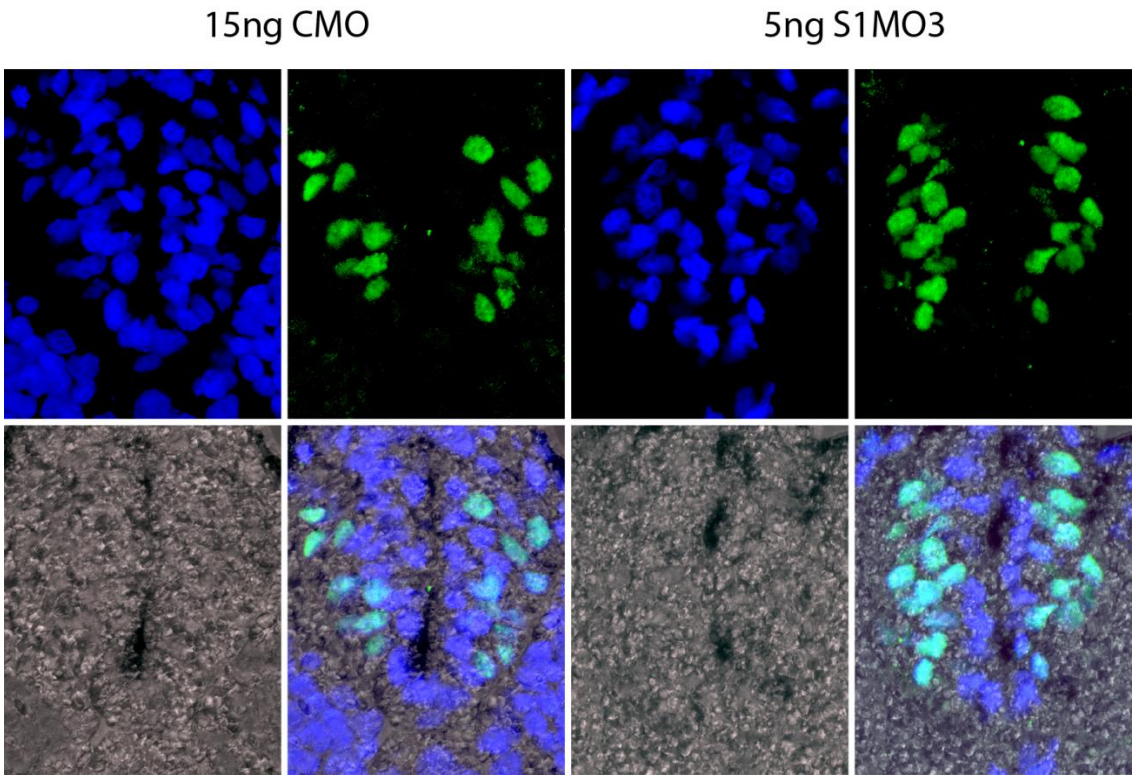

Figure 3.20 X-Myt1staining in transverse sections through *X. tropicalis* embryos at NF stage 23

Antibody staining with the pro-differentiation factor X-Myt1. Knockdown of Sulf1 changes the spatial distribution of positively stained cells such that they occupy a more medial position and are distributed further dorsally than in control embryos.

To quantify the differences observed between control and Sulf knockdown embryos, the position of X-Myt1 positive cells was measured as compared with the midline of the neural tube or with the floor plate. Figure 3.21 shows the average distance of each of the cells from the midline, and the distance of the most dorsal X-Myt1 positive cell from the floor plate. The average distance of X-Myt1 positive cells from the midline is greater and less variable in control

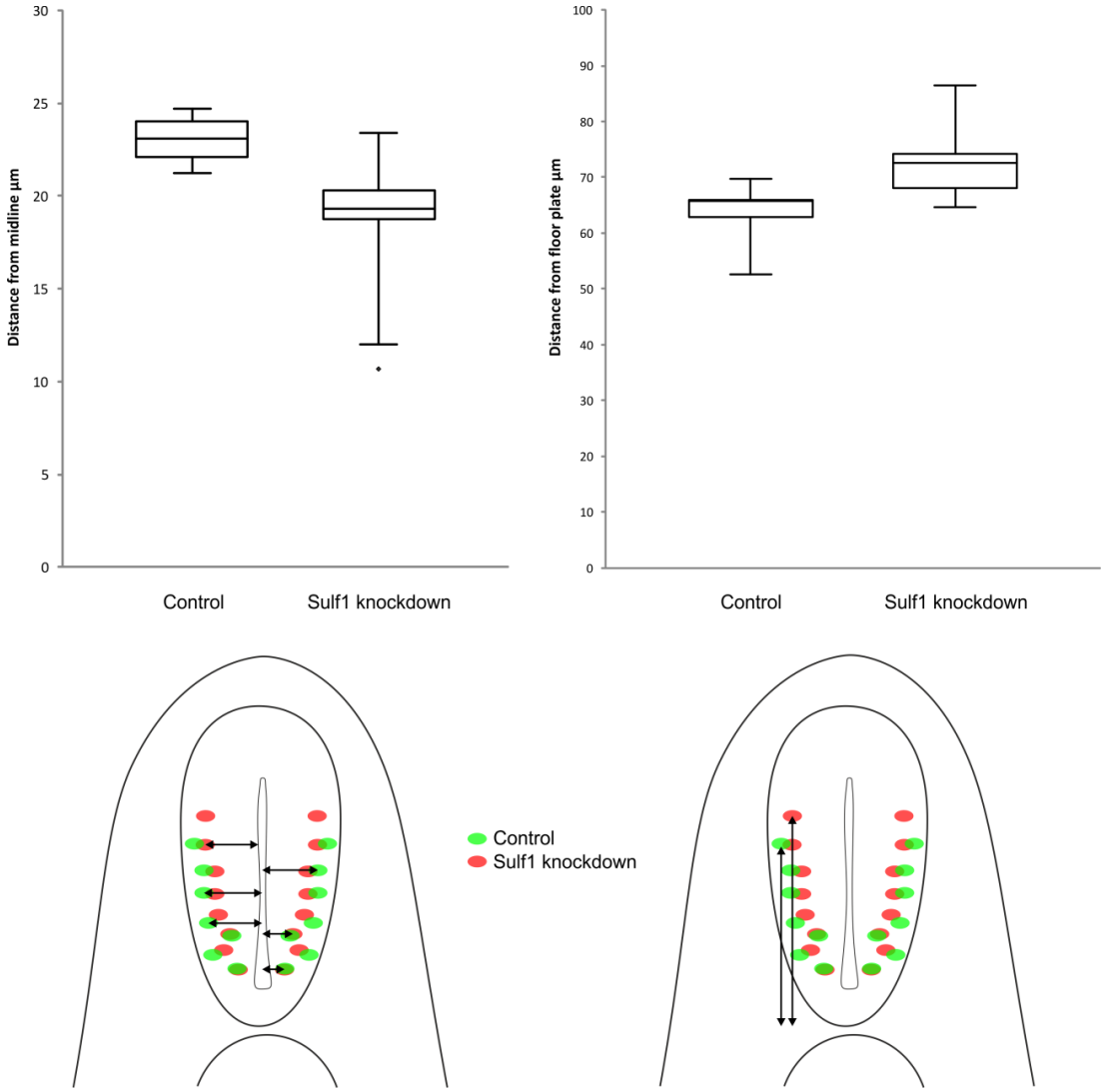

Figure 3.21 Box plots showing the position of X-Myt1 positive cells
The position of X-Myt1 positive cells was measured in relation to the midline or the floor plate**. Top left:** Following Sulf1 knockdown the average distance betweenf X-Myt1 positive cells and the midline is reduced to 19.4µm from 23µm as seen in control embryos. This change is significant (Student's t-test $p<0.01$, n= 10). **Top right:** X-Myt1 positive cells can be observed in more dorsal locations in Sulf1 morphant embryos (72.6µm from the floor plate) compared with control embryos (65.7µm). This change is significant (Student's t-test $p<0.05$, n= 10).
Bottom: The distance from the midline is shown as an average value of all of the X-Myt1 positive cells in a sample (diagram left), whereas the distance from the floor plate relates to the most dorsal positively stained cell (diagram right).

Box plots depict the maximum and minimum values, the interquartile range and the median. Any outlying values (greater than 3/2 of the quartile value) are also shown.

embryos as compared with Sulf1 morphants (Figure 3.21 left panel $p<0.01$). Following Sulf1 knockdown however the most dorsal X-Myt1 positive cells are located further from the floor plate than in control embryos (Figure 3.21 right panel $p<0.05$). These data indicate that knockdown of Sulf1 not only affects the specification of neuronal precursors but also spatial distribution of these cells as they undergo differentiation.

3.4.13 Sulf knockdown affects cell fate

The results thus far have shown that knockdown of Sulf1 leads to changes in the expression of genes which define subsets of precursor populations. To see how this affects the organisation of differentiated cells later during development, histological staining was performed. Stage 42 *X. tropicalis* embryos were stained with Borax carmine, then sectioned and counterstained with picro blue-black. Figure 3.22 shows transverse sections of the neural tube of embryos following knockdown of Sulf1 or Sulf1 and Sulf2. The neural tube in control embryos shows a high degree of structure. Axonal fibres (turquoise) form bundles in the lateral neural tube, with nuclei (red) arranged medially (Figure 3.22A). Although the overall arrangement is similar in the neural tube of Sulf1 morphants, the high degree of structure seen in control embryos is lost. Bundles of axons can be seen in medial regions (arrow) and further dorsally than in controls (arrow head) (Figure 3.22B). Knockdown of Sulf1 and Sulf2 together leads to major disruption in the structure of the neural tube (Figure 3.22C).

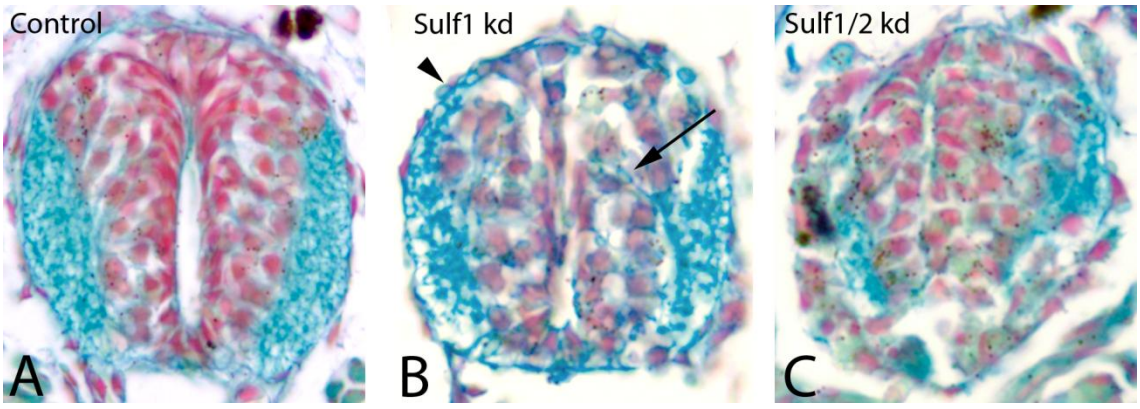

Figure 3.22 Histological staining of transverse sections of stage 42 *X. tropicals* embryos. (A) The neural tube of stage 42 embryos is higly ordered. Bundles of axons can be seen laterally (turquoise) with nuclei (red) tightly packed medially. (B) Knockdown of Sulf1disrupts the general structure of the neural tube. Fewer nuclei can be seen, axons are less tightly packed and are no longer restricted laterally (arrow). Axons also project further dorsally than seen in controls (arrow head). (C) Knockdown of Sulf2 alongside Sulf1 further disrupts this structure.

3.5 Discussion

3.5.1 A conserved patterning mechanism of the vertebrate neural tube

The transcription factors that define neural progenitor populations show a striking amount of similarity from flies through to mice. Ventral neural identity in vertebrates is specified by the nkx family of genes. Members of this family are expressed medially at open neural plate stages, and later on within the ventral neural tube. The *Drosophila* homologue *ventral nervous system defective* (*vnd),* shows comparable positional and temporal expression suggesting a conserved role. Msx genes similarly show expression within the open neural plate of zebrafish and *Xenopus*, which mirrors that of *muscle-specific homeobox* (*msh*) in *Drosophila*. In the intermediate region, members of the gsx family, which share sequence homology with *intermediate neuroblasts defective* (*ind*) in *Drosophila*, are expressed within the open neural plate of *Xenopus*, but not seen until closed neural tube stages in mice. With the exception of the lack of temporal conservation within intermediate regions, homologous transcription factors display a high degree of conservation both in terms of their positional and temporal expression. (Cornell and Ohlen, 2000; Winterbottom et al., 2010).

With the high degree of conservation in the positions of transcription factor expression, it might be expected that the mechanisms which determine these expression domains and their resulting neural identities would be similarly conserved. Support can be found in the existence of graded BMP/Dpp activity as a dorsal ventral patterning mechanism in both vertebrates and *Drosophila*. BMP expression within the roof plate creates a dorsal to ventral concentration gradient within the vertebrate neural tube, defining the boundaries of transcription factor expression (Liem et al., 1997). Dpp similarly acts as a morphogen within the *Drosophila* neurectoderm but differentially represses the expression of homeobox genes at different concentrations (Mizutani et al., 2006). The authors of this paper argue for a potential conservation of the repressive activity of BMP homologues as a mechanism for dorsal ventral patterning. Repression of ventral neuronal identities in vertebrates however seems to be indirect, whereby BMPs promote the expression of more dorsal genes which then repress ventral fates. An example of this can be found in the *small eye* (sey) mutation in mouse, which leads to a point mutation within Pax6. In *S*ey mutants, Nkx2.2 expression, which is normally repressed by Pax6, is

expanded dorsally, indicating that the dorsal boundary of Nkx2.2 is not defined by inhibition by BMP but instead by Pax6, which itself is activated by BMP (Ericson et al., 1997b). It has however not been shown that the repressive activity of Dpp is direct, so a conserved mechanism may exist in flies whereby Dpp signalling promotes transcription factor expression, which then acts in an inhibitory manner, in a similar way to BMP and Pax6.

In contrast to the relatively conserved role of BMP in positional determination, the role of hedgehog is not at all conserved between *Drosophila* and vertebrates in terms of dorsal ventral neural identity. Where *Shh* is expressed along the midline in vertebrates and is required to specify ventral neural cell types, hedgehog is expressed in transverse stripes of neurectoderm in *Drosophila (Lee et al., 1992)*, which suggests it does not play any role in vnd induction. Additionally the overall layout of neuron specification is not conserved. While in vertebrates, motor neuron populations are established in ventral domains, the establishment of motor neurons in flies occurs both dorsally and ventrally within the neurectoderm (Bossing et al., 1996; Schmidt et al., 1997).

The specific requirement for Shh in the establishment of the floor plate within vertebrates also shows some degree of divergence. In mouse and chick, Shh is essential for floor plate specification and the induction of ventral neural genes (Chiang et al., 1996; Ericson et al., 1996). In zebrafish however, Shh seems to play a minor role in floor plate specification, a function which is replaced by Nodal signalling (Hatta et al., 1991; Sampath et al., 1998; Strahle et al., 1997). Recent work in *Xenopus*, similarly suggests a reduced role for Shh in floor plate specification (Peyrot et al., 2011). The data presented in this thesis supports an important role for Shh in the establishment of floor plate identity, as has some previous research (Lopez et al., 2003; Ruiz i Altaba et al., 1995). In contrast to work in mice, loss of Shh signalling in *Xenopus* does not lead to a total loss of *FoxA2* expression. This may reflect the differential requirement for Shh in different floor plate populations, as seen in zebrafish, indicating that while the role of Shh during floor plate specification in *Xenopus* may be diminished compared with mice, it is still a requisite componant. Within vertebrates, Shh does have a conserved role in the determination of ventral neural cell types by

inducing the expression of class II homeodomain transcription factors (Nkx2.2, Nkx6.1) and inhibiting class I transcription factors (Pax6, Irx3) (Briscoe and Ericson, 1999; Briscoe et al., 2000; Guner and Karlstrom, 2007).

3.5.2 Sulf1 can promote *Nkx2.2* expression within the ventral neural tube

It has been shown in chick that *Sulf1* over expression is able to induce the expression of *Nkx2.2* cell autonomously (Danesin et al., 2006). To investigate whether Sulf1 was similarly able to promote *Nkx2.2* expression in *Xenopus*, Sulf1 was over expressed, and *Nkx2.2* expression analysed at stage 23. As seen in chick, *Sulf1* over expression results in up regulation of *Nkx2.2* expression (Figure 3.6). The expansion of the expression domain, rather than induction of ectopic sites indicates a permissive role for Sulf1 rather than a direct role. The ability of Sulf1 to promote cell-autonomous surface retention of Shh in chick (Danesin et al., 2006), suggests that Sulf1 induces *Nkx2.2* expression by potentiating Shh signalling. The ability of Sulf1, to extend the range over which Shh can induce *Nkx2.2* expression in *Xenopus* similarly suggests that it acts to promote Shh signalling.

3.5.3 Sulf1 is required for correct neural patterning

Loss of Sulf1 leads to changes in the patterning of the neural tube. *FoxA2*, which is expressed throughout the floor plate in control embryos, is much reduced following Sulf knockdown (Figure 3.7A-C). The spatial distribution of the ventral marker *Nkx2.2* similarly shows a significant reduction in its expression level in Sulf morphants. The ventral boundary of *Nkx2.2* is normally located at the dorsal boundary of the floor plate, however following Sulf1 knockdown expression of *Nkx2.2* can be seen within the floor plate region (Figure 3.7G-L). The dorsal markers Dbx1 and Pax6 are also affected by the loss of Sulf. The most ventral cells expressing *Pax6* are normally found juxtaposed to those expressing *Nkx2.2* (Figure 3.7P), and the cross inhibition of these transcription factors sets up a sharp boundary. In Sulf1 morphants however the expression region of *Pax6* is dorsally retracted from its normal position and expanded laterally filling the entire width of the neural tube (Figure 3.7Q). This expansion of the expression region is increased when Sulf1 and Sulf2 are knocked down together; so much so that the ventral border is similar to that seen in control embryos (Figure 3.7R).

Shh inhibition by treatment with cyclopamine results in a reduction in the expression region of *FoxA2* (Figure 3.5). *FoxA2* expression in Sulf morphants appears very similar to the expression seen in cyclopamine treated embryos, suggesting that Sulf1 knockdown results in reduced Shh signalling within the ventral neural tube. Furthermore the expression domain changes of *Nkx2.2* and *Olig2* are reminiscent of the changes observed in *Gas1* and *Cdo* mutant mice. Gas1 and Cdo are cell surface proteins which act as co-receptors to positively regulate Shh signalling (Allen et al., 2007; Tenzen et al., 2006). $Gas1^{-/-}$ mice show a ventral shift in the boundary of Nkx2.2 and Olig2 (Allen et al., 2007) in a similar manner observed following Sulf1 knockdown (Figure 3.7E,H). $Cdo^{-/-}$ embryos also display a ventral shift in the boundary of Nkx2.2 as well as a reduction in FoxA2 expression (Tenzen et al., 2006), an effect which is again seen following Sulf1 knockdown (Figure 3.7B). The similarity of the observed changes between Gas1/Cdo mutants and Sulf morphants suggests that they may act in a similar manner, elevating Shh signalling levels within the ventral neural tube.

Analysis of whole embryos reveals that changes to expression are much more dynamic following Sulf knockdown than would be suggested from the sections (Figure 3.8). There is not only a change to the distribution of expression in the dorsal ventral axis, but also in the anterior posterior axis, indicating a more extensive role for Sulf in neural patterning. As discussed previously, neural patterning is control by a variety in inputs during development in addition to BMP and Shh signalling. As Sulf1 is able to regulate various signalling pathways, it is unsurprising that knockdown of Sulf1 leads to a number of defects that are not directly related to dorsal ventral patterning of the neural tube. Sulf1 is a known negative regulator of FGF signalling (Freeman et al., 2008; Wang et al., 2004), and FGF is a major regulator of posterior identity in *Xenopus* (Pownall et al., 1996). Sulf1 is expressed in the posterior mesoderm of the early embryo, and knockdown of Sulf1 results in increased activation of FGF signalling (Freeman et al., 2008). This role for Sulf1 may therefore account for the posterior shift in the anterior expression boundary of certain genes, following Sulf1 knockdown.

3.5.4 A microarray to identity targets of Shh and Sulf1

Many of the neural markers used in this chapter were selected based on the paradigm of dorsoventral patterning in the vertebrate neural tube (Briscoe and Ericson, 1999; Briscoe et al., 2000; Ericson et al., 1997b). These genes mark progenitor cell populations in *Xenopus* as they have been shown to in chick and mouse. In order to investigate whether there are any additional gene targets of Shh or Sulf1 in *Xenopus* that were not predicted by studies in other vertebrates, a microarray based screen was used. The genes identified in this screen were mostly expressed in the telencephalon eye and neural crest, which all exhibit morphological changes following Sulf over expression and knockdown. Targets were validated by *in situ* hybridisation, and it was determined that these genes were regulated by Sulf1 in the way suggested by the mircroarray.

Changes to the pattern of *Dlx2a* expression within the neural crest following knockdown or over expression of Sulf, show that migration defects are consistent with previous findings (Guiral et al., 2010). Furthermore, loss of *Dlx2a* in the neural crest following sulf knockdown suggests a defect in Shh signalling. Zebrafish dispatched mutants, which exhibit a reduced ability to release Shh, fail to maintain *Dlx2a* expression within the neural crest. While some crest markers fail to migrate, the loss of *Dlx2a* in this region suggests an additional role for Sulf in regulating hedgehog signalling within the migrating crest cells. While *Evi-1* and *Dlx2a* are lost and *Vent2* expanded in the forebrain following Sulf knockdown, *Foxg1* does not seem to exhibit much of a change in expression as suggested by the microarray. This indicates that Sulf1 has a very specific role during forebrain development, and that the observed changes to gene expression are not just a result of non-specific effects. Changes to *Vent2* expression suggest a reduction in the size of the diencephalon following Sulf knockdown. Interestingly, *Shh* mutant mice exhibit a significant reduction in the size of the diencephalon, compared with other regions of the brain (Chiang et al., 1996). Additionally, loss of Dbx1 can be seen in the mice lacking Shh (Ishibashi and McMahon, 2002), while in Sulf1/2 knockdown embryos, *Dbx1* is significantly reduced within the brain. These results therefore suggest that Shh signalling is perturbed within the brain following Sulf knockdown.

3.5.5 Sulf1 can increase the efficacy of Shh

The ability of Sulf1 to promote Nxk2.2 expression, along with the observed changes to marker gene expression within the neural tube suggest that Sulf1 acts to potentiate Shh signalling. To investigate the ability of Sulf1 to increase the efficacy of Shh, Sulf1 and Shh were co-injected to establish whether the presence of Sulf1 leads to an increase in Shh activity. As Sulf1 has previously been shown to promote the expression of *Nkx2.2* (Danesin et al., 2006), injected mRNA levels of *Sulf1* were reduced such that no change in expression could be observed. Similarly only low levels of *Shh* were injected to allow for a measurable increase in signalling. Sulf1 was found to be able to increase the potency of Shh anteriorly within the embryo, promoting ectopic expression of *Nkx2.2* and *Vent2* (Figure 3.15). Analysis of *Nkx2.2* expression within the neural tube revealed a significant increase in the ability of Shh to extend the dorsal boundary of *Nkx2.2* expression. This suggests that Sulf1 does indeed act to increase levels of Shh signalling in *Xenopus*.

3.5.6 More to patterning than Sonic hedgehog?

Although the concentration of Shh is a major determinant in the specification of neuronal progenitors, all of the genes involved in patterning the neural tube are influenced by various different cues including BMP, Wnt and FGF signalling, which as previously discussed are regulated by Sulf1. It is important therefore to consider the extent to which knockdown of Sulf1 impacts on Shh signalling compared with other signalling pathways. As Sulf1 can inhibit the activity of BMPs (Freeman et al., 2008) which play a significant role in patterning the neural tube, one question that arises is whether or not the observed effects are not due to changes in hedgehog signalling, but in BMP signalling instead. The increase in the level of *Pax6* expression within the neural tube would certainly suggest that the level of BMP activity is increased following Sulf1 knockdown, and the further increase following Sulf2 knockdown would support this (Figure 3.7P-R). Although Sulf1 is able to inhibit BMP activity, it is not expressed in a region where it would be able to have a significant impact. *Sulf2* however is expressed in a region where BMP activity is high, so the additional increase in *Pax6* expression in the double knockdown is probably accounted for by the effect of Sulf2 on BMP signalling (Figure 3.7R). Nevertheless loss of Sulf1 alone is sufficient to affect neuronal patterning, and the majority of the genes analysed

showed no significant difference between the single and double knockdown. These results therefore do not suggest that BMP signalling within the neural tube is significantly affected by the loss of Sulf1.

Ptc2 is up regulated in response to increased levels of Shh and so provides a good readout of Shh activity levels. In chapter 2, *Ptc2* expression was shown to be significantly reduced following the knockdown of Sulf1. This indicates that although knockdown of Sulf1 will impact many different signalling pathways, perturbations to Shh signalling form a significant part of the changes observed.

3.5.7 Sulf1 and motor neurons

From expression analysis of certain transcription factors, it is apparent that loss of Sulf1 affects patterning of the neural tube. Despite the changes seen following Sulf1 knockdown, the genes responsible for defining the motor neuron domain are still present, although in different regions, and so motor neuron specification may still occur. Following hyper-sulfation of HSPGs by injection of 6-OST expression of the motor neuron marker Isl1 is no longer observed ventrally within the neural tube. Conversely over expression of Sulf1 leads to an expansion in the ventral Isl1 expression domain in a similar manner to Shh over expression (Figure 3.17B,E). The loss of Isl1 following over expression of 6-OST suggests that motor neurons are not specified, as Isl1 is a pre-requisite for motor neuron differentiation (Pfaff et al., 1996; Shi et al., 2009). In *Xenopus*, *Isl1* is not only expressed within the motor neuron domain, but in multiple domains which correspond to ventral and dorsal interneuron domains (Shi et al., 2009). The presence of Isl1 in dorsal domains following 6-OST injection may indicate that hyper-sulfation of HSPGs results in a dorsal shift of the motor neuron domain. It has been demonstrated however that motor neuron differentiation requires sustained levels of Shh signalling (Ericson et al., 1996), which over expression of 6-OST has been shown to inhibit (Figure 3.17). It is therefore unlikely that these dorsal populations of Isl1 positive cells represent motor neurons. Examination of a more specific marker such as xHB9 (Saha et al., 1997), may be used to ascertain the extent to which 6-OST can inhibit the differentiation of motor neurons.

Knockdown of Sulf1 also reveals a shift in the expression domains of Isl1 positive cells. The effects of the inhibition of Sulf1 however are much more subtle than those observed following 6-OST over expression. The presence of three distinct domains of Isl1 positive cells indicates that all three populations are present in Sulf1 morphants. The ventral and intermediate Isl1 positive cell populations are however shifted ventrally following Sulf1 knockdown. As shown previously, the genes responsible for defining the subsets of progenitor populations within the ventral neural tube, Nkx2.2 and Olig2, are also ventrally shifted following Sulf1 knockdown. Loss of Nkx2.2 from the p3 region permits the differentiation of motor neurons further ventrally than in controls as Nkx2.2 normally acts to repress motor neuron fate (Briscoe et al., 1999). This suggests that changes seen in the expression of transcription factors responsible for defining progenitor cell populations, as a result of Sulf1 knockdown, gives rise to detectable changes later on in development.

3.5.8 Increase in the width of the dorsal neural tube

As well as the change to patterning, a change to the general morphology of the neural tube was observed. To investigate whether this was due to a rise in the number of proliferative cells within the dorsal neural tube, actively proliferating cells were stained using the mitosis marker PH3. It was observed however that there was not an increase, but actually a decrease in the number of actively proliferating cells following Sulf1 knockdown. Knockdown of Sulf1 has been shown to decrease levels of Shh activity generally, as shown by reduced *Ptc2* expression. As Shh has been shown to promote cell proliferation in a number of neuronal cell types (Dahmane and Ruiz i Altaba, 1999; Palma et al., 2005), a reduction in Shh signalling following Sulf1 knockdown may explain the observed decline in the number of proliferative cells.

What may explain the change to the shape of the neural tube is failure to correctly undergo folding of the neural plate. Although the neural tube does close fully in Sulf1 morphants, it was observed that neural tube closure is slightly delayed. During neural tube closure cells within the midline undergo intercalation and convergent extension movements which drive the folding of the neural plate. During this process, the polarised rearrangement of cells is regulated by the planar cell polarity (PCP) cascade under the control of

dishevelled (Dsh) (Tada and Smith, 2000). Inhibition of Dsh signalling within the midline results in failure of convergent extension and neural tube closure (Wallingford and Harland, 2001; Wallingford and Harland, 2002). Sulf1is able to promote translocation of Dsh to the membrane in response to Wnt signalling (Simon Fellgett unpublished observations). As Sulf1 is first seen within the midline precisely at the time when neural tube closure begins in *Xenopus*, the loss of Sulf1 within the midline may lead to aberrant signalling thus disrupting correct neural tube closure. Failure to correctly fold the neural tube as a result of Sulf1 loss may explain the change in neural tube shape at the time embryos were analysed.

3.5.9 Loss of sulf1 leads to a change in differentiation

As discussed above, it was observed that there is a reduction in the number of proliferative cells within the neural tube at stage 23 (Figure 3.19). As this reduction in actively mitotic cells could indicate an early onset of differentiation, the post mitotic neuronal marker X-Myt1 was used to investigate whether cells were exiting the cell cycle earlier in Sulf1 morphants. X-Myt1 staining showed that the position of Myt1 positive cells was altered in Sulf1 morphants, but although the number of X-Myt1 positive cells was elevated, this increase was not statistically significant. In control embryos X-Myt1 positive cells are predominantly located within the ventral neural tube. Following Sulf1 knockdown however X-Myt1 positive cells are found further dorsally within the neural tube and staining is generally found to be more medial than seen in control embryos. This indicates that Sulf1 knockdown not only impacts on the spatial distribution of populations of precursor cells, but also affects the localisation of post-mitotic cells.

Histological staining of stage 42 embryos indicates that as development progresses, loss of Sulf activity leads to abnormal structure within the neural tube. While the neural tube is normally highly ordered, with cell bodies located medially and projecting axons laterally, loss of Sulf1 affects this organisation such that axon projections are not as tightly bundled and can be found in more dorsal and medial locations than in controls. The existence of imprecisely guided axons following Sulf knockdown suggests a possible reduction in guidance cues. Shh has been shown to act as a guidance cue, directing

commissural axons towards the ventral neural tube (Charron et al., 2003), and a reduction of ventral Shh may explain the reduction in axonal bundle structure. There also appear to be fewer cells within the neural tube at this time, in agreement with a reduction in PH3 staining seen earlier on in development.

3.6 A potential mechanism for the action of Sulf1

It is clear from these results that Sulf1 is an important factor during the development of the neural tube in *Xenopus*. Sulf1 is required for the correct positioning of transcription factors which define subsets of neural progenitors. Loss of Sulf1 phenocopies mouse mutants of the positive regulators of hedgehog signalling Cdo and Gas1, with respect to changes in *Nkx2.2* and *FoxA2* expression. Taken together with the data presented in chapter 2 whereby Sulf1 is able to influence the level of Shh and its downstream target Ptc2 within the embryo, it may be that Sulf1 acts to control neuronal patterning through regulation of Shh signalling.

Over expression of Sulf1 is able to raise levels of the direct downstream target of Shh, Ptc2 while knockdown of Sulf1 results in a reduction in the level of Ptc2 within the ventral neural tube. All of the observed changes to transcription factor expression are consistent with a change in the level of Shh activity within the ventral neural tube. The ventral marker Nkx2.2 and the floor plate marker FoxA2 require a high level of hedgehog activity for their expression. Experiments in tissue explants have shown that very high hedgehog levels promote the specification of floor plate identity at the expense of motor neurons (Roelink et al., 1995). If hedgehog levels are reduced, a decrease in cells with floor plate identity would be expected, concomitant with a shift towards a more dorsal identity. Within the ventral neural tube of Sulf1 morphants, *FoxA2* expression is reduced, while *Nkx2.2* and *Olig2* are expressed in a more ventral location (Figure 3.7B,E,H). Interestingly however, further dorsally, changes to *Nkx6.1* and *Dbx1* expression suggest a possible increase in Shh levels (Figure 3.7K,N). This suggests that the role of Sulf1 may not just be to promote ventral Shh signalling, but also to regulate the diffusion of Shh throughout the neural tube. The next chapter will focus on the distribution of the Shh protein, and how Sulf1 is able to influence its ability to diffuse.

4.0 The effects of Sulf1 on Shh diffusion

4.1 Introduction

4.1.1 Hedgehog interacts with the extracellular environment

Heparan sulphate proteoglycans (HSPGs) form a significant part of the extracellular matrix and are key in the regulation of multiple signalling pathways. Shh contains the consensus sequence for HSPG binding and has been shown to interact with the sulfate groups located on glycosaminoglycan (GAG) chains (Rubin et al., 2002). In flies it has been shown that this interaction with HSPGs is required for Hh to diffuse through a field of cells (The et al., 1999). *Tout-velu* (*ttv*), or the vertebrate homologue EXT1, codes for a co-polymerase and is essential for HSPG synthesis (The et al., 1999). In the absence of *ttv*, Hh is unable to diffuse even very short distances, indicating that its movement is dependent on the presence of HSPGs (Bellaiche et al., 1998; The et al., 1999). Other members of this family, *Brother of tout- velu* (*botv*) and *Sister of tout-velu* (*sotv*), which code for an N-acetylglucosaminyl transferase and co-polymerase respectively are similarly required for Hh diffusion (Bornemann et al., 2004; Han et al., 2004). The lipid modifications of Hh are also an important factor in the Hh-HSPG interaction. Hh-N which lacks the cholesterol moiety is able to diffuse in *ttv* mutants while wild-type Hh is not (Callejo et al., 2006), suggesting that HSPGs form an integral part in the mechanism allowing cholesterol modified Hh to diffuse.

Dally and *Dally-like* (*dlp*) code for glypicans in *Drosophila*. RNAi silencing of *dlp* gives rise to a phenotype very similar to that of Hh mutants, showing a requirement of dlp in Hh signalling (Desbordes and Sanson, 2003). *Dlp* mutants display defects in hedgehog signalling, which can be rescued following over expression of either wildtype *dlp*, or a mutant *dlp* where the attachment sites for heparan sulphate (HS) have been removed (Williams et al., 2010; Yan et al., 2010). This suggests that Hh interacts with the core protein of *dlp* and not the HS chains, however although Yan et al., (2010) showed direct Hh binding to Dlp(–HS), Williams et al., (2010) were unable to do so. Hh signalling cannot be restored by over expression of other HSPGs (*Dally*, *Syndecan*, *Trol)*, suggesting a specific role for *dlp* in Hh signalling. The mammalian homologues of *dlp, glypican4* (*gpc4*) and *glypican6* (*gpc6*), are similarly able to rescue *dlp* mutants (Williams et al., 2010). Other glypicans which are more related to *dally (gpc3 and gpc5)*, cannot rescue *dlp* mutants however. When over expressed in

a control background *dlp*, *gpc4* and *gpc6* act to potentiate hedgehog signalling whereas *dally*, *gpc2*, *gpc3* and *gpc5* act to inhibit hedgehog signalling (Williams et al., 2010). Gpc3 null mice exhibit enhanced levels of Shh signalling and over expression of Gpc3 in mouse embryonic fibroblasts inhibits hedgehog signalling (Capurro et al., 2008). Gpc3 is able to interact with Shh through its core protein in a similar manner to *dlp* in *Drosophila*, and this interaction promotes internalisation of Shh, thus inhibiting the amount of Shh available for signalling (Capurro et al., 2008). In *Drosophila* however dlp is found to be internalised with Hh in a complex with Ptc, and internalisation potentiates Hh signalling (Gallet et al., 2008), whereas gpc3 mediated internalisation is not associated with Ptc and leads to a inhibition of Shh signalling (Capurro et al., 2008). The potentiation of hedgehog signalling by dlp, gpc4 and gpc6 and inhibition of signalling by dally, gpc2, gpc3 and gpc5 points to a complex role for HSPGs in modifying hedgehog sigalling.

There are also co-factors that may mediate the interaction between Hh and HSPGs. *Shifted* (*Shf*) codes for a secreted protein orthologous to the vertebrate Wnt inhibitory factor (WIF), which interacts with both Hh and HSPG proteins. In *Shf* mutants wild type Hh protein is unable accumulate at high levels in the posterior compartment of the *Drosophila* wing pouch, and diffusion into the anterior compartment appears reduced (Glise et al., 2005). Mutant Hh lacking either cholesterol or palmitic acid modification however is able to diffuse in *Shf* mutants (Gorfinkiel et al., 2005), again indicating that for the physiologically relevant lipid modified hedgehog protein, interaction with the extracellular matrix is essential.

4.1.2 The formation of multimeric complexes aids diffusion

The formation of multimers of fully processed Shh (Shh-Np) depends on the N-terminal palmitoylation and addition of cholesterol (Chen et al., 2004; Gallet et al., 2006; Goetz et al., 2006; Zeng et al., 2001). This formation of multimeric complexes may increase the ability of the protein to diffuse, and it has been shown that Shh is very stable in its multimeric form (Goetz et al., 2006), a property conducive for long range signalling. This multimeric form is not only stable but shows a greater level of activity than that of the monomeric form (Chen et al., 2004). Within the limb bud, Shh-N, which lacks palmitate and is

therefore unable to form multimeric complexes, retains the biological activity of Shh-Np in that it can activate downstream signalling, but is unable to effectively signal over a long distance (Lewis et al., 2001). Work so far has concentrated on the relevance of palmitoyl and cholesterol adducts in multimerisation. It has been suggested however that HSPGs may provide a scaffold to allow the formation of hedgehog multimers (Goetz et al., 2006), presenting a platform to promote the accumulation of Shh at the surface of producing cells, and in this way facilitating Shh oligomerisation. A change to this platform would therefore further stabilise or potentially destabilise Shh complex formation. As Sulf1 modifies the GAG chains which potentially provide this scaffold, it may promote or inhibit Shh multimer assembly, influencing the diffusion of Shh.

4.1.3 Sulf1 has been shown to modify sonic distribution

Sulf1 has shown to be regulated by Shh in quail embryos (Dhoot et al., 2001). Implantation of beads containing Shh induces ectopic Sulf1 expression while antagonising Shh signalling using anti-sense oligonucleotides inhibits Sulf1 within its usual expression domain (Dhoot et al., 2001). In chick neuroepithelium, over-expression of *Shh* leads to ectopic and precocious oligodendrocyte formation. Over-expression of *Sulf1* leads to the accumulation of Shh at the cell surface in a cell autonomous manner suggesting that it could be the contributing factor to this switch, although overexpression of *Sulf1* can not by itself induce ectopic oligodendrocyte formation (Danesin et al., 2006). In *Xenopus*, Sulf1 expands the domain of *Nkx2.2* expression within the neural tube (Chapter 3). One possible mechanism by which Sulf1 could have this effect is by increasing the ability of Shh to diffuse, thereby extending its range of activity (Briscoe and Ericson, 1999; Craven et al., 2004). Sulf1 modifies the GAG chains of HSPGs and this modification may be important in regulating how Shh interacts with heparan sulphate.

The *Drosophila* mutant Sulf1$^{\Delta P1}$, which lacks most of its protein coding region, displays defects associated with increased Wg and Hh signalling (Kleinschmit et al., 2010; Wojcinski et al., 2011). Although this suggests a negative role for Sulf1 in the regulation of Hh signalling, the defects observed are very mild. Work analysing clones of *Sulf* mutant cells in the *Drosophila* wing disc has possibly indicated a bimodal role for Sulf1, whereby it acts positively to regulate

Hh when expressed in the same cell, but negatively when expressed in cells receiving the Hh signal (Wojcinski et al., 2011). In the two previous chapters it has been demonstrated that *Shh* and *Sulf1* are co-expressed in the floor plate and ventral CNS, that Shh is able to regulate the expression of *Sulf1* and that Sulf1 is able to influence the activity of Shh. Additionally loss of Sulf1 gives rise to alterations in neuronal patterning consistent with a change in the levels of Shh activity. Together with previous research showing that over expression of *Sulf1* leads to the accumulation of Shh at the cell surface in a cell autonomous manner which promotes the expression of Shh sensitive genes (Danesin et al., 2006), it is possible that by modifying the extracellular environment, Sulf1 modulates the distribution of the Shh protein.

4.2 Aims

The aims for this chapter are to analyse the effects of Sulf1 on the diffusion of Shh. This will be undertaken *in vitro* using fluorescently tagged Shh fusion proteins, and *in vivo* by immunohistochemistry. This chapter will investigate the following hypotheses:

- Sulf1 affects the distribution of Shh when globally expressed
- Sulf1 affects the distribution of Shh when co-expressed with *Shh* but not in cells receiving the Shh signal
- Sulf1 is able to regulate the distribution of Shh when expressed only in cells receiving the Shh signal
- Sulf1 is able to inhibit the formation of Shh multimeric complexes
- Loss of Sulf1 affects the distribution of Shh in vivo

4.3 Methods

4.3.1 Synthesis of Shh-GFP construct

Due to the large amount of processing which hedgehog undergoes during its synthesis, any addition of GFP to the end of the Shh protein would lead to it being cleaved. To generate a fusion construct the GFP coding region was therefore inserted between the N-terminal signal peptide and the C-terminal catalytic domain, such that C-terminal cholesterol modification occurs at the C-termnus of GFP instead of Shh-N. Fortunately, a Shh-GFP knock-in construct had previously been synthesied (Chamberlain et al., 2008) so generation of this construct from scratch was not necessary. The coding region of the Shh-GFP protein was cloned out of the knock-in cassette and inserted into the pCS2+ vector for use in *Xenopus*. A kozak sequence was added to the construct to increase the level of protein generated. Figure 4.1 shows the changes made to Shh to generate a functional Shh-GFP fusion protein. mRNA coding for the construct shown in Figure 4.1B was synthesised *in vitro* and injected into *Xenopus* embryos. Shh-GFP is then translated and processed *in vivo* to form the functional protein (Figure 4.1C).

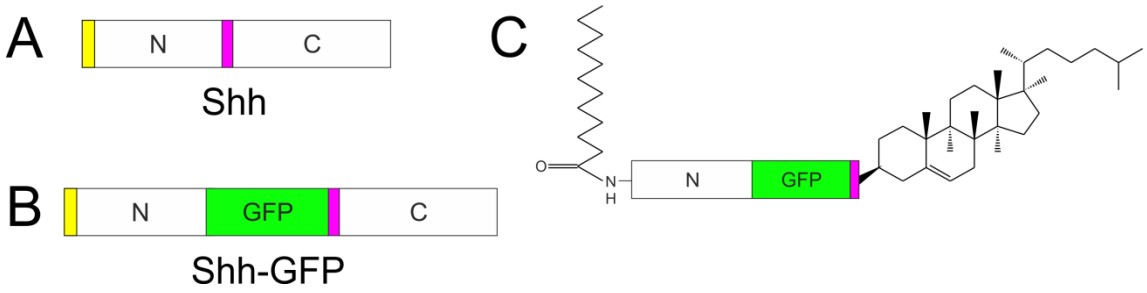

Figure 4.1 Synthesis of Shh-GFP
(A) Autoproteolysis and cholesterol addition in Shh take place at a specific site at the C-terminal end of the N-terminal fragment (magenta). N-terminal palmitoylation takes place at the N-terminal region after cleavage of the signal peptide (yellow). (B) To prevent GFP being cleaved off Shh-N during synthesis, the sequence defining the processing site was tranferred to the C-terminal end of GFP, and GFP was inserted between then N- and C-terminal fragments of Shh. (C) mRNA coding for the construct shown in (B) is injected into *Xenopus* embryos. Shh-GFP is translated and processed *in vivo* as Shh-Np, with the cholesterol being added to the end of GFP.

To investigate the ability of Sulf1 to affect the diffusion of the Shh protein, mRNA coding for Shh-GFP and Sulf1 was injected in a number of different ways. To dissect out the role of Sulf1 in Shh expressing and Shh receiving cells Shh-GFP and Sulf1 were injected as outlined below.

4.3.2 Shh-GFP diffusion within *Sulf1* expressing region

Embryos were injected with mRNA coding for Sulf1 at the 2 cell stage so that all of the cells would express *Sulf1*. Embryos were then cultured to the 32 cell stage, when one of the cells was injected with mRNA coding for *Shh-GFP* along with a membrane marker giving rise to a small group of cells that express *Shh-GFP*. Embryos were then cultured to stage 8 when animal caps were taken, which were cultured further for two hours at 23°C.

4.3.3 Shh-GFP diffusion out of a *Sulf1* expressing region

Embryos were cultured to the 32 cell stage, when one cell at this stage was injected with mRNA coding for *Shh-GFP* and *Sulf1* along with a membrane marker giving rise to a small group of cells that express *Shh-GFP* and *Sulf1*. Further processing of embryos was undertaken as described in 4.3.2.

4.3.4 Shh-GFP diffusion into a *Sulf1* expressing region

Embryos were injected with mRNA coding for *Sulf1* in one cell at the 32 cell stage so that only a small group of cells expressed *Sulf1*. Membrane RFP was co-injected with *Sulf1* so that *Sulf1* expressing cells could be identified. Embryos were then injected with mRNA coding for *Shh-GFP* in an adjacent cell, or a cell close to the *Sulf1* expressing region, along with CFP-GPI, giving rise to a small group of cells that express *Shh-GFP* that can be distinguished by a distinct membrane marker. Further processing of embryos was undertaken as described in 4.3.2.

4.3.5 Förster resonance energy transfer (FRET)

The Shh-GFP construct was modified such that the GFP was replaced with cyan fluorescent protein (CFP) and yellow fluorescent protein (YFP). These constructs were injected into 32 cell stage embryos following injection at the two cell satge with either *LacZ* or *Sulf1* RNA, as described previously. Figure 4.2 outlines how these constructs were used to determine the interaction between Shh monomers in the presence or absence of Sulf1.

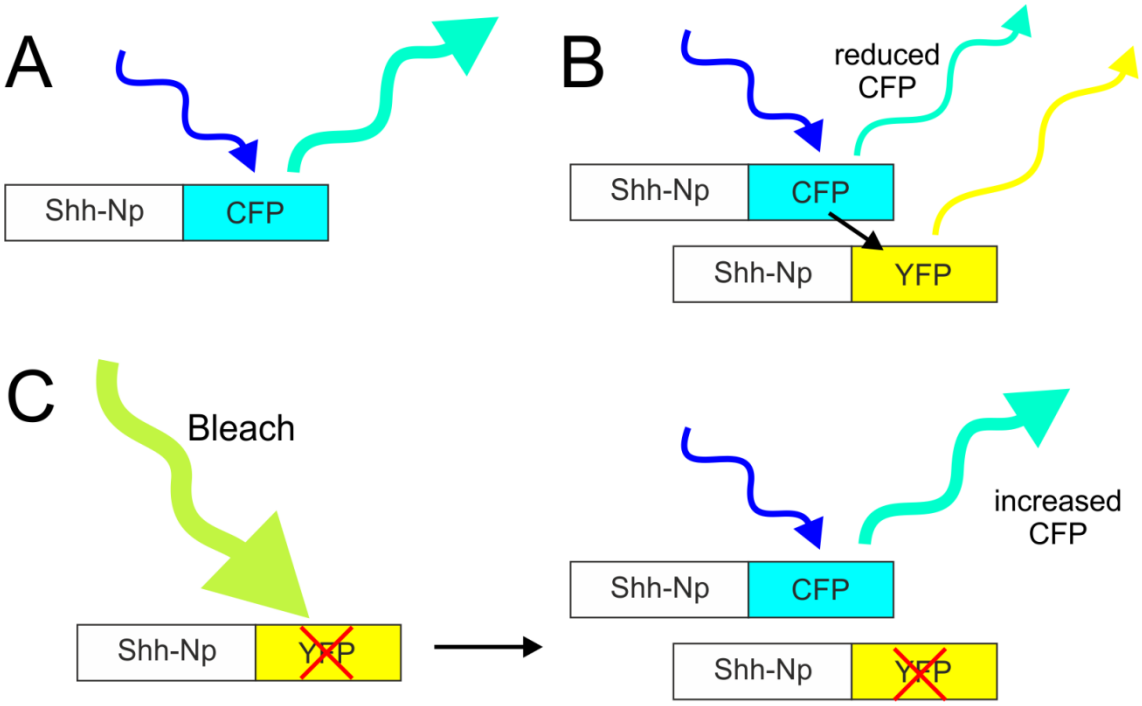

Figure 4.2 Energy transfer between FRET partners
(A) CFP fluoresces when illuminated with blue light. (B) If YFP is in close proximity (<~10nm), some of the energy which would normally be given out as blue/green light is directly transferred to YFP, which is subsequently emmited as yellow light. As a result, blue/green light emmision is reduced. This energy tranfer is known as Förster resonance energy transfer (FRET). As fluorophores move closer together, the amount of energy which is directly transferred increases. (C) Bleaching of YFP with a high intensity 514nm laser prevents energy transfer between CFP and YFP. With no energy transfer between FRET partners, all energy is emitted as blue/green light. The difference in blue/green light intensity before and after bleaching can be measured. This difference is termed the FRET efficiency, and can be used to determine the relative proximity of FRET partners.

4.4 Results

4.4.1 Shh-GFP diffuses differently in Sulf1 over expressing embryos

To analyse the effects of Sulf on the distribution of the hedgehog protein, a GFP fusion construct was synthesised allowing direct visualisation of the Shh protein in live cells. This fusion protein was derived from a construct used in mouse which has previously been shown to be active (Chamberlain et al., 2008). To analyse the effects of Sulf1 on Shh-diffusion, embryos were injected so that all cells within the embryo express *Sulf1* and only a few cells express *Shh-GFP*. By co-injecting mRNA coding for GPI linked CFP (CFP-GPI) with *Shh-GFP*, the cells that are expressing *Shh-GFP* can be differentiated from those not expressing *Shh-GFP*. Any GFP observed outside of this clone therefore represents Shh-GFP that has diffused away from the source cells. As a control embryos were injected with *LacZ* RNA instead of *Sulf1* RNA at the 2 cell stage. These will be referred to as control embryos for the remainder of this section. Figure 4.3 shows confocal images of clones of cells expressing *Shh-GFP* (green) and CFP-GPI (magenta) which are also expressing either *LacZ* or *Sulf1*. In control embryos Shh-GFP protein can be seen surrounding *Shh-GFP* expressing cells (magenta) and at a distance from these cells in the extracellular space (Figure 4.3A-C). When magnified, Shh-GFP is observed to be present in discrete foci (Figure 4.3D), suggesting that it is present in a complex, which as described previously, is the physiologically relevant and active form of Shh (Goetz et al., 2006; Zeng et al., 2001). In embryos injected with Sulf1 at the two cell stage, Shh-GFP is observed surrounding Shh-GFP expressing cells (Figure 4.3E-G). In contrast to control embryos however, very little Shh-GFP is found outside of the *Shh-GFP* positive clone of cells. On closer inspection, it is not only the quantity but also the character of the diffusive particles that is altered by the presence of Sulf1. Whereas in control embryos, Shh-GFP was present in discrete foci, in *Sulf1* over expressing embryos, Shh-GFP seems to form large aggregates which are not evenly spread around the cells, but seem to collect proximal to the source (Figure 4.3H). This suggests that Sulf1 may either promote aggregation of Shh particles, or may promote association of Shh with the cell surface.

.

Figure 4.3 Shh-GFP diffusion through a field of *Sulf1* expressing cells

X. laevis embryos were bilaterally injected at the 2-cell stage with 4ng *LacZ* RNA, as a control, or 4ng *Sulf1* RNA (1), cultured to the 32-cell stage and then injected with *Shh-GFP* in one cell, along with GPI linked CFP as a membrane marker (2). Animal caps were taken at NF stage 8 (3) and were imaged after 2 hours. All images shown are at the edge of the *Shh-GFP* positive group of cells (4, red bounding box). (A-C) In control embryos, Shh-GFP freely diffuses away from its site of synthesis. (D) A closer look reveals that Shh-GFP is abundant and surrounds cells far from its source. (E-G) In embryos injected with 4ng *Sulf1*, Shh GFP does not move as far, only being found within the first 3- 4 rows of cells away from its source. (H) Shh-GFP is not dispersed evenly around *Sulf1* positive cells but instead forms clumps around a few cells.

Shh-GFP expressing cells are marked by CFP-GPI (Magenta)

Shh-GFP protein is shown in green

Magnified images (D,H) are taken from the bounding boxes shown (C,G) and displayed in white to improve contrast

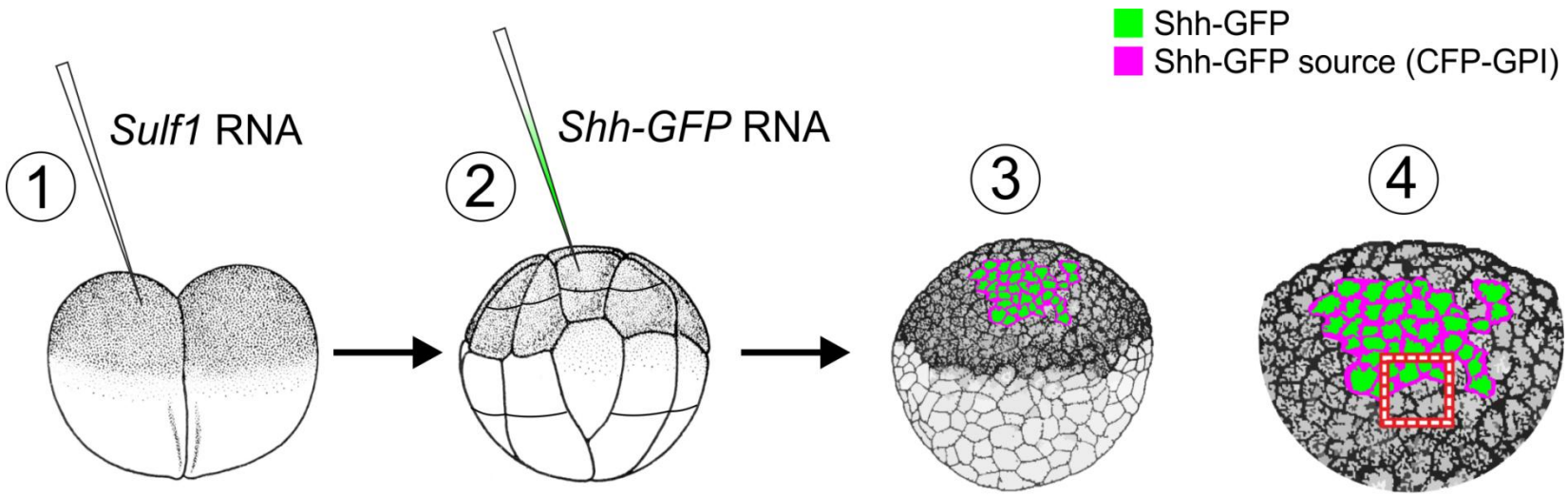

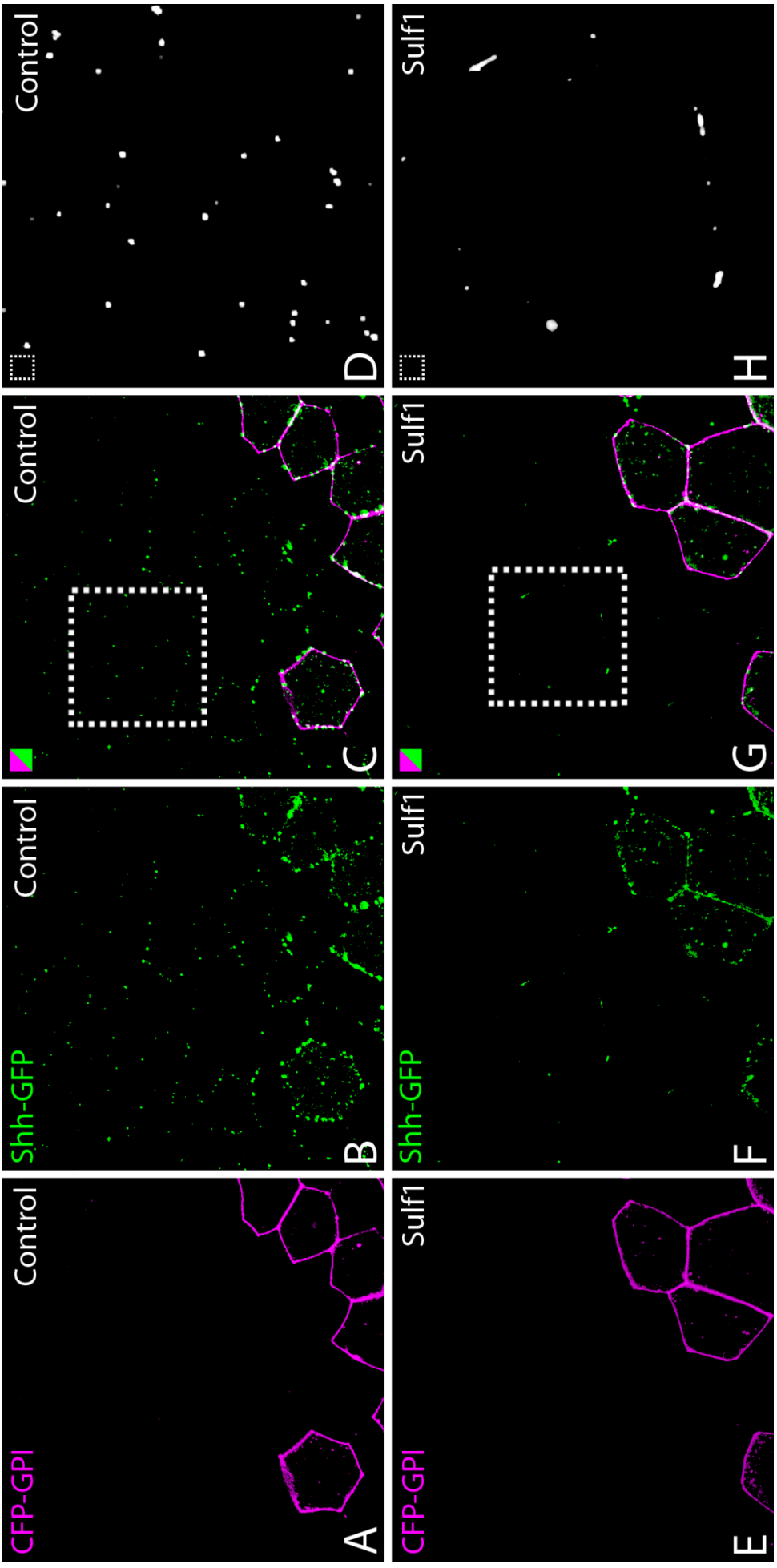
CFP-GPI
Control
A
Shh-GFP
Control
B
Control
C
Control
D
CFP-GPI
Sulf1
E
Shh-GFP
Sulf1
F
Sulf1
G
Sulf1
H

4.4.2 Sulf1 functions at both Shh-GFP expressing and receiving cells

The previous experiment investigated the diffusion of Shh-GFP in a field of *Sulf1* expressing cells. To determine the effects of Sulf1 activity on cells producing Shh-GFP compared to the effects of Sulf1 on cells receiving Shh-GFP the following experiments were done. *Sulf1* was expressed in a specific subset of cells; either in those also expressing *Shh*, or in the cells receiving the Shh signal. Injections were carried out such that cells either co-expressed *Shh-GFP* and *Sulf1*, or expressed *Shh-GFP* only but were adjacent to cells expressing *Sulf1* (as described in 4.3.3 and 4.3.4). To differentiate between cells expressing *Shh-GFP* or *Sulf1*, cells were co-injected with membrane RFP or GPI-linked CFP respectively; doubly labelled cells therefore indicate co-expression of *Shh* and *Sulf1*.

When *Shh-GFP* is expressed in control cells it is able to diffuse away from its site of synthesis as seen previously (Figure 4.4A-E). When cells co-express *Shh-GFP* and *Sulf1* however, the Shh-GFP protein is distributed as aggregates around and close to the *Shh-GFP* expressing cells instead of discrete particles (Figure 4.4F-I). When Sulf1 is not present in receiving cells, Shh-GFP particles are found in greater abundance, and can be seen far from the source, suggesting that Sulf1 reduces Shh mobility only when expressed in receiving cells.

To assess whether the presence of Sulf1 on the surface of cells which receive the Shh signal is enough to impede the diffusion of Shh, embryos were injected so that *Shh-GFP* expressing cells juxtaposed those expressing *Sulf1* (as described in 4.3.4). As demonstrated previously, Shh-GFP is able to freely diffuse between control cells (Figure 4.5A-E). In stark contrast however, when *Sulf1* is expressed in receiving cells only, Shh-GFP does not diffuse at all (Figure 4.5F-J). To see whether this is a result of Sulf activity directly at the edge of the *Shh-GFP* expressing clone, the experiment was repeated, with a slight modification so that the *Sulf1* positive and *Shh-GFP* positive clones were separated slightly by non-*Sulf1* expressing cells. As seen in Figure 4.6, *Shh-GFP* which freely diffuses in a control background, is unable to diffuse into an area of cells expressing *Sulf1*, even when at a distance from the source (Figure 4.6F-J).

Figure 4.4 Shh-GFP away from cells co-expressing Sulf1

(1) *X. laevis* embryos were injected at the 32-cell stage with *Shh-GFP* or *Shh-GFP* + *Sulf1* in one cell. (2) Animal caps were taken at NF stage 8 and were imaged at after 2 hours. All images shown are at the edge of the Shh-GFP positive group of cells (3, red bounding box). (A-D) Shh-GFP (green) freely diffuses away from its site of synthesis (magenta) in control cells, and evenly surrounds cells far from its source (E). (F-I) In cells co-injected with *Sulf1* (yellow), Shh-GFP does not freely diffuse away from its source but forms aggregates, which when magnified seem to group predominantly on one side of the cells (J).

Shh-GFP expressing cells are marked by CFP-GPI (Magenta)

Sulf1 expressing cells are marked by mRFP (Yellow)

Shh-GFP protein is shown in green

Magnified images (E,J) are taken from the bounding boxes shown (D,I) and displayed in white to improve contrast

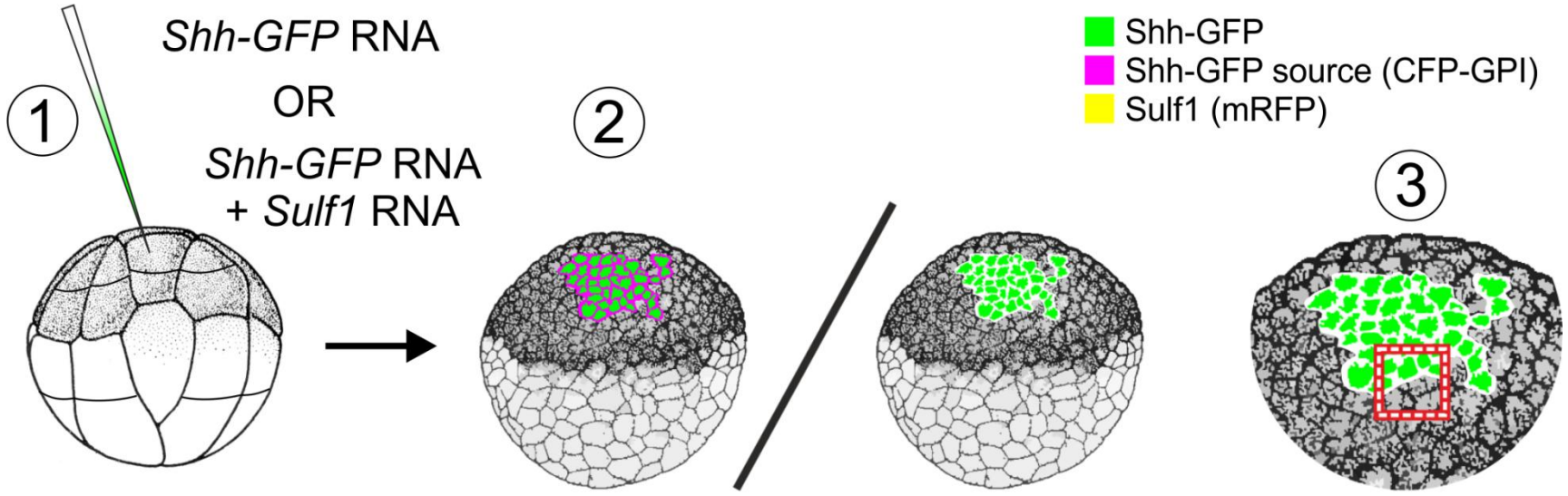

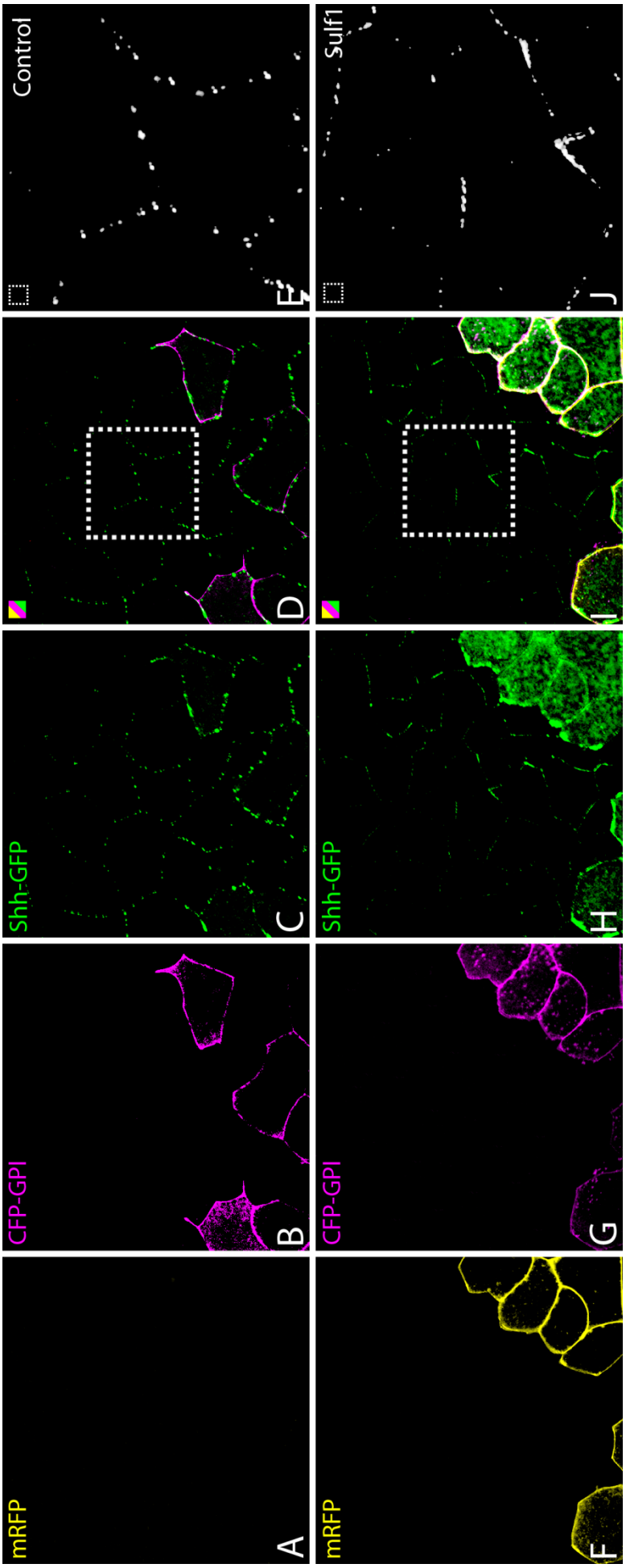
mRFP
A
CFP-GPI
B
Shh-GFP
C
D
Control
E
mRFP
F
CFP-GPI
G
Shh-GFP
H
I
Sulf1
J

Figure 4.5 Shh-GFP fails to diffuse into adjacent cells expressing Sulf1

(1) *X. laevis* embryos were injected at the 32-cell stage with *Shh-GFP* in one cell, along with GPI linked CFP as a membrane marker, and with *Sulf1* and mRFP in an adjacent cell. (2) Animal caps were taken at NF stage 8 and were imaged after 2 hours. Images A-E are from the edge of the Shh-GFP positive group of cells (3, red bounding box), while images F-J are from the opposite edge of the clone which juxtaposes *Sulf1* positive cells (3, blue bounding box). (A-D) Shh-GFP (green) is released from its source (magenta) and freely diffuses around control cells (unmarked). (E) When magnified, Shh-GFP is observed to freely surround cells. (F-I) At the opposing edge of the clone, *Shh-GFP* expressing cells are juxtaposed to those expressing *Sulf1* (yellow). (J) When the *Sulf1* positive region is magnified, no Shh-GFP can be observed diffusing between the cells.

Shh-GFP expressing cells are marked by CFP-GPI (Magenta)

Sulf1 expressing cells are marked by mRFP (Yellow)

Shh-GFP protein is shown in green

Magnified images (E,J) are taken from the bounding boxes shown (D,I) and displayed in white to improve contrast

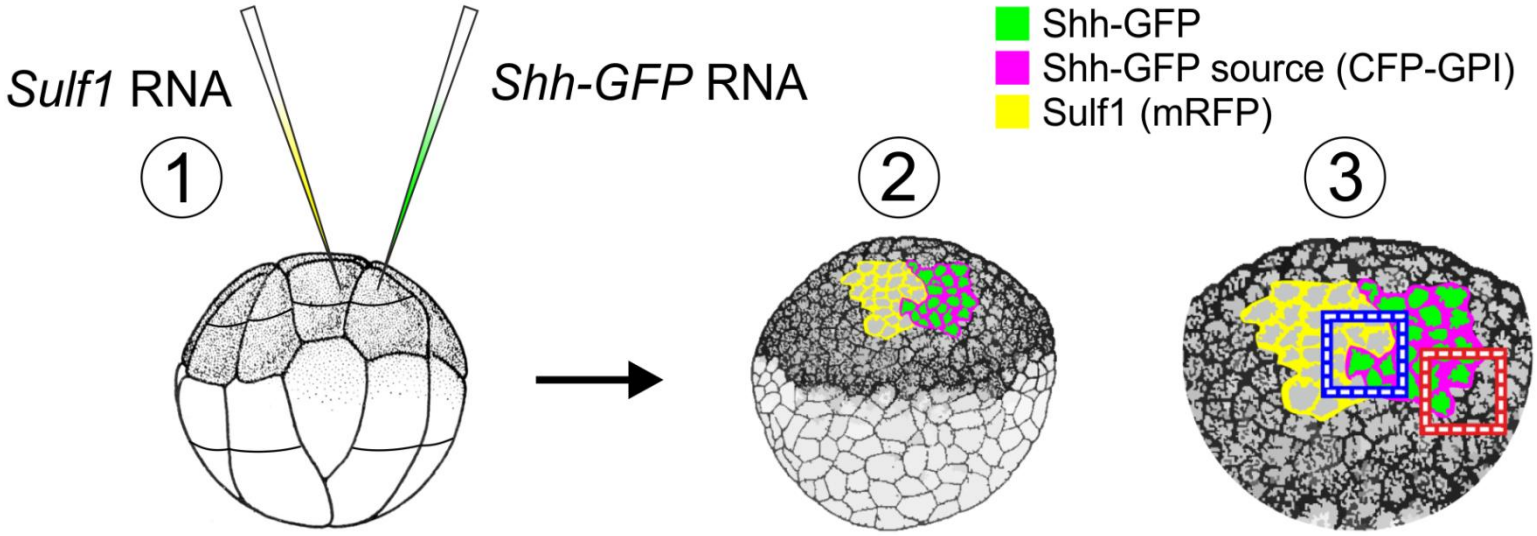

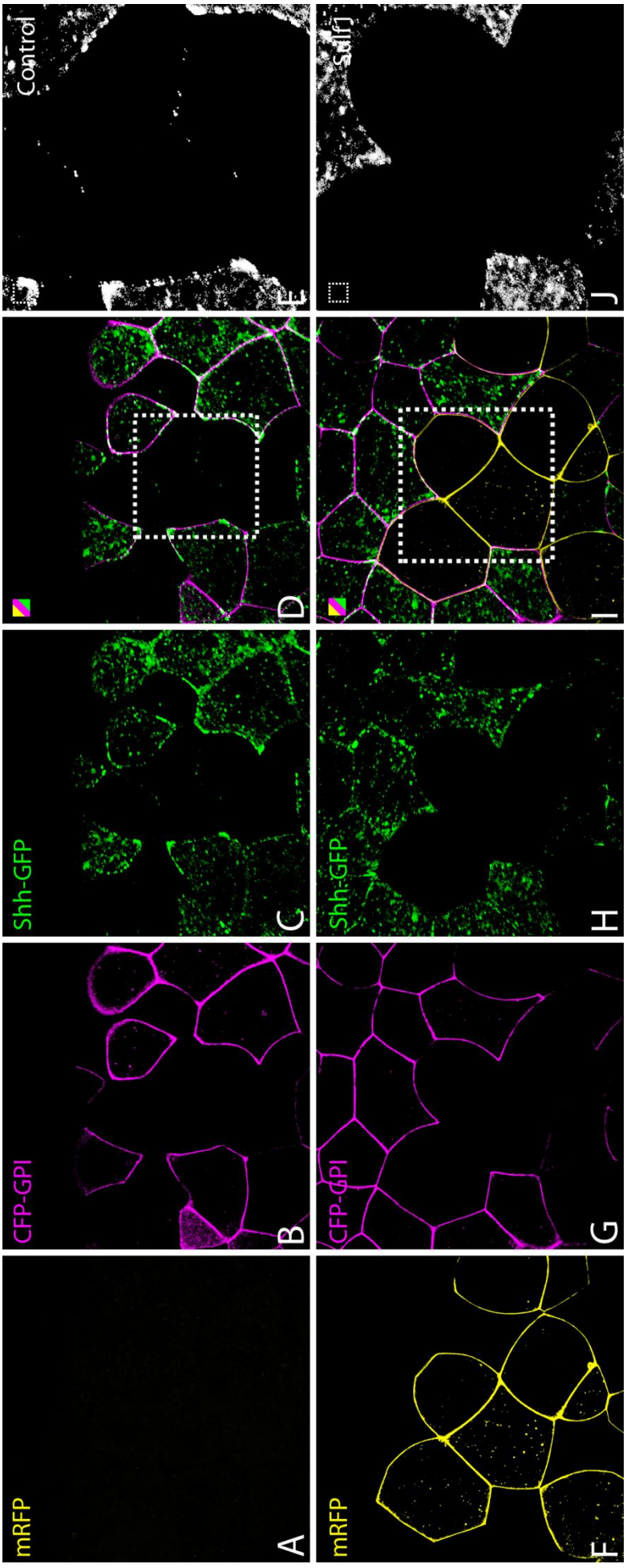
mRFP
A
CFP-GPI
B
Shh-GFP
C
D
Control
E
mRFP
F
CFP-GPI
G
Shh-GFP
H
I
Sulf1
J

Figure 4.6 Shh-GFP fails to diffuse into distant cells expressing Sulf1

(1) *X. laevis* embryos were injected at the 32-cell stage with *Shh-GFP* in one cell, along with GPI linked CFP as a membrane marker, and with *Sulf1* and mRFP in a nearby cell. (2) Animal caps were taken at NF stage 8 and were imaged after 2 hours. Images A-E are from the edge of the *Shh-GFP* positive group of cells (3, red bounding box), while images F-J are from the opposite edge of the clone which lies close to *Sulf1* positive cells (3, blue bounding box). (A-D) Shh-GFP (green) is released from its source (magenta) and freely diffuses around control cells (unmarked). (E) When magnified, Shh-GFP is observed to freely surround cells. (F-I) At the opposing edge of the clone, *Shh-GFP* expressing cells are close but not abbuting those expressing *Sulf1* (yellow), so that a gap of control cells lies between them. (J) While Shh-GFP is able to diffuse through the region of control cells, no Shh-GFP can be observed diffusing between *Sulf1* expressing cells.
Shh-GFP expressing cells are marked by CFP-GPI (Magenta)
Sulf1 expressing cells are marked by mRFP (Yellow)
Shh-GFP protein is shown in green
Magnified images (E,J) are taken from the bounding boxes shown (D,I) and displayed in white to improve contrast

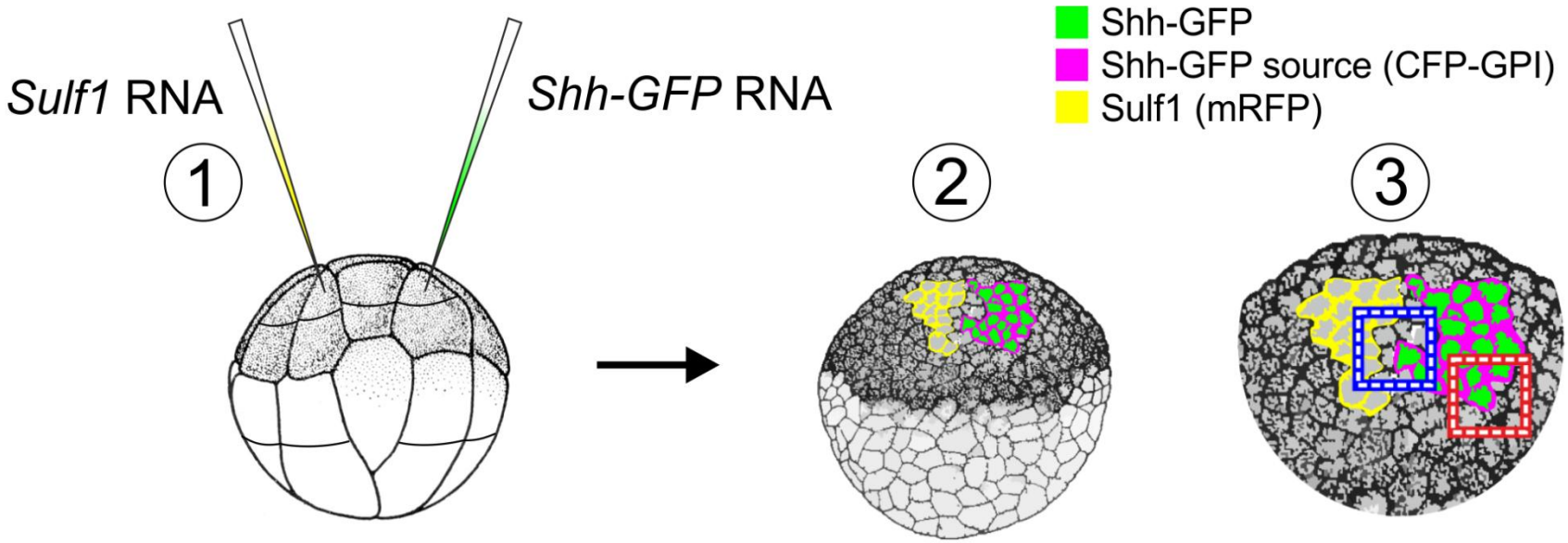

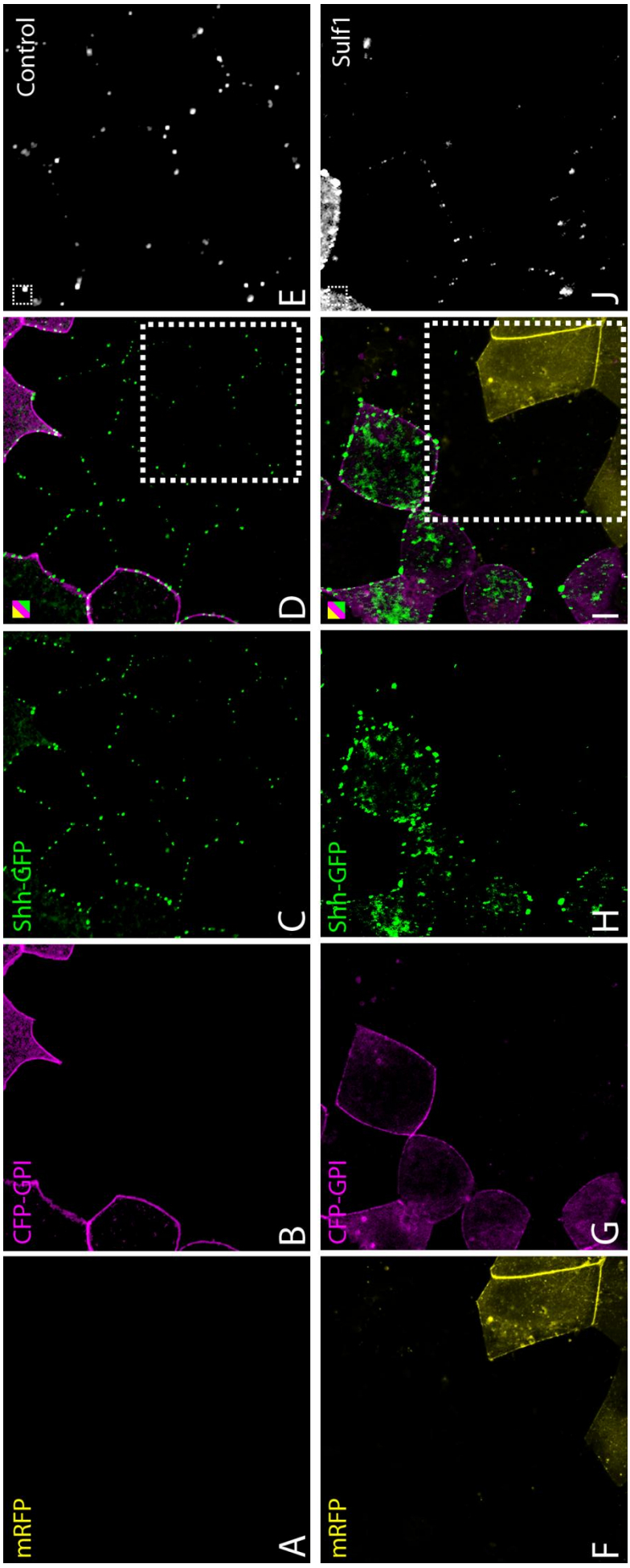
mRFP
A
CFP-GPI
B
Shh-GFP
C
D
Control
E
mRFP
F
CFP-GPI
G
Shh-GFP
H
I
Sulf1
J

This data suggests that Sulf1 alters the way in which Shh is able to diffuse. The way in which Sulf1 changes Shh diffusion appears to depend on whether Shh and Sulf1 are co-expressed, or expressed in adjacent cells. As Shh and Sulf1 are co-expressed within floor plate of the neural tube, the experiment shown in Figure 4.4 is most likely to recapitulate the role of Sulf1 within the floor plate in vivo. When Shh and Sulf1 are co-expressed, Sulf1 appears to promote the formation of aggregates. Interestingly however, upon close examination of these samples, aggregates only appear to be present close to the Shh expressing cells. Shh futher away from these cells however appears more punctuate as seen in control embryos. Figure 4.7 shows animal caps in which a region of cells co-expresses Shh-GFP and Sulf1. Bounding boxes show Shh-GFP ouside of the Shh-GFP expressing region, close to (1) and far away

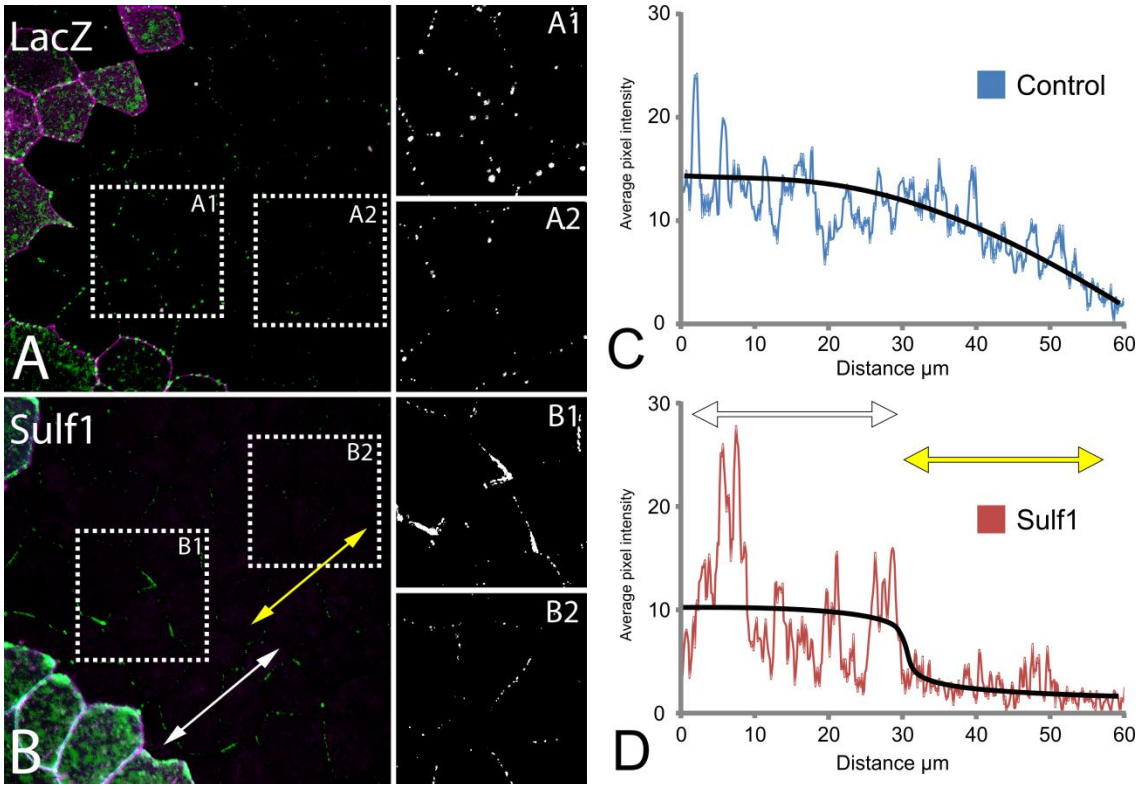

Figure 4.7 Sulf1 modifies the distribution of Shh-GFP when co-expressed in signalling cells
(A) Shh-GFP diffusion in control animal caps. Shh forms evenly distributed discrete foci around cells close to (A1) and far from (A2) the source. (B) Shh-GFP diffusion away from cells co-expressing *Sulf1* and *Shh-GFP*. Close to the source, Shh-GFP forms aggregates (B1). Far from the source, Shh-GFP is evenly distributed around cells (B2). (C,D) Average pixel intensity of Shh-GFP outside of the expressing region in control (C) and *Sulf1* expressing (D) animal caps. While levels in controls exhibit a gradual decrease, levels from *Sulf1* expressing caps show a sudden drop 30µm from the source.
Arrows show regions which represent high (white) and low (yellow) levels of Shh-GFP.
Control n=8, Sulf1 n=7

(2) from the region. In control embryos, Shh-GFP is more abundant near the site of synthesis (Figure 4.7A1) than far away (Figure 4.7A2) as would be expected with a diffusing molecule. The distribution of Shh-GFP particles around cells however does not change, with discrete foci being evenly distributed around cells. Shh-GFP which is released from Sulf1 expressing cells however forms aggregates around cells (Figure 4.7B1). Aggregation of Shh-GFP however is only seen close to the site of synthesis; analysis of particles far from the clone, reveal discrete evenly distributed foci similar to that seen in controls (Figure 4.7B2). Measurement of the average pixel intensity of Shh-GFP outside of Shh-GFP expressing cells reveals that this change in Shh aggregation is associated with a change in the level of Shh-GFP. Shh released from cells co-expressing LacZ (blue line) is present at high levels close to the clone, and this level gradually drops. Shh that is released from Sulf1 co-expressing cells (red line) is again present in high levels close to the source. Rather than a gradual decrease, however Shh-GFP displays a sudden drop in level after ~30µm. Due to the size of the caps, it is not possible to know whether Sulf1 extends or restricts the overall range of Shh diffusion. This data does however suggest that Sulf1 modifies the release of Shh into the environment. Additionally it was noted that cells expressing Sulf1 exhibit raised levels of intracellular Shh-GFP. This is likely to represent an increase in trafficking, suggesting that Sulf1 may modulate Shh diffusion by regulating which proteins Shh interacts with prior to its release.

4.4.3 Shh oligomerisation in Sulf1 expressing cells

The above results indicate that Sulf1 is able to alter the way in which hedgehog diffuses both when it is co-expressed with Shh and when it is expressed in cells responding to the hedgehog signal. This suggests that Sulf1 not only plays a role in altering the environment through which Shh moves but also may play a role during the release of hedgehog from the membrane. One way in which it may affect the release of hedgehog is by changing the way Shh forms multimeric complexes. HSPGs may provide a platform for Shh multimerisation (Goetz et al., 2006) and so changing the sulfation state of HSPGs could impact the formation of Shh complexes, so affecting its diffusive ability.

To initially assess the interaction between Shh monomers forming multimeric complexes, two fluorescent constructs were synthesised, replacing the GFP in the Shh-GFP construct with cyan fluorescent protein (CFP) and yellow fluorescent protein (YFP). When in close proximity, energy is directly transferred from a donor fluorphore (CFP) to an acceptor fluorophore (YFP), in a process known as Förster resonance energy transfer (FRET). When the acceptor fluorophore is bleached, energy is no longer transferred from the donor to the acceptor but is instead given out by the donor. This increase in donor intensity can be used to determine whether the two proteins interact. Figure 4.8 shows intensity traces of Shh-CFP and Shh-YFP over a 40 second period. After 20 seconds the YFP fluorophore was bleached away, and in both control and *Sulf1* over expressing samples, a corresponding increase in CFP intensity levels could be seen. This shows that, Shh-CFP is interacting with Shh-YFP, and that over expression of *Sulf1* does not inhibit the formation of hedgehog complexes.

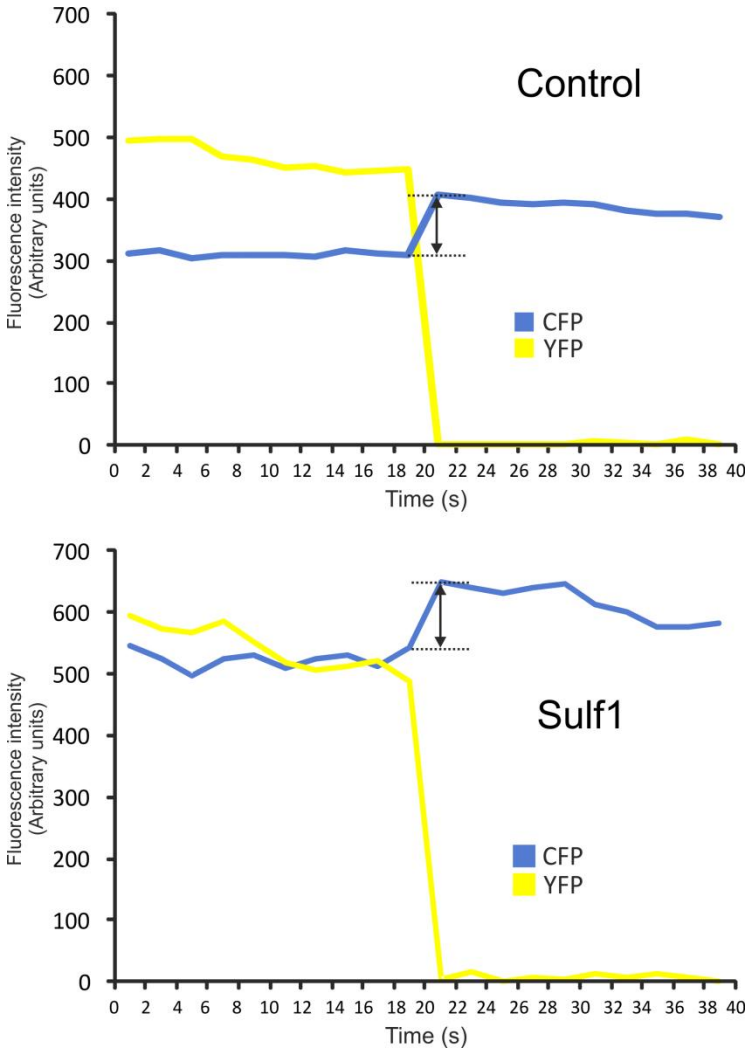

Figure 4.8 Intensity of Shh-CFP and Shh-YFP before and after photobleaching
Top: In control embryos, Shh-CFP and Shh-YFP show a steady state of fluorescence prior to bleaching. Following bleaching of YFP after 20 seconds with a high intensity 514 laser, Shh-CFP shows an increase in signal (arrow), indicating that Shh-CFP and Shh-YFP were undergoing FRET prior to bleaching.

Bottom: In embryos over expressing *Sulf1*, Shh-CFP and Shh-YFP also exhibit a steady state of fluorescence. Bleaching of YFP similarly leads to an increase in CFP intensity indicating that Shh FRET pairs also form in *Sulf1* over expressing embryos.

The efficiency of energy transfer between CFP and YFP can be calculated from the increase in intensity following photobleaching taking the difference between the intensity of the donor before and after bleaching as a percentage of the intensity after bleaching. This measurement gives an indication of the relative proximity of FRET partners, as the closer the FRET pairs, the greater the energy transfer between them. Using the numbers from the intensity plots showin in Figure 4.8, the FRET efficiencies were calculated for control and *Sulf1* over expressing samples. Although Sulf1 does not completely inhibit the formation of hedgehog multimers, it may act to destabalise them, reducing the number of monomers within the multimer. If this is the case it would be expected that the FRET efficiency between Shh-CFP and Shh-YFP moieties would be reduced, as there would be fewer CFP and YFP fluorophores in close proximity. Figure 4.9 shows the FRET efficiency in control and *Sulf1* over expressing samples. Only a slight drop in FRET efficiency is observed in *Sulf1* over expressing samples, suggesting that Sulf does not affect hedgehog multimerisation.

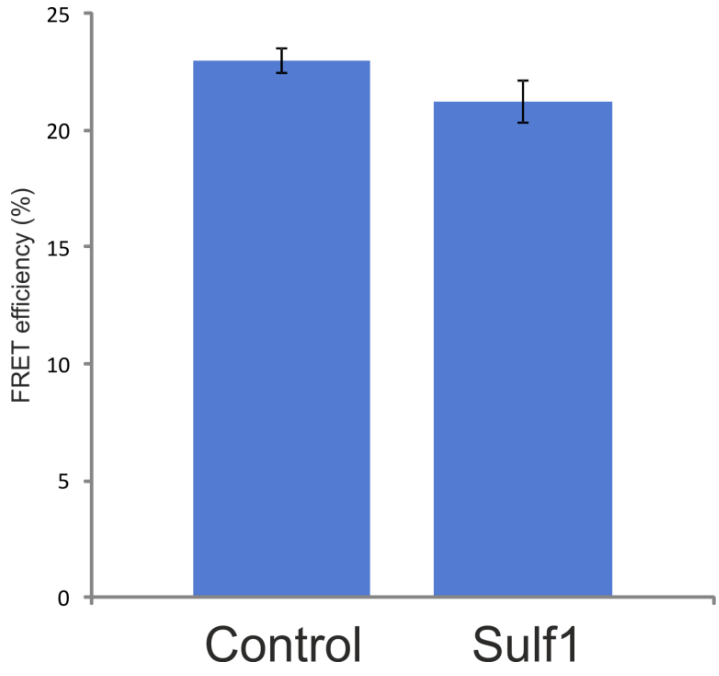

Figure 4.9 FRET efficiency between Shh-YFP and Shh-CFP within multimeric complexes
Measurement of the difference in the intensity of Shh-CFP before and after photobleaching. In control samples, CFP increases in intensity by 22.96% following photobleaching of Shh-YFP. In samples over expressing *Sulf1* this difference drops to 21.23%. This however does not represent a significant change (Student's t-test p=0.122, n=8)

4.4.4 Sulf1 affects the distribution of Shh *in vivo*

The experiments described above indicate a role for Sulf1 in controlling the distribution of Shh in animal caps. Although this methodology provides insights into the ability of Sulf1 to affect Shh distribution and allows separation of the activity of Sulf1 within cells expressing Shh and cells receiving Shh, it does not provide any indication as to the endogenous role which Sulf1 has within the neural tube. To characterise the function of Sulf1 within the neural tube and understand whether its ability to alter the distribution of Shh within animal caps is relevant in vivo, the distribution of Shh protein was analysed using the antibody 5E1. Sulf1 was knocked down using the AMO S1MO3 as described previously, and antibody staining was carried out in whole embryos which were sectioned for analysis by confocal microscopy. Figure 4.10 shows cross sections of stage 23 X. tropicalis embryos stained for the Shh protein using the 5E1 antibody. In control embryos, Shh staining is strong within the notochord and ventral neural tube, with particularly intense staining at the medial tip of the floor plate (Figure 4.10A). Following Sulf1 knockdown Shh staining is reduced within the ventral neural tube and notochord (Figure 4.10B). To quantify this observation the average intensity of Shh staining across the width of the neural tube was measured (measured area shown in Figure 4.10C). In control embryos, staining intensity shows a broad peak around the medial tip of the floor plate. After around 25µm the level of staining drops off fairly quickly (Figure 4.10D blue line). In Sulf1 morphant embryos, the peak level of staining is seen within the same region. After only 10µm however, the level of staining drops quickly, and staining further dorsally remains low (Figure 4.10D red line). These results suggest that Sulf1 normally acts to regulate the distribution of Shh, and that in the absence of Sulf1, Shh levels are reduced significantly.

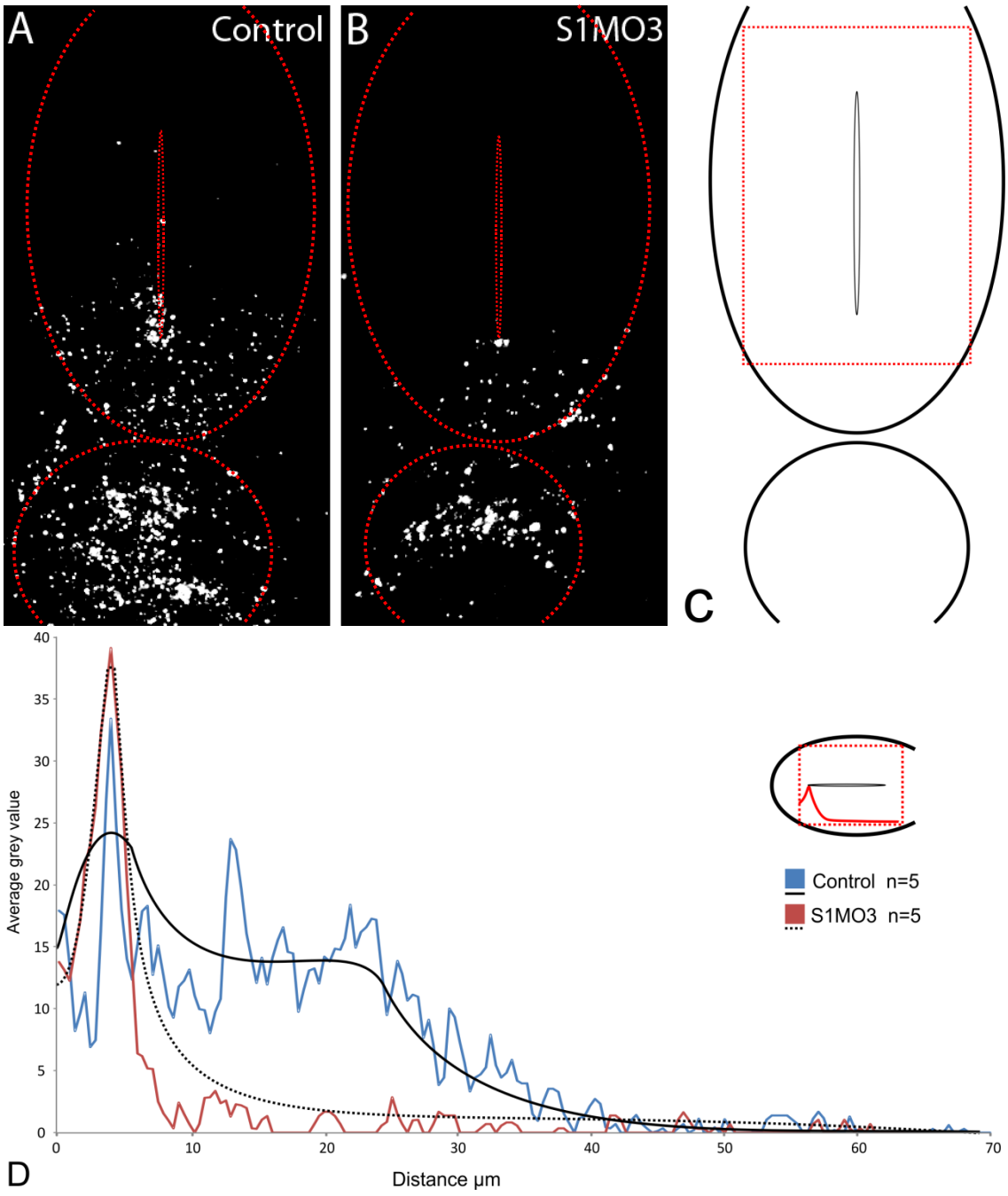

Figure 4.10 Distribution of Shh protein within the neural tube of stage 23 *X. tropicalis*

(A) Shh can be detected at high levels within the notochord (red dashed circle) and ventrally within the neural tube (elipse). Low levels can also be seen further dorsally within the neural tube, which show the highest intensity medially. (B) Following Sulf1 knockdown, the level of Shh is greatly reduced. (C) Schematic outlining the area over which the average intensity of staining across the width of the neural tube was measured. (D) Plot of the average grey level measured as described in C. The highest level in both control and morphant embryos is located at the medial tip of the floor plate. The overall distribution of Shh protein is however different. In control embryos (blue line), the level of Shh remais high around the peak, and drops off after 25µm. In Sulf1 morphant embryos (red line) high staining is only seen over a very narrow region; staining drops to almost nothing after 10µm.

(A) and (B) display representative images from 12µm Z-stacks and show the total pixel intensity over the stack. In (D) graphs show the average grey level over the width of the neural from the ventral to dorsal end, taken from 5 control and 5 knockdown embryos. Image in the top right corner indicates how the graph relates to the measured area as shown in (C).Trend of control (solid black line) and Sulf1 morphants (dashed line) is shown.

4.5 Discussion

The results presented in the previous chapter suggested that changes in neuronal patterning were due to a change in the diffusion of the Shh protein. To understand the ability of Sulf1 to affect the distribution of Shh, analysis of Shh was undertaken in live cells and fixed specimens. To allow visualisation of Shh in live cells, a GFP tagged Shh was synthesised. This was based on a mouse knock-in construct, which was shown to diffuse within the neural tube of mice in the same way as endogenous Shh, and was also able to activate Shh signalling (Chamberlain et al., 2008).

To initially test the ability of Shh to diffuse in the presence or absence of Sulf1, embryos were injected so that *Sulf1* was expressed globally while a subset of cells also expressed *Shh-GFP*. In control embryos, Shh-GFP diffused away from its site of synthesis in discrete foci that were evenly distributed around cells. In embryos expressing *Sulf1* however, Shh-GFP did not appear to diffuse as easily and could be seen to form clumps around cells receiving the Shh signal. To assess the relative importance of *Sulf1* expression in *Shh* expressing cells or cells through which Shh diffuses, embryos were injected such that small regions of cells either co-expressed *Shh* and *Sulf1* or expressed *Shh-GFP* but lay adjacent to a *Sulf1* expressing region. When *Shh-GFP* and *Sulf1* were co-expressed, the clumps of Shh-GFP that formed previously were still present, suggesting that this aggregation of Shh was a function of the activity of Sulf1 in Shh producing cells instead of those receiving the signal. Further analysis of these cells showed that while Shh aggregates formed close to the source, far from the source Shh-GFP appeared the same as that released from control cells, albeit at a lower level. Additionally, while levels of Shh-GFP released from control cells exhibit a gradual decrease as they diffuse away from the source, Shh-GFP released from Sulf1 expressing cells shows a sudden drop in level around 30µm from expressing cells. This suggests that Sulf1 may promote short distance diffusion away from cells at the expense of long range, thus raising the local concentration of Shh protein.

When *Sulf1* was expressed only in cells receiving the Shh signal, Shh could not be detected in the Sulf1 positive region. This was seen when Sulf1 positive cells were directly adjacent to Shh producing cells, and also when they lay at a

distance from the Shh source. It is not apparent from this analysis whether the absence of Shh from the *Sulf1* expressing region represents the exclusion of Shh, or whether over expression of *Sulf1* promotes rapid internalisation in Shh receiving cells. Future analysis on the downstream signalling and interaction of Ptc with Shh in receiving cells will help to decipher whether Sulf1 acts to positively or negatively regulate Shh signalling within Shh receiving cells.

4.5.1 Shh multimer formation is unaffected by Sulf1

In both embryos expressing *Sulf1* globally, and those co-expressing *Sulf1* and *Shh-GFP*, Shh protein was found to be in clumps surrounding cells and not in discrete foci distributed evenly. As the physiologically relevant form of Shh forms multimeric complexes, a change to the ability of Shh to oligomerise in the presence of Sulf1 may explain the change in the distribution of Shh. The interaction of Shh proteins was analysed with CFP and YFP fusion proteins using Förster resonance energy transfer as a measure of Shh proximity. This method was used as it allowed analysis of interaction in live cells, and avoided potential artefacts introduced during experiments involving the cross-linking of proteins such as pulldown experiments. The FRET efficiency of Shh-CFP/YFP FRET partners analysed in control samples was found to be about 23%. This represents a relatively high amount of energy transfer which possibly indicates the presence of multiple FRET partners within close proximity, as would be expected form a large multimeric complex. In samples over expressing *Sulf1*, the FRET efficiency is slightly reduced, but this reduction does not represent a statistically significant change. This suggests that Sulf1 does not act to modify Shh distribution by promoting the formation of multimeric complexes. The ability of Sulf1 to affect Shh dispersal when expressed exclusively in Shh expressing cells does however suggests that Sulf1 either modifies the ability of cells to release Shh into the surrounding environment, or changes the way in which co-factors interact with Shh as it is released. These possibilities will be discussed below.

4.5.2 Sulf1 knockdown affects endogenous Shh diffusion

The level of Shh within the neural tube is a crucial contributing factor in the determination of populations of precursor cells which define specific neuronal subtypes as development progresses. Inhibition of Shh signalling affects the

expression level and spatial distribution of transcription factors which act to specify the identity of these precursor populations, and this has a dramatic effect on the overall patterning and structure of the neural tube. Following Sulf1 knockdown, the overall level of Shh is reduced (Figure 4.10). In the previous chapter, knockdown of Sulf1 was shown to affect the regional expression of transcription factors which define certain regions of the neural tube. These observed changes in gene expression correspond to a reduction in the level of Shh, such that genes requiring high levels of Shh are shifted and reduced in size (FoxA2, Isl1), while those which are less dependent on Shh levels for expression show only minor changes (Nkx6.1, Dbx1). Figure 4.11 shows how the change in the level of Shh corresponds to the changes observed in gene expression. Reduced ventral levels of Shh results in a narrowing of the *FoxA2* positive region, and a ventral shift in *Nkx2.2* expression (Figure 4.11A,B) The steep reduction in the concentration of Shh close to the peak results in a narrowing of the permissive zone for *Isl1* expression (Figure 4.11C).

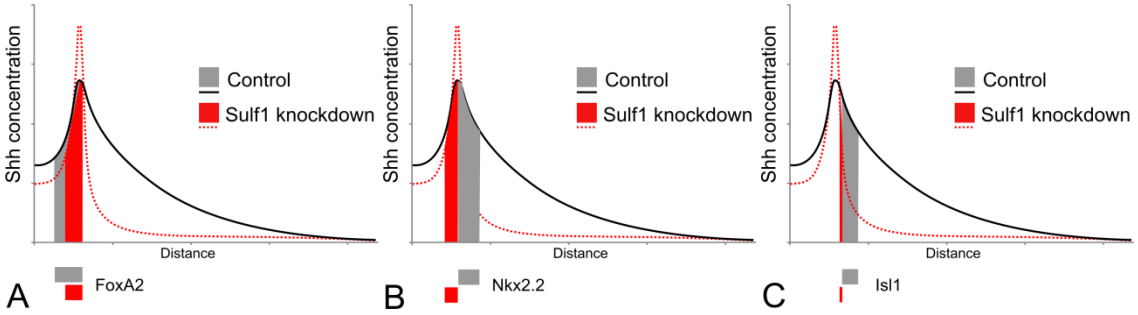

Figure 4.11 Changes to Shh concentration affects patterning of the neural tube
(A) A reduced level of Shh within the floor plate region following Sulf1 knockdown correlates with a narrowing of the region which expresses *FoxA2*. (B) Reduced levels of Shh result in *Nkx2.2* being expressed further vetrally within the neural tube such that it lies within the floor plate region. (C) Isl1 positive cells within the ventral neural tube lie further ventrally and occupy a narrower region following Sulf1 knockdown.
Expression region in control embryos represented by grey bar, and in sulf1 morphants by a red bar. X-axis shows distance along the dorsoventral axis of the neural tube from the ventral (left) to the dorsal (right) poles.

Interestingly however, not all changes in marker expression appear to reflect a reduction in the level of Shh. *Nkx6.1* expression, shows a very slight dorsal expansion following Sulf1 knockdown, although this can only be seen medially. This suggests that Shh levels may be increased rather than reduced. In Sulf1

morphants, a high level of Shh can still be seen at the medial tip of the floor plate. From this point, Shh can be released into the ventricular region and can move along cells apically (side toward lumen of the neural tube). In *Drosophila*, over expression of Sulf1 leads to a reduction of apical Shh (Wojcinski et al., 2011). Loss of Sulf1 in the ventral neural tube therefore may bias apical translocation of Shh, which could raise Shh levels medially. In animal cap experiments, Shh-GFP was seen to accumulate at higher levels close to the Shh-source when co-expressed with *Sulf1*. Further from the source however, Shh-GFP levels appeared slightly reduced. *In vivo*, Sulf1 may also act to promote short range Shh-diffusion over long range, thus raising ventral levels of Shh protein. Loss of Sulf1 would therefore lead to increased dorsal levels of Shh, and this may explain why Nkx6.1 exhibits a dorsal expansion in its expression domain. Although no Shh could be observed dorsally following Sulf1 knockdown *in vivo*, it may just have been below detectable levels. Further optimisation of Shh detection in *Xenopus* is therefore required to assess whether this is the case.

In the *Drosophila* wing, it has been suggested that Sulf1 has a bimodal role, whereby it promotes Hh release from *Hh* expressing cells, but reduces the perceived level of Hh signalling within receiving cells (Wojcinski et al., 2011). In vertebrates Sulf1 appears to promote Shh signalling within the ventral neural tube. In chick, over expression of *Sulf1* leads to Shh accumulation at the cell surface in a cell-autonomous manner and up-regulation of the Shh target *Nkx2.2* (Danesin et al., 2006). Inhibition of Sulf1 in *Xenopus* leads to reduced levels of the Shh protein *in* vivo (Figure 4.10) concomitant with a reduction in the level of *Ptc2* expression, a decrease in the size of the *FoxA2* expression region and a ventral shift of Shh targets. In animal caps co-expression of *Sulf1* results in the formation of Shh-GFP aggregates and a raised level of Shh-GFP close to Shh-GFP expressing cells (Figure 4.4). Taken together these results indicate that Sulf1 potentiates Shh signalling within the ventral neural tube, and suggest a mechanism whereby Sulf1 promotes the local accumulation of Shh thus increasing the level of Shh signalling ventrally.

5.0 Discussion

5.1.1 Morphogen gradient regulation by Sulf1

Although the focus of this work was the role of Sulf1 in regulating Shh during neuronal patterning, Sulf1 has the ability to modulate many different signalling pathways. One pathway that shares similarity with hedgehog signalling in particular is Wnt. Like hedgehog proteins, Wnts are lipidated during their synthesis (Doubravska et al., 2011) and are released into the surrounding environment to pattern tissues. Furthermore, many of the HSPG synthesis mutants that have been mentioned as affecting Hh signalling in *Drosophila*, also exhibit changes associated with Wg signalling (Bornemann et al., 2004). The expression of Hh and Wg is known to be interdependent in *Drosophila* and so perturbation of either pathway as a result of aberrant HSPG synthesis will impact on the other. It has been shown however that both Wg and Hh, display changes to their spatial distribution following changes to HSPG synthesis or Sulf expression. At the DV border of the *Drosophila* wing disc Sulf1 acts to facilitate the lateral diffusion of Wg protein (Kleinschmit et al., 2010; You et al., 2011). These studies also show that Wg signalling is up regulated in Sulf mutants, whereas over expression of Sulf1 leads to reduced Wg signalling and extracellular Wg protein levels (Kleinschmit et al., 2010; You et al., 2011). The work presented here suggests a role for Sulf1 in regulating Shh signalling in vertebrates, and work currently being undertaken in the Pownall lab has indicated a role for Sulf1 in regulating vertebrate Wnt signalling (Simon Fellgett personal communication). Together with the numerous studies in *Drosophila*, this suggests that Sulf1 modification of HSPGs may provide a general mechanism to shape morphogen gradients and fine tune patterning within a variety of tissues, and that this mechanism is not only used to regulate a number of different pathways, but is conserved between species.

5.1.2 Changing the range

In *Drosophila* it has been suggested that short and long range Hh signalling can be separated, where long range signalling is located apically, whereas short range signalling occurs basolaterally (Ayers et al., 2010). The HSPG dally has been shown to affect long range Hh signalling; *dally* mutant discs exhibit a reduction in the activation of long range Hh targets (Eugster et al., 2007). Furthermore, *dally* mutants display reduced levels of apical Hh, whereas increased dally levels promote apical accumulation (Ayers et al., 2010). When

dally-GFP is over expressed in the posterior compartment, *dpp* expression is expanded greatly, while *En* expression is reduced. Over expression of *dally* in Hh receiving cells however does not affect *dpp* expression. This suggests that long range signalling is mediated by dally, which promotes Hh accumulation apically, favouring long range (*dpp*) over short range (En) signalling (Ayers et al., 2010). Using a mutant form of Ptc (Ptc^{1130X}) which sequesters Hh but is not internalised, (Ayers et al., 2010) further show that apical Hh forms large puncta and can be detected far from the source, while basolateral Hh is only located close to the source. Additionally, basolateral Hh does not form discrete puncta, and appears closely associated with the membrane.

In *Xenopus* animal caps, over expression of *Sulf1* in *Shh* expressing cells leads to an increase in the accumulation of Shh close to the source (Chapter4). Furthermore, Shh released from *Sulf1* expressing cells which remains close to the source forms large aggregates around cells instead of the discrete puncta seen in controls. Shh far from *Sulf1* expressing clones however forms discrete foci. This pattern of Shh accumulation resembles that seen in *Drosophila*. The ability of Sulf1 to raise the proximal level of Shh therefore suggests that it may promote short range over long range signalling, and that as suggested in *Drosophila,* short and long range hedgehog signalling in *Xenopus* may be dependent on two discrete gradients. Figure 5.1 shows the distribution of Hh in the *Drosophila* wing disc. Hh is expressed posteriorly and diffuses into the anterior compartment. A cross section through the wing disc (Figure 5.1B) shows how Hh moves both apically and basolaterally to create two discrete gradients which are spatially and characteristically discrete, with basolateral Hh being more closely associated with the membrane. The ability of Sulf1 to reduce apical levels of Hh, together with the change from an apical to basolateral type distribution in *Xenopus* cells over expressing *Sulf1,* suggests a mechanism whereby Sulf1 promotes short range over long range signalling (Figure 5.1C).

Xenopus animal caps injected with *Sulf1*, exhibit increased levels of intracellular Shh-GFP (Chapter 4). This increase in intracellular accumulation of Shh-GFP in the presence of Sulf1 agrees with the hypothesis that Sulf1 promotes vesicular trafficking between the apical and basolateral plasma membranes. In *Drosophila*, (Wojcinski et al., 2011) report a reduced level of Hh in *Sulf*

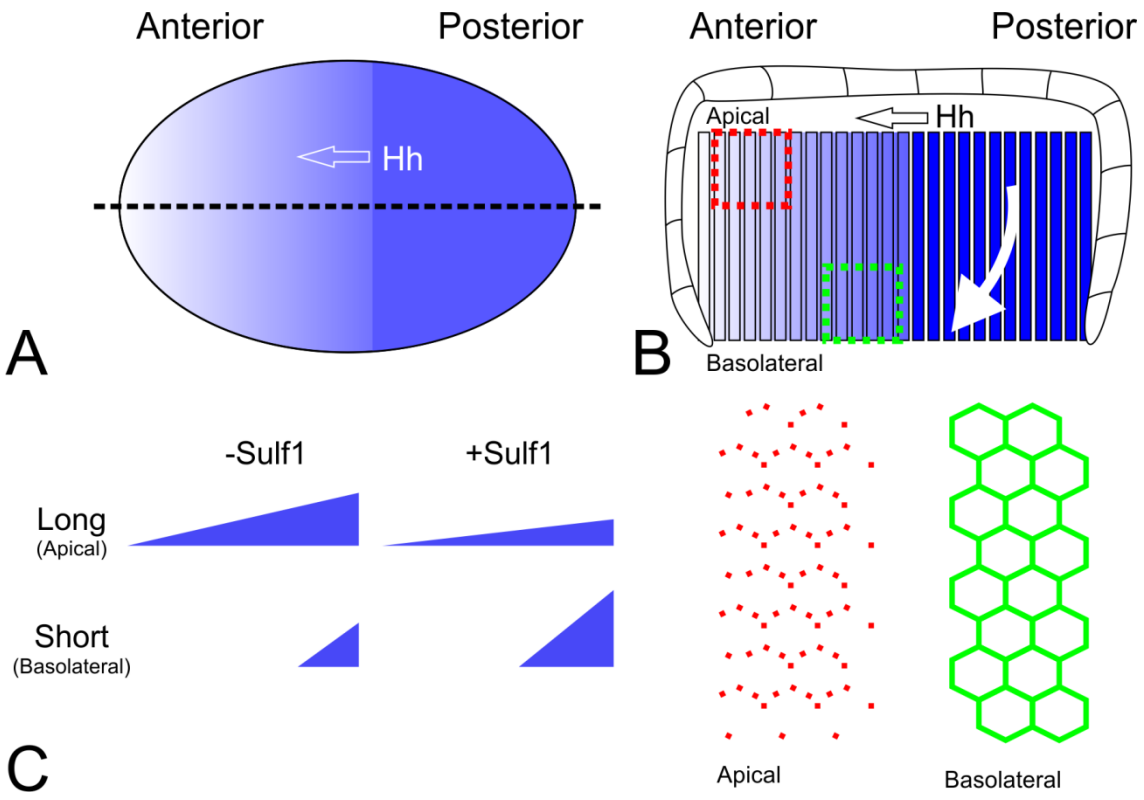

Figure 5.1 Sulf1 and the Hh gradient
(A) In the *Drosophila* wing disc, *Hh* is expressed in the posterior compartment and diffuses through the anterior compartment, forming a gradient. (B) Cross section through the wing disc as shown by the dashed line in (A). The disc is comprised of two discrete epithelia, the disc proper which will form the adult wing and a second squamous-like peripodial membrane which surrounds it. Hh protein is released from the apical side to affect long range signalling,and from the basolateral membrane to induce short range targets. While apically released Hh (red) forms discrete punta basolaterally released Hh (green) is closely associated with the membrane.
(C) Sulf1 acts to increase basolateral levels of Hh, raising the local level of Hh signalling, while reducing the level which activates longer range targets.
Schematics and localisation of Hh adapted from (Ayers et al., 2010).

expressing cells. Analysis however focused on the apical plain and so basolateral translocation may account for the observed reduction in Hh staining. Furthermore when Z-stacks are analysed the authors report reduced apical Hh staining in *Sulf* over expressing cells, indicating that Sulf1 does reduce apical Hh levels which may be achieved through the promotion of trafficking.

5.1.3 Dally or dlp

Dally is closely related to glypican 3 (gpc3) and glypican 5 (gpc5) in vertebrates. If these glypicans promote long range signalling in *Xenopus* as dally has been shown to in *Drosophila*, Sulf1 may act to inhibit their association with Shh.

Alternately Sulf1 may promote the association of Shh with other factors, one of which may by the closely related glypican dally-like protein (dlp). In *Drosphila* dlp is transcytosed from the apical to the basolateral plasma membrane. (Callejo et al., 2011). *Dlp* mutants display increased levels of Hh within expressing cells suggesting that Hh release is impaired. In agreement with this, knockdown of Dlp by RNAi in the posterior compartment, inhbits *Ptc* expression at the compartment border, indicating a reduced level of Hh signalling. (Callejo et al., 2011). The ability of Dlp to promote hedgehog release and high level Hh signalling close to the source, coupled with its subcellular localisation, makes it an attractive candidate for Sulf1 in respect to regulating hedgehog signalling. By promoting association with dlp over dally, Sulf1 could regulate the way in which Shh is released, thus promoting short range over long range signalling. A mechanism by which this may occur will be discussed below.

Work in chick has indicated that in the ventral neural tube, the majority of Shh is released basolaterally, and that this is under the control of Dispatched (disp). Blocking disp by co-transfection of miRNA constructs against *Disp1* reduces basolaterally released Shh (Etheridge et al., 2010). Interestingly however apical release of Shh is disp-independent. It has been argued that basolaterally released Shh forms the gradient that results in long range signalling, as $Disp^{-/-}$ cells are unable to induce the motor neuron specific marker HB9 or inhibit the expression of Pax7, as far from the source as $Disp^{+/+}$ cells (Etheridge et al., 2010). However, in mice it has been shown that apically restricted Shh forms a gradient far from the source which is co-incident with the specification of ventral cell identities (Chamberlain et al., 2008). Early notochord derived Shh appears to be restricted apically, whereas later Shh is found increasingly on the basolateral side (Chamberlain et al., 2008; Etheridge et al., 2010). It is interesting to note that in chick, Shh mRNA can be detected in the floor plate at E3, whereas Sulf1 expression is not seen until E4.5/5 (Danesin et al., 2006). The switch from apical, to predominantly basolateral accumulation therefore occurs over the period of *Sulf1* induction, which could explain the change in distribution.

5.1.4 A dual role for Sulf1

In chick, Sulf1 over expression leads to accumulation of Shh at the cell surface and the induction of *Nkx2.2* expression in a cell-autonomous manner (Danesin et al., 2006). The cell-autonomous nature of this indicates that Sulf1 is able to act not only at the level of Shh release, but also at the level of Shh reception. Interestingly, a mechanism whereby Sulf1 promotes the association of Shh with dlp could similarly explain why Sulf1 promotes hedgehog signalling in receiving cells. Apically located dlp in cells receiving Hh is rapidly internalised and transcytosed to the basolateral membrane, and is localised with Ptc and Hh in endocytic vesicles (Gallet et al., 2008). Blocking endocytosis of dlp leads to a depletion of basolaterally located dlp and a decrease in Hh signalling, indicating that endocytosis of dlp is required for optimal Hh signalling (Gallet et al., 2008). Endocytosis of hedgehog proteins in a complex with other glypicans however has been shown to inhibit signalling. In mouse embryonic fibroblasts, Shh is internalised in a complex with gpc3 in the absence of Ptc, and this leads to down regulation of signalling (Capurro et al., 2008). If Sulf1 acts to promote association with dlp (gpc4,6) over that with dally (gpc2,3,5), then it may raise the level of signalling by increasing the amount of hedgehog that is endocytosed in a complex with Ptc, thus leading to activation downstream signalling. It must be noted that while an inhibitory role for dally and gpc3 has been shown, dally which lacks its gpi link (dally$^{\Delta gpi}$) has been shown to be associated with Ptc and Hh in endocytic vesicles (Eugster et al., 2007), while cleaved dally has been shown to activate long range Hh signalling (Ayers et al., 2010). It may be therefore that gpi-linked dally may inhibit signalling in receiving cells, while cleaved dally released from Hh expressing cells acts to positively regulate signalling.

5.1.5 A conserved mechanism for Hh and Wg?

Wnt/Wg signalling has been shown to require HSPGs in a similar manner to Hh (Bornemann et al., 2004). Additionally it has been shown that Sulf1 is able to regulate the distribution of the Wg protein (Kleinschmit et al., 2010). Loss of Sulf1 in the wing disc leads to an increase in the level of Wg at the DV border indicating a role for Sulf1 in promoting its diffusion. It appears therefore that the way in which Sulf1 modulates the distribution of Wg is opposite to the way in which it regulates Hh, promoting long range dispersal instead of short range

signal activation. This divergence of activity however may be explained by the differential role that dlp has with either protein. While dlp has been shown to potentiate Hh signalling (Williams et al., 2010), dlp acts in an antagonistic manner with respect to Wg signalling; it has been suggested that dlp promotes transcytosis of Wg in the absence of its receptors DFrizzled2 (Dfz2) and Arrow, and hence prevents downstream signal activation (Gallet et al., 2008). Dally however has been shown to promote Wg signalling (Lin and Perrimon, 1999), indicating a divergent role for glypicans in modulating signal transduction. One other factor is the spatial distribution of the glypicans. While *Sulf1* and *dlp* are co-expressed in the posterior compartment where *Hh* is expressed and released, *dlp* is not expressed at the source of the wingless protein, along the dorsoventral border (Kleinschmit et al., 2010). Instead, dally is located proximal to the Wg source, while dlp is only present in distant cells. Immunodetection of Sulf1 and dlp reveal that they do not overlap in this region (Wojcinski et al., 2011), suggesting that dally is the main substrate for Sulf1, and this may explain the differential function of Sulf1 on protein dispersal. Figure 5.2 shows the spatial distribution of Sulf1, Wg, Hh, dlp and dally within the Drosophila wing disc. While *dally* is expressed ubiquitously, dlp is excluded form the dorsoventral border. Hh protein can be detected at high levels within the posterior compartment, but the level decreases further anteriorly. Wg is expressed at the dorsoventral border and the protein diffuses out from this region. Sulf1 is dynamically expressed, with two stripes of expression flanking both the dorsoventral and anteroposterior boundaries. While changes to the level of dlp are reflected by the levels of Hh, regions of dlp and Wg are mutually exclusive. From these patterns of protein distribution it can be seen that while

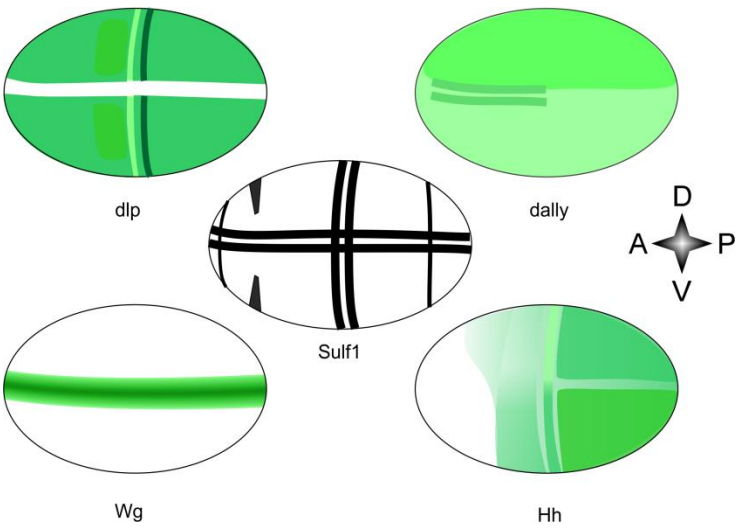

Figure 5.2 Sulf1 regulates Wg and Hh dispersal in the wing disc
Protein distribution of the glypicans dlp and dally, the signalling proteins Wg and Hh, and Sulf1 within the *Drosophila* wing disc.
Orientation is shown on the right.
Protein distribtuions from antibody stains as shown in (Kleinschmit et al., 2010; Wojcinski et al., 2011).

both dally and dlp overlap with Sulf1 at the anteroposterior border, only dally significantly overlaps with Sulf1 at the dorsoventral border. The availability of substrate for Sulf1 therefore affects the way in which it can modify the distribution of Wg and Hh.

5.1.6 HSPGs and hedgehog binding

The suggested mechanism above seems at odds with the idea that Shh specifically interacts with sulphated HS chains (Rubin et al., 2002), as it assumes that Sulf1 promotes the association of Shh with glypicans. Recently however it has been shown that HS chains are not required for Hh to bind glypicans (Yan et al., 2010). However while dlp(-HS) is only able to restore a null allele of dlp cell autonomously, wild type dlp is able to act in a non cell-autonomous manner, suggesting that while the core protein is important for Hh signalling, the HS side chains confer additional functionality (Yan et al., 2010). Together with the weight of evidence showing that HS synthesis is required for Hh diffusion, this indicates that while Hh may be able to bind the core proteins of glypicans, it appears that this interaction is not able to fully account for the role of dlp during Hh signalling. It is also Interesting to note that while (Yan et al., 2010) show that Hh is able to bind dlp independently of HS, other research has indicated that Dlp(-HS) is not able to bind Hh (Williams et al., 2010). The disparity in these results may be due to the presence of a co-factor which mediates this interaction. One candidate which may fill this role is the protein Shifted (Shf). Shf is a diffusible protein which interacts with HSPGs and Hh, accumulates in regions of high Hh levels and when mutated gives rise to similar diffusion defects seen following loss of HS synthesis (Glise et al., 2005; Gorfinkiel et al., 2005). It has been proposed that Shf acts to stabilise the interaction between Hh and HSPGs, thus facilitating signalling (Glise et al., 2005). Shf requires HS for its interaction with HSPGs; tout-velu mutant clones which lack HS exhibit reduced Shf accumulation (Glise et al., 2005). A requirement of Shf for Hh-HSPG stabilisation explains why Hh is unable to move through a region lacking HS synthesis. This may also explain the ability of wild type dlp but not dlp(-HS) to non cell-autonomously restore a dlp null.

One other question that arises from this potential mechanism is how Sulf1 promotes the association of Hh with dlp over dally, as Sulf1 is only able to

modify the HS chains on either protein. Interestingly, while Hh binding to the core protein of dlp has been shown (Yan et al., 2010), a similar interaction with dally has not been investigated. The ability of Shh to interact with gpc3 however (Capurro et al., 2008) suggests that dally will associate with Hh in a similar manner to dlp. As previously mentioned, the interaction between dlp and Hh may be mediated by Shf, and specificity for either glypican therefore may be Shf-dependent. Additionally, the HS complement of dlp and dally has been shown to differ, with dally having a greater level of HS (Kreuger et al., 2004). Sulf1 may therefore be able to more easily promote Hh association with dlp as its HS chains may be more rapidly modified compared with those of dally.

One other potential mechanism may be that Sulf1 does not confer preferential binding of Hh for either protein but instead changes the ability of either to be released from the membrane. Cleavage of the gpi-link both proteins by notum has been shown, resulting in their release form the membrane. When the HS of dlp is removed however, although notum is still able to cleave dlp, the efficiency of cleavage is reduced (Kreuger et al., 2004). The attached HS may therefore provide a scaffold to increase the ability of notum to cleave dally and dlp. If the sulphate groups of HS chains are required for this interaction, then Sulf1 would reduce the level of dlp and dally cleavage. In this way, dlp and dally would be retained at the membrane of Hh producing cells, allowing more dlp to be transcytosed, to affect short range signalling. Another mechanism of release of Hh in *Drosophila* is through the association of Hh with the lipoprotein lipophorin, and this association is important for long but not short range activity (Panakova et al., 2005). Association of glypicans with lipophorin can be through their gpi-link or through HS. (Eugster et al., 2007). Sulf1 may therefore reduce the ability of glypicans to associate with lipophorin through their HS chains, and subsequently reduce the level of Hh release, thus promoting short over long range signalling.

Figure 5.3 shows a model by which Sulf1 may control Shh signalling. In the absence of Sulf activity, Shh associates with the HS chains of HSPGs, and this association is stabilised by a co-factor (such as WIF-1). Shh may then move freely from cell to cell using the HSPGs on adjacent cells. Cleavage by notum, allows the Shh/HSPG complex to be released from the cell surface in association with a lipoprotein particle, facilitating long range signalling. Co-expression of *Sulf1* with *Shh*, promotes association with a dlp homologue, which is transcytosed to the basolateral membrane, where release of Shh under the control of Disp induces the expression of high level Shh targets close to the source.

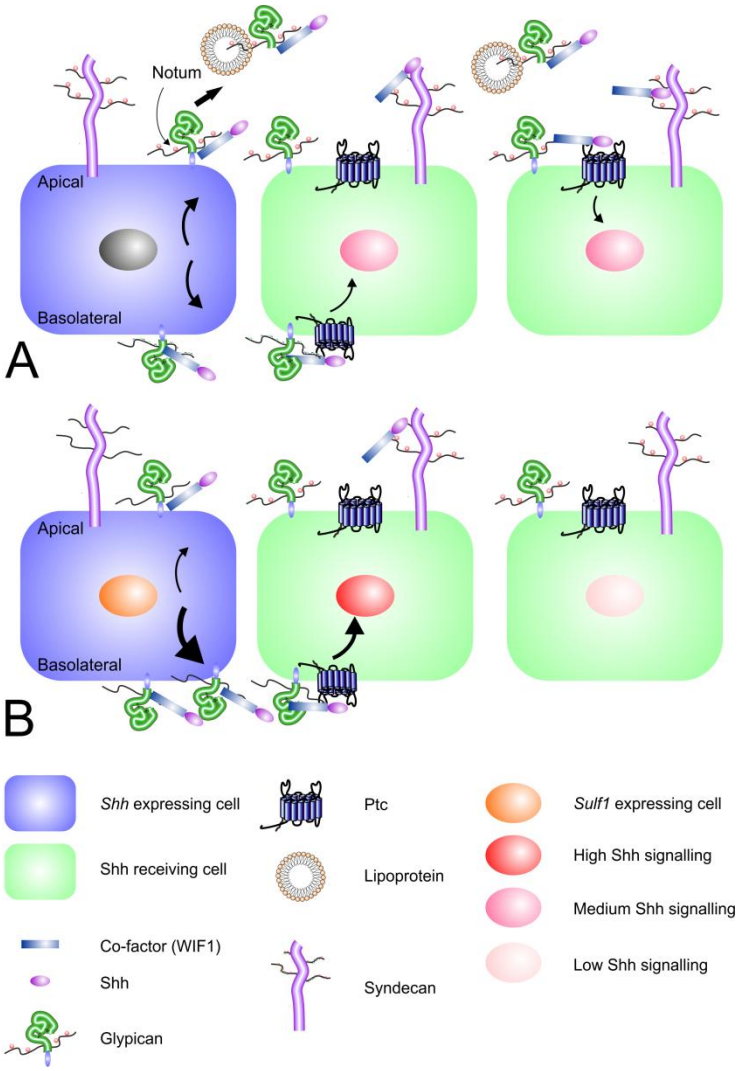

Figure 5.3 Potential mechanism for the regulation of Shh signalling by Sulf1
(A) In cells not expressing *Sulf1*, Shh associates with HSPGs along with a co-factor. Shh then moves along from cell to cell through interaction with HSPGs on adjacent cells. If associated with dally, Shh can be released into the extracellular space when dally is cleaved by notum, elicitng long range signalling. Shh can also associate with dlp, and be transcytosed to the basolateral membrane where it activates short range signalling.
(B) Co-expression of *Sulf1* with *Shh* promotes basolateral over apical Shh accumulation, such that Shh signalling is up regulated close to the source. Long range signalling is consequently reduced.

While this mechanism provides a possible explanation for the changes in Hh diffusion, it does require that Shf be present in all regions in which Hh is released. Additionally, while Shf has been shown to interact with Hh in

Drosophila, the ability of its vertebrate homologue WIF-1 to bind Shh has not yet been established. Additionally vertebrate WIF-1 is unable to rescue Shf mutants (Glise et al., 2005), suggesting their roles in respect to hedgehog signalling may not be conserved. Another interpretation could be that the HS chains simply provide a platform to allow Hh diffusion. In this way Hh is released from the signalling cell and interaction with the HS chains prevents interaction with the membrane, allowing diffusion. In the presence of Sulf1 therefore, Hh has a lower affinity for the HS chains, and so associates with the membrane. The inability of Hh to be lifted away from the membrane results in restricted movement such that longer range signalling is inhibited. It is unlikely however that the mechanism of Hh dispersal *in vivo* is this simple, as mutation of a number of factors other than HSPG synthesis inhibits Hh diffusion (Callejo et al., 2011; Glise et al., 2005), while over expression of proteins, such as an un-cleavable form of dally, restricts movement away from the site of synthesis (Ayers et al., 2010). A simple diffusion model cannot account for these discrepancies, and so while a conserved role for Shf has not yet been shown, it is likely that if the role of Shf is not conserved, there are other Shh binding proteins which perform a similar role.

5.1.7 Sonic or banded?

While this thesis has focused on the role of Shh, it is possible the some of the effects seen following Sulf1 over expression and knockdown could be due to modulation of other hedgehog signalling pathways. While *Shh* expression is confined to the midline, expression of *banded hedgehog* (*bhh*) the *Xenopus* homologue of Indian hedgehog, can be seen within the lateral neural plate during open neural plate stages. Later on, expression can be seen within the eye, otic vesicle branchial arches and somites, the banded expression pattern in this region giving rise to its name (Ekker et al., 1995). Following over expression of *Sulf1*, an increase in *Ptc2* expression can be seen within the somites, a region in which *Bhh* but not *Shh* is expressed. This may therefore represent an increase in Bhh signalling within this region, rather than Shh. Other hedgehog genes are not present in regions that overlap with Sulf1 until much later during development. Despite the possibility that this effect could be due to a different ligand, Sulf1 is still able to potentiate hedgehog signalling. Furthermore, effects can clearly be seen in region which are specifically

associated with Shh and so although this one experiment doesn't rule out the possibility that both Bhh and Shh signalling could be affected, the majority of this work applies specifically to Shh signalling only.

5.1.8 Future work

The results presented in this thesis show that Sulf1 is able to promote hedgehog signalling and modify the distribution of the Shh ligand. The mechanism by which Sulf1 regulates Shh dispersal and signalling however remains unknown. The model proposed above suggests that Sulf1 may act to promote the association of Shh with dlp homologues over that of dally homologues. It would be interesting therefore to investigate whether Shh is able to interact with these two glypicans *in vivo*, and how Sulf1 changes the dynamics of these interactions. Further to this, the observation that dlp is co-localised with Ptc in endocytic vesicles, while gp3 is not raises the question as to whether changing the sulfation state of the ECM will impact in the endocytosis of the Shh ligand.

The lack of observable Shh moving from control cells to *Sulf1* expressing cells in animal caps suggests that Shh is not able to migrate though an environment deficient in 6-O sulphated HSPGs. Alternatively Shh may simply be endocytosed more rapidly, although the cell-autonomous accumulation of Shh at the cell membrane of *Sulf1* over expressing cells in chick suggests that this may not be the case. Shh was however seen to be able to diffuse, albeit less efficiently, when expressed in a global region of *Sulf1* expression. While Sulf1 does not appear to modulate the ability of Shh to form multimeric complexes, this reduced ability to diffuse suggests that Shh may be in a different state when released from *Sulf1* co-expressing cells, possibly being associated with different co-factors. The requirement for Shf in the *Drosophila* wing disc points to a potential role for Wif1 in the regulation of Shh signalling. It would be interesting therefore to investigate whether Wif1 interacts with Shh, if it is present within the right place and at the right time to impact on Shh signalling and whether or not Sulf1 is able to affect the interaction between Shh and Wif1, or modify the distribution of Wif1.

5.1.9 Conclusions

It is unlikely that there is a universal mechanism for the establishment of a Hh gradient, as the specific environment in which Hh has to move through will differ not only between species but will also differ depending on the specific region in which the gradient is set up. Additionally, the requirement for long versus short range signalling also differs between tissues; in the wing disc Hh activates dpp at a distance from the source (Ayers et al., 2010) whereas in the ectoderm, Hh activates Rho and Wg in cells close to the source (Gallet et al., 2003). The differential expression of certain factors therefore will reflect the requirements of gradient formation. In the vertebrate neural tube, *Sulf1* is expressed throughout the floor plate region, such that all cells expressing *Shh* also express *Sulf1*. In the *Drosophila* wing disc however, *Sulf1* is only expressed by a strip of cells within the *Hh* expressing region. Despite these differences however it does appear that in both systems, Sulf1 acts to regulate the distribution of the hedgehog protein.

This study considered the role of Sulf1 during neuronal patterning in vertebrates, using *Xenopus* as a model organism. Co-expression of *Sulf1* with *Shh* in the floor plate suggested that it may act to regulate Shh signalling, and experiments analysing the expression of downstream targets of Shh signalling indicated that this was the case. Using knockdown experiments, the requirement of Sulf1 for the proper establishment of neuronal precursor populations was shown. The redistribution of these populations of cells suggested that Sulf1 acts to regulate the diffusion of Shh within the ventral neural tube, and that in the absence of Sulf1, Shh is able to diffuse more freely. Analysis of Shh, firstly in animal caps and then *in vivo* indicated that in the absence of Sulf1, the distribution of Shh is altered. While in animal caps it was possible to see that Sulf1 increased the amount of protein close to the source, it is difficult to establish a precise role for Sulf1 *in vivo* as Shh protein levels appear significantly reduced. The changes to dorsal markers does however suggest that as in animal caps, Sulf1 acts to concentrate Shh levels near the source, giving rise to a steep concentration gradient. While this thesis has not established the exact mechanism by which Sulf1 functions, this work has identified a role for Sulf1 in the modulation of Shh signalling in vertebrates, and shown that it is crucial for the correct patterning of the neural tube.

6.0 Materials & Methods

6.1 Embryological methods

6.1.1 *Xenopus laevis in vitro* fertilization and embryo culture

Females to be used for *in vitro* fertilization were primed with 50 units human chorionic gonadotrophin (hCG: Chorulon), from 1 day to 1 month prior to use. Laying was induced within 16 hours by injection of 250-350 units of hCG. Eggs were fertilized with a suspension of freshly crushed testis in distilled water from a sacrificed male. Embryos were cultured in NAM/10 (1/10 Normal Amphibian Medium) at 14-24◦C, in 60mm dishes coated with 1% agarose. Jelly coats were removed prior to first cleavage in NAM containing 2.5% L-cysteine hydrochlorate monohydrate (Sigma), pH7.8-8. Embryos were staged according to (Nieuwkoop and Faber, 1994).

6.1.2 *Xenopus tropicalis in vitro* fertilization and embryo culture

Females to be used for *in vitro* fertilization were primed with 20 units of hCG 16 hours prior to use. Laying was induced in ~2.5 hours by injection of 100 units of hCG. Eggs were fertilized with a suspension of freshly crushed testes, homogenized in L-15 medium (Sigma) + 10% foetal calf serum. Embryos were cultured in MRS/9 (1/9 Modified Ringer's Solution) prior to gastrulation, and in MRS/20 thereafter, at 21.5-27◦C, in 60mm dishes coated with 1% agarose. Jelly coats were removed prior to first cleavage in MRS/9 containing 3% L-cysteine (Sigma), pH7.8-8. Embryos were staged according to (Nieuwkoop and Faber, 1994).

6.1.3 Microinjection

mRNA for microinjection was synthesized as described in section 6.2.11. *X. tropicalis* embryos were injected in MRS/9 + 3% ficoll (manufacturer) and transferred to MRS/20 after one hour. Injections were performed using using a pneumatic microinjector (Harvard apparatus/ Narishige) or a Drummond microinjector with glass needles pulled from capillary tubes (DrummondNarishige). *X. laevis* embryos were injected in NAM/3 + 5% ficoll (Sigma) and transferred to NAM/10 after one hour. Embryos were injected into the animal hemisphere using a maximum total volume of 20nl (10nl or 5nl per cell at the 2 cell and 4 cell stages respectively). For the Shh-GFP diffusion assay (Chapter4) embryos were injected at the 2-cell stage with a total volume

of 20nl and then again at the 32-cell stage with a volume of 1.25nl into a single cell.

6.1.4 Generation of animal caps for confocal microscopy

Following injection at the 2-cell and 32-cell stage, *X. laevis* embryos were cultured to blastula stage 8 in NAM/10 at 12°C overnight. Vitelline membranes were removed on the vegetal side of the embryos to avoid damage to the animal pole of the embryo. The presumptive ectoderm at the animal pole was excised using tungsten needles washed with ethanol and NAM/10 to remove residual sodium hydroxide. Membrane removal and cap excision were performed in high salt (NAM/2). Animal caps were cultured for two hours at 21°C in NAM/2 to allow them to heal fully before mounting. Relief slides were generated using Superfrost slides (Thermo Fisher Scientific) and a double layer of plastic tape in which a depression 7mm by 11mm was cut. Healed animal caps were placed into the depression in NAM/2 and covered with a cover slip cut to 15mm by 22mm. The slides were left to dry for 15 minutes and sealed with nail varnish to prevent movement of samples during imaging. Samples were imaged by confocal microscopy using the Laser Scanning Microscope LSM 710 (Carl Zeiss) using Zen software (2008-2010) (Carl Zeiss).

6.1.5 Drug treatments

Cyclopamine was stored at a concentration of 5mM in ethanol at -20°C.The stock solution was diluted in MRS/20 to give a final concentration of 100µM. For treatment, vitteline membranes were removed from embryos at stage 9 inhibiting the hedgehog pathway before the onset of hedgehog expression. Embryos were immediately added to cyclopamine in MRS/20 in a 6 well plate containing 3 ml of the medium. Plated were coated with a thin layer of 1% agarose to prevent embryos sticking to the plastic. At the appropriate stage embryos were washed in MRS/20 and collected for analysis via *in situ* hybridisation or qRT-PCR as described in sections 6.2.18 and 6.2.13.

6.1.6 Microtome sectioning and histological staining of embryos

Embryos were fixed in 4% paraformaldehyde (Sigma) at 4°C for 60 hours, and then washed in PBS at 4◦C. Embryos were stained overnight with 1ml 10% borax carmine in 35% ethanol (Fluka), then de-stained in acid alcohol (70%

ethanol, 0.32% HCl) for several hours, with washes being changed every hour until all excess stain was removed. Embryos were washed in 70% ethanol and stored in 100% ethanol. Embryos were transferred into Histoclear (National Diagnostics) through a series of graded washes and then to Paraplast paraffin wax (Sigma) at 60°C. Embryos were oriented in moulds (Cellpath) containing molten wax which was allowed to set at room temperature, then trimmed to size and affixed to wooden blocks with hot wax. 5µm sections were cut with a Bright 5040 microtome, mounted on to Superfrost glass slides (Thermo Fisher Scientific) and dried overnight. Wax was removed from the sections via heating followed by washes in Histoclear. Sections were taken through a series of ethanol washes into water and then counterstained with picro blue black (97.5% saturated picric acid, 0.025% naphthalene blue black- diluted from a 1% aqueous solution). Following staining slides were taken through the wash series in reverse and mounted in Histomount (National Diagnostics).

6.1.7 Vibratome sectioning of embryos

For vibratome sectioning following *in situ* hybridisation, embryos were embedded in 15mm moulds (Cellpath) in PBS containing 15% gelatin from porcine skin (Sigma Aldrich), warmed to 60°C. Trimmed gelatin blocks were attached with superglue to the specimen plate of a Leica VT1000 S vibratome. Sections were cut at a thickness of 50µm in PBS cooled to 4°C, transferred to Superfrost glass slides (Thermo Fisher Scientific) and mounted with Hydromount (National Diagnostics).

Following immunohistochemistry, embryos were sectioned in a similar fashion but were embedded in low melt agarose (Invitrogen) warmed to 42°C, and mounted with VectaShield (Vector labs) to maintain fluorophore intensity. In both cases embryos were left unbleached to maintain tissue integrity.

6.1.8 Cryo-sectioning of embryos

Embryos were prepared as for *in situ* hybridisation as described in section 6.2.18. Embryos were re-hydrated in 100mMTrisHcl + 100mM NaCl (pH7.4) for 30 minutes. Embryos were then washed overnight at 4°C in PBST containing 15% fish gelatin (sigma) and 7.5% sucrose. Embryos were transferred to PBST containing 25% cold water fish gelatin (sigma) and 7.5% sucrose and washed

overnight at 4°C. Embryos were transferred to fresh 25% gelatin solution and placed in 5mm square moulds (Cellpath) in groups of up to 10 embryos. Samples were oriented and then placed on dry ice to freeze the blocks. Blocks were trimmed to size and sectioned using a Leica CM1900 Cryostat. Slides were stored at -80°C until required.

6.1.9 Photography

Whole embryos were photographed using a SPOT 14.2 Color Mosaic camera (Diagnostic Instruments Inc.) and SPOT Advanced software, with a Leica MZ FLIII microscope. Sections were photographed using an 18.2 Color Mosaic camera (Diagnostic Instruments Inc.) and SPOT Advanced software with a Leica DM2500 microscope. Images were processed using Adobe Photoshop CS5 (64 Bit).

6.2 Molecular biological methods

6.2.1 Generation of Shh-GFP

The Shh-GFP mouse knock-in construct was donated by Andrew McMahon (Chamberlain et al., 2008). PCR primers for amplification of the MmShh gene were designed with restriction sites (EcoRI and XbaI) to allow in-frame insertion into the pCS2+ plasmid, as shown in Table 6.1. Additionally the forward primer was designed to include a Kozak sequence to improve mRNA translation. PCRs were conducted using the Shh-GFP (Chamberlain et al., 2008) as a template which contained the MmShh-GFP coding region and additional regulatory elements.

Name	Sequence 5' to 3'
Shh-GFP fwd	AGA GAG GAA TTC **ACC** ATG **G**TG CTG CTG CTG GCC AGA TGT TTT
Shh-GFP rev	AGA GAG TCT AGA TCA GCT GGA CTT GAC CGC CAT TCC

Table 6.1 Primers used to generate Shh-GFP
EcoR1 and Xba1 recognition sequences are shown in red and blue respectively. Nucleotides changed to create the kozak sequence are shown in bold, and the stop codon is underlined.

The PCR reaction was set up as follows:

- 1.5µl 10µM forward primer
- 1.5µl 10µM reverse primer
- 1µl 10mM dNTP
- 1µl template
- 5µl 10X Pfu buffer
- 2µl Pfu
- Nuclease free water to 50µl

The PCR programme was as follows:

5 minutes	95°C	
45 seconds	95°C	} X 25
45 seconds	75°C	
4 minutes	76°C	
20 minutes	76°C	

The size of amplified PCR products was checked by agarose gel electrophoresis (section 6.2.8), and purified and concentrated as in section 6.2.12. To create complementary sticky ends, restriction the PCR product and pCS2+, were digested with both EcoR1 and XbaI in a total volume of 30µl. After digestion, the PCR product and vector were purified using the QIAquick Gel-Extraction Kit (Qiagen). Ligation reactions were set up as follows:

- 1µl vector (pCS2+)
- 4-7*µl *Shh-GFP* insert, or water for control (depending on concentration*)
- 1µl 10X ligase buffer (Promega)
- 1µl T4 DNA ligase (Promega)
- Nuclease-free water to 10µl

Reactions were incubated at 4◦C overnight or for 3 hours at 15°C, 5µl of each ligation reaction was used to transform DH5α competent cells (section 6.2.3). Colonies were picked and cultured in LB-amp medium (10g/l bactotryptone, 5g/l bacto-yeast, 10g/l NaCl, plus 100µg/ml ampicillin), and DNA was extracted by miniprep, purified, checked by colony PCR and sequenced.

6.2.2 Generation of Shh-CFP/YFP

To generate the Shh-CFP and Shh-YFP constructs the Not1 site 3' of the SV40 in the pCS2+ vector had to be knocked out as the GFP in the mouse knock in construct was cloned in with Not1. Primers were designed to replace GCGGCCGC with GCCATGGC to remove the Not1 site in pCS2+ (see Table

6.2). The resulting plasmid will be referred to as pCS2+$^{\Delta Not1}$. For a plasmid map showing the deletion site see appendix 2.

Name	Sequence 5' to 3'
Removal of Not1 in pCS2+ fwd	AGA GAG GC*C ATG* GCG GCG CCA ATG CAT TGG CCC
Removal of Not1 in pCS2+ rev	AGA GAG GC*C ATG* GCG AAT TAA AAA ACC TCC CAC

Table 6.2 Primers designed to mutate the Not1 site in pCS2+
Recognition sequence of Not1 is shown underlined and the nucleotides replaced to mutate the Not1 site are shown in red.

The PCR reaction was set up as follows:

- 2µl 10µM forward primer
- 2µl 10µM reverse primer
- 1µl pCS2+
- 2µl 10mM dNTP
- 5µl 10X Pfu Fusion buffer
- 2µl Pfu Fusion
- Nuclease free water to 50µl

The PCR programme was as follows:

2 minutes	95°C	
30 seconds 45 seconds 3.5 minutes	95°C 62°C 72°C	} X 30
20 minutes	72°C	

The size of amplified PCR products was checked by agarose gel electrophoresis (section6.2.8), and purified and concentrated as in section 6.2.12

To replace GFP with CFP or YFP, primers were designed to amplify CFP from the CFP-GPI construct (donated by Jim Smith) and the YFP-Venus contruct (donated by M. Mochii) containing theNot1 site at the 5' end of the GFP and PflM1 at the 3' end to allow in-frame insertion into the pCS2+ plasmid, as shown in Table 6.3. For a map of this construct see appendix 3.

Name	Sequence 5' to 3'
Shh-CFP/YFP fwd	AG AGA GGC GGC CGC **GTG AGC AAG GGC**
Shh-CFP/YFP rev	AGA GAC CAC GGA TTG GCC GCC **CTT GTA CAG CTC GTC**

Table 6.3 Primers used to generate Shh-CFP/YFP fusion constructs
Recognition sequence of Not1 and PflM1 are shown in red and blue respectively. The start and end of the CFP/YFP coding region is shown in bold.

The PCR reaction was set up as follows:

- 2.5µl 10µM forward primer
- 2.5µl 10µM reverse primer
- 1µl template
- 2µl 10mM dNTP
- 5µl 10X Pfu
- 2µl Pfu
- Nuclease free water to 50µl

The PCR programme was as follows:

5 minutes	95°C	
30 seconds	95°C	} X 2
30 seconds	30°C	
3 minutes	72°C	
30 seconds	95°C	} 25
30 seconds	65°C	
3 minutes	72°C	
10 minutes	72°C	

The size of amplified PCR products was checked by agarose gel electrophoresis (section 6.2.8), and purified and concentrated as in section 6.2.12. Subsequent processing was carried out as described in section 6.2.1, with the exception that the pCS2+$^{\Delta Not1}$ was used as the vector during the ligation.

6.2.3 Bacterial transformation

DH5α competent cells (Invitrogen) were transformed by heat shock (90 seconds at 42°C followed by 90s on ice). Cells were cultured in LB medium at 37°Cfor 1 hour and plated out on LB- agar plates (LB-plus15g/l agar) containing 100µg/ml ampicillin, at dilutions of 0.1X, 1X and 10X.

6.2.4 Colony PCR

Following transformation, colonies were screened for the presence of an insert of the correct size using colony PCR. The reaction was set up as follows:

- 1.5µl 10µM SP6 primer
- 1.5µl 10µM T7 primer
- 5µl nuclease-free water
- 10µl 2x PCR Master Mix (Promega)
- 2µl colony (+ water)

2µl of water was added to each colony on the plate, mixed and the resulting suspension was added to the PCR mix. The pipette tip was subsequently streaked onto an LB-amp plate and numbered for identification.

The PCR programme was as follows:

2 minutes	95°C	
30 seconds	95°C	} X 30
1 minute (per kb)	50°C	
30 seconds	72°C	
10 minutes	72°C	

The products were checked via agarose gel electrophoresis (secton 6.2.8), and colonies were selected for miniprep and sequencing if they yielded products of the correct size.

6.2.5 DNA minipreps

Plasmid DNA was purified from competent DH5α (Invitrogen). Single colonies were cultured in 10ml LB-ampicillin medium in a shaker at 37◦C for 14 hours. Cells were pelleted by centrifugation (13,000 RPM at 4°C) and DNA isolated using the QIAprep Spin Miniprep Kit (Qiagen), according to the manufacturer's instructions.

6.2.6 Quantification of DNA and RNA

DNA and RNA were quantified using the NanoDrop 2000/8000 Spectrophotometer (Thermo Scientific) to measure absorbance at 260nm.

6.2.7 Sequencing

Plasmid DNA was sequenced by the genomics lab within the Technology facility at the University of York, using the 3130 Genetic Analyzer (Applied Biosystems).

6.2.8 Gel electrophoresis

DNA and RNA were run on 1-2% agarose gels in TAE (4mM Tris-acetate, 1mM EDTA) and stained with ethidium bromide. Alternatively DNA was run on a 15% polyacrylamide gel (7.5ml 30% polyacrylamide, 6ml H_2O, 1.5ml 10X TBE (890 mM Tris base, 890 mM Boric acid, 20mM EDTA), 100µl APS, 15µl TEMED). For gel-extraction, samples were run on low met agarose (Invitrogen) and stained with SYBR Safe (Invitrogen).

6.2.9 Linearisation of plasmid DNA

For synthesis of functional (sense) mRNA, sequences were cloned into the pCS2+ or pCS107 vectors as they contain the SV40 polyadenylation sequence which gives mRNA increased stability. Sequences were oriented with the 5' end next to the SP6 promoter. Plasmids were linearised by restriction digestion using an enzyme that cuts downstream of the SV40 signal to give a template. The enzymes used for linearisation are listed in Table 6.4.

Name	Vector	Linearisation	Source
6-OST	pCS2+	Not1	Subclone from EST: TEgg139n13 M. Pownall
CFP-GPI	pCS2+	Not1	J. Smith
GFP	pCS2+	Not1	J.C.Illes
mRFP	pCS2+	Not1	R. Tsien
Shh	pCS2+	kpn1 + blunt	Subclone from EST: TNeu023n04
Shh-CFP	pCS2+	kpn1 + blunt	Subcloned from Shh-GFP Section 6.2.2
Shh-GFP	pCS2+	kpn1 + blunt	Subclone from mouse knock-in construct A. Mcmahon Section 6.2.1
Shh-YFP	pCS2+	kpn1 + blunt	Subcloned from Shh-GFP Section 6.2.2
Sulf1	pCS2+	Not1	Cloned from genomic DNA S.Freeman

Table 6.4 Plasmids used for functional mRNA synthesis

Linearisation reactions were set up as follows:

- 10µg plasmid DNA
- 10µl appropriate10x restriction buffer
- 2-3µl appropriate restriction enzyme
- Nuclease-free water to total volume of 100µl

Reactions were incubated at 37°C for 2-2.5 hours, and samples were checked by agarose gel electrophoresis (section 6.2.8) to ensure complete digestion.

If linearised products required blunting they were mixed with:

- T4 DNA Polymerase
- 10X reaction buffer
- 20µm dNTPs

and incubated at 15°C for 30 minutes. The polymerase was heat inactivated at 75°C for 10 minutes. Products were cleaned using the using the QIAquick Gel Extraction kit (Qiagen), and eluted in 50µl nuclease-free water.

6.2.10 DNA purification

Following restriction digestion and other enzymatic reactions, DNA samples were extracted using an equal volume of phenol/chloroform, followed by an equal volume of chloroform. Samples were then purified by sodium acetate precipitation. Precipitated DNA was pelleted by centrifugation, washed with 70% ethanol, dried and re-suspended in an appropriate volume of nuclease-free water.

6.2.11 *In vitro* transcription of functional mRNA

Functional mRNA was transcribed using the SP6 MEGAScript Kit (Ambion). The manufacturer's instructions were adapted as follows:

- The concentration of GTP was reduced from 50mM to 5mM,
- 2.5µl of 40mM methyl GTP cap analog (Ambion) was added to the reaction

Addition of methyl GTP is required for synthesis of capped mRNA, which is more efficiently translated *in vivo*. The GTP concentration is lowered to give a ratio of 10:1 methyl GTP to GTP to promote synthesis of capped mRNA. Following transcription at 37°C over a period of 3-4 hours, synthesised RNA was checked via electrophoresis, and the DNA template was removed by

treatment with 1µl DNAse I at 37◦C for 10 minutes. The sample was then extracted using phenol/chloroform and concentrated using isopropanol precipitation according to the manufacturer's instructions. The resulting mRNA was re-suspended in nuclease-free water to 400ng/µl and stored in aliquots at -80°C.

6.2.12 PCR cloning of *X. tropicalis* genomic fragments

To generate some of the antisense RNA probes used in this project, fragments of the genes of interest were amplified from the *Xenopus tropicalis* genome by PCR and cloned into the pGEM-T-Easy vector (Promega). Primers were designed to amplify 300-500bp products. See Table 6.5 for primer sequences.

Name	Forward 5' to 3'	Reverse 5' to 3'
Dlx2a	ACCGGAGTGTTTGACAGCTTGGTG	GTGTGGCGGGGAAGGACTTGTC
Evi-1	TGTTTGGGCAAGGCATTTCT	ACGGCAGTCTGTTCCTCTAAGC
Fezf2	GCTGCGCCTTTGGAGAC	CCGGAGGGTGGAAGGAAGAGT
Foxg1	TGCCCCGCCACTACGATGACC	AGGGCGGCTGCAGTGAGATGG
Fz8	CAAGTACCCAGAGCGCCCCATCAT	GAGACAAAGCCGGCCAGGAGGAAC
Olig2	TGCGGCAGCGGGCGACAAGTT	TGGGGTGGGCAGGAGAGG
Vent2	AAAGCAGCCGGAGATCTCACAAAG	AGCAGCATCTTCATTGGAAGTGGT

Table 6.5 Primers used for PCR cloning of *X. tropicalis* genomic fragments

PCR was performed as follows:

- 1µl forward primer
- 1µl reverse primer
- 100ng *X. tropicalis* genomic DNA
- Nuclease-free water to 10µl
- 10µl 2x PCR Master Mix (Promega)

The PCR programme was as follows:

5 minutes	95°C	
30 seconds	95°C	} X 30
30 seconds	60°C	
30 seconds	74°C	
10 minutes	74°C	

The products were checked via agarose gel electrophoresis (secton 6.2.8), and colonies were selected for miniprep and sequencing if they yielded products of the correct size. Ligations were set up using the pGEM-T-Easy Vector, as directed by the manufacturer, using 3µl of the PCR product per 10µl reaction and incubating overnight at 4◦C. 5µl of the ligation was used to transform DH5α competent cells as described in section 6.2.3.

6.2.13 First-strand cDNA synthesis

For expression analysis via qRT-PCR, embryos were snap frozen on dry ice at the appropriate developmental stage following either microinjection or drug treatment. 10 *X. tropicalis* embryos were collected per sample. Total RNA extraction was carried out using 1ml Tri-Reagent (Sigma) per sample, according to the manufacturer's instructions. Samples were checked by agarose gel electrophoresis (section 6.2.8), and quantified via spectrophotometry (section 6.2.6).

The first-strand cDNA synthesis was set up as follows:

- 1µg RNA
- 1µl OligodT
- Nuclease-free water to 12µl

Samples were placed at 65°C for 2 minutes then placed on ice for another 2 minutes. The following was then added:

- 1µl nuclease-free water
- 2µl DTT
- 4µl 5X First strand buffer

Sample was placed at 42°C for 2 minutes. While at 42°C 1µl Superscript (or water for controls), was added to samples. Samples were then incubated at 42°C for 1 hour.

cDNA was checked via PCR amplification using L8 (sequence shown in Table 6.6).

The PCR reaction was set up as follows:

- 1µl 10µM forward primer
- 1µl 10µM reverse primer
- 7.5µl nuclease-free water
- 3µl cDNA
- 12.5µl PCR Master mix (Promega)

PCR products were checked by gel electrophoresis. cDNA samples were stored at -20°C.until required.

6.2.14 qRT-PCR

qRT-PCR reactions were set up in 96 well plates as follows:

- 1.5µl 10µM forward primer
- 1.5µl 10µM reverse primer
- 5.5µl nuclease-free water
- 5µl cDNA
- 12.5µl SYBR-green (Applied Biosystems)

Primers were designed to amplify a 90bp fragment of the mRNA of interest, when possible from a region flanking an intron in the genomic sequence, to eliminate the possibility of contamination by genomic DNA. Sequences of the primers used are given in Table 6.6.

Gene	Forward primer 5' to 3'	Reverse primer 5' to 3'
Dbx1	GGAGAGGAGGAGCCAATGTG	TGCTCCGGGCATTGATATG
FoxA2	ATGCGAAGCCCCCCTACT	CTCGCTGAGAGTGAGCATCTTG
Gsh2	GTCTGCAGCCCAACCTACAAC	CTCTGCTCCACCCATTGTCA
Nkx2.2	CCCCAGACAACGACAAGGA	ACCCGGCGCTTTCTCTTT
Pax6	CGTCCCTGCGACATTTCT	CGATCCAGTCTCGTAATATCTCC
Ptch2	CCCCTTGGCTATGCAGCTT	TGGTGTCATATCGGTCATGTATCC
Shh	CGACTCATGACTCAGAGATGTAAGG	CCCGGCCACTGGTTCA
ODC	AAAGCTTGTTCTGCGCATAGCAACT	AGGGTGGCACCAAATTTTAC
L8	GGGCTRTCGACTTYGCTGAA	ATACGACCACCWCCAGCAAC

Table 6.6 Primers used in qPCR reactions

qRT-PCR was carried out using the ABI Prism or 7300 Real-Time PCR system (Applied Biosystems), using the following programme:

2 minutes	50°C	
10 minutes	95°C	
15 seconds	95°C	} X 40
1 minute	60°C	
15 seconds	95°C	
20 seconds	60°C	
15 seconds	95°C	

Results were analysed using 7000 system SDS software (Applied Biosystems) using $2^{-\Delta CT}$ method.

6.2.15 Confirmation of Sulf1 knockdown

To confirm that the Sulf1 antisense morpholino S1MO3 effectively blocks splicing, cDNA was generated from Sulf1 morphant embryos and analysed by PCR using the primers shown in Table 6.7.

Name	Forward 5' to 3'	Reverse 5' to 3'
Exon2	GCAAATGGAGATTCCTGTGG	TGGGCCTGATATTCCTTCTG
Exon2/3 boundary	CCAAATTCAGAGGGCGAGTA	TGAAGCTCCTCCTTCTTCCA

Table 6.7 Primers used to identify mis-splicing in Sulf1 morphants

The PCR reaction was set up as follows:

- 1µl forward primer
- 1µl reverse primer
- 5µl cDNA
- 2µl nuclease-free water
- 10µl 2x PCR Master Mix (Promega)

The PCR programme was as follows:

2 minutes	95°C	
30 seconds	95°C	} X 30
30 seconds	60°C	
2 minutes	72°C	
10 minutes	72°C	

Products were analysed by gel electrophoresis on both agarose and acrylamide gels (section 6.2.8).

6.2.16 Microarray analysis

Following microinjection and incubation to the required stage, embryos were snapfrozen on dry ice and stored at -80◦C until required. Twenty *X. laevis* embryos were used per sample. Total RNA extraction was carried out using Tri-reagent (Sigma), according to the manufacturer's instructions, with the following adaptations: The optional extra centrifugation step was included, an additional chloroform extraction was performed and the isopropanol precipitation was performed for 1 hour on dry ice. After resuspension, the RNA was re-purified using the RNeasy Mini Kit (Qiagen), followed by LiCl precipitation overnight at -80◦C. The quality of the purified total RNA samples was verified using the Agilent 2100 Bioanalyzer (Agilent). The Message Amp II-Biotin Enhanced Kit (Ambion) was then used to perform reverse transcription, second-strand cDNA synthesis and generation of biotin-labelled amplified (a)RNA, according to the manufacturer's instructions. 20µg of each aRNA sample was fragmented in a total volume of 40µl.After checking quality on the 2100 Bioanalyzer, fragmented aRNA was hybridized to *Xenopus laevis* Genome 2.0 Array GeneChips (Affymetrix), and the chips were washed, stained and scanned according to the manufacturer's instructions. Data was analysed using the BRB array tools plugin for Micosoft Excel. RNA quality checking and all steps after LiCl precipitation were carried out by Celina Whalley at the Department of Biology Technology Facility, University of York.

6.2.17 *In vitro* transcription of digoxigenin-labelled antisense RNA probes

For synthesis of labelled antisense RNA, templates were generated as described for functional mRNA (6.2.9). Enzymes were selected on the basis that they cut between 300bp and 1kb from the 3' end of the insert sequence.

When this was not possible plasmid was cut at the 5' end of the insert and the probe was hydrolyzed (see below). Table 6.8 gives details of the linearization and transcription of the probes used:

Name	Vector	Linearisation	Polymerase	Source
Dbx1	pGEM T- easy	SpeI	T7	Subclone from genomic DNA, E. Winterbottom
Dlx2a	pGEM T- easy	Sal1	T7	Subclone from genomic DNA, Section 6.2.12
Evi1	pGEM T- easy	Nco1	SP6	Subclone from genomic DNA, Section 6.2.12
FoxA2	pCS107	HindIII	T7	EST: TNeu069I04
Foxg1	pGEM T- easy	Nco1	SP6	Subclone from genomic DNA, Section 6.2.12
Isl1	pCS107	EcoR1 + hydro	T7	EST: BX736684
Nkx2.2	pGEM T- easy	Sal1	T7	Subclone from EST: IMAGE:9019890
Nkx6.1	PCS107	EcoR1 + hydro	T7	EST: AL894846
Olig2	pGEM T- easy	Sal1	T7	Subclone from genomic DNA, Section 6.2.12
Pax6	pBSKS+	EcoR1	T7	J.Illes
Ptc2	pGEM T- easy	Sal1	T7	Subclone from EST: IMAGE:7615868
Shh	pCS107	BamH1	T7	EST: TNeu023n04
Sulf1	pBSKS+	Xho1	T7	Subclone from genomic DNA, S. Freeman
Sulf2	pCS107	Nco1	T7	EST: Tegg037d24
Vent2	pGEM T- easy	Nco1	SP6	Subclone from genomic DNA, Section6.2.12

Table 6.8 Details of plasmids used for synthesis of antisense RNA probes for *in situ* hybridisation

For *in vitro* transcription, the following reaction was set up:

- 10µl 5x transcription buffer (Promega)
- 2.5µl 10x DIG (digoxigenin) RNA labeling mix (Roche)
- 5µl 100mM dithiothretiol (DTT)
- 2µl RNase inhibitor (Promega)
- 3µl SP6/T7/T3 RNA polymerase, as appropriate (Promega)
- 1-2µg linear DNA template
- Nuclease-free water to a total volume of 50µl

The reaction was incubated at 37°C for 4 hours, adding an additional1µl of the appropriate polymerase after 2 hours. 2µl was checked by electrophoresis on a 2% agarose gel, before removal of the template by incubation with 1µlRNase-free DNase I (Promega) at 37°C for 15 minutes. After checking again by

electrophoresis, probes were precipitated (25µl water, 50µl 5M NH_4OAc and 312.5µl 100% ethanol) and incubating on dry ice for 1 hour or at -80°C overnight. Probes were pelleted by centrifugation at 4°C at 13,000rpm for 15-minutes, washed in70% ethanol and dried in a desiccator for 5-10 minutes. After re-suspension in 50µlnuclease-free water, probes were checked on a 2% gel and stored at -80°C. When hydrolysis of a probe was required, it was re-suspended after precipitation in25µl. After checking the probe on a gel, 25µl of 2x hydrolysis solution (2x: 80mM$NaHCO_3$, 120mM Na_2CO_3) was added and the probe was incubated at 60°C for the time *t* determined by the following formula:

$$\text{t (minutes)} = \frac{\text{(starting length, kb) - (desired length, kb)}}{0.11\ \text{(starting length)(desired length)}}$$

where the starting length was the approximate insert size and the desired length was500bp. After hydrolysis, probes were re-precipitated as described above.

6.2.18 Whole-mount *in situ* hybridization

Fixation:

Vitelline membranes were manually removed using forceps. Embryos were fixed in MEMFA (0.1M MOPS pH7.4, 2mM EGTA, 1mM $MgSO_4$, 3.7% formaldehyde) for 1 hour at room temperature, dehydrated in 100% methanol and stored at -20◦C in methanol until required.

Whole-mount *in situ* hybridization:

Antisense digoxigenin (DIG)-labeled probes were synthesized as described above.

Embryos were rehydrated with a series of washes in methanol and PBST (1X PBS + 0.1% Tween), then washed in PBST. Embryos were treated with Proteinase K (10µg/ml ;Roche) at 37°C for a period of time depending on the stage. Table 6.9 outlines the period of proteinase K treatment for each stage that was analysed.

Stage	Time (mins)
10.5	2.5
12.5	2.5
15	3
23	4
37	6

Table 6.9 Time of proteinase K treatment

Embryos were subsequently treated with acetic anhydride in 0.1M triethanolamine (pH7.8), washed again in PBST and re-fixed in 10% formalin (PBST) for 20 minutes. After additional washes in PBST, embryos were washed in hybridization buffer (50% formamide, 5x SSC (pH7), 1mg/ml total yeast RNA, 100µg/ml heparin, 1x Denhart's, 0.1% Tween, 0.1% CHAPS, 10mM EDTA) at 60°C for 2 hours. This was replaced with hybridization buffer containing DIG RNA probe, left to hybridize overnight at 60◦C. To remove excess probe, embryos were washed in hybridization buffer followed by a series of washes in SSC (2X + 0.1% Tween followed by 0.2X + 0.1% Tween) at 60°C, and then with maleic acid buffer (1X MAB; 100mM maleic acid, 150mM NaCl, 0.1% Tween, pH7.8) at room temperature. Embryos were blocked in MABBMBHTLS (MAB + 2% BMB, 20% heat-treated lamb serum) for 2 hours at room temperature, and incubated in 1/2000 sheep anti-DIG antibody (coupled to alkaline phosphatase (AP) (Roche) overnight at 4◦C in blocking solution.

Washes in MAB were carried out at room temperature for a minimum of 3 hours to remove excess antibody. Subsequently embryos were washed for 10 minutes in AP buffer (100mM Trizma, 50mM $MgCl_2$, 100mM NaCl, 0.1% Tween). To block endogenous alkaline phosphatise activity, embryos were incubated in AP buffer containing 2mM levamisole. The antibody was detected by incubation with a 1/3 dilution of BM purple (Roche) in AP buffer, containing 1mM levamisole, at room temperature. The period of detection is dependent on the probe taking 2 to 48 hours. To stop the reaction, embryos were washed in PBST and re-fixed in 10% formalin and stored at room temperature. Embryos were bleached (5%H_2O_2, 2.5% SSC, 5% Formamide in PBST) under bright light to remove pigmentation. Embryos were washed in PBST and re-fixed and stored in 10% formalin at room temperature. Embryos required for vibratome sectioning as described in section 6.1.7 were not bleached.

6.2.19 Detection of endogenous Shh

Following microinjection and incubation to the required stage, vitelline membranes were manually removed using forceps and embryos were fixed in MEMFA (0.1M MOPS pH7.4, 2mM EGTA, 1mM $MgSO_4$, 3.7% formaldehyde) for 20 minutes at 4°C Embryos were washed in PBSTx (1X PBS + 0.1% TritonX-100) and blocked (PBSTx + 1%BSA) for 1 hour at room temperature. Embryos were then incubated in 1/4 anti-Shh antibody (5E1 DSHB) in PBSTx (1%BSA) for 60 hours at 4°C. Washes in PBSTx were carried out at room temperature for a minimum of 3 hours to remove excess antibody. Embryos were blocked again in PBSTx (1%BSA) for 30 minutes at room temperature. The following steps were all carried out in the dark. Embryos were incubated in 1/250 anti-mouse Alexa-568 antibody (Invitrogen) in PBSTx (1%BSA) overnight at 4°C. Washes in PBSTx were carried out at room temperature for a minimum of 3 hours to remove excess antibody. Embryos were fixed in 10% formalin for 1 hour at room temperature. Embryos were sectioned as described in section 6.1.7with the exception that samples were mounted in Vectashield hard set mounting medium (Vector labs). Samples were analysed by confocal microscopy as described in section 6.1.4.

6.2.20 Detection of X-Myt1 and PH3

Following microinjection and incubation to the required stage, embryos were fixed and stored as described in section 6.2.18. Embryos were prepared and cryo-sectioned as described in section 6.1.8 and stored at -80°Cuntil required. Samples were dried for 1 hour at room temperature, washed in acetone for 2 minutes, re-dried and washed in PBSTx. Samples were then blocked for 1 hour at room temperature in PBSTx (5% heat treated lamb serum (HTLS)). Blocking was undertaken vertically in a rack immersed in blocking solution to prevent sections separating from the slide. Slides were incubated in 1/1000 anti-X-Myt1 antibody (Donated by Nancy Papalopulu) in PBSTx (5% HTLS) or 1/500 anti PH3 antibody (Millipore) in PBSTx (5% HTLS) for 2 hours at room temperature. Slides were washed (3X15 mins) in PBSTx to remove excess antibody. Slides were re-blocked in PBSTx (5% HTLS) for 30 minutes at room temperature. Samples were incubated in 1/1000 anti-rabbit Alexa488 antibody (Invitrogen) for 90 minutes at room temperature. Slides were washed (3X15 mins) in PBSTx to remove excess antibody. Samples were mounted in Vectashield mounting

medium +DAPI (Vector labs), and analysed by confocal microscopy as described in section 6.1.4.

6.2.21 Lineage tracing with GFP or ß-galactosidase

When embryos were unilaterally injected, the injected side of the embryo was identified by co-injection of *GFP* mRNA at a concentration of 200pg per cell in a 2-cell stage embryo. Visualization was carried out before fixing using the Leica MZ FLIII microscope GFP fluorescence filter set. Alternatively, lineage tracing with ß-galactosidase was sometimes used, as follows: *LacZ* mRNA was co-injected at a concentration of 1ng per cell at the 2-cell stage, and embryos were allowed to develop and fixed for 1 hour in MEMFA as usual. Immediately after fixing, embryos were washed several times in PBST, then incubated in 1.5mg/ml Red-Gal (5-Bromo-6-chloro-3-indolyl β-D galactopyranoside; Sigma, from a stock of 80mg/ml in methanol) or X-Gal (5-Bromo-4 chloro -3 indoyl β-D galactose) in 1ml LacZ staining solution (20 mM $K_3Fe(CN)_6$, 20mM $K_4Fe(CN)_6$, 2mM $MgCl_2$, 0.01% deoxycholate, 0.02% NP-40). Staining was carried out at 37◦C for 45 minutes to 1 hour until red/blue colour developed. Embryos were then rinsed several times in PBSAT, transferred to 100% methanol and stored at -20°C.

Appendices

Appendix 1 Plasmid maps

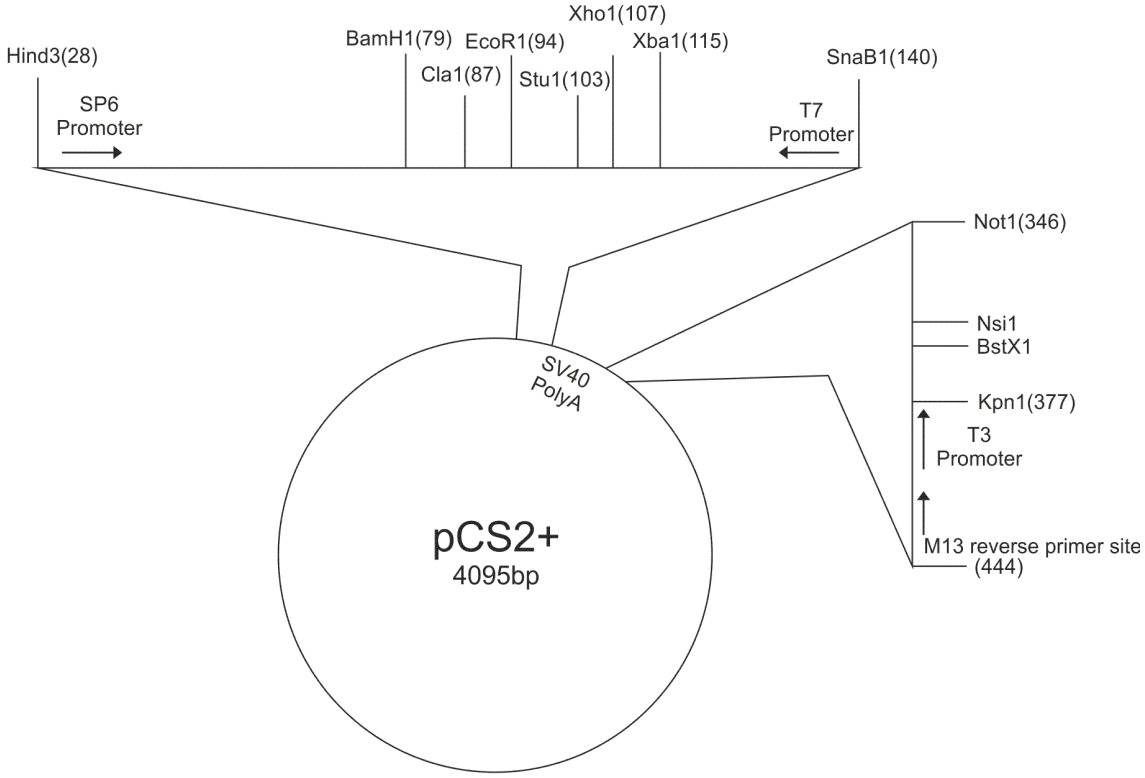

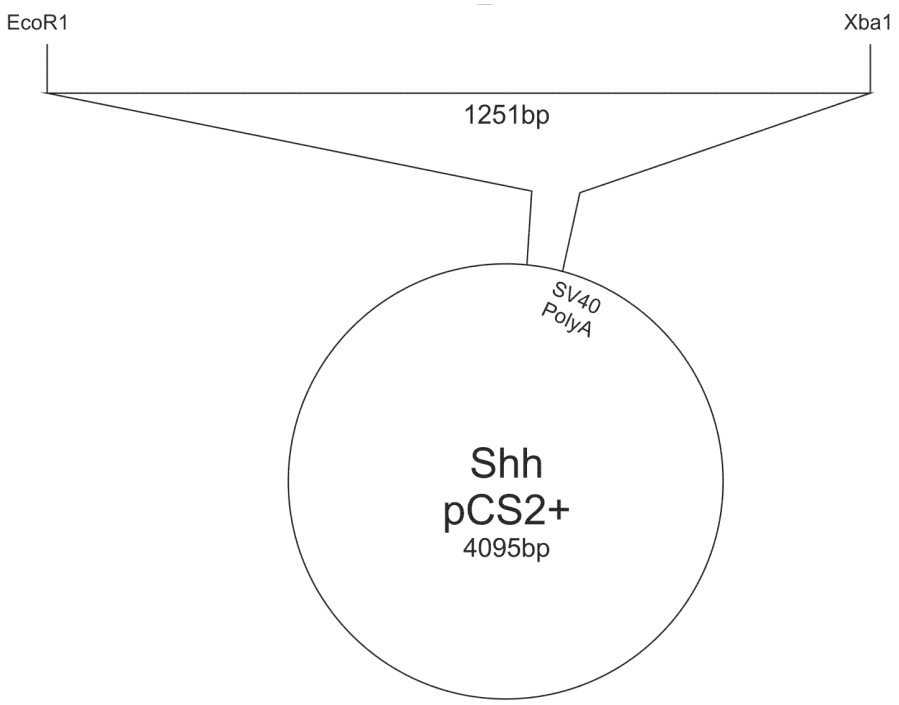

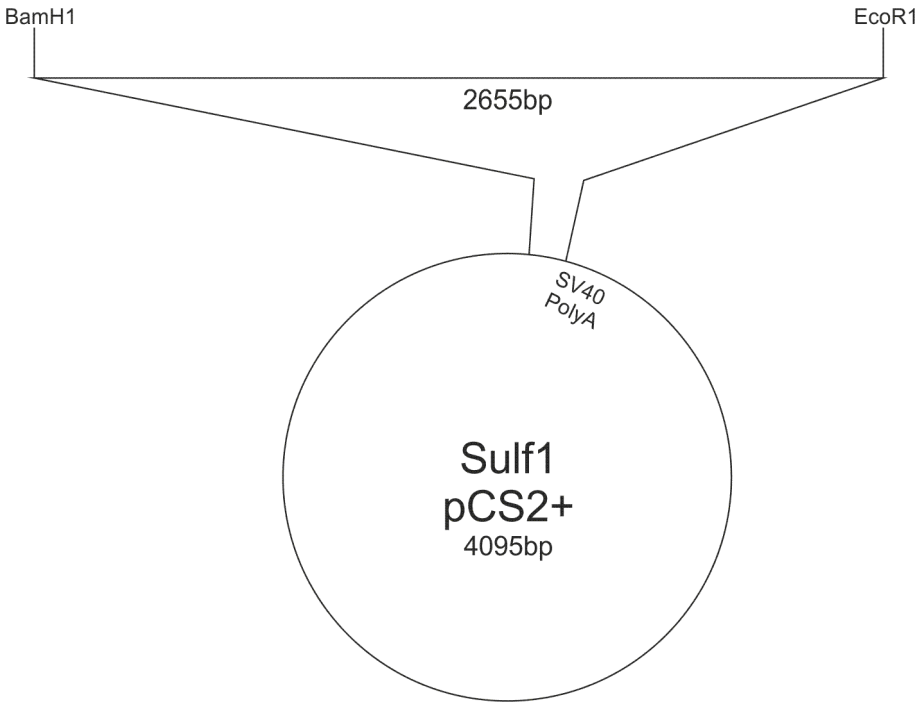
BamH1
EcoR1
2655bp
SV40
PolyA
Sulf1
pCS2+
4095bp

Appendix 2 Generation of pCS2+$^{\Delta Not1}$

To allow insertion of CFP or YFP into the GFP locus in Shh-GFP, the Not1 site in pCS2+ downstream of the insertion site of Shh-GFP was mutated. This was achieved using a PCR based method as described in section 6.2.2.

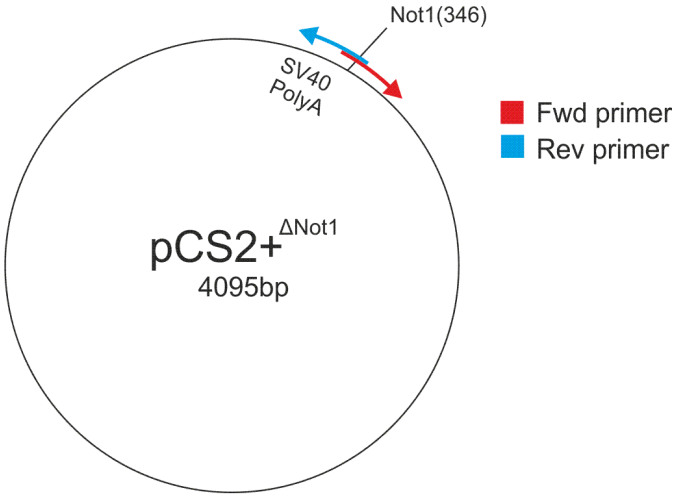

Appendix 3 Cloning of Shh-CFP/YFP

CFP and YFP were amplified and inserted into the GFP locus in Shh-GFPpCS2+$^{\Delta Not1}$ as described in section 6.2.2.

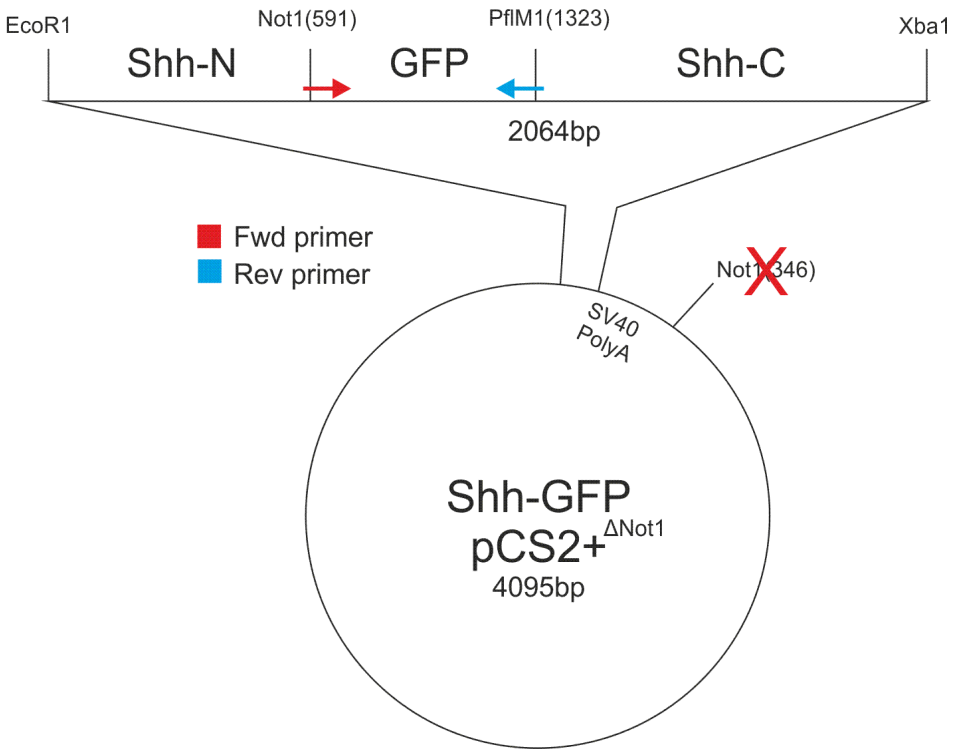

Abbreviations

2-OST	2-O Sulfotransferase
3-OST	3-O Sulfotransferase
6-OST	6-O Sulfotransferase
AER	Apical ectodermal ridge
AMO	Antisense morpholino oligo
AP	Anteroposterior
bFGF	Basic FGF
Bhh	Banded hedgehog
bHLH	Basic helix-loop-helix
BM	Mammillary band
BMP	Bone Morphogenetic Protein
Boc	Biregional cell adhesion molecule-related
Boi	Brother of Ihog
Botv	Brother of Tout-velu
BSA	Bovine serum albumin
CBP	CREB binding protein
Cdo	Cysteine dioxygenase type I
Ci	Cubitus interruptus
CKI	Casein kinase I
CFP	Cyan fluorescent protein
CFP-GPI	Glycosylphosphatidylinositol linked Cyan fluorescent protein
CMO	Control morpholino
CNS	Central nervous system
Cos-2	Costal 2
CS	Chondroitin sulphate
Cyc	Cyclops
Dally	Division abnormally delayed
Dbx	Developing brain homeobox
Dhh	Desert hedgehog
DIN	Dorsal interneuron
Disp	Dispatched
Dlp	Dally-like protein
Dlx2a	Distal-less homeobox 2a
DNA	Deoxyribonucleic acid
Dpp	Decapentaplegic
DS	Dermatan Sulphate
Dsh	Dishevelled
DSHB	Developmental studies hybridoma bank
Dync2h1	Dynein 2 heavy chain
DV	Dorsoventral
e	Eye
ECD	Extracellular domain
ECM	Extracellular matrix
EDTA	Ethylenediaminetetraacetic acid
eFGF	embryonic FGF
EGTA	Ethylene glycol tetraacetic acid
En	Engrailed
ERK	Extracellular signal-regulated kinase
EST	Expressed sequence tag
Evi-1	Enhanced viral integration site 1

Ext	Exostosin
EXTL	Exostosin -like
Ey	Eyeless
fb	Forebrain
Fezf2	Forebrain embryonic zinc finger f2
FGF	Fibroblast growth factor
Fox	Forkhead box
Flh	Floating head
fp	Floor plate
FRET	Förster resonance energy transfer
Fu	Fused
Fxo	Flexo
Fz	Frizzled
GAG	Glycosaminoglycan
Gas1	Growth arrest specific 1
GDNF	Glial cell line derived neurotrophic factor
GFP	Green fluorescent protein
Gli1	Glioma-associated oncogene 1
Gli2	Glioma-associated oncogene 2
Gli3	Glioma-associated oncogene 3
Gpc	Glypican
GPI	Glycosylphosphatidylinositol
Gsk3β	Glycogen synthase kinase 3 beta
Gsx/Gsh	Genomic screened homeobox
hb	Hindbrain
Hcg	Human chorionic gonadotrophin
Hh	Hedgehog
Hhat	Hedgehog acetyl transferase
Hh-Np	Processed hedgehog
Hh-Nu	Unprocessed hedgehog
Hip	Hedgehog interacting protein
HNF3β	Human necrosis factor 3 beta
HS	Heparan Sulphate
HS2ST	Heparan Sulphate 2 Sulfotransferase
HSPG	Heparan Sulphate proteoglycan
HTLS	Heat-treated lamb serum
IFT	Intraflagellar transport
Ihh	Indian hedgehog
Ihog	Interference hedgehog
IN	Interneuron
Ind	Intermediate neuroblasts defective
Iro/Irx	Iroquois/Iroquois homeobox
Isl1	Inhibitor of Serine protease Like protein family member1
mb	Midbrain
MAB	Maleic acid buffer
MBT	Mid-blastula transition
MEF	Mouse embryonic fibroblast
MDCK	Madin-Darby canine kidney
MN	Motor neuron
miRNA	Micro RNA
mRNA	Messenger Ribonucleic acid
mRFP	Membrane linked Red fluorescent protein

MRS	Modified Ringers solution
Msx/Msh	Muscle segment homeobox
MyoD	Myogenic differentiation 1
Myf5	Myogenic regulatory factor 5
NAM	Normal amphibian medium
nc	Neural crest
Ndr2	Nodal-related 2
NDST1	N-deacetylase/N-sulfotransferase 1
Nkx	NK-related homeobox
NF	Nieuwkoop and Faber stage
NHLF	Normal human lung fibroblast
Nsps	Neurospheres
Ntl	No tail
Oep	One eyed pinhead
Olig	Oligodendrocyte transcription factor
P1	Diencephalic prosomere1
P2	Diencephalic prosomere2
P3	Diencephalic prosomere3
Pa	Pallium
Pax	Paired box
PBS	Phosphate buffered saline
PBST	Phosphate buffered saline with tween
PBSTx	Phosphate buffered saline with triton X-100
PCP	Planar cell polarity
PCR	Polymerase chain reaction
PH3	Phospho-histone 3
PKA	Protein kinase A
pn	Pronephros
PO	Preoptic area
POC	Preoptic commissural area
Ptc	Patched
qRT-PCR	Quantitative reverse transcriptase PCR
RA	Retinoic acid
RGC	Retinal ganglion cell
RNA	Ribonucleic acid
rp	Roof plate
RT-PCR	Reverse transcriptase PCR
S1MO3	Sulf1 antisense morpholino 3
S2MO4	Sulf2 antisense morpholino 4
SAG	Smoothened agonist
SANT	Smoothened antagonist
SC	Suprachiasmatic nucleus
Sey	Small eyes
Sfl	Sulfateless
Sgl	Sugarless
Shf	Shifted
Shh	Sonic hedgehog
Sit	Sightless
SiRNA	Small interfering RNA
Ski/Skn	Skinny hedgehog
Slmb	Supernumary limbs
Smo	Smoothened

Sog	Short gastrulation
Sotv	Sister of Tout-velu
som	Somite
Sox	Sry-related box
Spa	Subpallium
SPV	Supraoptoparaventricular area
Sry	Sex-determining region of chromosome Y
SSD	Sterol sensing domain
Sulf1	Heparan Sulphate 6-O endosulfatase1
Sulf2	Heparan Sulphate 6-O endosulfatase2
Su(fu)	Suppressor of fused
SVZ	Subventricular zone
Syu	Sonic-you
TAE	Tris-acetate EDTA
TBE	Tis-borate EDTA
TGF-ß	Transforming growth factor beta
TP	Posterior tubercle
Ttv	Tout-velu
Tub	Tuberal area
UTR	Untranslated region
Vent2	Ventral homeobox1
VIN	Ventral interneuron
Vnd	Ventral nervous system defective
VP	Ventral pallium
Wg	Wingless
Wim	Wimple
WIF1	Wnt inhibitory factor 1
Wnt	Wingless-related MMTV integration site
Xbra	Xenopus brachyury
xHB9	Xenopus homeobox 9
X-Myt1	Xenopus myelin transcription factor 1
YFP	Yellow fluorescent protein
Zi	Zona incerta
Zli	Zona limitans intrathalamica
ZPA	Zone of polarising activity

References

Aanstad, P., Santos, N., Corbit, K. C., Scherz, P. J., Trinh le, A., Salvenmoser, W., Huisken, J., Reiter, J. F. and Stainier, D. Y. (2009). The extracellular domain of Smoothened regulates ciliary localization and is required for high-level Hh signaling. *Curr Biol* **19**, 1034-9.

Agius, E., Soukkarieh, C., Danesin, C., Kan, P., Takebayashi, H., Soula, C. and Cochard, P. (2004). Converse control of oligodendrocyte and astrocyte lineage development by Sonic hedgehog in the chick spinal cord. *Dev.Biol.* **270**, 308-321.

Ahn, J., Ludecke, H. J., Lindow, S., Horton, W. A., Lee, B., Wagner, M. J., Horsthemke, B. and Wells, D. E. (1995). Cloning of the putative tumour suppressor gene for hereditary multiple exostoses (EXT1). *Nat Genet* **11**, 137-43.

Ai, X., Do, A., Lozynska, O., Kusche-Gullberg, M., Lindahl, U. and Emerson, C. (2003a). QSulf1 remodels the 6-O sulfation states of cell surface heparan sulfate proteoglycans to promote Wnt signaling. *J Cell Biol* **162**, 341 - 351.

Ai, X., Do, A. T., Kusche-Gullberg, M., Lindahl, U., Lu, K. and Emerson, C. P., Jr. (2006). Substrate specificity and domain functions of extracellular heparan sulfate 6-O-endosulfatases, QSulf1 and QSulf2. *J Biol Chem* **281**, 4969-76.

Ai, X., Kitazawa, T., Do, A. T., Kusche-Gullberg, M., Labosky, P. A. and Emerson, C. P., Jr. (2007). SULF1 and SULF2 regulate heparan sulfate-mediated GDNF signaling for esophageal innervation. *Development* **134**, 3327-38.

Ai, X. B., Do, A. T., Lozynska, O., Kusche-Gullberg, M., Lindahl, U. and Emerson, C. P. (2003b). QSulf1 remodels the 6-O sulfation states of cell surface heparan sulfate proteoglycans to promote Wnt signaling. *Journal of Cell Biology* **162**, 341-351.

Akimaru, H., Chen, Y., Dai, P., Hou, D. X., Nonaka, M., Smolik, S. M., Armstrong, S., Goodman, R. H. and Ishii, S. (1997). Drosophila CBP is a co-activator of cubitus interruptus in hedgehog signalling. *Nature* **386**, 735-8.

Alcedo, J., Ayzenzon, M., Von Ohlen, T., Noll, M. and Hooper, J. E. (1996). The Drosophila smoothened gene encodes a seven-pass membrane protein, a putative receptor for the hedgehog signal. *Cell* **86**, 221-232.

Alcedo, J., Zou, Y. and Noll, M. (2000). Posttranscriptional regulation of smoothened is part of a self-correcting mechanism in the Hedgehog signaling system. *Mol.Cell* **6**, 457-465.

Allen, B. L., Tenzen, T. and McMahon, A. P. (2007). The Hedgehog-binding proteins Gas1 and Cdo cooperate to positively regulate Shh signaling during mouse development. *Genes Dev* **21**, 1244-57.

Altaba, A. R. I. (1998). Combinatorial Gli gene function in floor plate and neuronal inductions by sonic hedgehog. *Development* **125**, 2203-2212.

Ang, S. L. and Rossant, J. (1994). HNF-3 beta is essential for node and notochord formation in mouse development. *Cell* **78**, 561-74.

Apionishev, S., Katanayeva, N. M., Marks, S. A., Kalderon, D. and Tomlinson, A. (2005). Drosophila Smoothened phosphorylation sites essential for Hedgehog signal transduction. *Nat Cell Biol* **7**, 86-92.

Arikawa-Hirasawa, E., Watanabe, H., Takami, H., Hassell, J. R. and Yamada, Y. (1999). Perlecan is essential for cartilage and cephalic development. *Nat Genet* **23**, 354-8.

Ayers, K. L., Gallet, A., Staccini-Lavenant, L. and Therond, P. P. (2010). The long-range activity of Hedgehog is regulated in the apical extracellular space by the glypican Dally and the hydrolase Notum. *Dev Cell* **18**, 605-20.

AzaBlanc, P., RamirezWeber, F. A., Laget, M. P., Schwartz, C. and Kornberg, T. B. (1997). Proteolysis that is inhibited by Hedgehog targets Cubitus interruptus protein to the nucleus and converts it to a repressor. *Cell* **89**, 1043-1053.

Basler, K. and Struhl, G. (1994). Compartment boundaries and the control of Drosophila limb pattern by hedgehog protein. *Nature* **368**, 208-14.

Bellaiche, Y., The, I. and Perrimon, N. (1998). Tout-velu is a Drosophila homologue of the putative tumour suppressor EXT-1 and is needed for Hh diffusion. *Nature* **394**, 85-8.

Bellefroid, E. J., Bourguignon, C., Hollemann, T., Ma, Q., Anderson, D. J., Kintner, C. and Pieler, T. (1996). X-MyT1, a Xenopus C2HC-type zinc finger protein with a regulatory function in neuronal differentiation. *Cell* **87**, 1191-202.

Bernfield, M., Gotte, M., Park, P. W., Reizes, O., Fitzgerald, M. L., Lincecum, J. and Zako, M. (1999). Functions of cell surface heparan sulfate proteoglycans. *Annu.Rev.Biochem.* **68**, 729-777.

Bernfield, M., Kokenyesi, R., Kato, M., Hinkes, M. T., Spring, J., Gallo, R. L. and Lose, E. J. (1992). Biology of the syndecans: a family of transmembrane heparan sulfate proteoglycans. *Annu Rev Cell Biol* **8**, 365-93.

Bijlsma, M. F., Spek, C. A., Zivkovic, D., van de Water, S., Rezaee, F. and Peppelenbosch, M. P. (2006). Repression of smoothened by patched-dependent (pro-)vitamin D3 secretion. *PLoS Biol* **4**, e232.

Bishop, J. R., Schuksz, M. and Esko, J. D. (2007). Heparan sulphate proteoglycans fine-tune mammalian physiology. *Nature* **446**, 1030-7.

Bornemann, D. J., Duncan, J. E., Staatz, W., Selleck, S. and Warrior, R. (2004). Abrogation of heparan sulfate synthesis in Drosophila disrupts the Wingless, Hedgehog and Decapentaplegic signaling pathways. *Development* **131**, 1927-38.

Borycki, A. G., Brunk, B., Tajbakhsh, S., Buckingham, M., Chiang, C. and Emerson, C. P., Jr. (1999). Sonic hedgehog controls epaxial muscle determination through Myf5 activation. *Development* **126**, 4053-63.

Borycki, A. G., Mendham, L. and Emerson, C. P., Jr. (1998). Control of somite patterning by Sonic hedgehog and its downstream signal response genes. *Development* **125**, 777-790.

Bossing, T., Udolph, G., Doe, C. Q. and Technau, G. M. (1996). The embryonic central nervous system lineages of Drosophila melanogaster. I. Neuroblast lineages derived from the ventral half of the neuroectoderm. *Dev Biol* **179**, 41-64.

Bret, C., Moreaux, J., Schved, J. F., Hose, D. and Klein, B. (2011). SULFs in human neoplasia: implication as progression and prognosis factors. *J Transl Med* **9**, 72.

Briscoe, J. (2004). Hedgehog signaling: measuring ligand concentrations with receptor ratios. *Curr.Biol.* **14**, R889-R891.

Briscoe, J., Chen, Y., Jessell, T. M. and Struhl, G. (2001). A hedgehog-insensitive form of patched provides evidence for direct long-range morphogen activity of sonic hedgehog in the neural tube. *Mol.Cell* **7**, 1279-1291.

Briscoe, J. and Ericson, J. (1999). The specification of neuronal identity by graded Sonic Hedgehog signalling. *Semin.Cell Dev.Biol.* **10**, 353-362.

Briscoe, J. and Ericson, J. (2001). Specification of neuronal fates in the ventral neural tube. *Curr.Opin.Neurobiol.* **11**, 43-49.

Briscoe, J., Pierani, A., Jessell, T. M. and Ericson, J. (2000). A homeodomain protein code specifies progenitor cell identity and neuronal fate in the ventral neural tube. *Cell* **101**, 435-445.

Briscoe, J., Sussel, L., Serup, P., Hartigan-O'Connor, D., Jessell, T. M., Rubenstein, J. L. and Ericson, J. (1999). Homeobox gene Nkx2.2 and specification of neuronal identity by graded Sonic hedgehog signalling. *Nature* **398**, 622-627.

Buglino, J. A. and Resh, M. D. (2008). Hhat is a palmitoylacyl transferase with specificity for N-palmitoylation of sonic hedgehog. *J.Biol.Chem.*

Bullock, S. L., Fletcher, J. M., Beddington, R. S. and Wilson, V. A. (1998). Renal agenesis in mice homozygous for a gene trap mutation in the gene encoding heparan sulfate 2-sulfotransferase. *Genes Dev* **12**, 1894-906.

Bumcrot, D. A., Takada, R. and McMahon, A. P. (1995). Proteolytic processing yields two secreted forms of sonic hedgehog. *Mol Cell Biol* **15**, 2294-303.

Burke, R., Nellen, D., Bellotto, M., Hafen, E., Senti, K. A., Dickson, B. J. and Basler, K. (1999). Dispatched, a novel sterol-sensing domain protein dedicated to the release of cholesterol-modified hedgehog from signaling cells. *Cell* **99**, 803-15.

Callejo, A., Bilioni, A., Mollica, E., Gorfinkiel, N., Andres, G., Ibanez, C., Torroja, C., Doglio, L., Sierra, J. and Guerrero, I. (2011). Dispatched mediates Hedgehog basolateral release to form the long-range morphogenetic gradient in the Drosophila wing disk epithelium. *Proc Natl Acad Sci U S A* **108**, 12591-8.

Callejo, A., Torroja, C., Quijada, L. and Guerrero, I. (2006). Hedgehog lipid modifications are required for Hedgehog stabilization in the extracellular matrix. *Development* **133**, 471-83.

Camp, D., Currie, K., Labbe, A., van Meyel, D. J. and Charron, F. (2010). Ihog and Boi are essential for Hedgehog signaling in Drosophila. *Neural Dev* **5**, 28.

Capurro, M. I., Xu, P., Shi, W., Li, F., Jia, A. and Filmus, J. (2008). Glypican-3 inhibits Hedgehog signaling during development by competing with patched for Hedgehog binding. *Dev Cell* **14**, 700-11.

Carey, D. J. (1997). Syndecans: multifunctional cell-surface co-receptors. *Biochem J* **327 (Pt 1)**, 1-16.

Carpenter, D., Stone, D. M., Brush, J., Ryan, A., Armanini, M., Frantz, G., Rosenthal, A. and de Sauvage, F. J. (1998). Characterization of two patched receptors for the vertebrate hedgehog protein family. *Proc Natl Acad Sci U S A* **95**, 13630-4.

Castillo, G. M., Ngo, C., Cummings, J., Wight, T. N. and Snow, A. D. (1997). Perlecan binds to the beta-amyloid proteins (A beta) of Alzheimer's disease, accelerates A beta fibril formation, and maintains A beta fibril stability. *J Neurochem* **69**, 2452-65.

Chamberlain, C. E., Jeong, J., Guo, C., Allen, B. L. and McMahon, A. P. (2008). Notochord-derived Shh concentrates in close association with the apically positioned basal body in neural target cells and forms a dynamic gradient during neural patterning. *Development* **135**, 1097-1106.

Chamoun, Z., Mann, R. K., Nellen, D., von Kessler, D. P., Bellotto, M., Beachy, P. A. and Basler, K. (2001). Skinny hedgehog, an acyltransferase required for palmitoylation and activity of the hedgehog signal. *Science* **293**, 2080-4.

Charrier, J. B., Lapointe, F., Le Douarin, N. M. and Teillet, M. A. (2002). Dual origin of the floor plate in the avian embryo. *Development* **129**, 4785-96.
Charron, F., Stein, E., Jeong, J., McMahon, A. P. and Tessier-Lavigne, M. (2003). The morphogen sonic hedgehog is an axonal chemoattractant that collaborates with netrin-1 in midline axon guidance. *Cell* **113**, 11-23.
Chen, J. K., Taipale, J., Cooper, M. K. and Beachy, P. A. (2002). Inhibition of Hedgehog signaling by direct binding of cyclopamine to Smoothened. *Genes Dev* **16**, 2743-8.
Chen, M. H., Li, Y. J., Kawakami, T., Xu, S. M. and Chuang, P. T. (2004). Palmitoylation is required for the production of a soluble multimeric Hedgehog protein complex and long-range signaling in vertebrates. *Genes Dev* **18**, 641-59.
Chen, W., Burgess, S. and Hopkins, N. (2001). Analysis of the zebrafish smoothened mutant reveals conserved and divergent functions of hedgehog activity. *Development* **128**, 2385-96.
Chen, Y., Gallaher, N., Goodman, R. H. and Smolik, S. M. (1998). Protein kinase A directly regulates the activity and proteolysis of cubitus interruptus. *Proc Natl Acad Sci U S A* **95**, 2349-54.
Chen, Y. and Struhl, G. (1996). Dual roles for patched in sequestering and transducing Hedgehog. *Cell* **87**, 553-563.
Chen, Y. and Struhl, G. (1998). In vivo evidence that Patched and Smoothened constitute distinct binding and transducing components of a Hedgehog receptor complex. *Development* **125**, 4943-4948.
Chiang, C., Litingtung, Y., Lee, E., Young, K. E., Corden, J. L., Westphal, H. and Beachy, P. A. (1996). Cyclopia and defective axial patterning in mice lacking Sonic hedgehog gene function. *Nature* **383**, 407-13.
Chuang, P. T. and McMahon, A. P. (1999). Vertebrate Hedgehog signalling modulated by induction of a Hedgehog-binding protein. *Nature* **397**, 617-21.
Clegg, C. H., Linkhart, T. A., Olwin, B. B. and Hauschka, S. D. (1987). Growth factor control of skeletal muscle differentiation: commitment to terminal differentiation occurs in G1 phase and is repressed by fibroblast growth factor. *J Cell Biol* **105**, 949-56.
Corbit, K. C., Aanstad, P., Singla, V., Norman, A. R., Stainier, D. Y. and Reiter, J. F. (2005). Vertebrate Smoothened functions at the primary cilium. *Nature* **437**, 1018-21.
Corcoran, R. B. and Scott, M. P. (2006). Oxysterols stimulate Sonic hedgehog signal transduction and proliferation of medulloblastoma cells. *Proc Natl Acad Sci U S A* **103**, 8408-13.
Cornell, R. A. and Ohlen, T. V. (2000). Vnd/nkx, ind/gsh, and msh/msx: conserved regulators of dorsoventral neural patterning? *Curr Opin Neurobiol* **10**, 63-71.
Cossu, G. and Borello, U. (1999). Wnt signaling and the activation of myogenesis in mammals. *EMBO J* **18**, 6867-72.
Counce, S. J. (1956). Studies on female-sterility genes in Drosophila melanogaster. II. The effects of the gene fused on embryonic development. *Z Indukt Abstamm Vererbungsl* **87**, 462-81.
Craven, S. E., Lim, K. C., Ye, W., Engel, J. D., de, S. F. and Rosenthal, A. (2004). Gata2 specifies serotonergic neurons downstream of sonic hedgehog. *Development* **131**, 1165-1173.
Dahmane, N. and Ruiz i Altaba, A. (1999). Sonic hedgehog regulates the growth and patterning of the cerebellum. *Development* **126**, 3089-100.

Dahmane, N., Sanchez, P., Gitton, Y., Palma, V., Sun, T., Beyna, M., Weiner, H. and Altaba, A. (2001). The Sonic Hedgehog-Gli pathway regulates dorsal brain growth and tumorigenesis. *Development* **128**, 5201-5212.

Dai, P., Akimaru, H., Tanaka, Y., Maekawa, T., Nakafuku, M. and Ishii, S. (1999). Sonic Hedgehog-induced activation of the Gli1 promoter is mediated by GLI3. *J.Biol.Chem.* **274**, 8143-8152.

Dai, Y., Yang, Y., MacLeod, V., Yue, X., Rapraeger, A., Shriver, Z., Venkataraman, G., Sasisekharan, R. and Sanderson, R. (2005). HSulf-1 and HSulf-2 are potent inhibitors of myeloma tumor growth in vivo. *J Biol Chem* **280**, 40066 - 40073.

Danesin, C., Agius, E., Escalas, N., Ai, X., Emerson, C., Cochard, P. and Soula, C. (2006). Ventral neural progenitors switch toward an oligodendroglial fate in response to increased Sonic hedgehog (Shh) activity: involvement of Sulfatase 1 in modulating Shh signaling in the ventral spinal cord. *J.Neurosci.* **26**, 5037-5048.

Dann, C. E., Hsieh, J. C., Rattner, A., Sharma, D., Nathans, J. and Leahy, D. J. (2001). Insights into Wnt binding and signalling from the structures of two Frizzled cysteine-rich domains. *Nature* **412**, 86-90.

David, G. (1993). Integral membrane heparan sulfate proteoglycans. *FASEB J* **7**, 1023-30.

Del Sal, G., Ruaro, E. M., Utrera, R., Cole, C. N., Levine, A. J. and Schneider, C. (1995). Gas1-induced growth suppression requires a transactivation-independent p53 function. *Mol Cell Biol* **15**, 7152-60.

Del Sal, G., Ruaro, M. E., Philipson, L. and Schneider, C. (1992). The growth arrest-specific gene, gas1, is involved in growth suppression. *Cell* **70**, 595-607.

Denef, N., Neubuser, D., Perez, L. and Cohen, S. M. (2000). Hedgehog induces opposite changes in turnover and subcellular localization of patched and smoothened. *Cell* **102**, 521-31.

Desbordes, S. C. and Sanson, B. (2003). The glypican Dally-like is required for Hedgehog signalling in the embryonic epidermis of Drosophila. *Development* **130**, 6245-55.

Dessaud, E., Yang, L. L., Hill, K., Cox, B., Ulloa, F., Ribeiro, A., Mynett, A., Novitch, B. G. and Briscoe, J. (2007). Interpretation of the sonic hedgehog morphogen gradient by a temporal adaptation mechanism. *Nature* **450**, 717-20.

Dhoot, G. K., Gustafsson, M. K., Ai, X. B., Sun, W. T., Standiford, D. M. and Emerson, C. P. (2001). Regulation of Wnt signaling and embryo patterning by an extracellular sulfatase. *Science* **293**, 1663-1666.

DiNardo, S., Sher, E., Heemskerk-Jongens, J., Kassis, J. A. and O'Farrell, P. H. (1988). Two-tiered regulation of spatially patterned engrailed gene expression during Drosophila embryogenesis. *Nature* **332**, 604-9.

Ding, Q., Motoyama, J., Gasca, S., Mo, R., Sasaki, H., Rossant, J. and Hui, C. C. (1998). Diminished Sonic hedgehog signaling and lack of floor plate differentiation in Gli2 mutant mice. *Development* **125**, 2533-43.

Dominguez, L., Gonzalez, A. and Moreno, N. (2010). Sonic hedgehog expression during Xenopus laevis forebrain development. *Brain Res* **1347**, 19-32.

Dominguez, M. (1999). Dual role for Hedgehog in the regulation of the proneural gene atonal during ommatidia development. *Development* **126**, 2345-53.

Doubravska, L., Krausova, M., Gradl, D., Vojtechova, M., Tumova, L., Lukas, J., Valenta, T., Pospichalova, V., Fafilek, B., Plachy, J. et al. (2011).

Fatty acid modification of Wnt1 and Wnt3a at serine is prerequisite for lipidation at cysteine and is essential for Wnt signalling. *Cell Signal* **23**, 837-48.

Duprez, D., Bell, E. J., Richardson, M. K., Archer, C. W., Wolpert, L., Brickell, P. M. and Francis-West, P. H. (1996). Overexpression of BMP-2 and BMP-4 alters the size and shape of developing skeletal elements in the chick limb. *Mech Dev* **57**, 145-57.

Ekker, S. C., McGrew, L. L., Lai, C. J., Lee, J. J., von Kessler, D. P., Moon, R. T. and Beachy, P. A. (1995). Distinct expression and shared activities of members of the hedgehog gene family of Xenopus laevis. *Development* **121**, 2337-47.

Ericson, J., Briscoe, J., Rashbass, P., van, H. V. and Jessell, T. M. (1997a). Graded sonic hedgehog signaling and the specification of cell fate in the ventral neural tube. *Cold Spring Harb.Symp.Quant.Biol.* **62**, 451-466.

Ericson, J., Morton, S., Kawakami, A., Roelink, H. and Jessell, T. M. (1996). Two critical periods of Sonic Hedgehog signaling required for the specification of motor neuron identity. *Cell* **87**, 661-73.

Ericson, J., Rashbass, P., Schedl, A., Brenner-Morton, S., Kawakami, A., van, H. V., Jessell, T. M. and Briscoe, J. (1997b). Pax6 controls progenitor cell identity and neuronal fate in response to graded Shh signaling. *Cell* **90**, 169-180.

Esko, J. D. and Selleck, S. B. (2002). Order out of chaos: assembly of ligand binding sites in heparan sulfate. *Annu Rev Biochem* **71**, 435-71.

Etheridge, L. A., Crawford, T. Q., Zhang, S. and Roelink, H. (2010). Evidence for a role of vertebrate Disp1 in long-range Shh signaling. *Development* **137**, 133-40.

Eugster, C., Panakova, D., Mahmoud, A. and Eaton, S. (2007). Lipoprotein-heparan sulfate interactions in the Hh pathway. *Dev Cell* **13**, 57-71.

Fan, C. M. and Tessier-Lavigne, M. (1994). Patterning of mammalian somites by surface ectoderm and notochord: evidence for sclerotome induction by a hedgehog homolog. *Cell* **79**, 1175-86.

Fan, G., Xiao, L., Cheng, L., Wang, X., Sun, B. and Hu, G. (2000). Targeted disruption of NDST-1 gene leads to pulmonary hypoplasia and neonatal respiratory distress in mice. *FEBS Lett* **467**, 7-11.

Fletcher, R. B. and Harland, R. M. (2008). The role of FGF signaling in the establishment and maintenance of mesodermal gene expression in Xenopus. *Dev Dyn* **237**, 1243-54.

Forbes, A. J., Nakano, Y., Taylor, A. M. and Ingham, P. W. (1993). Genetic analysis of hedgehog signalling in the Drosophila embryo. *Dev.Suppl*, 115-124.

Freeman, S. D., Moore, W. M., Guiral, E. C., Holme, A. D., Turnbull, J. E. and Pownall, M. E. (2008). Extracellular regulation of developmental cell signaling by XtSulf1. *Dev.Biol.* **320**, 436-445.

Fuse, N., Maiti, T., Wang, B., Porter, J. A., Hall, T. M., Leahy, D. J. and Beachy, P. A. (1999). Sonic hedgehog protein signals not as a hydrolytic enzyme but as an apparent ligand for patched. *Proc.Natl.Acad.Sci.U.S.A* **96**, 10992-10999.

Gallet, A., Rodriguez, R., Ruel, L. and Therond, P. P. (2003). Cholesterol modification of hedgehog is required for trafficking and movement, revealing an asymmetric cellular response to hedgehog. *Dev.Cell* **4**, 191-204.

Gallet, A., Ruel, L., Staccini-Lavenant, L. and Therond, P. P. (2006). Cholesterol modification is necessary for controlled planar long-range activity of Hedgehog in Drosophila epithelia. *Development* **133**, 407-18.

Gallet, A., Staccini-Lavenant, L. and Therond, P. P. (2008). Cellular trafficking of the glypican Dally-like is required for full-strength Hedgehog signaling and wingless transcytosis. *Dev Cell* **14**, 712-25.

Giraldez, A. J., Copley, R. R. and Cohen, S. M. (2002). HSPG modification by the secreted enzyme Notum shapes the Wingless morphogen gradient. *Dev Cell* **2**, 667-76.

Glise, B., Miller, C. A., Crozatier, M., Halbisen, M. A., Wise, S., Olson, D. J., Vincent, A. and Blair, S. S. (2005). Shifted, the Drosophila ortholog of Wnt inhibitory factor-1, controls the distribution and movement of Hedgehog. *Dev.Cell* **8**, 255-266.

Goetz, J. A., Singh, S., Suber, L. M., Kull, F. J. and Robbins, D. J. (2006). A highly conserved amino-terminal region of sonic hedgehog is required for the formation of its freely diffusible multimeric form. *J.Biol.Chem.* **281**, 4087-4093.

Goodrich, L. V., Johnson, R. L., Milenkovic, L., McMahon, J. A. and Scott, M. P. (1996). Conservation of the hedgehog/patched signaling pathway from flies to mice: induction of a mouse patched gene by Hedgehog. *Genes Dev.* **10**, 301-312.

Goodrich, L. V., Milenkovic, L., Higgins, K. M. and Scott, M. P. (1997). Altered neural cell fates and medulloblastoma in mouse patched mutants. *Science* **277**, 1109-13.

Gorfinkiel, N., Sierra, J., Callejo, A., Ibanez, C. and Guerrero, I. (2005). The Drosophila ortholog of the human Wnt inhibitor factor Shifted controls the diffusion of lipid-modified Hedgehog. *Dev Cell* **8**, 241-53.

Gritsman, K., Zhang, J., Cheng, S., Heckscher, E., Talbot, W. S. and Schier, A. F. (1999). The EGF-CFC protein one-eyed pinhead is essential for nodal signaling. *Cell* **97**, 121-32.

Guiral, E. C., Faas, L. and Pownall, M. E. (2010). Neural crest migration requires the activity of the extracellular sulphatases XtSulf1 and XtSulf2. *Dev Biol* **341**, 375-88.

Guner, B. and Karlstrom, R. O. (2007). Cloning of zebrafish nkx6.2 and a comprehensive analysis of the conserved transcriptional response to Hedgehog/Gli signaling in the zebrafish neural tube. *Gene Expr Patterns* **7**, 596-605.

Gurdon, J. B., Standley, H., Dyson, S., Butler, K., Langon, T., Ryan, K., Stennard, F., Shimizu, K. and Zorn, A. (1999). Single cells can sense their position in a morphogen gradient. *Development* **126**, 5309-5317.

Gustafsson, M. K., Pan, H., Pinney, D. F., Liu, Y., Lewandowski, A., Epstein, D. J. and Emerson, C. P., Jr. (2002). Myf5 is a direct target of long-range Shh signaling and Gli regulation for muscle specification. *Genes Dev* **16**, 114-26.

Häcker, U., Lin, X. and Perrimon, N. (1997). The Drosophila sugarless gene modulates Wingless signaling and encodes an enzyme involved in polysaccharide biosynthesis. *Development* **124**, 3565-73.

Hacker, U., Nybakken, K. and Perrimon, N. (2005). Heparan sulphate proteoglycans: the sweet side of development. *Nat Rev Mol Cell Biol* **6**, 530 - 541.

Hagner-McWhirter, A., Li, J. P., Oscarson, S. and Lindahl, U. (2004). Irreversible glucuronyl C5-epimerization in the biosynthesis of heparan sulfate. *J Biol Chem* **279**, 14631-8.

Halfter, W., Dong, S., Schurer, B. and Cole, G. J. (1998). Collagen XVIII is a basement membrane heparan sulfate proteoglycan. *J Biol Chem* **273**, 25404-12.

Halfter, W., Schurer, B., Yip, J., Yip, L., Tsen, G., Lee, J. A. and Cole, G. J. (1997). Distribution and substrate properties of agrin, a heparan sulfate proteoglycan of developing axonal pathways. *J Comp Neurol* **383**, 1-17.

Halpern, M. E., Ho, R. K., Walker, C. and Kimmel, C. B. (1993). Induction of muscle pioneers and floor plate is distinguished by the zebrafish no tail mutation. *Cell* **75**, 99-111.

Han, C., Belenkaya, T. Y., Khodoun, M., Tauchi, M. and Lin, X. (2004). Distinct and collaborative roles of Drosophila EXT family proteins in morphogen signalling and gradient formation. *Development* **131**, 1563-1575.

Hatta, K., Kimmel, C. B., Ho, R. K. and Walker, C. (1991). The cyclops mutation blocks specification of the floor plate of the zebrafish central nervous system. *Nature* **350**, 339-41.

Hayashi, S., Itoh, M., Taira, S., Agata, K. and Taira, M. (2004). Expression patterns of Xenopus FGF receptor-like 1/nou-darake in early Xenopus development resemble those of planarian nou-darake and Xenopus FGF8. *Dev Dyn* **230**, 700-7.

Haycraft, C. J., Banizs, B., Aydin-Son, Y., Zhang, Q., Michaud, E. J. and Yoder, B. K. (2005). Gli2 and Gli3 localize to cilia and require the intraflagellar transport protein polaris for processing and function. *PLoS Genet* **1**, e53.

Holst, C. R., Bou-Reslan, H., Gore, B. B., Wong, K., Grant, D., Chalasani, S., Carano, R. A., Frantz, G. D., Tessier-Lavigne, M., Bolon, B. et al. (2007). Secreted sulfatases Sulf1 and Sulf2 have overlapping yet essential roles in mouse neonatal survival. *PLoS One* **2**, e575.

Hook, M., Lindahl, U., Backstrom, G., Malmstrom, A. and Fransson, L. (1974). Biosynthesis of heparin. 3. Formation of iduronic acid residues. *J Biol Chem* **249**, 3908-15.

Hooper, J. E. and Scott, M. P. (2005). Communicating with Hedgehogs. *Nat Rev Mol Cell Biol* **6**, 306-17.

Huangfu, D. and Anderson, K. V. (2005). Cilia and Hedgehog responsiveness in the mouse. *Proc Natl Acad Sci U S A* **102**, 11325-30.

Huangfu, D., Liu, A., Rakeman, A. S., Murcia, N. S., Niswander, L. and Anderson, K. V. (2003). Hedgehog signalling in the mouse requires intraflagellar transport proteins. *Nature* **426**, 83-7.

Huze, C., Bauche, S., Richard, P., Chevessier, F., Goillot, E., Gaudon, K., Ben Ammar, A., Chaboud, A., Grosjean, I., Lecuyer, H. A. et al. (2009). Identification of an agrin mutation that causes congenital myasthenia and affects synapse function. *Am J Hum Genet* **85**, 155-67.

Hynes, M., Ye, W., Wang, K., Stone, D., Murone, M., Sauvage, F. and Rosenthal, A. (2000). The seven-transmembrane receptor smoothened cell-autonomously induces multiple ventral cell types. *Nat Neurosci* **3**, 41-6.

Inatani, M., Irie, F., Plump, A. S., Tessier-Lavigne, M. and Yamaguchi, Y. (2003). Mammalian brain morphogenesis and midline axon guidance require heparan sulfate. *Science* **302**, 1044-6.

Ingham, P. W. and McMahon, A. P. (2001). Hedgehog signaling in animal development: paradigms and principles. *Genes Dev.* **15**, 3059-3087.

Ingham, P. W., Taylor, A. M. and Nakano, Y. (1991). Role of the Drosophila patched gene in positional signalling. *Nature* **353**, 184-7.

Ishibashi, M. and McMahon, A. P. (2002). A sonic hedgehog-dependent signaling relay regulates growth of diencephalic and mesencephalic primordia in the early mouse embryo. *Development* **129**, 4807-19.

Itoh, K. and Sokol, S. Y. (1994). Heparan sulfate proteoglycans are required for mesoderm formation in Xenopus embryos. *Development* **120**, 2703-11.

Jia, J., Tong, C., Wang, B., Luo, L. and Jiang, J. (2004). Hedgehog signalling activity of Smoothened requires phosphorylation by protein kinase A and casein kinase I. *Nature* **432**, 1045-50.

Jiang, J. and Struhl, G. (1995). Protein kinase A and hedgehog signaling in Drosophila limb development. *Cell* **80**, 563-72.

Jiang, J. and Struhl, G. (1998). Regulation of the Hedgehog and Wingless signalling pathways by the F-box/WD40-repeat protein Slimb. *Nature* **391**, 493-6.

Johnson, R. L., Grenier, J. K. and Scott, M. P. (1995). patched overexpression alters wing disc size and pattern: transcriptional and post-transcriptional effects on hedgehog targets. *Development* **121**, 4161-70.

Johnson, R. L., Laufer, E., Riddle, R. D. and Tabin, C. (1994). Ectopic expression of Sonic hedgehog alters dorsal-ventral patterning of somites. *Cell* **79**, 1165-73.

Johnson, R. L., Milenkovic, L. and Scott, M. P. (2000). In vivo functions of the patched protein: requirement of the C terminus for target gene inactivation but not Hedgehog sequestration. *Mol Cell* **6**, 467-78.

Junnila, S., Kokkola, A., Mizuguchi, T., Hirata, K., Karjalainen-Lindsberg, M. L., Puolakkainen, P. and Monni, O. (2010). Gene expression analysis identifies over-expression of CXCL1, SPARC, SPP1, and SULF1 in gastric cancer. *Genes Chromosomes Cancer* **49**, 28-39.

Kang, J. S., Gao, M., Feinleib, J. L., Cotter, P. D., Guadagno, S. N. and Krauss, R. S. (1997). CDO: an oncogene-, serum-, and anchorage-regulated member of the Ig/fibronectin type III repeat family. *J Cell Biol* **138**, 203-13.

Kang, J. S., Mulieri, P. J., Hu, Y., Taliana, L. and Krauss, R. S. (2002). BOC, an Ig superfamily member, associates with CDO to positively regulate myogenic differentiation. *EMBO J* **21**, 114-24.

Kawakami, T., Kawcak, T., Li, Y. J., Zhang, W., Hu, Y. and Chuang, P. T. (2002). Mouse dispatched mutants fail to distribute hedgehog proteins and are defective in hedgehog signaling. *Development* **129**, 5753-65.

Khare, N. and Baumgartner, S. (2000). Dally-like protein, a new Drosophila glypican with expression overlapping with wingless. *Mech Dev* **99**, 199-202.

Kim, B. T., Kitagawa, H., Tamura, J., Saito, T., Kusche-Gullberg, M., Lindahl, U. and Sugahara, K. (2001). Human tumor suppressor EXT gene family members EXTL1 and EXTL3 encode alpha 1,4- N-acetylglucosaminyltransferases that likely are involved in heparan sulfate/ heparin biosynthesis. *Proc Natl Acad Sci U S A* **98**, 7176-81.

Kim, B. T., Kitagawa, H., Tamura Ji, J., Kusche-Gullberg, M., Lindahl, U. and Sugahara, K. (2002). Demonstration of a novel gene DEXT3 of Drosophila melanogaster as the essential N-acetylglucosamine transferase in the heparan sulfate biosynthesis: chain initiation and elongation. *J Biol Chem* **277**, 13659-65.

Kim, J., Kato, M. and Beachy, P. A. (2009). Gli2 trafficking links Hedgehog-dependent activation of Smoothened in the primary cilium to transcriptional activation in the nucleus. *Proc Natl Acad Sci U S A* **106**, 21666-71.

Kitagawa, H., Shimakawa, H. and Sugahara, K. (1999). The tumor suppressor EXT-like gene EXTL2 encodes an alpha1, 4-N-acetylhexosaminyltransferase that transfers N-acetylgalactosamine and N-acetylglucosamine to the common glycosaminoglycan-protein linkage region. The key enzyme for the chain initiation of heparan sulfate. *J Biol Chem* **274**, 13933-7.

Kleinschmit, A., Koyama, T., Dejima, K., Hayashi, Y., Kamimura, K. and Nakato, H. (2010). Drosophila heparan sulfate 6-O endosulfatase regulates Wingless morphogen gradient formation. *Dev Biol* **345**, 204-14.

Knaust, A., Schmidt, B., Dierks, T., von Bulow, R. and von Figura, K. (1998). Residues critical for formylglycine formation and/or catalytic activity of arylsulfatase A. *Biochemistry* **37**, 13941-6.

Kobayashi, T., Habuchi, H., Nogami, K., Ashikari-Hada, S., Tamura, K., Ide, H. and Kimata, K. (2010). Functional analysis of chick heparan sulfate 6-O-sulfotransferases in limb bud development. *Dev Growth Differ* **52**, 146-56.

Kobayashi, T., Habuchi, H., Tamura, K., Ide, H. and Kimata, K. (2007). Essential role of heparan sulfate 2-O-sulfotransferase in chick limb bud patterning and development. *J Biol Chem* **282**, 19589-97.

Kokenyesi, R. and Bernfield, M. (1994). Core protein structure and sequence determine the site and presence of heparan sulfate and chondroitin sulfate on syndecan-1. *J Biol Chem* **269**, 12304-9.

Kreuger, J., Perez, L., Giraldez, A. J. and Cohen, S. M. (2004). Opposing activities of Dally-like glypican at high and low levels of Wingless morphogen activity. *Dev Cell* **7**, 503-12.

Lai, J., Chien, J., Staub, J., Avula, R., Greene, E. L., Matthews, T. A., Smith, D. I., Kaufmann, S. H., Roberts, L. R. and Shridhar, V. (2003). Loss of HSulf-1 up-regulates heparin-binding growth factor signaling in cancer. *J Biol Chem* **278**, 23107-17.

Lai, J. P., Chien, J., Strome, S. E., Staub, J., Montoya, D. P., Greene, E. L., Smith, D. I., Roberts, L. R. and Shridhar, V. (2004a). HSulf-1 modulates HGF-mediated tumor cell invasion and signaling in head and neck squamous carcinoma. *Oncogene* **23**, 1439-47.

Lai, J. P., Chien, J. R., Moser, D. R., Staub, J. K., Aderca, I., Montoya, D. P., Matthews, T. A., Nagorney, D. M., Cunningham, J. M., Smith, D. I. et al. (2004b). hSulf1 Sulfatase promotes apoptosis of hepatocellular cancer cells by decreasing heparin-binding growth factor signaling. *Gastroenterology* **126**, 231-48.

Lamanna, W. C., Baldwin, R. J., Padva, M., Kalus, I., ten Dam, G., van Kuppevelt, T. H., Gallagher, J. T., von Figura, K., Dierks, T. and Merry, C. L. R. (2006). Heparan sulfate 6-O-endosulfatases: discrete in vivo activities and functional co-operativity. *Biochemical Journal* **400**, 63-73.

Lamanna, W. C., Kalus, I., Padva, M., Baldwin, R. J., Merry, C. L. R. and Dierks, T. (2007). The heparanome - The enigma of encoding and decoding heparan sulfate sulfation. *Journal of Biotechnology* **129**, 290-307.

Laufer, E., Nelson, C. E., Johnson, R. L., Morgan, B. A. and Tabin, C. (1994). Sonic hedgehog and Fgf-4 act through a signaling cascade and feedback loop to integrate growth and patterning of the developing limb bud. *Cell* **79**, 993-1003.

Lea, R., Papalopulu, N., Amaya, E. and Dorey, K. (2009). Temporal and spatial expression of FGF ligands and receptors during Xenopus development. *Dev Dyn* **238**, 1467-79.

LeClair, E. E., Mui, S. R., Huang, A., Topczewska, J. M. and Topczewski, J. (2009). Craniofacial skeletal defects of adult zebrafish Glypican 4 (knypek) mutants. *Dev Dyn* **238**, 2550-63.

Lee, C. S., Buttitta, L. and Fan, C. M. (2001). Evidence that the WNT-inducible growth arrest-specific gene 1 encodes an antagonist of sonic hedgehog signaling in the somite. *Proc Natl Acad Sci U S A* **98**, 11347-52.

Lee, J., Platt, K. A., Censullo, P. and Altaba, A. R. I. (1997). Gli1 is a target of Sonic hedgehog that induces ventral neural tube development. *Development* **124**, 2537-2552.

Lee, J. D. and Treisman, J. E. (2001). Sightless has homology to transmembrane acyltransferases and is required to generate active Hedgehog protein. *Curr Biol* **11**, 1147-52.

Lee, J. J., Ekker, S. C., von Kessler, D. P., Porter, J. A., Sun, B. I. and Beachy, P. A. (1994). Autoproteolysis in hedgehog protein biogenesis. *Science* **266**, 1528-1537.

Lee, J. J., von Kessler, D. P., Parks, S. and Beachy, P. A. (1992). Secretion and localized transcription suggest a role in positional signaling for products of the segmentation gene hedgehog. *Cell* **71**, 33-50.

Lee, P. H., Trowbridge, J. M., Taylor, K. R., Morhenn, V. B. and Gallo, R. L. (2004). Dermatan sulfate proteoglycan and glycosaminoglycan synthesis is induced in fibroblasts by transfer to a three-dimensional extracellular environment. *J Biol Chem* **279**, 48640-6.

Lee, S. K. and Pfaff, S. L. (2001). Transcriptional networks regulating neuronal identity in the developing spinal cord. *Nat Neurosci* **4 Suppl**, 1183-91.

Lemjabbar-Alaoui, H., van Zante, A., Singer, M. S., Xue, Q., Wang, Y. Q., Tsay, D., He, B., Jablons, D. M. and Rosen, S. D. (2010). Sulf-2, a heparan sulfate endosulfatase, promotes human lung carcinogenesis. *Oncogene* **29**, 635-46.

Lewis, K. E., Concordet, J. P. and Ingham, P. W. (1999). Characterisation of a second patched gene in the zebrafish Danio rerio and the differential response of patched genes to Hedgehog signalling. *Dev Biol* **208**, 14-29.

Lewis, P. M., Dunn, M. P., McMahon, J. A., Logan, M., Martin, J. F., St-Jacques, B. and McMahon, A. P. (2001). Cholesterol modification of sonic hedgehog is required for long-range signaling activity and effective modulation of signaling by Ptc1. *Cell* **105**, 599-612.

Liem, K. F., Jessell, T. M. and Briscoe, J. (2000). Regulation of the neural patterning activity of sonic hedgehog by secreted BMP inhibitors expressed by notochord and somites. *Development* **127**, 4855-4866.

Liem, K. F., Jr., Tremml, G. and Jessell, T. M. (1997). A role for the roof plate and its resident TGFbeta-related proteins in neuronal patterning in the dorsal spinal cord. *Cell* **91**, 127-38.

Lin, X. (2004). Functions of heparan sulfate proteoglycans in cell signaling during development. *Development* **131**, 6009 - 6021.

Lin, X., Buff, E. M., Perrimon, N. and Michelson, A. M. (1999). Heparan sulfate proteoglycans are essential for FGF receptor signaling during Drosophila embryonic development. *Development* **126**, 3715-3723.

Lin, X. and Perrimon, N. (1999). Dally cooperates with Drosophila Frizzled 2 to transduce Wingless signalling. *Nature* **400**, 281-4.

Lind, T., Tufaro, F., McCormick, C., Lindahl, U. and Lidholt, K. (1998). The putative tumor suppressors EXT1 and EXT2 are glycosyltransferases required for the biosynthesis of heparan sulfate. *J Biol Chem* **273**, 26265-8.

Loo, B. M. and Salmivirta, M. (2002). Heparin/Heparan sulfate domains in binding and signaling of fibroblast growth factor 8b. *J Biol Chem* **277**, 32616-23.

Lopez, S. L., Paganelli, A. R., Siri, M. V., Ocana, O. H., Franco, P. G. and Carrasco, A. E. (2003). Notch activates sonic hedgehog and both are involved in the specification of dorsal midline cell-fates in Xenopus. *Development* **130**, 2225-38.

Lundin, L., Larsson, H., Kreuger, J., Kanda, S., Lindahl, U., Salmivirta, M. and Claesson-Welsh, L. (2000). Selectively desulfated heparin inhibits fibroblast growth factor-induced mitogenicity and angiogenesis. *J Biol Chem* **275**, 24653-60.

Maccarana, M., Sakura, Y., Tawada, A., Yoshida, K. and Lindahl, U. (1996). Domain structure of heparan sulfates from bovine organs. *J Biol Chem* **271**, 17804-10.

Madsen, E. C., Morcos, P. A., Mendelsohn, B. A. and Gitlin, J. D. (2008). In vivo correction of a Menkes disease model using antisense oligonucleotides. *Proc Natl Acad Sci U S A* **105**, 3909-14.

Marigo, V., Davey, R. A., Zuo, Y., Cunningham, J. M. and Tabin, C. J. (1996). Biochemical evidence that patched is the Hedgehog receptor. *Nature* **384**, 176-9.

Marlow, F., Zwartkruis, F., Malicki, J., Neuhauss, S. C., Abbas, L., Weaver, M., Driever, W. and Solnica-Krezel, L. (1998). Functional interactions of genes mediating convergent extension, knypek and trilobite, during the partitioning of the eye primordium in zebrafish. *Dev Biol* **203**, 382-99.

Martin, V., Carrillo, G., Torroja, C. and Guerrero, I. (2001). The sterol-sensing domain of Patched protein seems to control Smoothened activity through Patched vesicular trafficking. *Curr Biol* **11**, 601-7.

Martinez Arias, A., Baker, N. E. and Ingham, P. W. (1988). Role of segment polarity genes in the definition and maintenance of cell states in the Drosophila embryo. *Development* **103**, 157-70.

May, S. R., Ashique, A. M., Karlen, M., Wang, B., Shen, Y., Zarbalis, K., Reiter, J., Ericson, J. and Peterson, A. S. (2005). Loss of the retrograde motor for IFT disrupts localization of Smo to cilia and prevents the expression of both activator and repressor functions of Gli. *Dev Biol* **287**, 378-89.

McLaughlin, D., Karlsson, F., Tian, N., Pratt, T., Bullock, S. L., Wilson, V. A., Price, D. J. and Mason, J. O. (2003). Specific modification of heparan sulphate is required for normal cerebral cortical development. *Mech Dev* **120**, 1481-8.

Methot, N. and Basler, K. (2000). Suppressor of fused opposes hedgehog signal transduction by impeding nuclear accumulation of the activator form of Cubitus interruptus. *Development* **127**, 4001-10.

Micchelli, C. A., The, I., Selva, E., Mogila, V. and Perrimon, N. (2002). Rasp, a putative transmembrane acyltransferase, is required for Hedgehog signaling. *Development* **129**, 843-51.

Miller, R. H., Dinsio, K., Wang, R., Geertman, R., Maier, C. E. and Hall, A. K. (2004). Patterning of spinal cord oligodendrocyte development by dorsally derived BMP4. *J Neurosci Res* **76**, 9-19.

Mizutani, C. M., Meyer, N., Roelink, H. and Bier, E. (2006). Threshold-dependent BMP-mediated repression: a model for a conserved mechanism that patterns the neuroectoderm. *PLoS Biol* **4**, e313.

Morimoto-Tomita, M., Uchimura, K., Werb, Z., Hemmerich, S. and Rosen, S. D. (2002). Cloning and characterization of two extracellular heparin-degrading endosulfatases in mice and humans. *J Biol Chem* **277**, 49175-85.

Motoyama, J., Heng, H., Crackower, M. A., Takabatake, T., Takeshima, K., Tsui, L. C. and Hui, C. (1998). Overlapping and non-overlapping Ptch2 expression with Shh during mouse embryogenesis. *Mech Dev* **78**, 81-4.

Murdoch, A. D., Liu, B., Schwarting, R., Tuan, R. S. and Iozzo, R. V. (1994). Widespread expression of perlecan proteoglycan in basement membranes and extracellular matrices of human tissues as detected by a novel monoclonal

antibody against domain III and by in situ hybridization. *J Histochem Cytochem* **42**, 239-49.

Nakato, H., Futch, T. A. and Selleck, S. B. (1995). The division abnormally delayed (dally) gene: a putative integral membrane proteoglycan required for cell division patterning during postembryonic development of the nervous system in Drosophila. *Development* **121**, 3687-702.

Narita, K., Staub, J., Chien, J., Meyer, K., Bauer, M., Friedl, A., Ramakrishnan, S. and Shridhar, V. (2006). HSulf-1 inhibits angiogenesis and tumorigenesis in vivo. *Cancer Res* **66**, 6025 - 6032.

Newport, J. and Kirschner, M. (1982). A major developmental transition in early Xenopus embryos: I. characterization and timing of cellular changes at the midblastula stage. *Cell* **30**, 675-86.

Nieuwkoop, P. D. and Faber, J. (1994). Normal Table of *Xenopus laevis* (Daudin). New York: Garland Publishing Inc.

Niswander, L., Jeffrey, S., Martin, G. R. and Tickle, C. (1994). A positive feedback loop coordinates growth and patterning in the vertebrate limb. *Nature* **371**, 609-12.

Nitkin, R. M., Smith, M. A., Magill, C., Fallon, J. R., Yao, Y. M., Wallace, B. G. and McMahan, U. J. (1987). Identification of agrin, a synaptic organizing protein from Torpedo electric organ. *J Cell Biol* **105**, 2471-8.

Noonan, D. M., Fulle, A., Valente, P., Cai, S., Horigan, E., Sasaki, M., Yamada, Y. and Hassell, J. R. (1991). The complete sequence of perlecan, a basement membrane heparan sulfate proteoglycan, reveals extensive similarity with laminin A chain, low density lipoprotein-receptor, and the neural cell adhesion molecule. *J Biol Chem* **266**, 22939-47.

Nusslein-Volhard, C. and Wieschaus, E. (1980). Mutations affecting segment number and polarity in Drosophila. *Nature* **287**, 795-801.

Odenthal, J., van Eeden, F. J., Haffter, P., Ingham, P. W. and Nüsslein-Volhard, C. (2000). Two distinct cell populations in the floor plate of the zebrafish are induced by different pathways. *Dev Biol* **219**, 350-63.

Ogden, S. K., Ascano, M., Jr., Stegman, M. A., Suber, L. M., Hooper, J. E. and Robbins, D. J. (2003). Identification of a functional interaction between the transmembrane protein Smoothened and the kinesin-related protein Costal2. *Curr Biol* **13**, 1998-2003.

Okada, A., Charron, F., Morin, S., Shin, D. S., Wong, K., Fabre, P. J., Tessier-Lavigne, M. and McConnell, S. K. (2006). Boc is a receptor for sonic hedgehog in the guidance of commissural axons. *Nature* **444**, 369-73.

Paine-Saunders, S., Viviano, B. L., Economides, A. N. and Saunders, S. (2002). Heparan sulfate proteoglycans retain Noggin at the cell surface: a potential mechanism for shaping bone morphogenetic protein gradients. *J Biol Chem* **277**, 2089-96.

Palma, V. and Altaba, A. R. I. (2004). Hedgehog-GLI signaling regulates the behavior of cells with stem cell properties in the developing neocortex. *Development* **131**, 337-345.

Palma, V., Lim, D. A., Dahmane, N., Sanchez, P., Brionne, T. C., Herzberg, C. D., Gitton, Y., Carleton, A., varez-Buylla, A. and Altaba, A. (2005). Sonic hedgehog controls stem cell behavior in the postnatal and adult brain. *Development* **132**, 335-344.

Pan, Y., Bai, C. B., Joyner, A. L. and Wang, B. (2006). Sonic hedgehog signaling regulates Gli2 transcriptional activity by suppressing its processing and degradation. *Mol Cell Biol* **26**, 3365-77.

Panakova, D., Sprong, H., Marois, E., Thiele, C. and Eaton, S. (2005). Lipoprotein particles are required for Hedgehog and Wingless signalling. *Nature* **435**, 58-65.

Passos-Bueno, M. R., Suzuki, O. T., Armelin-Correa, L. M., Sertie, A. L., Errera, F. I., Bagatini, K., Kok, F. and Leite, K. R. (2006). Mutations in collagen 18A1 and their relevance to the human phenotype. *An Acad Bras Cienc* **78**, 123-31.

Patten, I., Kulesa, P., Shen, M. M., Fraser, S. and Placzek, M. (2003). Distinct modes of floor plate induction in the chick embryo. *Development* **130**, 4809-21.

Patten, I. and Placzek, M. (2002). Opponent activities of Shh and BMP signaling during floor plate induction in vivo. *Curr Biol* **12**, 47-52.

Pepinsky, R. B., Zeng, C., Wen, D., Rayhorn, P., Baker, D. P., Williams, K. P., Bixler, S. A., Ambrose, C. M., Garber, E. A., Miatkowski, K. et al. (1998). Identification of a palmitic acid-modified form of human Sonic hedgehog. *J.Biol.Chem.* **273**, 14037-14045.

Peterson, S., Iskenderian, A., Cook, L., Romashko, A., Tobin, K., Jones, M., Norton, A., Gomez-Yafal, A., Heartlein, M., Concino, M. et al. (2010). Human Sulfatase 2 inhibits in vivo tumor growth of MDA-MB-231 human breast cancer xenografts. *BMC Cancer* **10**, 427.

Peyrot, S. M., Wallingford, J. B. and Harland, R. M. (2011). A revised model of Xenopus dorsal midline development: differential and separable requirements for Notch and Shh signaling. *Dev Biol* **352**, 254-66.

Pfaff, S. L., Mendelsohn, M., Stewart, C. L., Edlund, T. and Jessell, T. M. (1996). Requirement for LIM homeobox gene Isl1 in motor neuron generation reveals a motor neuron-dependent step in interneuron differentiation. *Cell* **84**, 309-20.

Pierani, A., Brenner-Morton, S., Chiang, C. and Jessell, T. M. (1999). A sonic hedgehog-independent, retinoid-activated pathway of neurogenesis in the ventral spinal cord. *Cell* **97**, 903-915.

Placzek, M. and Briscoe, J. (2005). The floor plate: multiple cells, multiple signals. *Nat Rev Neurosci* **6**, 230-40.

Placzek, M., Jessell, T. M. and Dodd, J. (1993). Induction of floor plate differentiation by contact-dependent, homeogenetic signals. *Development* **117**, 205-18.

Placzek, M., Tessier-Lavigne, M., Yamada, T., Jessell, T. and Dodd, J. (1990). Mesodermal control of neural cell identity: floor plate induction by the notochord. *Science* **250**, 985-8.

Porter, J. A., Ekker, S. C., Park, W. J., von Kessler, D. P., Young, K. E., Chen, C. H., Ma, Y., Woods, A. S., Cotter, R. J., Koonin, E. V. et al. (1996a). Hedgehog patterning activity: role of a lipophilic modification mediated by the carboxy-terminal autoprocessing domain. *Cell* **86**, 21-34.

Porter, J. A., von Kessler, D. P., Ekker, S. C., Young, K. E., Lee, J. J., Moses, K. and Beachy, P. A. (1995). The product of hedgehog autoproteolytic cleavage active in local and long-range signalling. *Nature* **374**, 363-6.

Porter, J. A., Young, K. E. and Beachy, P. A. (1996b). Cholesterol modification of hedgehog signaling proteins in animal development. *Science* **274**, 255-259.

Pownall, M. E., Tucker, A. S., Slack, J. M. and Isaacs, H. V. (1996). eFGF, Xcad3 and Hox genes form a molecular pathway that establishes the anteroposterior axis in Xenopus. *Development* **122**, 3881-92.

Pratt, T., Conway, C. D., Tian, N. M., Price, D. J. and Mason, J. O. (2006). Heparan sulphation patterns generated by specific heparan sulfotransferase

enzymes direct distinct aspects of retinal axon guidance at the optic chiasm. *J Neurosci* **26**, 6911-23.

Pye, D. A., Vives, R. R., Hyde, P. and Gallagher, J. T. (2000). Regulation of FGF-1 mitogenic activity by heparan sulfate oligosaccharides is dependent on specific structural features: differential requirements for the modulation of FGF-1 and FGF-2. *Glycobiology* **10**, 1183-92.

Radhakrishnan, A., Sun, L. P., Kwon, H. J., Brown, M. S. and Goldstein, J. L. (2004). Direct binding of cholesterol to the purified membrane region of SCAP: mechanism for a sterol-sensing domain. *Mol Cell* **15**, 259-68.

Rapraeger, A., Jalkanen, M., Endo, E., Koda, J. and Bernfield, M. (1985). The cell surface proteoglycan from mouse mammary epithelial cells bears chondroitin sulfate and heparan sulfate glycosaminoglycans. *J Biol Chem* **260**, 11046-52.

Rapraeger, A. C., Krufka, A. and Olwin, B. B. (1991). Requirement of heparan sulfate for bFGF-mediated fibroblast growth and myoblast differentiation. *Science* **252**, 1705-8.

Reichsman, F., Smith, L. and Cumberledge, S. (1996). Glycosaminoglycans can modulate extracellular localization of the wingless protein and promote signal transduction. *J Cell Biol* **135**, 819-27.

Ribes, V., Balaskas, N., Sasai, N., Cruz, C., Dessaud, E., Cayuso, J., Tozer, S., Yang, L. L., Novitch, B., Marti, E. et al. (2010). Distinct Sonic Hedgehog signaling dynamics specify floor plate and ventral neuronal progenitors in the vertebrate neural tube. *Genes Dev* **24**, 1186-200.

Robbins, D. J., Nybakken, K. E., Kobayashi, R., Sisson, J. C., Bishop, J. M. and Therond, P. P. (1997). Hedgehog elicits signal transduction by means of a large complex containing the kinesin-related protein costal2. *Cell* **90**, 225-34.

Robertson, D. A., Freeman, C., Morris, C. P. and Hopwood, J. J. (1992). A cDNA clone for human glucosamine-6-sulphatase reveals differences between arylsulphatases and non-arylsulphatases. *Biochem J* **288 (Pt 2)**, 539-44.

Roelink, H., Augsburger, A., Heemskerk, J., Korzh, V., Norlin, S., Altaba, A., Tanabe, Y., Placzek, M., Edlund, T. and Jessell, T. M. (1994). Floor plate and motor neuron induction by vhh-1, a vertebrate homolog of hedgehog expressed by the notochord. *Cell* **76**, 761-775.

Roelink, H., Porter, J. A., Chiang, C., Tanabe, Y., Chang, D. T., Beachy, P. A. and Jessell, T. M. (1995). Floor plate and motor neuron induction by different concentrations of the amino-terminal cleavage product of sonic hedgehog autoproteolysis. *Cell* **81**, 445-455.

Rogalski, T. M., Williams, B. D., Mullen, G. P. and Moerman, D. G. (1993). Products of the unc-52 gene in Caenorhabditis elegans are homologous to the core protein of the mammalian basement membrane heparan sulfate proteoglycan. *Genes Dev* **7**, 1471-84.

Rohatgi, R., Milenkovic, L., Corcoran, R. B. and Scott, M. P. (2009). Hedgehog signal transduction by Smoothened: pharmacologic evidence for a 2-step activation process. *Proc Natl Acad Sci U S A* **106**, 3196-201.

Rohatgi, R., Milenkovic, L. and Scott, M. P. (2007). Patched1 regulates hedgehog signaling at the primary cilium. *Science* **317**, 372-6.

Rosenbaum, J. L. and Witman, G. B. (2002). Intraflagellar transport. *Nat Rev Mol Cell Biol* **3**, 813-25.

Rubin, J. B., Choi, Y. J. and Segal, R. A. (2002). Cerebellar proteoglycans regulate sonic hedgehog responses during development. *Development* **129**, 2223-2232.

Ruiz i Altaba, A., Jessell, T. M. and Roelink, H. (1995). Restrictions to floor plate induction by hedgehog and winged-helix genes in the neural tube of frog embryos. *Mol Cell Neurosci* **6**, 106-21.

Rupp, F., Payan, D. G., Magill-Solc, C., Cowan, D. M. and Scheller, R. H. (1991). Structure and expression of a rat agrin. *Neuron* **6**, 811-23.

Saha, M. S., Miles, R. R. and Grainger, R. M. (1997). Dorsal-ventral patterning during neural induction in Xenopus: assessment of spinal cord regionalization with xHB9, a marker for the motor neuron region. *Dev Biol* **187**, 209-23.

Sampath, K., Rubinstein, A. L., Cheng, A. M., Liang, J. O., Fekany, K., Solnica-Krezel, L., Korzh, V., Halpern, M. E. and Wright, C. V. (1998). Induction of the zebrafish ventral brain and floorplate requires cyclops/nodal signalling. *Nature* **395**, 185-9.

Sasaki, N., Hirano, T., Kobayashi, K., Toyoda, M., Miyakawa, Y., Okita, H., Kiyokawa, N., Akutsu, H., Umezawa, A. and Nishihara, S. (2010). Chemical inhibition of sulfation accelerates neural differentiation of mouse embryonic stem cells and human induced pluripotent stem cells. *Biochem Biophys Res Commun* **401**, 480-6.

Schauerte, H. E., van Eeden, F. J., Fricke, C., Odenthal, J., Strahle, U. and Haffter, P. (1998). Sonic hedgehog is not required for the induction of medial floor plate cells in the zebrafish. *Development* **125**, 2983-93.

Schier, A. F., Neuhauss, S. C., Helde, K. A., Talbot, W. S. and Driever, W. (1997). The one-eyed pinhead gene functions in mesoderm and endoderm formation in zebrafish and interacts with no tail. *Development* **124**, 327-42.

Schmidt, H., Rickert, C., Bossing, T., Vef, O., Urban, J. and Technau, G. M. (1997). The embryonic central nervous system lineages of Drosophila melanogaster. II. Neuroblast lineages derived from the dorsal part of the neuroectoderm. *Dev Biol* **189**, 186-204.

Schneider, C., King, R. M. and Philipson, L. (1988). Genes specifically expressed at growth arrest of mammalian cells. *Cell* **54**, 787-93.

Schoenwolf, G. C. and Franks, M. V. (1984). Quantitative analyses of changes in cell shapes during bending of the avian neural plate. *Dev Biol* **105**, 257-72.

Sertie, A. L., Sossi, V., Camargo, A. A., Zatz, M., Brahe, C. and Passos-Bueno, M. R. (2000). Collagen XVIII, containing an endogenous inhibitor of angiogenesis and tumor growth, plays a critical role in the maintenance of retinal structure and in neural tube closure (Knobloch syndrome). *Hum Mol Genet* **9**, 2051-8.

Sharma, R. P. and Chopra, V. L. (1976). Effect of the Wingless (wg1) mutation on wing and haltere development in Drosophila melanogaster. *Dev Biol* **48**, 461-5.

Shi, Y., Zhao, S., Li, J. and Mao, B. (2009). Islet-1 is required for ventral neuron survival in Xenopus. *Biochem Biophys Res Commun* **388**, 506-10.

Shih, J. and Fraser, S. E. (1996). Characterizing the zebrafish organizer: microsurgical analysis at the early-shield stage. *Development* **122**, 1313-22.

Sisson, J. C., Ho, K. S., Suyama, K. and Scott, M. P. (1997). Costal2, a novel kinesin-related protein in the Hedgehog signaling pathway. *Cell* **90**, 235-45.

Smith, J. L. and Schoenwolf, G. C. (1989). Notochordal induction of cell wedging in the chick neural plate and its role in neural tube formation. *J Exp Zool* **250**, 49-62.

Smyth, I., Narang, M. A., Evans, T., Heimann, C., Nakamura, Y., Chenevix-Trench, G., Pietsch, T., Wicking, C. and Wainwright, B. J. (1999). Isolation and characterization of human patched 2 (PTCH2), a putative tumour

suppressor gene inbasal cell carcinoma and medulloblastoma on chromosome 1p32. *Hum Mol Genet* **8**, 291-7.

Solnica-Krezel, L., Stemple, D. L., Mountcastle-Shah, E., Rangini, Z., Neuhauss, S. C., Malicki, J., Schier, A. F., Stainier, D. Y., Zwartkruis, F., Abdelilah, S. et al. (1996). Mutations affecting cell fates and cellular rearrangements during gastrulation in zebrafish. *Development* **123**, 67-80.

Spring, J., Paine-Saunders, S. E., Hynes, R. O. and Bernfield, M. (1994). Drosophila syndecan: conservation of a cell-surface heparan sulfate proteoglycan. *Proc Natl Acad Sci U S A* **91**, 3334-8.

Stebel, M., Vatta, P., Ruaro, M. E., Del Sal, G., Parton, R. G. and Schneider, C. (2000). The growth suppressing gas1 product is a GPI-linked protein. *FEBS Lett* **481**, 152-8.

Stickens, D., Clines, G., Burbee, D., Ramos, P., Thomas, S., Hogue, D., Hecht, J. T., Lovett, M. and Evans, G. A. (1996). The EXT2 multiple exostoses gene defines a family of putative tumour suppressor genes. *Nat Genet* **14**, 25-32.

Strahle, U., Jesuthasan, S., Blader, P., Garcia-Villalba, P., Hatta, K. and Ingham, P. W. (1997). one-eyed pinhead is required for development of the ventral midline of the zebrafish (Danio rerio) neural tube. *Genes Funct* **1**, 131-48.

Strutt, H., Thomas, C., Nakano, Y., Stark, D., Neave, B., Taylor, A. M. and Ingham, P. W. (2001). Mutations in the sterol-sensing domain of Patched suggest a role for vesicular trafficking in Smoothened regulation. *Curr Biol* **11**, 608-13.

Tada, M. and Smith, J. C. (2000). Xwnt11 is a target of Xenopus Brachyury: regulation of gastrulation movements via Dishevelled, but not through the canonical Wnt pathway. *Development* **127**, 2227-38.

Taipale, J., Cooper, M. K., Maiti, T. and Beachy, P. A. (2002). Patched acts catalytically to suppress the activity of Smoothened. *Nature* **418**, 892-7.

Takabatake, T., Takahashi, T. C., Takabatake, Y., Yamada, K., Ogawa, M. and Takeshima, K. (2000). Distinct expression of two types of Xenopus Patched genes during early embryogenesis and hindlimb development. *Mech Dev* **98**, 99-104.

Talbot, W. S., Trevarrow, B., Halpern, M. E., Melby, A. E., Farr, G., Postlethwait, J. H., Jowett, T., Kimmel, C. B. and Kimelman, D. (1995). A homeobox gene essential for zebrafish notochord development. *Nature* **378**, 150-7.

Tannahill, D., Isaacs, H. V., Close, M. J., Peters, G. and Slack, J. M. (1992). Developmental expression of the Xenopus int-2 (FGF-3) gene: activation by mesodermal and neural induction. *Development* **115**, 695-702.

Taylor, F. R., Wen, D., Garber, E. A., Carmillo, A. N., Baker, D. P., Arduini, R. M., Williams, K. P., Weinreb, P. H., Rayhorn, P., Hronowski, X. et al. (2001). Enhanced potency of human Sonic hedgehog by hydrophobic modification. *Biochemistry* **40**, 4359-4371.

Tenzen, T., Allen, B. L., Cole, F., Kang, J. S., Krauss, R. S. and McMahon, A. P. (2006). The cell surface membrane proteins Cdo and Boc are components and targets of the Hedgehog signaling pathway and feedback network in mice. *Dev Cell* **10**, 647-56.

Tessier-Lavigne, M., Placzek, M., Lumsden, A. G., Dodd, J. and Jessell, T. M. (1988). Chemotropic guidance of developing axons in the mammalian central nervous system. *Nature* **336**, 775-8.

The, I., Bellaiche, Y. and Perrimon, N. (1999). Hedgehog movement is regulated through tout velu-dependent synthesis of a heparan sulfate proteoglycan. *Mol.Cell* **4**, 633-639.

Timmer, J. R., Wang, C. and Niswander, L. (2002). BMP signaling patterns the dorsal and intermediate neural tube via regulation of homeobox and helix-loop-helix transcription factors. *Development* **129**, 2459-2472.

Topczewski, J., Sepich, D. S., Myers, D. C., Walker, C., Amores, A., Lele, Z., Hammerschmidt, M., Postlethwait, J. and Solnica-Krezel, L. (2001). The zebrafish glypican knypek controls cell polarity during gastrulation movements of convergent extension. *Dev Cell* **1**, 251-64.

Torroja, C., Gorfinkiel, N. and Guerrero, I. (2004). Patched controls the Hedgehog gradient by endocytosis in a dynamin-dependent manner, but this internalization does not play a major role in signal transduction. *Development* **131**, 2395-408.

Traister, A., Shi, W. and Filmus, J. (2007). Mammalian Notum induces the release of glypicans and other GPI-anchored proteins from the cell surface. *Biochem J*.

Trousse, F., Marti, E., Gruss, P., Torres, M. and Bovolenta, P. (2001). Control of retinal ganglion cell axon growth: a new role for Sonic hedgehog. *Development* **128**, 3927-36.

Tsen, G., Halfter, W., Kroger, S. and Cole, G. J. (1995). Agrin is a heparan sulfate proteoglycan. *J Biol Chem* **270**, 3392-9.

Turnbull, J., Powell, A. and Guimond, S. (2001). Heparan sulfate: decoding a dynamic multifunctional cell regulator. *Trends Cell Biol.* **11**, 75-82.

van den Heuvel, M. and Ingham, P. W. (1996). smoothened encodes a receptor-like serpentine protein required for hedgehog signalling. *Nature* **382**, 547-51.

Viviano, B. L., Paine-Saunders, S., Gasiunas, N., Gallagher, J. and Saunders, S. (2004). Domain-specific modification of heparan sulfate by Qsulf1 modulates the binding of the bone morphogenetic protein antagonist Noggin. *J.Biol.Chem.* **279**, 5604-5611.

Voigt, A., Pflanz, R., Schafer, U. and Jackle, H. (2002). Perlecan participates in proliferation activation of quiescent Drosophila neuroblasts. *Dev Dyn* **224**, 403 - 412.

Wallingford, J. B. and Harland, R. M. (2001). Xenopus Dishevelled signaling regulates both neural and mesodermal convergent extension: parallel forces elongating the body axis. *Development* **128**, 2581-92.

Wallingford, J. B. and Harland, R. M. (2002). Neural tube closure requires Dishevelled-dependent convergent extension of the midline. *Development* **129**, 5815-25.

Wang, G., Amanai, K., Wang, B. and Jiang, J. (2000). Interactions with Costal2 and suppressor of fused regulate nuclear translocation and activity of cubitus interruptus. *Genes Dev* **14**, 2893-905.

Wang, G. and Jiang, J. (2004). Multiple Cos2/Ci interactions regulate Ci subcellular localization through microtubule dependent and independent mechanisms. *Dev Biol* **268**, 493-505.

Wang, Q. T. and Holmgren, R. A. (1999). The subcellular localization and activity of Drosophila cubitus interruptus are regulated at multiple levels. *Development* **126**, 5097-106.

Wang, S. W., Ai, X. B., Freeman, S. D., Pownall, M. E., Lu, Q., Kessler, D. S. and Emerson, C. P. (2004). QSulf1, a heparan sulfate 6-O-endosulfatase,

inhibits fibroblast growth factor signaling in mesoderm induction and angiogenesis. *Proc Natl Acad Sci U S A* **101**, 4833-4838.

Wang, Y., Zhou, Z., Walsh, C. T. and McMahon, A. P. (2009). Selective translocation of intracellular Smoothened to the primary cilium in response to Hedgehog pathway modulation. *Proc Natl Acad Sci U S A* **106**, 2623-8.

Weinstein, D. C., Ruiz i Altaba, A., Chen, W. S., Hoodless, P., Prezioso, V. R., Jessell, T. M. and Darnell, J. E. (1994). The winged-helix transcription factor HNF-3 beta is required for notochord development in the mouse embryo. *Cell* **78**, 575-88.

Williams, E. H., Pappano, W. N., Saunders, A. M., Kim, M. S., Leahy, D. J. and Beachy, P. A. (2010). Dally-like core protein and its mammalian homologues mediate stimulatory and inhibitory effects on Hedgehog signal response. *Proc Natl Acad Sci U S A* **107**, 5869-74.

Winterbottom, E. F., Illes, J. C., Faas, L. and Isaacs, H. V. (2010). Conserved and novel roles for the Gsh2 transcription factor in primary neurogenesis. *Development* **137**, 2623-31.

Winterbottom, E. F. and Pownall, M. E. (2008). Complementary expression of HSPG 6-O-endosulfatases and 6-O-sulfotransferase in the hindbrain of Xenopus laevis. *Gene Expr Patterns*.

Wojcinski, A., Nakato, H., Soula, C. and Glise, B. (2011). DSulfatase-1 fine-tunes Hedgehog patterning activity through a novel regulatory feedback loop. *Dev Biol*.

Wu, Y., Belenkaya, T. Y. and Lin, X. (2010). Dual roles of Drosophila glypican Dally-like in Wingless/Wnt signaling and distribution. *Methods Enzymol* **480**, 33-50.

Yamada, T., Placzek, M., Tanaka, H., Dodd, J. and Jessell, T. M. (1991). Control of cell pattern in the developing nervous system: polarizing activity of the floor plate and notochord. *Cell* **64**, 635-47.

Yan, D., Wu, Y., Yang, Y., Belenkaya, T. Y., Tang, X. and Lin, X. (2010). The cell-surface proteins Dally-like and Ihog differentially regulate Hedgehog signaling strength and range during development. *Development* **137**, 2033-44.

Yang, Y., Drossopoulou, G., Chuang, P. T., Duprez, D., Marti, E., Bumcrot, D., Vargesson, N., Clarke, J., Niswander, L., McMahon, A. et al. (1997). Relationship between dose, distance and time in Sonic Hedgehog-mediated regulation of anteroposterior polarity in the chick limb. *Development* **124**, 4393-404.

Yao, S., Lum, L. and Beachy, P. (2006). The ihog cell-surface proteins bind Hedgehog and mediate pathway activation. *Cell* **125**, 343-57.

Yayon, A., Klagsbrun, M., Esko, J. D., Leder, P. and Ornitz, D. M. (1991). Cell surface, heparin-like molecules are required for binding of basic fibroblast growth factor to its high affinity receptor. *Cell* **64**, 841-8.

You, J., Belenkaya, T. and Lin, X. (2011). Sulfated is a negative feedback regulator of wingless in Drosophila. *Dev Dyn* **240**, 640-8.

Yue, X., Li, X., Nguyen, H. T., Chin, D. R., Sullivan, D. E. and Lasky, J. A. (2008). Transforming growth factor-beta1 induces heparan sulfate 6-O-endosulfatase 1 expression in vitro and in vivo. *J Biol Chem* **283**, 20397-407.

Zaphiropoulos, P. G., Unden, A. B., Rahnama, F., Hollingsworth, R. E. and Toftgard, R. (1999). PTCH2, a novel human patched gene, undergoing alternative splicing and up-regulated in basal cell carcinomas. *Cancer Res* **59**, 787-92.

Zeng, X., Goetz, J. A., Suber, L. M., Scott, W. J., Jr., Schreiner, C. M. and Robbins, D. J. (2001). A freely diffusible form of Sonic hedgehog mediates long-range signalling. *Nature* **411**, 716-720.

Zhang, W., Zhao, Y., Tong, C., Wang, G., Wang, B., Jia, J. and Jiang, J. (2005). Hedgehog-regulated Costal2-kinase complexes control phosphorylation and proteolytic processing of Cubitus interruptus. *Dev Cell* **8**, 267-78.

Zhang, X. M., Ramalho-Santos, M. and McMahon, A. P. (2001). Smoothened mutants reveal redundant roles for Shh and Ihh signaling including regulation of L/R asymmetry by the mouse node. *Cell* **105**, 781-92.

Zhao, W., Allen, S. and Dhoot, G. K. (2007). FGF mediated Sulf1 regulation. *FEBS Lett* **581**, 4960-4.

Zhou, Q. and Kalderon, D. (2011). Hedgehog Activates Fused through Phosphorylation to Elicit a Full Spectrum of Pathway Responses. *Dev Cell* **20**, 802-14.

Zhu, A. J., Zheng, L., Suyama, K. and Scott, M. P. (2003). Altered localization of Drosophila Smoothened protein activates Hedgehog signal transduction. *Genes Dev* **17**, 1240-52.